THE EXTRACTION OF TRICHLOROSTANNATO-RHODIUM COMPLEXES BY POLYURETHANE FOAM

A thesis submitted to the

UNIVERSITY OF CAPE TOWN

in fulfilment of the requirements for the degree of

DOCTOR OF PHILOSOPHY

by

IRIS HALL (née NEL)

B.Sc(Hons.) (University of Cape Town)

Department of Chemistry

University of Cape Town

Rondebosch 7700

South Africa

June 1990

"IT IS BY LOGIC THAT WE PROVE,

BUT BY INTUITION THAT WE DISCOVER."

Jules Henri Poincare

(1854 - 1912)

ACKNOWLEDGEMENTS

I would like to sincerely thank :

- My supervisor, Prof. Klaus Koch, for the chemistry he has taught me and for all the time he has spent recording nmr spectra,
- Mammi and Uncle Alan, who have always stood by me,
- Prof. Graham Jackson for his kind interest and invaluable help with the computer simulation,
- Dr. Gary Watkins for proofreading this thesis,
- Mr. Tony Jutzen and Mr. Fred Smith for their friendly assistance,
- Mr. Rodney Wright for his invaluable assistance with the gel permeation chromatography, and the Polymer Science Institute of Stellenbosch University for the use of their apparatus,
- Mr. Joaquin Schoch of Dow Chemical Company (S.A.) for useful discussions on the preparation of polyurethane foam,
- Dow Chemical Company (S.A.) and Flexaire Foams (S.A.) for donating chemicals and the polyurethane foam used in this work,
- The University of Cape Town, the South African Council for Scientific and Industrial Research and the African Explosives and Chemical Industry for financial assistance,
- And all my friends, especially Ms Cheryl Sacht, in the Chemistry Department for making my study enjoyable.
- I would also like to especially thank my husband, Dr. Philip Hall, for the many hours he spent typing this thesis and for his friendship and invaluable moral support.

ABSTRACT

Polyurethane foam (polyether based) has been found to efficiently extract rhodium from hydrochloric acid solutions containing stannous chloride. The amount of rhodium extracted is significantly influenced by *inter alia* temperature, acid concentration, the Sn(II):Rh mol ratio and the presence of alkali metal cations. The extraction efficiency is promoted by increased acid concentration and high Sn(II):Rh ratios. The presence of K^+ inhibits the extraction of rhodium, while the effect of Li^+ and Na^+ is small.

A series of model urethane compounds (diurethane podands and linear polyurethanes) have been synthesized and characterized. These model compounds allowed the direct determination of the extracted trichlorostannato-rhodium complex anions by ^{119}Sn nmr spectroscopy. Conditions favouring the formation of $[Rh(SnCl_3)_5]^{4-}$ were found to result in the extraction of increased amounts of rhodium. The predominant species in the urethane phase was identified as the hydrido complex, $[RhH(SnCl_3)_5]^{3-}$, which is formed by protonation of $[Rh(SnCl_3)_5]^{4-}$. The protonation reaction has been shown to be reversible. The ^{119}Sn nmr study showed the formation of a new rhodium-hydrido complex formulated to be $[RhH(SnCl_3)_4Cl]^{3-}$. In the presence of low tin(II) concentrations {Sn(II):Rh = 4:1}, $[Rh(SnCl_3)_3Cl_3]^{3-}$ is predominantly extracted by the foam phase.

Analysis of the acid-decomposed polyurethane foam phase by atomic absorption spectroscopy and of the model urethane compound phase by ^7Li nmr spectroscopy, confirmed the extraction of alkali metal cations from aqueous solutions containing alkali metal salts. Our studies indicate that the polyether chains of polyurethane

foam play a major role in the extraction process, and that the flexibility of the chains influences the efficiency of polyurethane foam as an extractant.

The creation of cationic sites within the foam matrix, which facilitate the extraction of the rhodium-tin complex anions, is postulated to occur by protonation of the donor oxygen atoms as well as by chelation of cations such as H_3O^+, Li^+, Na^+ and K^+ by the polyether chains. A working model for the extraction of the trichlorostannato-rhodium complexes by polyurethane foam is proposed.

ABBREVIATIONS

AAS	=	atomic absorption spectroscopy
Aliquat 336	=	tricaprylylmethylammonium chloride
C	=	maximum capacity of polyurethane foam for rhodium ($mmol.g^{-1}$)
CCM	=	cation chelation mechanism
COV	=	coefficient of variation
D	=	dispersity (in gel permeation chromatography)
D	=	distribution ratio (in extraction experiments)
Diϕ150U	=	a diurethane podand synthesized from a polyethylene glycol with a molecular weight of 150
D'_m	=	the amount of metal (rhodium or cobalt) extracted per unit mass of polymer ($mmol.g^{-1}$)
%E	=	the percentage of the total amount of metal (rhodium or cobalt) extracted
EOP	=	ethylene oxide protons
GPC	=	gel permeation chromatography
$\bar{M}_n$	=	number average molecular weight
$\bar{M}_w$	=	weight average molecular weight
MP	=	methyl protons
n	=	oligo(ethylene oxide) chain length
η	=	viscosity
$[\eta]$	=	intrinsic viscosity
PEG	=	polyethylene glycol
PEO	=	poly(ethylene oxide)
PGM	=	platinum group metals

Pol400U(1:2) = a soluble linear polyurethane synthesized from a PEG with a molecular weight of 400. The number in parenthesis indicates the NCO:OH ratio used during synthesis.

PPO = poly(propylene oxide)

R_t = retention time

s = standard deviation

TDI = toluene diisocyanate

ν = stretching frequency {although not strictly correct, the units of cm^{-1} are given since ν(frequency) and $\tilde{\nu}$(wavenumber) are used interchangeably in the literature}

V_e = elution volume

TABLE OF CONTENTS

CHAPTER 1

INTRODUCTION

1. The Use of Polyurethane Foams in Separation Science

There is an enormous demand for flexible polyurethane foam. It serves as comfort cushioning in furniture and mattresses, carpet underlay, air filters in the automobile industry, shock absorbent packaging material, and linings for fabrics in the clothing industry, to mention but a few of the numerous applications. Thus polyurethane foam is mass produced in multi-million kilogram quantities every year, making it readily available and relatively inexpensive.

The use of foamed material for chemical separation is not entirely novel. Natural sponge was used as a solid support more than four centuries ago, when Brunschwig loaded the foam with olive oil for the purification of ethanol in a distillation system [3]. This ancient method was tested by Bayer in 1962 [4], who found that it operates well.

The first use of polyurethane foam in separation science was reported in 1965, when Bauman *et al.* [1] immobilized an enzyme-containing starch onto polyurethane foam in order to monitor air and water for enzymic-inhibiting atmospheric pollutants. In 1967, Van Venrooy [2] patented the use of polyurethane foam as a column support to facilitate the resolution of a mixture containing heptane, benzene, toluene, ethylbenzene, pentylbenzene and 2-ethylphenol by gas chromatography. The separation was achieved in twenty minutes using helium as the carrier gas.

It was not until 1970 that Bowen [5] reported the capability of untreated polyurethane foam to extract a variety of substances with relatively high efficiency. He was able to absorb iodine, benzene, chloroform, and phenol from water, and Hg(II), Au(III), Fe(III), Sb(V), Tl(III), Mo(VI) and Re(III) from hydrochloric acid

solutions, and U(VI) from a saturated aluminium nitrate solution. According to Bowen, "the separations require simple apparatus and are rapid and specific". He found capacities of the different foams investigated to vary from 0.5 to 1.5 $mol.kg^{-1}$ foam, and that desorption could usually be achieved without difficulty.

Since 1970, the number of publications involving polyurethane foam has grown dramatically, with an impressive variety in the applications reported for polyurethane foam sorbents. The sorptive capacity of polyurethane foams can be exploited in two ways:

a) the untreated, or unloaded, polyurethane foam can be used directly for the separation of a host of inorganic [5-27], as well as organic substances [28-31] from dilute solution (mainly aqueous, but also non-aqueous [14]),

b) active substances, such as solvent extractants [7,32-36], chelate compounds [37-47], liquid ion-exchangers [48,49], anchored extracting groups [50,51], and powdered ion-exchangers [51,52], are immobilized, or loaded onto the polyurethane foam to effect separation.

In the latter case, the polyurethane foam acts mainly as a solid support, with the capability of immobilizing an active substance. Usually, the organic extractants are immobilized on the foam matrix by allowing the foam material to swell in solutions of the extractants.

The physical nature of polyurethane foam largely contributes to its usefulness in analytical chemistry. Polyurethane foam can be described as a cellular plastic material in which part of the solid phase has been replaced by gas. Typically, around 97% of the bulk volume of polyurethane foam is occupied by the cells (bubbles), which appear as pentagonal dodecahedra, see Figure 1.1.

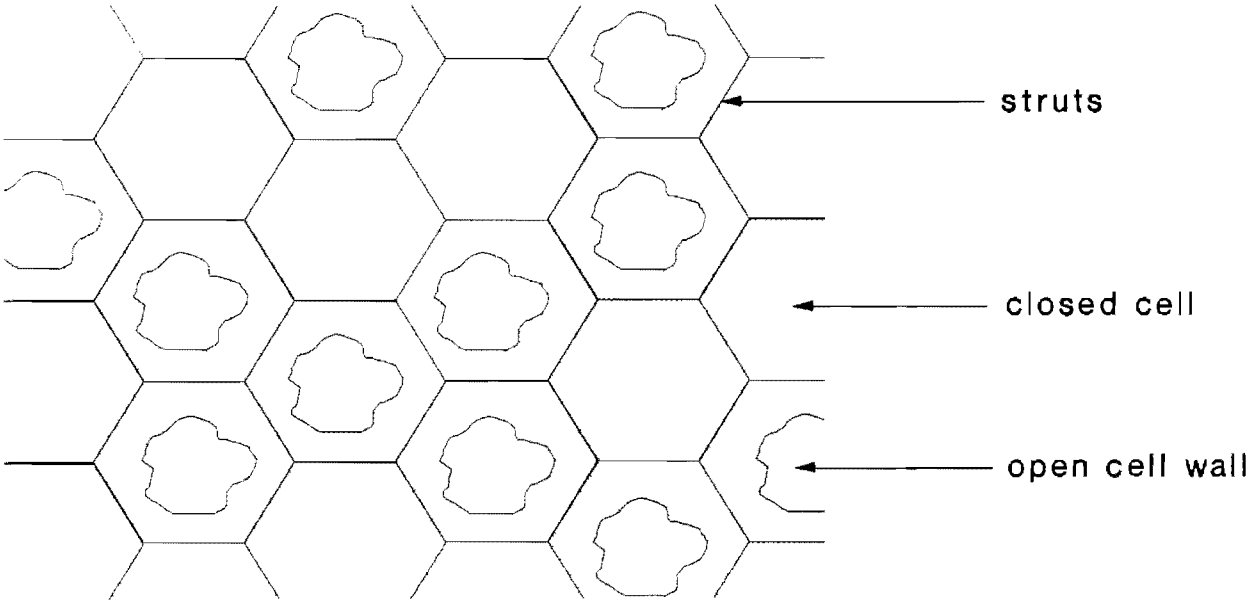

Figure 1.1 Diagrammatic representation of the morphology of polyurethane foam.

Usually rigid polyurethane foams tend to have closed cells, while flexible polyurethane foams are formed when the cell walls rupture in the final stages of expansion. In open-cell flexible polyurethane foam, at least two windows in each cell must be ruptured for fluids to pass freely through the foam. It is the latter class of open cell polyurethane foam that has found such wide application in analytical chemistry.

The physical nature of the polyurethane foam facilitates easy handling. Since the reaction systems are always heterogeneous, the solid foam phase is easily recovered from the reaction vessel for subsequent manipulation (for example, for analysis, or stripping of the extracted species from the foam.) Several authors have achieved extraction by simply shaking small pieces of polyurethane foam in the sample solution [5,13,17,36,41,42]. This procedure is referred to as a batch shaking method [53]. The unique resilience of polyurethane foam also lends itself to the more

efficient batch squeezing [9,11,12,14-16,18,19,25,27,29,45,54,55] and pulsating column methods [21,56,57]. The batch squeezing method involves squeezing of the polyurethane foam pieces to establish sorption equilibrium. The various squeezing methods that have been reported range from periodical manual compression of the foam with the back of a measuring cylinder [16], to an automated squeezing device operated by an electric motor [9,11,12,14-16,18,19,27,29,55]. In the pulsating column method a syringe is loaded with polyurethane foam. Compression and release of the foam column with the plunger of the syringe while the syringe tip is submerged in the sample solution, brings the foam in contact with the solution and results in extraction.

Polyurethane foam also has been utilized for the trapping of pesticide vapours in air [58-62]. The porous, cellular structure of the foam material offers little resistance to air passage, hence the polyurethane foam has been successfully incorporated into a high-volume air sampler [59,62]. In addition, polyurethane foam was found to be reusable [58,59,62] and allowed the use of elementary apparatus [58]. Arguably the most popular use of polyurethane foam has been as a solid stationary phase [7,8,10,13,17,21,28,30,63] or a solid support [13,32-35,37-40,42-44,46,48,49,51,52,64-66] in column separations due to the excellent hydrodynamic properties of foam-filled columns, which obviates the need for forced flow conditions. Braun and Farag [32] remarked "that chromatographic adsorption, exchange and partition processes could be favourably influenced by giving the adsorbent a hollow spherical (cellular) form, and effecting the adsorption on the internal surface of the cells". Since open-cell polyurethane foam, "may be regarded as a relatively regular stack of hollow spheres (cells)," [32] and exhibits good sorptive properties, the material proved to be a promising sorbent for truly chromatographic separations. Polyurethane foam was found to retain relatively high loads of organic complexing

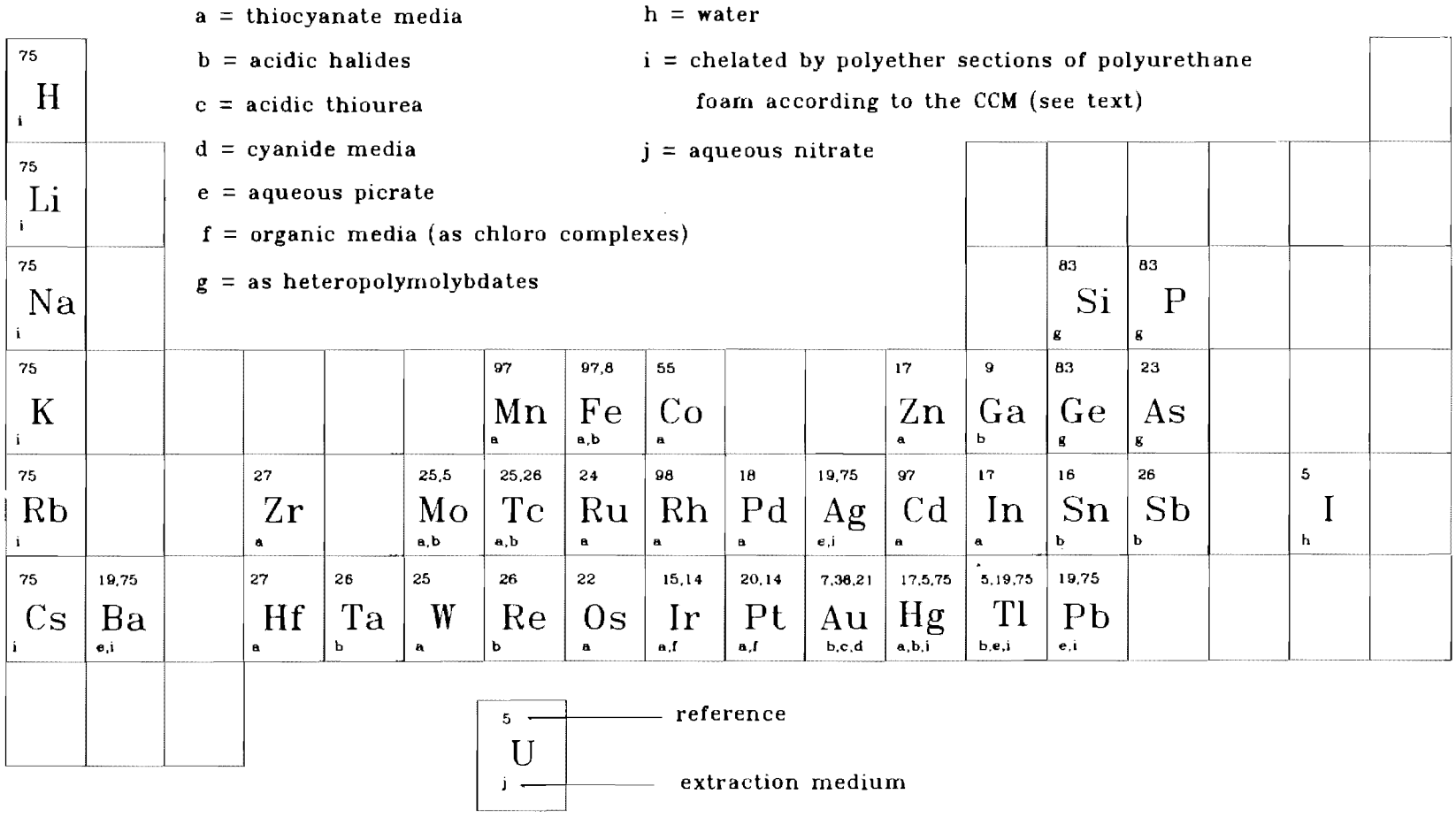

Figure 1.2 A summary of the elements that are reportedly sorbed by polyurethane foam.

agents and to permit high flow rates [32]. This preliminary communication by Braun and Farag [32] pioneered a series of publications on reverse-phase foam chromatography [33-35,40,48,64] and ion-exchange chromatography [51,52].

A detailed report of the myriad of diverse analytical applications reported for polyurethane foam is beyond the scope of this work. The topic has been discussed intensively in review articles [67-69] and books [53,70]. We shall limit the remainder of the introduction to the sorption of mainly metal ions by untreated polyurethane foam, with special reference to the mechanism by which extraction occurs. A brief summary of the various elements sorbed by untreated polyurethane foam is presented in Figure 1.2.

2. A Chemical Description of Polyurethane Foam

Any attempt at obtaining insight into the sorption mechanism must necessarily be accompanied by a knowledge of the chemical nature and structure of polyurethane foam. Therefore, we shall provide a brief overview of the substances and reactions involved in the synthesis of polyurethane foam.

Polyurethanes are not, as the name might suggest, derived by polymerizing a monomeric urethane molecule, nor do they consist primarily of urethane groups [71]. The synthesis of foamed polyurethanes depends largely upon the condensation-polymerization reaction between a diisocyanate (typically an 80:20 or 60:40 isomer mixture of 2,4- and 2,6-toluene diisocyanate) and di- or multi-functional hydroxyl compounds (mainly polyester or polyether polyols). This reaction is considered to be a chain propagation reaction as shown below:

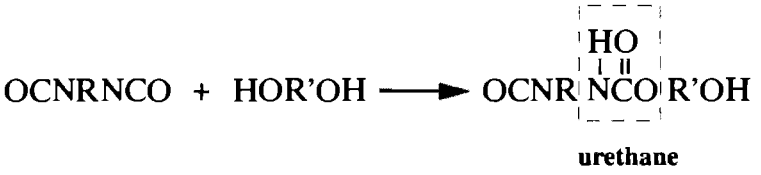

(1)

Another important reaction is the reaction between isocyanate and water to form an unstable carbamic acid, which decomposes to form carbon dioxide and an amine.

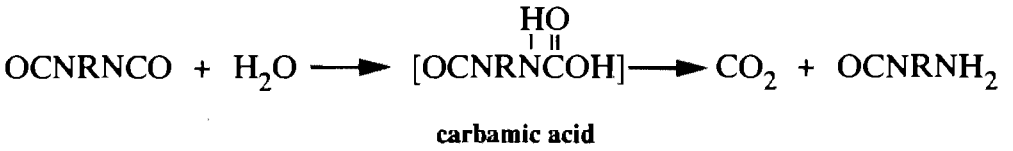

(2)

The liberation of CO_2 during this reaction acts as an *in situ* blowing agent and is responsible for foam formation, hence the foam-like morphology of the solid polyurethane foam.

The amine formed in reaction 2 may react with an additional isocyanate to form substituted ureas and result in further chain extension.

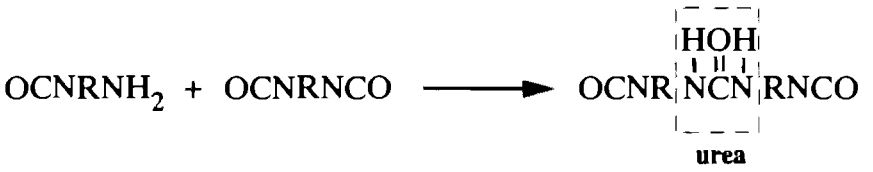

(3)

Alternatively, the carbamic acid may react with an isocyanate to produce an anhydride which decomposes to provide further urea bridges and blowing action.

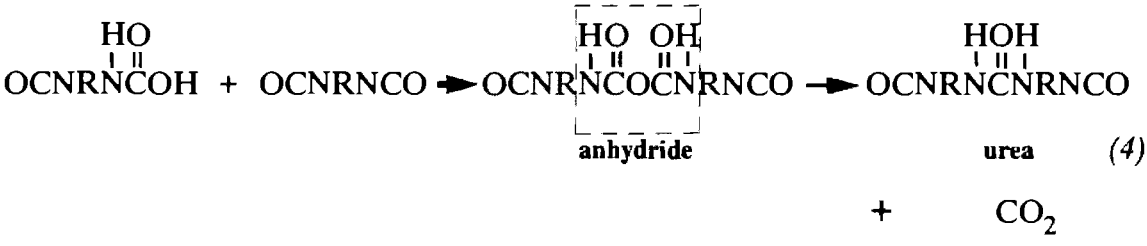

(4)

In addition to the chain propagation reactions, side reactions occur which lead to branching and cross-linking. Thus the isocyanate-urethane reaction produces allophanate linkages and the isocyanate-urea reaction produces biuret units.

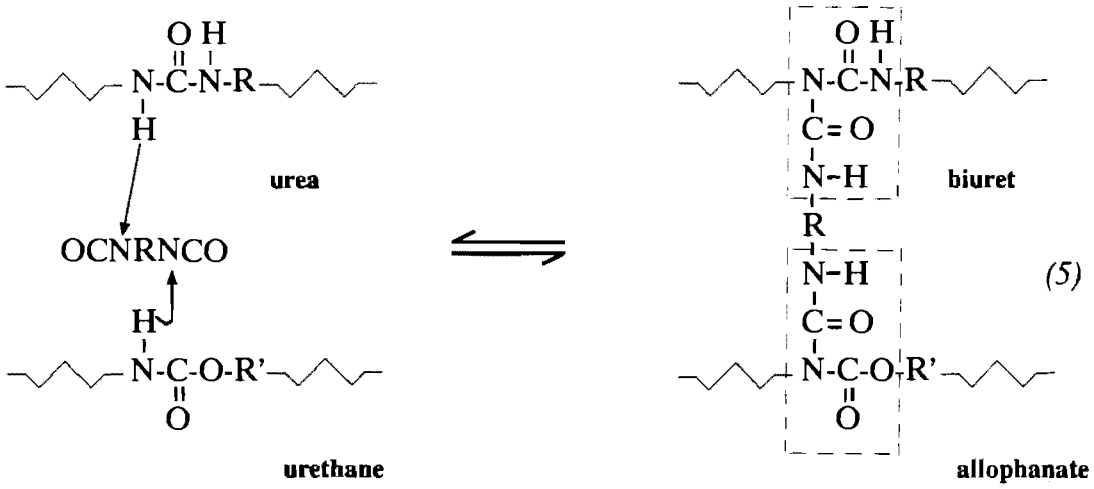

(5)

A simplified representation of the formation of biuret and allophanate groups can be found in equations 6 and 7.

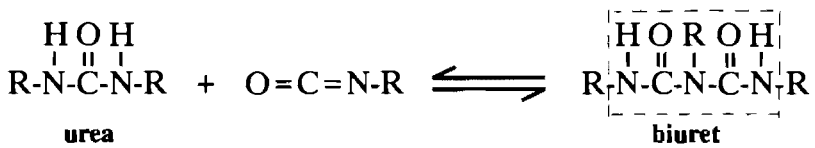

(6)

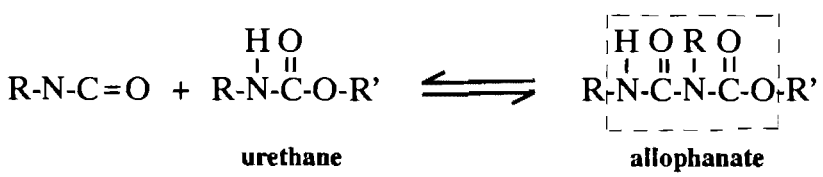

(7)

Evidently then, polyurethane foams consist of a complex network of polyether or polyester chains, urethane, urea, allophanate, and biuret linkages, as well as aromatic hydrocarbons sections.

3. Mechanistic Considerations

3.1 Surface Adsorption

Insight into the nature of the sorption process was first reached by Bowen when he showed that *absorption* into the foam material occurred rather than *adsorption* onto the foam surface [5]. By shaking portions of polyurethane foam in a *n*-heptane solution of [carboxy-^{14}C]-stearic acid, and assuming that the stearic acid is *adsorbed* as a uniform monolayer, Bowen was able to calculate the surface area of the polyurethane foam portion after the *adsorbed* stearic acid had been quantified. The surface area was found to be far too small to account for the foam extractions. Hence, 1-3 x 10^{-4} mol of adsorbent could be accommodated on the surface of 1 kg of the foam under investigation, where up to 1.5 mol.kg^{-1} foam had actually been extracted. These results clearly indicated *absorption* into the bulk of the polymer rather than surface *adsorption*. Although the assumption that stearic acid was *adsorbed* as a monolayer could be criticized, this conclusion was confirmed by a microscopic study of cross-sections of the foam fibrils after the extraction of iodine. The iodine colour was found to be uniformly distributed throughout the fibril, and not confined to its surface. Subsequently, authors have determined surface areas of polyurethane foams by the BET method using Krypton [9,16], and also rejected surface *adsorption* as a possible extraction mechanism based on the relatively low surface areas measured.

3.2 Solvent Extraction

Bowen [5] noted that two classes of substances were extracted by polyurethane foam:

a) easily polarizable free molecules such as iodine, aromatic compounds and metal dithizonates, and

b) singly charged anions with high polarizability, such as $AuCl_4^-$, $TlCl_4^-$ and $FeCl_4^-$.

It was found that all the substances in the latter class were also readily extracted into diethyl ether from aqueous acids.

The concept of polyurethane foam acting as a type of "solid solvent extractant" was developed by several authors, whose results were consistent with a solvent extraction type of mechanism [8-12,16]. Gesser *et al.* [9] reported that the extraction of gallium by polyurethane foam from acidic chloride solutions was similar to that of liquid ether. Gallium was thought to be extracted as the $HGaCl_4$ complex, and it was found that the concentrations of the H^+, Ga^{3+}, and Cl^- ions affected the capacity of the foam. The authors proposed two possible mechanisms:

Mechanism I

$$GaCl_4^- + H^+ \rightleftharpoons HGaCl_4\,(aq) \qquad (8)$$

$$HGaCl_4\,(aq) \rightleftharpoons HGaCl_4\,(foam) \qquad (9)$$

Mechanism II

$$H^+ + (\text{-}CH_2\text{-}O\text{-}CH_2\text{-})_{foam} \rightleftharpoons (\text{-}CH_2\text{-}\overset{H}{\underset{+}{O}}\text{-}CH_2\text{-})_{foam} \qquad (10)$$

$$(\text{-}CH_2\text{-}\overset{H}{\underset{+}{O}}\text{-}CH_2\text{-})_{foam} + GaCl_4^- \rightleftharpoons (\text{-}CH_2\text{-}\overset{H}{\underset{GaCl_4}{O}}\text{-}CH_2\text{-})_{foam} \qquad (11)$$

The first mechanism describes a true solvent extraction type of process where a neutral metal complex is first formed in the aqueous phase followed by dissolution into the solid foam "solvent". The second mechanism is more descriptive of an

anion exchange process, relying on the protonation of the ether groups to create cationic sites for the extraction of the $GaCl_4^-$ anion. Unfortunately, the results of Gesser *et al.* [9] did not allow them to distinguish between the two mechanisms. The transport of the $HGaCl_4$ complex through a polyurethane film was considered to be further evidence that the complex "dissolves" in the polyurethane foam [9,72]. The above-mentioned mechanisms I and II also plausibly explain the active transport of gallium through the polyurethane film.

Braun and Farag [10] also considered polyether-type polyurethane foams to act as solid ether solvents for cobalt(II) and iron(III) thiocyanato complexes. (Polyester-type polyurethane foams were found not to extract either species under comparable conditions.) Similarly, antimony (as $HSbCl_4$ and $HSbCl_6$) [11] and tin(IV) (possibly as the $HSnCl_5$ molecule) [16] were thought to be extracted by a solvent extraction type of mechanism.

A detailed comparison between the liquid solvent and polyurethane foam extractant systems for the removal of Fe(III) from acidic chloride solutions was reported by Oren *et al.* [12]. They found that in a plot of the change in the distribution ratio (**D**) with changing H^+, Fe^{3+} and Cl^- concentrations, most of the slopes predicted from liquid solvent extraction results reported in the literature [73], were confirmed for polyurethane foam extractions. Hence, the authors concluded [12] that the species absorbed by the foam would be the same as the species extracted in the reported solvent extraction study, namely, $FeCl_3$ and $HFeCl_4$ in the low and high hydrogen ion concentration regions respectively [73]. Epr spectra of the iron(III) loaded foam supported the hypothesis that $HFeCl_4$ (or the ion pair $H^+FeCl_4^-$) was dissolved in the solid foam. Finally, the solid polyurethane foam was considered similar to a liquid extractant of a moderate dielectric constant.

Further evidence for the similarity in the species extracted by liquid solvent extraction and polyurethane foam, was found in a Mössbauer speciation study on the extraction of ferric ions from thiocyanate media [74]. These spectra seemed to indicate that a neutral $Fe(SCN)_3$ species was extracted by polyether and polyester based polyurethane foams as well as by diethyl ether.

For a well-rounded discussion on the proposed solvent extraction mechanism, it is worthwhile to digress briefly from metal ion sorption to a report on the extraction of aromatic organic compounds by polyurethane foam from aqueous media [31]. Schumack *et al.* [31] found that their observations were consistent with a solvent extraction mechanism. The time required for establishing extraction equilibrium was short, and the addition of inert salts caused an increase in extraction due to a salting-out phenomenon. The effect of cations on extraction was found to increase as the charge-density on the ion increased. Schumack *et al.* [31] understood this to be due to increased solvation of ions with larger charge densities, which would reduce the number of solvent molecules available to solvate the organic compounds, hence forcing the organic molecules out of the aqueous phase into the foam. Varying the acidity of the aqueous phase had no effect on the extraction of compounds which exist as neutral species irrespective of pH, whereas compounds which could be involved in equilibria with protons were only extracted by polyurethane foam at pH values at which they were in the neutral form. Hence, no evidence for a mechanism requiring ionic species was found. Decreasing the polarity of the aqueous phase (with increasing amounts of ethanol) decreased extraction, a phenomenon which is commonly observed for solvent extraction. Finally, the authors also put forward strong evidence suggesting hydrogen bonding between extracted organic compounds (with groups capable of hydrogen bonding) and polyurethane foam.

Solvent extraction as a sorption mechanism for metal ions has been challenged and rejected as an only mechanism by several authors [14,75,76]. Moore and Chow [14] studied the extraction of chloro complexes of iridium and platinum from acetone and ethyl acetate solutions. They found the distribution ratio, **D** (where **D** is the ratio at equilibrium of the metal concentration in the foam relative to the aqueous phase) to remain constant over a range of iridium concentrations, after which the **D** values fell as the iridium concentration was raised. The authors proposed the following chemical equilibria,

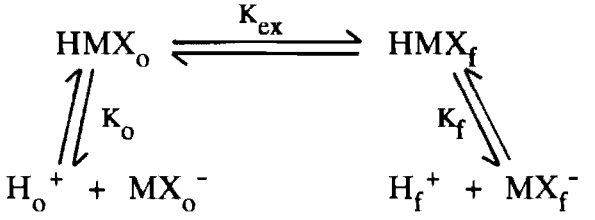

(12)

where HMX represents the undissociated complex and the subscripts "o" and "f" represent the organic solvent and foam phase respectively. By manipulation and substitution of the expressions describing K_o, K_{ex} and K_f, an expression for **D** was formulated as follows,

$$\mathbf{D} = \frac{K_{ex}[HMX]_o^{1/2} + K_{ex}^{1/2} K_f^{1/2}}{[HMX]_o^{1/2} + K_o^{1/2}}$$

This expression implies that a fall-off of **D** with increasing $[HMX]_o$ should only occur if $K_f >> K_o$. Since one might expect the dielectric constant of acetone (20.7 at 25 °C) to be considerably greater than that of the foam [14], it would seem unlikely for K_f to be greater than K_o when the complex is extracted from acetone. Ethyl acetate has a much lower dielectric constant (6.02 at 25 °C) and presumably K_f might approach K_o in this case. However, since the condition $K_f >> K_o$ could not be

satisfied, the results could not be explained by a simple solvent extraction mechanism. In their discussion on polyurethane foam sorption mechanisms, Hamon *et al.* [75] referred to the Moore and Chow [14] study and pointed out that it was difficult to justify treating the polymer as an analogue of diethyl ether, since neither $IrCl_6^{2-}$ nor $PtCl_6^{2-}$ shows any appreciable solubility in that solvent. They also mentioned that the polarity of polyurethanes had been determined from swelling measurements to be similar to that of acetone [77]. Hence, one would expect **D** values of approximately 1 $l.kg^{-1}$ for the distribution of $IrCl_6^{2-}$ between acetone and polyurethane foam instead of the 225 $l.kg^{-1}$ observed experimentally. If solvent extraction is the sorption mechanism these high distribution ratios would imply superior solvating powers of polyurethane foam.

Hamon *et al.* [75] examined the extraction of $Co(NCS)_4^{2-}$ by polyurethane foam. They found that sorption was essentially independent of hydrogen ion concentration over a wide pH range (pH = 1-9) when the solution ionic strength was constant. The formation of the neutral $H_2Co(NCS)_4$ species required for solvent extraction, under these conditions, is highly improbable. This fact, together with the high distribution ratios measured for polyurethane foam sorption (3×10^6 for $Co(NCS)_4^{2-}$) relative to the **D** values observed for liquid organic solvents (3 or less for $Co(NCS)_4^{2-}$), suggests that factors other than simple ether-like solvent extraction facilitate metal ion sorption and that some specific interactions with the polymer should exist.

The findings of Hamon *et al.* [75] were echoed by Al-Bazi and Chow [76] in their report on the extraction of palladium(II) thiocyanate complexes by polyether based polyurethane foam. These authors [76] found that 40% of the palladium was extracted from basic solutions where the formation of the neutral species

$H_2Pd(SCN)_4$ was not possible. They also reported distribution coefficients for polyurethane foam sorption that were orders of magnitude higher than those reported for extractions by diethyl ether. Furthermore, the fact that the polarity of urethane polymers had been measured to be similar to that of acetone [77] was in conflict with a solvent extraction mechanism, when one considered the complete recovery of the $Pd(SCN)_4^{2-}$ complex from the foam by acetone. Once again, it was concluded that factors other than a simple ether-like solvent extraction mechanism should be operative in the distribution of $Pd(SCN)_4^{2-}$ between foam and aqueous phase.

3.3 Ligand Addition and Ligand Exchange

The presence of ~~loan~~ lone pairs on the many nitrogen and oxygen atoms has brought ligand addition and ligand exchange into consideration as possible extraction mechanisms. The polyurethane donor atoms or "ligands" (L) can complex the extracted species either by addition

$$MX_n^{y-} + mL \rightleftharpoons MX_nL_m^{y-} \qquad (13)$$

or by ligand exchange

$$MX_n^{y-} + mL \rightleftharpoons MX_{n-m}L_m^{(y-m)-} + mX^- \qquad (14)$$

Abbas *et al.* [74] indicated the formation of the $Fe(SCN)_3L_3$ species, where L represents the donor groups of the polymer, from their Mössbauer studies on the sorption of ferric ions. Ligand addition has also been suggested as the most probable mechanism for the extraction of palladium from low thiocyanate conditions [76]. The authors deduced the extractable species to be the neutral

$PdCl_2$ complex in the absence of thiocyanate, and $Pd(SCN)_2$ from solutions containing low thiocyanate concentrations, and proposed that extraction occurred as follows

$$PdCl_2 + \overline{2L} \rightleftharpoons \overline{PdCl_2L_2} \qquad (15)$$

$$\text{and} \quad PdCl_2 + 2SCN^- \rightleftharpoons Pd(SCN)_2 \overset{SCN^-}{\rightleftharpoons} Pd(SCN)_4^{2-}$$
$$\Big\| \qquad (16)$$
$$\overline{2L} + Pd(SCN)_2 \rightleftharpoons \overline{Pd(SCN)_2L_2}$$

where the bars indicate the foam phase.

However, ligand addition/exchange has not found general acceptance and has been discarded as a possible mechanism for the extraction of $Co(NCS)_4^{2-}$ [75] and $Pd(SCN)_4^{2-}$ [76].

In the case of cobalt [75], an increase in coordination number caused by ligand addition would most probably result in a hexacoordinate complex. The change from tetrahedral to octahedral geometry is accompanied by a large change in the absorption spectrum, resulting in a colour change from blue to pink. However, no such colour change was observed on extraction (the foam adopted the blue colour of the tetrahedral $Co(NCS)_4^{2-}$ species.) Similarly, ligand exchange would cause a symmetry change in the complex which should also be accompanied by some alteration in the UV/visible spectrum. The spectrum of the sorbed species that had been rapidly recovered from polyurethane foam into several organic solvents, was again that of $Co(NCS)_4^{2-}$.

Ligand addition and ligand exchange were ruled out as possible mechanisms for the extraction of $Pd(SCN)_4^{2-}$, using similar arguments as above [76]. Five- or six-coordinate Pd(II)-complexes were reported to be rare and had not been observed in the solvent extraction of Pd(II). In addition, the replacement of the strongly bound sulphur atom by the nitrogen or oxygen atoms on the foam was considered unlikely, since such substitution had not been reported even for strongly donating solvents.

3.4 Anion Exchange

Weak-base anion exchange is another mechanism made feasible by the donor nitrogen and oxygen atoms present in polyurethane foam. These atoms may become protonated to create cationic sites which can act as anion exchangers. The protonation of cyclic and non-cyclic polyethers has been reported in the literature [78-82].

$$-CH_2\text{-}O\text{-}CH_2- \; + \; H^+ \rightleftharpoons -CH_2\text{-}\overset{\overset{H}{|}}{\overset{+}{O}}\text{-}CH_2- \qquad (17)$$

polyether oxygen atoms

$$\text{-O-}\overset{\overset{O}{\|}}{\overset{|}{C}}\text{-}\overset{\overset{H}{|}}{N}\text{-} \; + \; H^+ \rightleftharpoons \text{-O-}\overset{\overset{O}{\|}}{\overset{|}{C}}\text{-}\overset{\overset{H}{|}}{\overset{+}{N}}\text{-} \rightleftharpoons \text{-O-}\overset{\overset{OH}{|}}{C}\text{=}\overset{+}{N}\text{-} \qquad (18)$$

urethane nitrogen atoms

Bowen, in his original paper on polyurethane foam sorption [5], suggested the possibility of the foam acting as a weak anion exchanger with a low capacity, since it contains amido and perhaps amino groups. However, the marked specificity in anion absorption led him to remark that the process taking place could not be ion exchange alone.

Ion exchange has tentatively been suggested as a possible mechanism for the extraction of iridium from ethyl acetate and acetone [14], while the extraction of phosphomolybdate by anion exchange has also been considered feasible [83]. Gesser *et al.* [9] proposed two possible mechanisms for the extraction of gallium from acidic chloride solutions, one of which was an anion exchange mechanism (see reactions 10 and 11).

Weak-base anion exchange might be expected to contribute significantly to the sorption of anionic metal complexes in the presence of high concentrations of strong acids. However, high distribution ratios have been recorded for extractions in the absence of appreciable amounts of strong acid, for example, for the extraction of $Co(NCS)_4^{2-}$ [75] and $Pd(SCN)_4^{2-}$ [76]. Under these conditions, weak-base anion exchange should not play a significant role. In neutral or basic solution conditions, only a strong-base anion exchange mechanism could be expected to be operative, where permanent cationic sites such as quaternary ammonium groups would be involved. Since no such sites are typical of polyurethane foams, Hamon *et al.* [75] concluded that if anion exchange did occur, it took place at sites generated by some other mechanism. The most substantiated mechanism to date, namely the cation chelation mechanism, evolved from their observations.

3.5 The Cation Chelation Mechanism (CCM)

According to the cation chelation mechanism [75], many cations can be chelated by the polyether chains of polyurethane foams, in much the same way as chelation occurs by crown ethers [84]. Cations of the alkali, alkali-earth and some transition metals, as well as NH_4^+, RNH_3^+ and H_3O^+, are thought to be chelated, thus creating a cationic site in the foam matrix as shown below.

$$M^{p+} + \overline{site} \rightleftharpoons (\overline{M.site})^{p+}$$

Electroneutrality would demand the simultaneous accompaniment of anions. In the presence of only one extractable anion, for example MeX_n^{m-}, the mechanism resembles a solvent extraction process, where the chelated cation and accompanied anion may be associated within the polymer.

$$mM^{p+} + pMeX_n^{m-} + m(\overline{site}) \rightleftharpoons m(\overline{M.site})^{p+} + p\overline{MeX}_n^{m-}$$

However, should the solution contain some other moderately extractable anion, which becomes associated with the cationic site before, or concurrently with the sorption of MeX_n^{m-}, the process can conveniently be regarded as a type of anion exchange mechanism. The anions A^- are exchanged for the species MeX_n^{m-} at the positive site which was formed by the chelation of the M^{p+} by the polymer.

$$M^{p+} + pA^- + \overline{site} \rightleftharpoons (\overline{M.site})^{p+} + \overline{pA}^-$$

$$MeX_n^{m-} + \overline{mA}^- \rightleftharpoons \overline{MeX}_n^{m-} + mA^-$$

The polyether chains have been ideally proposed by Hamon *et al.* [75] to form helical conformations with inwardly directed oxygen atoms. This configuration is conducive to ion-dipole interactions between the poly(ethylene oxide) oxygen atoms and a chelated cation, and simulates cation associations with macrocycles such as 18-crown-6.

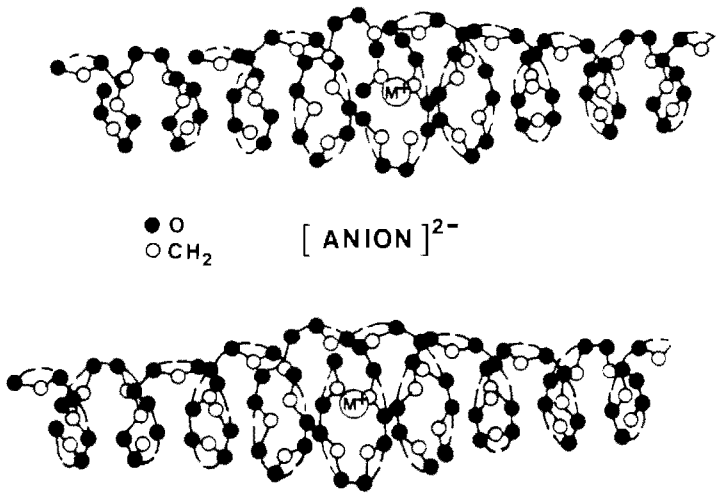

Figure 1.3 Diagrammatic representation of extraction by the cation chelation mechanism (CCM) facilitated by helical polyether chains.

Interactions between long chain non-cyclic poly(ethylene oxide) polymers and inorganic salts have been reported [85,86]. Significant support for the helical conformation of the polyether chains of polyurethane foam can be found in the literature. Pure poly(ethylene oxide) is known to adopt a helical conformation in the crystalline state [87] and to retain a large part of this structure in aqueous solution [88]. X-ray crystallographic data of shorter chain poly(ethylene oxide) complexes with alkali metal salts [89], for example of the NaSCN complex with $CH_3OC_6H_5O(CH_2CH_2O)_3C_6H_5OCH_3$, show that the polyether forms a spiral about the cation with inwardly directed oxygen atoms. Hamon *et al.* [75] mentioned that "extension of the spiral-type configuration of oxygen atoms about a cation complexed by shorter polyethers, would logically lead to a helical pattern of inwardly directed oxygen atoms in longer chains".

The evidence in support of helical conformations of long chain poly(ethylene oxides) on chelation with cations is not unequivocal. Saenger *et al.* [89] found that for "very long" ligands, that is for 1,5-bis{2-[5-(2-nitrophenoxy)-3-oxapentyloxy]-

phenoxy}-3-oxapentane, a 1:2 complex of polyether : KSCN was formed. While the two K^+ cations were coordinated in circular complex structures, these were not stacked "on top" of each other to form a helix, but were "side-by-side" in an s-like configuration. The reason for this structure could be the neutralization of the dipole moments of the two K^+ complexes. A further reason could be the observed coordination between the oxygen atoms of the nitro end groups, which would not be possible in a helical conformation.

The crystal structure of the complex of poly(ethylene oxide) with mercuric chloride ($(CH_2CH_2O)_4HgCl_2$), [90] showed a deviation from the helical conformation on complexation of the poly(ethylene oxide). However, the difference in conformation of poly(ethylene oxide) before and after complexation was not large.

The reduced extraction capability of polyurethane foams with higher poly(propylene oxide) content relative to poly(ethylene oxide) content observed by Hamon *et al.* [75] was ascribed to the steric effect of the poly(propylene oxide) methyl groups. These authors [75] state that the steric effect of the methyl group lowers the tendency for the polyether chains to assume a helical configuration. Poly(propylene oxide) glycols have been found to have a non-planar zig-zag conformation [91]. Yanagida *et al.* [85] reported a low extracting power for poly(propylene oxide) glycols relative to poly(ethylene oxide) glycols and similarly cited the non-helical conformation of the poly(propylene oxide) glycols to be responsible. On the other hand, the above mentioned hypotheses are contradicted by Sotobayashi *et al.* [92,93] who reported a higher extracting power for poly(propylene oxide) glycols than poly(ethylene oxide) glycols in the solvent extraction of certain metals.

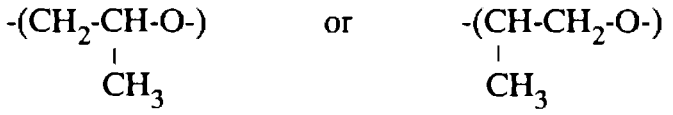

poly(propylene oxide) repeating units

Hamon *et al.* [75] predicted that polyurethane foams should exhibit a selectivity towards cation complexation depending on the size and other properties of the cation related to solvation. This prediction was based upon similar cation chelation selectivities reported for crown ethers [94,95] as well as non-cyclic polyethers [84]. These authors [75] proceeded to study the effect of a whole host of cations on the extraction of $Co(NCS)_4^{2-}$, and reported the affinity of polyether based polyurethane foam for various cations as

$$Li^+ < Na^+ < Cs^+ < Rb^+ < K^+ \approx NH_4^+ < Ag^+ < Tl^+$$

and $Ca^{2+} < Ba^{2+} < Hg^{2+} < Pb^{2+}$

The resemblance of this series with the order of stability constants reported by Christensen *et al.* [95] for dicyclohexyl-18-crown-6 was striking. Hamon *et al.* [75] linked this similarity to a report by Mattice [96] who studied the cyclization of poly(ethylene oxide) chains of some length and whose results indicated that 18-crown-6 was the most easily formed macrocycle.

The nature of the anions present in solution may limit the extent to which any cation is extracted, depending on the size and polarizability of the anion. Sorption of a given cation was found to increase in the order of NO_3^- < 2,4-dinitrophenolate$^-$ = 2,6-dinitrophenolate$^-$ < ClO_4^- < picrate$^-$ < ANS$^-$ < $(C_6H_5)_4B^-$, where ANS represents 8-anilino-1-naphthalenesulphonate [75]. Selective anion sorption has been reported by, amongst others, Bowen [5] and Al-Bazi *et al.* [20] who reported

negligible sorption of the chloro complexes of platinum and **D** > 10^4 for thiocyanato platinum complexes.

Infrared spectra provided compelling evidence in support of strong polyether involvement in the extraction of ion pairs [75]. The sorption of Co(II) from sodium thiocyanate solution induced a shift of about 30 cm^{-1} in the ν(C-O) of the ether modes of poly(ethylene oxide). An increase in the glass transition temperature of the foam (i.e. the foam fails to return to its original shape when compressed and becomes brittle) after virtual saturation with Co(II) thiocyanate, was also put forward as evidence of strong polyether-metal ion interactions.

The CCM has found wide-spread recognition. The extraction behaviour of Pt [20], Pd [18,76], Co, Fe, Zn, Cd, Mn [97], Ru [24], Os [22], Mo, W, Tc [25], Zr and Hf [27] from thiocyanate media, Ta, Sb, Re and Tc from hydrofluoric acid solutions [26] and Ag, Tl, Ba and Pb from aqueous picrate solutions [19], was consistent with the predictions of the CCM.

However, it is noteworthy that in some cases the CCM does not adequately explain all extraction phenomena. Al-Bazi *et al.* [98] studied the extraction of rhodium from thiocyanate media and found the presence of alkali metal salts to increase extraction in the order $Li^+ > Na^+ > K^+$, an observation considered to be in conflict with the CCM. This series corresponds to a decrease in the hydration number of the cations. The conclusion was made, therefore, that extraction took place by a simple solvent extraction mechanism, and that the salts affected sorption by a salting out process.

The extraction of phosphomolybdate by polyether polyurethane foam [83] showed a drop in **D** values with increasing LiCl concentration, which led Khan *et al.* to suggest that possibly sorption did not take place by the CCM. These authors suggested weak-base anion exchange and solvent extraction as possible alternate mechanisms. It was also proposed that the drop in **D** values with increasing LiCl concentration might be attributed to competitive sorption of MoO_4^{2-} (or any other suitable anion) by cation chelation of the Li^+ cations.

Polyester polyurethane foams have been found inferior to polyether based foams for metal ion sorption [10,16,75]. Hamon *et al.* [75] explained this phenomenon in terms of the CCM, to be partly due to the inherent inability of polyesters to become helically orientated about a central axis, and partly to a decrease in the density of oxygen atoms available for chelation. However, the decreased sorption ability by polyester polyurethane foam was not a universal observation. Braun *et al.* [17] found that polyether and polyester polyurethane foams extracted Zn, Hg and In equally well.

4. Separation and Preconcentration of the Platinum Group Metals

Rhodium is found in very low levels in the earth's crust, while no notable presence of rhodium in sea water has been detected [99]. The cosmic abundance of rhodium was estimated by H.C. Urey to be 0.0067 relative to a figure of 10000 for silicon [99]. Rhodium, as do the platinum group metals (PGMs) in general, exhibits distinctive properties, including resistance to chemical attack, excellent high temperature characteristics, the ability to catalyze chemical reactions, and stable electrical properties. Rhodium is commonly alloyed with platinum to increase the hardness and high temperature stability of platinum [100]. In 1988, 73% of the total

demand for rhodium in the western world, arose out of the autocatalyst sector for the reduction of NO_x gases [101]. Other important markets are the electrical, glass and chemical industries.

Secondary platinum group metals (PGMs), that is PGMs recovered from PGM scrap can be of the same purity as primary PGMs (unlike the secondary base metals which usually contain a wide range of impurities and are limited in their application). The high cost of the PGMs (in 1988 rhodium fetched about $1200 per ounce [101]) stresses the importance of recycling these metals. The autocatalyst industry is expected to grow even larger as more countries (in particular nations of the European Community) commence fitment of platinum-rhodium three-way catalysts. Hence, spent automobile catalytic converters are potentially an excellent source of secondary PGMs.

It is evident, therefore, that there is an ever-growing interest in efficient and cost-effective methods for preconcentration and separation of PGMs. Solvent extraction and ion exchange methods have been proposed for this purpose [102-105]. Ion exchange resins are frequently expensive and handling large volumes of organic solvents often present practical difficulties. Polyurethane foams seem an attractive alternative as a means of separation and preconcentration of the PGMs. It is readily available, inexpensive, allows for the use of simple apparatus and has been found to be reusable.

Many reports have appeared in the literature on the extraction by polyurethane foams of the platinum group metals as thiocyanato complexes [18,20,22,24,76,98]. However, a whole host of base metals and other elements are also complexed by thiocyanate and may be extracted as the thiocyanate complexes [25,27,55,97].

Hence, thiocyanate as a complexing agent has obvious disadvantages in any separation procedure.

The trichlorostannato anion ($SnCl_3^-$) is a more selective ligand with a particular affinity for the platinum group metals [106]. Several workers in our laboratory have studied the solvent extraction of PGMs as trichlorostannato complexes [107,108]. We sought to extend the study to the extraction of trichlorostannato complexes of rhodium by polyurethane foam. Such a study has also been reported for the extraction of platinum [109,110].

5. Reactions of Rhodium with Stannous Chloride in Hydrochloric Acid Medium

Salts of the platinum group metals react with stannous chloride in hydrochloric acid medium to give intensely coloured solutions. This phenomenon was observed by Wohler as early as 1907 [111]. In 1918, Ivanov [112,113] reportedly utilized the colour of rhodium(III)-stannous chloride solutions for both qualitative tests and for quantitative measurements by visual comparison with standard solutions. In his textbook of colourimetric analyses, Sandell [114] described a spectrophotometric method for the determination of rhodium using stannous chloride as the colour reagent. According to Sandell, "by far the best colour reaction for rhodium is that with stannous chloride".

Forerunners in the field used the reaction between stannous chloride and Rh(III) purely as a colour reaction to facilitate spectrophotometric determination of rhodium, without speculation about the nature of the coloured products formed [113,115,116]. Rhodium was quantified in the presence of other elements such as

iridium [115] and uranium [113] without prior separation. The simultaneous determination of platinum and rhodium was also performed [116].

Although the nature of the trichlorostannato-rhodium species was unknown, Sandell [114] referred to a red and a yellow "form" of rhodium. According to Sandell, the red "form" exists in approximately 2 M HCl and has an absorbance maximum around 480 nm, whereas the yellow "form" is produced on dilution with water (λ_{max} = 435 nm). Sandell stated that "it seems likely that rhodium is reduced to a lower valency state (but not to the colloidal metal) and that the formation of one or more chloro complexes is involved. The colour change is reversible". Increasing the chloride concentration reportedly restores the "red form of reduced rhodium," which was found to be stable.

A paper electrophoresis study of the platinum group metals in stannous chloride-hydrochloric acid medium by Shukla [117], revealed that the complexes formed were anionic. This finding refuted the existence of the $[Pt^0Sn_4Cl_4]^{4+}$ cation which was postulated by Meyer and Ayres [118]. The anionic nature of the coloured complexes in question was confirmed by simple ion exchange experiments [119].

The first attempt at isolating and determining the structure of the trichlorostannato-rhodium species in solution was made by Davies *et al.* [120]. Using the Job method and visible absorption spectrophotometry, it was shown that the Rh:Sn ratio required for the formation of the red complex was 1:3. This evidence, together with the microanalytical data of the orange-yellow precipitates obtained on addition of tetramethylammonium chloride to their solutions, led them to suggest the formation of the complex below:

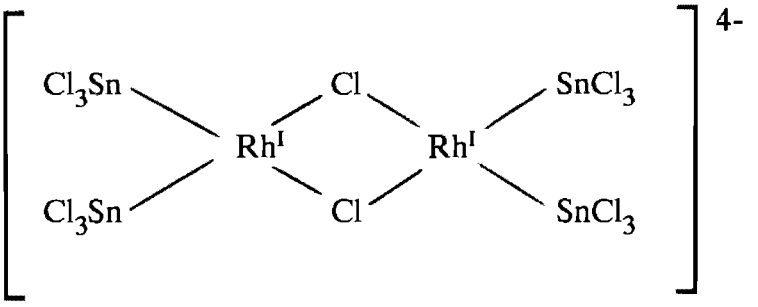

according to the following interaction:

$$2RhCl_3 + 6SnCl_3^- \rightleftharpoons [Rh_2Sn_4Cl_{14}]^{4-} + 2SnCl_5^-$$

Far infrared spectra of the red trichlorostannato-rhodium species reported by Adams and Chandler [121], were consistent with the proposed binuclear $[Rh_2Cl_2(SnCl_3)_4]^{4-}$ complex. The position of bands assigned to M-Cl bond stretching, and their observed shift on halogen substitution, corresponded well with those recorded for the related $[Rh_2Cl_2(COD)_2]$ (COD = cyclooctadiene) complex, which has been shown by x-ray diffraction to have a planar bridge system [122,123].

Subsequent publications have reported uncertainty in the existence of the binuclear rhodium(I) species postulated by Davies *et al.* [120]. Furlani and co-workers [124] found two species in aqueous solution. The red "form" was characterized by absorbance maxima at 470 and 296 nm, and the yellow "form" by maxima at 314 and 420 nm. They also reported an intermediate with a maximum absorbance at 373 nm which disappeared when the red solution had reached equilibrium. The authors mentioned the possibility that the intermediate might be the binuclear species postulated by Davies *et al.*, but stressed that this was purely speculative. Furlani *et al.* concluded that their results did not indicate a binuclear rhodium complex, but that a threefold lower rhodium concentration and a difference in ambient reaction conditions may have influenced the complexes in solution.

The early assignments of the reaction products in the $Rh/SnCl_2/HCl$ system, were usually based on the assumption that rhodium(III) would be reduced to rhodium(I), since tin(II) is easily oxidized to tin(IV). However, the more recent literature report the isolation of a series of six-coordinate rhodium(III) complexes of the type $[Rh(SnCl_3)_nCl_{6-n}]^{3-}$ [125-127].

While assigning the infrared modes of the $[(CH_3)_4N]_3[Rh(SnCl_3)_2Cl_4]$ complex, Kimura [126] noticed that the bands assigned to terminal ν(Rh-Cl) were in the region reported for bridged $\nu(Rh_2Cl_2)$ of the postulated dimer, $[(CH_3)_4N]_4[RhCl(SnCl_3)_2]_2$ [121]. Attempts to synthesize the binuclear salt following the procedure described by Young *et al.* [119] failed and produced only a yellow salt, similar to $[(CH_3)_4N]_3[RhCl_2(SnCl_3)_4]$ in the elemental analysis and the infrared spectrum.

Antonov *et al.* [127] remarked that the Mössbauer parameters for the six-coordinate trichlorostannato(II) complexes of rhodium(III) that they had isolated, were practically the same as the published parameters of the Mössbauer spectra of the trichlorostannato(II) complexes of rhodium(I). Mössbauer spectral evidence indicates that the σ-donor interaction of $SnCl_3^-$ with rhodium(I) is weaker than with rhodium(III) [127]. In addition, the conditions of preparation of the complexes previously published, that is $[Me_4N]_4[RhCl(SnCl_3)_2]_2$ [119,120], $[Me_4N]_3[Rh(SnCl_3)_4]$ [124] and $[Et_4N]_4[Rh(SnCl_3)_5]$ [128], were practically the same as those used by Antonov *et al.*. Hence, these authors [127] assumed that the cited authors [119,120,124,128] were in fact dealing with trichlorostannato(II) complexes of rhodium(III), and not the rhodium(I) complexes.

A recent ^{119}Sn Fourier Transform nmr study by Moriyama *et al.* [129], demonstrated the existence of the six-coordinate $[Rh(SnCl_3)_nCl_{6-n}]^{3-}$ (n = 1-5) as well as a mononuclear rhodium(I) complex associated with five $SnCl_3^-$ ligands. However, Moriyama and co-workers could not find evidence of the binuclear $[RhCl(SnCl_3)_2]_2^{4-}$ complex postulated by Davies *et al.* [120] and they stated: "we now believe non-existence of this dimeric complex, at least in the solution examined by him".

The existence of the binuclear $[RhCl(SnCl_3)_2]_2^{4-}$ dimer remains debatable. Analogous dimers, such as $[RhCl(CO)_2]_2$ [130] are well documented, and since the electronic properties of the carbonyl ligand are very similar to those of the $SnCl_3^-$ ligand [131], non-existence of the dimer would be surprising. It is possible that the $[RhCl(SnCl_3)_2]_2^{4-}$ dimer is short-lived in solution making it difficult to detect and isolate. The intermediate peak in the electronic spectra of the red rhodium-stannous chloride solutions reported by Furlani *et al.* [124] may well be the elusive dimer. In subsequent publications, the dimer was proposed as part of an ion-association formed with crystal violet [132] as well as victoria blue [133] in spectrophotometric determinations of rhodium. Mention of the formation of the dimer was also made in a recent review [134]. However, there seems to be no irrefutable evidence in support of the existence of the $[RhCl(SnCl_3)_2]_2^{4-}$ dimer.

The solution chemistry of rhodium and stannous chloride in hydrochloric acid medium is evidently very complex. Several reaction equilibria seem to exist, and the complexes present in solution apparently depend strongly on a variety of factors. Heating the reaction mixture appears to not only accelerate equilibrium attainment [116], but also to influence the dominant species in solution [126,129]. According to Kimura [126], $[Rh(SnCl_3)_nCl_{6-n}]^{3-}$, with n = 2 and 3, were precipitated from cold

solutions (<5 °C), whereas $[Rh(SnCl_3)_4Cl_2]$ was precipitated from a hot solution. Furlani *et al.* [124], came to the conclusion that the Cl^- : $SnCl_3^-$ ratio, rather than the Sn:Rh ratio, played the major role in determining the species in solution. The solution chemistry of the $Rh/SnCl_2/HCl$ system seems to be a dynamic process and it may take days for an overall equilibrium to be reached. This was revealed by Kimura [126], who reported that ten days at 35 °C was required for the full development of the purple solution from which $M_3[RhSn_5Cl_{15}]$ and $[Rh(NH_3)_6]_3[RhSn_6Cl_{22}]4H_2O$ were isolated. In a kinetic study of the reaction of $[(CH_3)_4N]_3[Rh(SnCl_3)_nCl_{6-n}]$ (n = 2,3,4) with tin(II) in hydrochloric acid, Iwasaki *et al.* [135] identified two independent reaction pathways for the formation of $[Rh(SnCl_3)_5]^{4-}$ (the purple species), a fast and a slow path. The main path was found to be fast, and the reaction orders were reported as 1, 2 and -2 with respect to the total rhodium(III), $SnCl_3^-$ and Cl^- concentrations, respectively.

The various electronic spectra recorded over the years illustrate the diversity of the rhodium-stannous chloride solutions. Table 1.1 is a summary of the absorbance maxima and the solution conditions from which the spectra were produced.

Kimura [126] isolated and recorded the electronic spectra of trichlorostannato-rhodium precipitates, which he had assigned to the complexes $[Rh(SnCl_3)_nCl_{6-n}]^{3-}$ with n = 2, 3 and 4. The absorbance maxima reported, and the solution conditions from which the complexes were precipitated, are summarized in Table 1.2.

TABLE 1.1 A summary of the absorbance maxima of reported electronic spectra and the corresponding solution conditions.

Ref.	$\lambda_{max}1$(nm)	$\lambda_{max}2$(nm)	[HCl] (M)	[Cl]/[$SnCl_2$]	[Sn]/[Rh]	[Rh] (moles.l^{-1})	Colour	Comment
114		480	2	19	5250 - 52500	2×10^{-6} - 2×10^{-5}	red	heated for 0.5 - 1 hour
114		435	0.4	4	5250 - 52500	2×10^{-6} - 2×10^{-5}	yellow	heated for 0.5 - 1 hour
115		470	2	19	500	2×10^{-4}		heated for 1 hour
116	330	475		2 - 20	500 - 5000	4×10^{-5} - 2×10^{-4}	pink/red	boiled for 10 minutes
119	303	425					orange salt	NMe_4^+ salt in 1:1 HCl solution
119		462						HCl solution containing 0.5 M $SnCl_2$
119	310	419						3 M HCl solution with 0.5 M $SnCl_2$
124	374		2	20	500	2×10^{-4}	red	intermediate
124	296	470	2	20	500	2×10^{-4}	red	470 nm stable, 296 nm varies with reaction conditions
124	314	420	12	600	100	2×10^{-4}	yellow	314 varies with reaction conditions
135		470	≤ 3	$[Cl^-] \leq 3.4$ M	$[Sn^{2+}] \leq 0.2$ M	7.5×10^{-5}	purple	assigned to $Rh^I(SnCl_3)_5^{4-}$
136		460	0.25	4	4900	1.3×10^{-5}	rose	after 1 hr at room temperature
136		425	0.25	4	4900	1.3×10^{-5}	yellow	after 2 - 3 days at room temperature
136	285	440	0.25	1 - 42	462 - 19000	1.3×10^{-5}		1 - 24 hrs equilibration
136	290	440	0.5	83	462	1.3×10^{-5}		24 hrs equilibration
136	305	425	0.5	83	462	1.3×10^{-5}		1 hr equilibration
136	305	425	2	333	462	1.3×10^{-5}		1 - 4 hrs equilibration
136	310	425	6	240 - 1000	462 - 1900	1.3×10^{-5}		1 - 24 hrs equilibration
136	315	425	12	2000	462	1.3×10^{-5}		1 - 4 hrs equilibration
136	305		6	24 - 100	4600 - 19200	1.3×10^{-5}		0.2 - 1 hr equilibration
136	315		12	48 - 200	4600 - 19200	1.3×10^{-5}		1 - 24 hrs equilibration
136	295	475	0.5	2	19200	1.3×10^{-5}		4 - 24 hrs equilibration
136	295	475	2	8 - 33	4600 - 19200	1.3×10^{-5}	rose	1 - 24 hrs equilibration
136	300	475	6	24 - 100	4600 - 19200	1.3×10^{-5}	red	4 - 24 hrs equilibration
137		612					red	In a Rh-Pt alloy, in strongly acidic $SnCl_2$ containing solution

Table 1.2. Electronic spectral data for $[(CH_3)_4N]_3[Rh(SnCl_3)_nCl_{6-n}]$ [126].

Complex	$\lambda_{max}1$	$\lambda_{max}2$	Sn:Rh	[HCl]	Conditions	Colour
n=2	323	450	1	3 M	boiled & cooled to -10 ^{o}C overnight	brown
n=3	310	450	3	3 M	boiled & cooled to -5 ^{o}C for 20 hrs.	orange
n=4	310	433	3	3 M	heated for 2 hrs. & filtered hot	yellow

Kimura [126] isolated a violet salt from the aged purple solution containing a Sn:Rh ratio of 7 : 1 in 3 M hydrochloric acid. This salt had a reduction equivalent of 14.0 and was diamagnetic, properties which suggested a new Rh(I) complex containing $SnCl_3^-$. The elemental analysis showed the composition to be $[Rh(NH_3)_6]_3[RhSn_6Cl_{22}]4H_2O$. The author speculated about the possible structure of the rhodium anion and finally suggested that it may be $[Rh(SnCl_3)_5]^{4-}$, analogous to the trigonal bipyramidal Pt(II) anion [138]. Mössbauer spectra of the violet salt indicated coordinated as well as non-coordinated $SnCl_3^-$ ligands.

It was only a year later when Kimura and Sakurai [139] determined the crystal structure of the violet salt, $[Rh(NH_3)_6]_3[Rh(SnCl_3)_4(SnCl_4)][SnCl_6]4H_2O$ and confirmed it to be a trigonal bipyramidal Rh(I) complex. Interestingly the Rh(I) anionic complex contained four coordinated $SnCl_3^-$ ligands and one coordinated $SnCl_4^{2-}$ ligand. Although the coordination of $SnCl_4^{2-}$ to a transition metal might be considered unusual, the crystallographic data are sound [140]. A non-coordinated $SnCl_6^{4-}$ ligand was also present. The three cations were rhodium(III) complexes. The anion can be represented as follows:

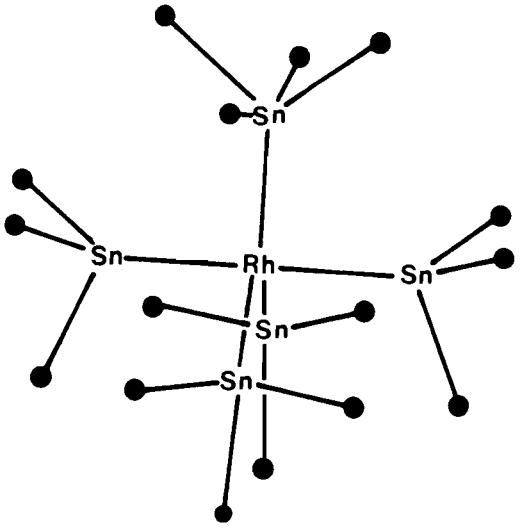

Figure 1.4 Molecular structure of $[Rh(SnCl_3)_4(SnCl_4)]^{5-}$ [139].

The yellow salts that were isolated from the purple solution by Kimura [126], appeared to be five-coordinated rhodium(II) complexes, according to the elemental analysis. However, the fact that they were diamagnetic was inconsistent with this proposed structure. The possibility of the yellow salt being a hydride, that is $M_3[RhH(SnCl_3)_5]$ was also considered. However, the infrared band at 1940 cm^{-1} that could most likely be assigned to ν(Rh-H), did not shift on deuteration of the yellow salt. The salt in question also exhibited "strange features". For example, on dissolution of the salt in concentrated hydrochloric acid, a yellow solution was obtained. However, in 3 M hydrochloric acid, the solution was purple. Increasing the chloride concentration to 12 M by the addition of LiCl did not alter the purple solution.

Krut'ko *et al.* [141] obtained a yellow precipitate from a purple, 3 M hydrochloric acid solution of $RhCl_34H_2O$ (3.6 mmoles) and $SnCl_2$ (42.6 mmoles) using bulky ligands. With the aid of ^{119}Sn and ^1H nmr spectroscopy, supported by elemental analysis, the composition of the yellow salt was found to be $[R_4N]_3[HRh(SnCl_3)_5]$

(R = butyl or ethyl groups). The infrared spectrum of the yellow salt showed ν(Rh-H) at 1940 cm^{-1}.

Krut'ko *et al.* [142] have also studied the reactivity of the above-mentioned rhodium-hydrido complex towards tributyl phosphine, as well as the reaction of one of the resulting products with molecular hydrogen.

6. The Nature of $SnCl_3^-$ as a Ligand

Apart from the effect of varying reaction conditions, the nature of the $SnCl_3^-$ ligand might be expected to influence the formation of the trichlorostannato-rhodium complexes. It has been shown that the $SnCl_3^-$ ligands are usually coordinated to the metal ion through the tin atom [127,134,139,143,]. However, the electronic nature of the trichlorostannato anion and its effect on an octahedral molecule upon coordination is surrounded by some controversy.

By means of ^{19}F nmr shielding parameters of fluorophenyl platinum complexes (where the $SnCl_3^-$ ligand was *trans* to the phenyl group), Parshall [131] showed the trichlorostannato anions to be weak σ-donors and strong π-acceptors. Graham *et al.* [144,145] independently obtained results that supported those of Parshall. Analysis of the carbonyl force constants of $(SnCl_3)Mn(CO)_5$ obtained by the Cotton and Kraihanzel method [146] led them, too, to conclude that the $SnCl_3^-$ group was a poor σ-donor and an excellent π-acceptor. Although the methods used by both Parshall and Graham *et al.* were criticized by Hartley [147], the results were, in general, accepted [126,148-150] and observations were made which were consistent with the above electronic characteristics [126,151].

The σ- and π-bonding characteristics of the $SnCl_3^-$ ligand could have several implications. Firstly, it is thought to result in the *trans* directing behaviour of the trichlorostannato(II) ions. No unanimous agreement has been reached on the best interpretation of the *trans* influence and the *trans* effect [147,152-154], and at present it is likely that no one theory completely accounts for these phenomena. However, there is evidence in support of the π-bonding theory and strong *trans* directors are often good π-acceptors (e.g. CN^-, CO) [152,155,156]. Hence, the d_π-d_π overlap between the transition metals and tin(II) is thought to be responsible for the *trans* activating nature of the $SnCl_3^-$ anion [119,150]. Opinions differ on the extent to which the $SnCl_3^-$ ligand acts as a *trans* directing ligand. Lindsay *et al.* [157] described it as a strongly *trans* directing ligand. These authors assessed the strength of $SnCl_3^-$ as a *trans* directing ligand by using a method described by Chatt and co-workers [158,159] for setting up a *trans* series. The method ranks ligands in terms of their ability to shift the Pt-H infrared stretching frequency and ^1H nmr frequency in *trans*-$[(C_2H_5)_3P]_2PtHX$ compounds. Their results allowed them to place the $SnCl_3^-$ ligand between NCS^- and CN^-, the two most powerful ligands in the Chatt series.

Care should be taken to avoid ambiguity when referring to the *trans* influence and the *trans* effect. The *trans* effect is a kinetic effect and relates to the influence of a coordinated group upon the *rate* of substitution of ligands *trans* to it. In contrast, the thermodynamic concept of the *trans* influence, describes the extent to which that ligand weakens the bond *trans* to it in the equilibrium state of the substrate [152].

Albinati *et al.* [160] studied the effect of the $SnCl_3^-$ ligand on the $^2J(Pt\text{-}CH_3)$ of the complex *trans*-$[Pt(SnCl_3)(CH_3)(PEt_3)_2]$. Their results suggested a moderate *trans* influence for the $SnCl_3^-$ ligand, similar to that of an olefin.

The *trans* influence of the $SnCl_3^-$ is consistent with M-Sn bond lengths in crystal structures of *trans*-$[Pt(SnCl_3)_2(P(OPh)_3)_2]$ [161] and $[N(C_2H_5)_4]_4[Ru(SnCl_3)_5Cl]$ [162]. The Pt-Sn bond length of the former complex falls at the high end of the reported M-Sn bond lengths. The Ru-Cl bond length of the latter compound, in which the chloride is *trans* to a $SnCl_3^-$ ligand, is greater than the range of observed Ru-Cl distances with mutually *trans* chloride ligands.

Most of the reports describing the *trans* effect, involve studies of square-planar Pt(II) complexes. Since the Rh(III) complexes are octahedral, there is some uncertainty about the prominence of the *trans* effect in the substitution reactions involved in the formation of $[Rh(SnCl_3)_nCl_{6-n}]^{3-}$ from $[Rh(H_2O)_{6-n}Cl_n]^{(3-n)+}$ and $SnCl_3^-$. The *trans* effect of a ligand has been described in terms of the stabilization of a trigonal bipyramidal intermediate by a π-accepting ligand [154,155,157]. These arguments cannot simply be extended to octahedral complexes.

An associative mechanism, involving a 7-coordinate intermediate has been postulated for the reaction of $[Rh(NH_3)_5(H_2O)]^{3+}$ with Cl^- or Br^- [152] and the *trans* effect has been reported for metal carbonyl complexes, where the reaction proceeds readily as long as there are carbonyls *trans* to each other [152].

Hartley [147] reported that the principal factor responsible for the *trans* influence in octahedral complexes was the σ-donor ability of the influencing ligand. Any π-acceptor ability of the influencing ligand would reduce the charge density on the metal. As a consequence, the *trans* influence due to σ-donation by the influencing ligand would be opposed. Appleton *et al.* [153] suggested that the *trans* effect appeared to parallel the *trans* influence in octahedral complexes, and ligands with high π-bonding ability did not have strong *trans* effects. These observations are

supported in the case of the carbonyl group in the $[RuHCl(CO)(PMe_2Ph)_3]$ complex [163].

Evidence in support of the *trans* effect of $SnCl_3^-$ being operative in octahedral hydrido and carbonyl-hydrido complexes of iridium containing stannous chloride, was presented by Taylor *et al.* [150]. Accordingly, Antonov [127] may well have been correct in suggesting that solutions having a Sn(II):Rh(III) ratio of 4 : 1 would contain mainly rhodium(III) complexes coordinatively saturated with respect to the $SnCl_3^-$ in the initial stage of the reaction, due to the strong *trans* effect of the $SnCl_3^-$ ligand. In his opinion, a slow redistribution of the $SnCl_3^-$ ligands takes place by reaction of the $[Rh(SnCl_3)_5X]^{3-}$ complexes with the original Rh(III) anions (e.g. $RhCl_6^{3-}$). Although the presence of the *trans* effect cannot be discounted, it can neither be assumed that the *trans* effect will determine the substitution reactions in octahedral complexes.

The *trans* influence has indeed been observed in octahedral complexes [152,162], and one might expect the stability of the isomers in solution to reflect the *trans* influence of the $SnCl_3^-$ anion. Hence, Kimura [125,126] suggested that the *fac*-isomer of the complex $[RhCl_3(SnCl_3)_3]^{3-}$ should be thermodynamically more stable than the *mer*-isomer.

7. Solvent Extraction of Trichlorostannato-Rhodium Complexes from Hydrochloric Acid Medium

Trichlorostannato(II) complexes of rhodium are extractable into oxygen- and nitrogen- containing organic solvents. This extractability has been exploited for the separation of rhodium from iridium using isopentyl alcohol, and the subsequent

determination of rhodium [164]. Furlani *et al.* [124] also extracted rhodium from the $Rh/SnCl_2/HCl/H_2O$ system using isopentyl alcohol and, as did Tertipis and Beamish [164], remarked that the organic extract was yellow. Furlani *et al.* were unable to extract the red species. They ascribed the observed colour change from red in the aqueous phase, to yellow in the organic phase, to a structure change on extraction. Using large amines, they precipitated the yellow species from organic solutions as an impure salt, and postulated an anionic structure to be a square planar Rh(I) species, $[Rh(SnCl_3)_4]^{3-}$.

Khattak and Magee [165] employed high molecular weight amines such as tri-*n*-octylamine dissolved in benzene, for the extraction of trichlorostannato-rhodium complexes. They too, found that the red species existing in the aqueous phase turned yellow on extraction into the organic phase. They reported that the electronic spectrum of the yellow organic phase did not coincide with that of the red aqueous species. When the red aqueous phase was diluted with water to a hydrochloric acid concentration lower than 0.4 M, or in hydrochloric acid concentrations higher than 7 M, the yellow species was formed, showing an absorption maximum at 415 nm. The yellow product in the amine phase was formed on extraction from red aqueous phase as well as from the yellow phase with a hydrochloric acid concentration higher than 7 M, and absorbed to a maximum at 415 nm. The similarity in their electronic spectra suggested that the yellow species in aqueous and organic phases were similar.

Kalinin *et al.* [166] chose *n*-tributyl phosphate for the extraction of trichlorostannato-rhodium complexes, because it is strongly basic and had previously been found to ensure higher distribution coefficients in most cases. They achieved quantitative extraction from 6 M hydrochloric acid solution containing Sn(II):Rh of

5000:1. A high hydrogen ion concentration was found to be more important for extraction than a high chloride ion concentration. Once again, the authors remarked on the colour change on transference of the trichlorostannato- rhodium complex(es) from aqueous to organic phases.

Koch and Wyrley-Birch [167] examined the yellow MIBK phase after solvent extraction from aqueous solution containing Sn(II):Rh(III) ratios of 5-6:1 in 2 M hydrochloric acid, by ^{119}Sn nmr. They found that the predominant species initially present, could best be described as the tetrakis(trichlorostannato)(chloro)rhodium(III)-hydrido anion, $[RhH(SnCl_3)_4Cl]^{3-}$. Furthermore, six-coordinate $[Rh(SnCl_3)_nCl_{6-n}]^{3-}$ (n = 3 and 5) complexes previously found in the aqueous phase by Moriyama *et al.* [129] were also identified in the organic phase. The resonance at $\delta(^{119}Sn)$ = –54,7 ppm was tentatively assigned to $[Rh(SnCl_3)_5]^{2-}$ in which a solvent molecule occupied a vacant coordination site, in accordance with the octahedral geometry normally preferred by rhodium(III).

8. Catalytic Properties of Trichlorostannato-Rhodium Complexes

Stannous chloride complexes of rhodium have been found to catalyze reactions such as dehydrogenation, hydrogen transfer reactions as well as isotopic exchange of hydrogen [168-172].

The dehydrogenation of isopropyl alcohol can be catalyzed by chloro complexes of rhodium(III) [173]. However, as the reaction proceeds, concurrent metal precipitation decreases the rate of dehydrogenation. In a subsequent study [168], it was found that the addition of stannous chloride (with Sn:Rh = 6:1) allowed the reaction to proceed at a steady rate. The authors reported "that $SnCl_3^-$, acting as a

ligand to rhodium, stabilizes the rhodium hydride intermediate against metal formation".

In a preliminary paper, Shinoda *et al.* [170] reported that photo-irradiation of a propan-2-ol solution of the rhodium-stannous chloride catalyst, considerably enhanced the rate of the endothermic dehydrogenation reaction, to produce acetone and hydrogen. The more detailed report followed [171], describing a large decrease in activation energy by photo-irradiation. A mechanism was proposed, assuming the generation of coordinatively unsaturated catalytically active species by the photocleavage of the Rh-Sn coordination bond. The mechanism also assumed the incorporation of a hydride complex in the dehydrogenation cycle. The hydride complex was detected by a change in the spectral pattern on decoupling, both in ^{1}H nmr as well as the ^{119}Sn nmr spectrum. The authors noted that this hydrido complex was not observed in the solution before the reaction.

In a subsequent publication [174], Yamakawa *et al.* reported a complete nmr analysis of the rhodium hydride complex present in the catalyst solution, as well as its iridium analogue. The ^{119}Sn nmr evidence showed the structure to be the octahedral $[RhH(SnCl_3)_5]^{3-}$ species reported by Krut'ko *et al.* [141].

9. Objectives

In the light of the above we aim to:

a) establish the effect of solution conditions on the extraction of trichlorostannato complexes of rhodium from hydrochloric acid media, and so to make possible the choice of optimum sorption conditions.

b) study the nature of the sorption process by a study of the extraction behaviour of a series of soluble model compounds, synthesized to model portions of the polyurethane foam, and

c) determine the nature of the sorbed metal species by instrumental analysis of the soluble model compounds after sorption of the trichlorostannato-rhodium complexes.

REFERENCES

1 E.K.BAUMAN, L.H.GOODSON, G.G.GUILBAULT AND D.N.KRAMER, *Anal. Chem.*, **37** (1965) 1378

2 J.J.VAN VENROOY, U.S. Patent 3,347,020 (1967)

3 H.BRUNSCHWIG, *Liber de Arte Distillandi*, (1512), (See also A.Bittel, Dissertation, Tübingen,1957)

4 E.BAYER, *Gaschromatographie*, 2nd. ed., Springer-Verlag, Heidelberg (1962) 4

5 H.J.M.BOWEN, *J. Chem. Soc.*, **A** (1970) 1082

6 P.SCHILLER AND G.B.COOK, *Anal. Chim. Acta*, **54** (1971) 364

7 S.SUKIMAN, *Radiochem. Radioanal. Letters*, **18** (1974) 129

8 H.D.GESSER, E.BOCK, W.G.BALDWIN, A.CHOW, D.W.MCBRIDE AND W.LIPINSKY, *Separation Science*, **11** (1976) 317

9 H.D.GESSER AND G.A.HORSFALL, *J. Chim. Phys. Phys.-Chim. Biol.*, **74** (1977) 1072

10 T.BRAUN AND A.B.FARAG, *Anal. Chim. Acta*, **98** (1978) 133

11 V.S.K.LO AND A.CHOW, *Anal. Chim. Acta*, **106** (1979) 161

12 J.J.OREN, K.M.GOUGH AND H.D.GESSER, *Can. J. Chem.*, **57** (1979) 2032

13 M.P.MALONEY, G.J.MOODY AND J.D.R.THOMAS, *Analyst*, **105** (1980) 1087

14 R.A.MOORE AND A.CHOW, *Talanta*, **27** (1980) 315

15 S.J.AL-BAZI AND A.CHOW, *Anal. Chem.*, **53** (1981) 1073

16 V.S.K.LO AND A.CHOW, *Talanta*, **28** (1981) 157

17 T.BRAUN AND M.N.ABBAS,
Anal. Chim. Acta, 134 (1982) 321

18 S.J.AL-BAZI AND A. CHOW,
Talanta, **29** (1982) 507

19 A.S.KHAN, W.G.BALDWIN AND A.CHOW,
Anal. Chim. Acta, **146** (1983) 201

20 S.J.AL-BAZI AND A.CHOW,
Anal. Chem., **55** (1983) 1094

21 T.BRAUN AND A.B.FARAG,
Anal. Chim. Acta, **153** (1983) 319

22 S.J.AL-BAZI AND A.CHOW,
Anal. Chim. Acta, **157** (1984) 83

23 A.S.KHAN AND A. CHOW,
Talanta, **31** (1984) 304

24 S.J.AL-BAZI AND A.CHOW,
Talanta, **31** (1984) 189

25 R.CALETKA, R.HAUSBECK AND V.KRIVAN,
Talanta, **33** (1986) 315

26 R.CALETKA, R.HAUSBECK AND V.KRIVAN,
Talanta, **33** (1986) 219

27 L.JIN-CHUN AND A.CHOW,
Talanta, **34** (1987) 331

28 H.D.GESSER, A.CHOW, F.C.DAVIS, J.F.UTHE AND J.REINKE,
Anal. Lettr., **4** (1971) 883

29 K.M.GOUGH AND H.D.GESSER,
J. Chromatogr., **115** (1975) 383

30 A.B.FARAG, H.N.A.HASSAN AND M.H.ABDEL-RAHMAN,
Acta Chimica Hungarica, **124** (1987) 289

31 L.SCHUMACK AND A.CHOW,
Talanta, **34** (1987) 957

32 T.BRAUN AND A.B.FARAG,
Talanta, **19** (1972) 828

33 T.BRAUN AND A.B.FARAG,
Anal. Chim. Acta, **61** (1972) 265

34 T.BRAUN AND A.B.FARAG,
Anal. Chim. Acta, **65** (1973) 115

35 T.BRAUN, L.BAKOS AND Z. SZABÓ,
Anal. Chim. Acta, **66** (1973) 57

36 T.BRAUN AND A.B.FARAG,
Anal. Chim. Acta, **66** (1973) 419

37 T.BRAUN AND A.B.FARAG,
Anal. Chim. Acta, **69** (1974) 85

38 T.BRAUN AND A.B.FARAG,
Anal. Chim. Acta, **71** (1974) 133

39 T.BRAUN AND A.B.FARAG,
Anal. Chim. Acta, **76** (1975) 107

40 G.N.LYPKA, H.D.GESSER, AND A.CHOW,
Anal. Chim. Acta, **78** (1975) 367

41 D.W.LEE AND M.HALMANN,
Anal. Chem., **48** (1976) 2214

42 I.VALENTE AND H.J.M.BOWEN,
Analyst, **102** (1977) 842

43 T.BRAUN, A.B.FARAG AND M.P.MALONEY,
Anal. Chim. Acta, **93** (1977) 191

44 T.BRAUN AND M.N.ABBAS,
Anal. Chim. Acta, **119** (1980) 113

45 A.S.KHAN, W.G.BALDWIN AND A. CHOW,
Can. J. Chem., **59** (1981) 1490

46 T.BRAUN, M.N.ABBAS, L.BAKOS AND A.ELEK,
Anal. Chim. Acta, **131** (1981) 311

47 T.BRAUN, M.N.ABBAS, S.TÖRÖK AND Z.SZÖKEFALVI-NAGY,
Anal. Chim. Acta, **160** (1984) 277

48 T.BRAUN, É.HUSZÁR AND L.BAKOS,
Anal. Chim. Acta, **64** (1973) 77

49 M.P.MALONEY, G.J.MOODY AND J.D.R.THOMAS,
Proc. Analyt. Div. Chem. Soc., (1977) 244

50 M.A.J.MAZURSKI, A.CHOW AND H.D.GESSER,
Anal. Chim. Acta, 65 (1973) 99

51 T.BRAUN, O.BÉKEFFY, I.HAKLITS, K.KÁDÁR AND G.MAJOROS,
Anal. Chim. Acta, **64** (1973) 45

52 T.BRAUN AND A.B.FARAG,
Anal. Chim. Acta, 68 (1974) 119

53 T.BRAUN, J.D.NAVRATIL AND A.B.FARAG,
"Polyurethane Foam Sorbents in Separation Science",
CRC press, Florida, (1985)

54 A.CHOW AND S.L.GINSBERG,
Talanta, **30** (1983) 620

55 R.F.HAMON AND A.CHOW,
Talanta, **31** (1984) 963

56 T.BRAUN AND A.B.FARAG,
Anal. Chim. Acta, **65** (1973) 139

57 T.BRAUN AND Š.PALÁGYI,
Anal. Chem., **51** (1979) 1697

58 B.C.TURNER AND D.E.GLOTFELTY,
Anal. Chem., **49** (1977) 7

59 R.G.LEWIS, A.R.BROWN AND M.D.JACKSON,
Anal. Chem., **49** (1977) 1668

60 C.G.SIMON AND T.F.BIDLEMAN,
Anal. Chem., **51** (1979) 1110

61 N.F.BURDICK AND T.F.BIDLEMAN,
Anal. Chem., **53** (1981) 1926

62 R.G.LEWIS AND M.D.JACKSON,
Anal. Chem., **54** (1982) 594

63 H.SCHNECKO AND O.BIEBER,
Chromatographia, **4** (1971) 109

64 T.BRAUN, A.B.FARAG AND A.KLIMES-SZMIK,
Anal. Chim. Acta, **64** (1973) 71

65 T.BRAUN AND A.B.FARAG,
Anal. Chim. Acta, **73** (1974) 301

66 A.CHOW AND D.BUKSAK,
Can. J. Chem., **53** (1975) 1373

67 T.BRAUN AND A.B.FARAG,
Talanta, **22** (1975) 699

68 T.BRAUN AND A.B.FARAG,
Anal. Chim. Acta, **99** (1978) 1

69 G.J.MOODY AND J.D.R.THOMAS,
Analyst, **104** (1979) 1234

70 G.J.MOODY AND J.D.R.THOMAS,
"Chromatographic Separation and Extraction with Foamed Plastics and Rubbers", (Chromatographic Science **21**), Marcel Dekker, New York (1982)

71 J.H.SAUNDERS AND K.C.FRISCH,
"Polyurethanes: Chemistry and Technology",(High Polymers, **16**(1)) Wiley & Sons, U.S.A., (1983)

72 H.D.GESSER, G.A.HORSFALL, K.M.GOUGH AND B.KRAWCHUK,
Nature, **268** (1977) 323

73 T.SEKINE, Y.ZENIA AND M.NITSU,
Bull. Chem. Soc. (Jpn.), **49** (1976) 2629

74 M.N.ABBAS, A.VÉRTES, AND T.BRAUN,
Radiochem. Radioanal. Lettr., **54** (1982) 17

75 R.F.HAMON, A.S.KHAN AND A.CHOW,
Talanta, **29** (1982) 313

76 S.J.AL-BAZI AND A.CHOW,
Talanta, **30** (1983) 487

77 A.CHAPIRO, M.LAMOTHE AND T.LE DOAN,
Eur. Polym. J., **14** (1978) 647

78 E.SHCHORI AND J.JAGUR-GRODZINSKI,
J. Amer. Chem. Soc., **94** (1972) 7957

79 I.M.KOLTHOFF, W.-J.WANG, M.K.CHANTOONI,
Anal. Chem., **55** (1983) 1202

80 J.JAGUR-GRODZINSKI,
Israel J. Chem., **25** (1985) 39

81 H.-J.BUSCHMANN,
Inorg. Chim. Acta, **118** (1986) 77

82 H.-J.BUSCHMANN,
Polyhedron, **6** (1987) 1469

83 A.S.KHAN AND A.CHOW,
Talanta, **30** (1983) 173

84 C.J.PEDERSEN,
J. Amer. Chem. Soc., **89** (1967) 7017

85 S.YANAGIDA, K.TAKAHASHI AND M.OKAHARA,
Bull. Chem. Soc. (Jpn.), **50** (1977) 1386

86 S.YANAGIDA, K.TAKAHASHI AND M.OKAHARA,
Bull. Chem. Soc. (Jpn.), **51** (1978) 1294

87 H.TADOKORO,
Macromol. Rev., 1 (1967) 119

88 J.L.KOENIG AND A.C.ANGOOD,
J. Polym. Sci., Part A-2, **8** (1970) 1787

89 W.SAENGER, I.-H.SUH AND G.WEBER,
Israel J. Chem., **18** (1979) 253

90 R.IWAMOTO, Y.SAITO, H.ISHIHARA AND H.TADOKORO,
J. Polym. Sci., Part A-2, **6** (1968) 1509

91 M.CESARI, G.PEREGO AND W.MARCONI,
Makromol. Chem., **94** (1966) 194

92 T.SOTOBAYASHI, T.SUZUKI AND K.YAMADA,
Chem. Lett. (Chem Soc. Jpn.), (1976) 77

93 T.SOTOBAYASHI, T.SUZUKI AND S.TONOUCHI,
Chem. Lett. (Chem Soc. Jpn.), (1976) 585

94 C.J.PEDERSEN,
Federation Proceedings, **27** (1968) 1305

95 J.J.CHRISTENSEN, D.J.EATOUGH AND R.M.IZATT,
Chem Rev., **74** (1974) 351

96 W.L.MATTICE,
Marcomolecules, **12** (1979) 944

97 G.J.MOODY, J.D.R.THOMAS AND M.A.YARMO,
Anal. Proc., **20** (1983) 132

98 S.J.AL-BAZI AND A.CHOW,
Talanta, **31** (1984) 431

99 *"Van Nostrand's Scientific Encyclopedia"*,
6th ed., Van Nostrand Reinhold Company, New York, (1983)

100 *"Kirk-Othmer Encyclopedia of Chemical Technology"*,
3rd ed., Wiley-Interscience, New York, (1982)

101 *"Platinum 1988"*, Johnson Matthey Publication, London, (1987)

102 A.DIAMANTATOS,
Anal. Chim. Acta, **131** (1981) 53

103 L.M.GINDIN,
Ion Exch. Solvent Extr., **8** (1981) 311

104 A.WARSHAWSKY,
Sep. Purif. Methods, **12** (1983)1

105 S.J.Al-BAZI AND A.CHOW,
Talanta, **31** (1984) 815

106 K.F.G.BRACKENBURY, L.JONES, I.NEL, K.R.KOCH AND J.M.WYRLEY-BIRCH,
Polyhedron, **6** (1987) 71

107 N.AHMED AND K.R.KOCH,
Anal. Chim. Acta, **162** (1984) 347

108 J.M.WYRLEY-BIRCH,
M.Sc. Thesis, University of Cape Town, (1984)

109 K.R.KOCH AND I.NEL,
Analyst, **110** (1985) 217

110 K.F.G.BRACKENBURY, L.JONES AND K.R.KOCH,
Analyst, **112** (1987) 459

111 L.WOHLER,
Chemiker Ztg., **31** (1907) 938

112 V.N.IVANOV,
J. Russ. Phys.-Chem. Soc., **50** (1918) 460

113 R.D.GARDNER AND A.D.HUES,
Anal. Chem., **31** (1959) 1488

114 E.B.SANDELL,
"Chemical Analysis v3*: Colorimetric Determination of Traces of Metals"*,
Interscience, New York, 2nd. (1950) p523-525

115 A.D.MAYNES AND W.A.E. MCBRYDE,
Analyst, **79** (1954) 230

116 G.H.AYRES, B.L.TUFFLY, J.S.FORRESTER,
Anal. Chem., **27** (1955) 1742

117 S.K.SHUKLA,
D.ès Sc. Thesis, Paris, May 1961

118 A.S.MEYER. AND G.H.AYRES,
J. Amer. Chem. Soc., **77** (1955) 2671

119 J.F.YOUNG, R.D.GILLARD AND G.WILKINSON,
J. Chem. Soc., (1964) 5176

120 A.G.DAVIES, G.WILKINSON AND J.F.YOUNG,
J. Amer. Chem. Soc., **85** (1963) 1692

121 D.M.ADAMS AND P.J.CHANDLER,
Chem. Ind. (London), (1965) 269

122 J.A.IBERS AND R.G.SNYDER,
J. Amer. Chem. Soc., **84** (1962) 495

123 J.A.IBERS AND R.G.SNYDER,
Acta Cryst., **15** (1962) 923

124 C.FURLANI, E.ZINATO AND F.FURLAN,
Atti Accad. Naz. Lincei, Cl. Sci. Fis., Mat. Nat., Rend., **38** (1965) 517

125 T.KIMURA, E.MIKI, K.MIZUMACHI AND T.ISHIMORI,
Chem. Lett. (Chem. Soc. Jpn.), (1976) 1325

126 T.KIMURA,
Sci. Pap. Inst. Phys. Chem. Res. (Jpn.), **73** (1979) 31

127 P.G.ANTONOV, YU.N.KUKUSHKIN, V.I.ANUFRIEV,
L.N.VASIL'EV AND L.V.KONOVALOV,
Russ. J. Inorg. Chem., **24** (1979) 231

128 E.N.YURCHENKO, V.A.VARNEK, G.L.ELIZAROVA,
L.G.MATVIENKO,AND M.S.IOFFE,
Koord. Khim., **1** (1975) 1406

129 H.MORIYAMA, T.AOKI, S.SHINODA AND Y.SAITO,
J. Chem. Soc. (Dalton Trans.), (1981) 639

130 L.F.DAHL, C.MARTELL AND D.L.WAMPLER,
J. Amer. Chem. Soc., **83** (1961) 1761

131 G.W.PARSHALL,
J. Amer. Chem. Soc., **88** (1966) 704

132 M.ZHAO,
Kexue Tongbao (Foreign Lang. Ed.), **31** (1986) 1547, **CA: 106** 148529g

133 W.ZHENG, M.ZHAO, Z.LI,
Yejin Fenxi, **7** (1987) 1 (Chinese), **CA: 109** 162460w

134 M.S.HOLT, W.L.WILSON, J.H.NELSON,
Chem. Rev., **89** (1989) 11

135 S.IWASAKI, T.NAGAI, E.MIKI, K.MIZUMACHI AND T.ISHIMORI,
Bull. Chem. Soc. (Jpn.), **57** (1984) 386

136 S.K.KALININ, K.P.STOLYAROV AND G.A.YAKOVLEVA,
J. Anal. Chem. USSR (Engl. Transl.), **25** (1970) 107

137 Y.YU AND W.LU,
Fenxi Huaxue, **13** (1985) 280, **CA: 104** 45049e

138 J.H.NELSON AND N.W.ALCOCK,
Inorg. Chem., **21** (1982) 1196

139 T.KIMURA AND T.SAKURAI,
J. Solid State Chem., **34** (1980) 369

140 M.NIVEN,
Private Communication

141 D.P.KRUT'KO, A.B.PERMIN, V.S.PETROSYAN AND O.A.REUTOV,
Bull. Acad. Sci. USSR, Div. Chem. Sci. (Engl. Transl.), **12** (1984) 2553

142 D.P.KRUT'KO, A.B.PERMIN, V.S.PETROSYAN AND O.A.REUTOV,
Bull. Acad. Sci. USSR, Div. Chem. Sci. (Engl. Transl.), **4** (1985) 829

143 YU.N.KUKUSHKIN, P.G.ANTONOV, K.I.DUBONOS AND L.V.KONOVALOV,
Russ. J. Inorg. Chem., **18** (1973) 1604

144 W.A.G.GRAHAM,
Inorg. Chem., **7** (1968) 315

145 W.JETZ, P.B.SIMONS, J.A.J.THOMPSON, W.A.G.GRAHAM,
Inorg. Chem., **5** (1966) 2217

146 F.A.COTTON AND C.S.KRAIHANZEL,
J. Amer. Chem. Soc., **84** (1962) 4432

147 F.R.HARTLEY
Chem. Soc. Rev., **2** (1973) 163

148 J.D.DONALDSON,
Progr. Inorg. Chem., **8** (1967) 287

149 J.R.SHAPLEY AND J.A.OSBORN,
Acc. Chem. Res., **6** (1973) 305

150 R.C.TAYLOR, J.F.YOUNG AND G.WILKINSON,
Inorg. Chem., **5** (1966) 20

151 M.KRETSCHMER, P.S.PREGOSIN AND H.RÜEGGER,
J. Organomet. Chem., **241** (1983) 87

152 J.E.HUHEEY
"Inorganic Chemistry", Harper & Row, New York, 2nd ed., (1978)

153 T.G.APPLETON, H.C.CLARK AND L.E.MANZER,
Coord. Chem. Rev., **10** (1973) 335

154 A.V.BABKOV,
Polyhedron, **7** (1988) 1203

155 J.CHATT, L.A.DUNCANSON AND L.M.VENANZI,
J. Chem. Soc., (1955) 4456

156 L.E.ORGEL,
J. Inorg. Nucl. Chem., **2** (1956) 137

157 R.V.LINDSEY, G.W.PARSHALL AND U.G.STOLBERG,
J. Amer. Chem. Soc., **87** (1965) 658

158 J.CHATT, L.A.DUNCANSON AND B.L.SHAW,
Chem. Ind. (London), (1958) 859

159 J.CHATT AND B.L.SHAW,
J. Chem. Soc., (1962) 5075

160 A.ALBINATI, U. VON GUNTEN, P.S.PREGOSIN AND H.J.RUEGG,
J. Organomet. Chem., **295** (1985) 239

161 A.ALBINATI, P.S.PREGOSIN AND H.RÜEGGER,
Inorg. Chem., **23** (1984) 3223

162 L.J.FARRUGIA, B.R.JAMES, C.R.LASSIGNE AND E.J.WELLS,
Can. J. Chem., **60** (1982) 1304

163 M.S.LUPIN AND B.L.SHAW,
J. Chem. Soc., **A** (1968) 741

164 G.G.TERTIPIS AND F.E.BEAMISH,
Anal. Chem., **34** (1962) 623

165 M.A.KHATTAK AND R.J.MAGEE,
Anal. Chim. Acta, **45** (1969) 297

166 S.K.KALININ, G.S.KATYKHIN, M.K.NIKITIN AND G.A.YAKOVLEVA,
J. Anal. Chem. USSR (Engl. Transl.), **25** (1970) 459

167 K.R.KOCH AND J.M.WYRLEY-BIRCH,
Inorg. Chim. Acta, **102** (1985) L5

168 H.B.CHARMAN,
J. Chem. Soc., **B** (1970) 584

169 I.YU.KLINSKAYA, M.B.ROSENKEVICH AND YU.A.SAKHAROVSKII,
Kinet. Catal. (Engl. Transl.), **19** (1978) 258

170 S.SHINODA, H.MORIYAMA, Y.KISE AND Y.SAITO,
J. Chem. Soc. (Chem. Commun.), (1978) 348

171 H.MORIYAMA, T.AOKI, S.SHINODA AND Y.SAITO
J. Chem. Soc. (Perkin (II)), (1982) 369

172 J.KASPAR, R.SPOGLIARICH AND M.GRAZIANI,
J. Organomet. Chem., **231** (1982) 71

173 H.B.CHARMAN,
J. Chem. Soc., **B** (1967) 629

174 T.YAMAKAWA, S.SHINODA, Y.SAITO, H.MORIYAMA AND P.S. PREGOSIN,
Magn. Reson. Chem., **23** (1985) 202

CHAPTER 2

THE EXTRACTION OF TRICHLOROSTANNATO-RHODIUM COMPLEXES BY POLYURETHANE FOAM

Introduction

A detailed study of polyurethane foam as an extractant for trichlorostannato complexes of rhodium, should address several important issues. Firstly, a knowledge of the effect of various factors on the amount of rhodium sorbed per unit mass of polyurethane foam, is imperative. In this regard, one might expect variables such as temperature, the hydrochloric acid concentration and the ratio of tin(II) to rhodium present in the solution, to influence the "efficiency" of polyurethane foam as an extractant of rhodium. Once the effect of these variables on the extraction of rhodium has been established, one would be in the position to suggest suitable conditions for a specific purpose. Hence, one may exploit this knowledge for optimum preconcentration of rhodium from dilute solutions, or for the effective separation of rhodium from other platinum group metals. Another important issue to be addressed is the mechanism by which the trichlorostannato-rhodium species are sorbed by the polyurethane foam. The latter issue is a more difficult one to resolve. Analyzing the effects of solution variables on the extraction of rhodium may assist in gaining insight into the extraction mechanism. Therefore, in this Chapter, we shall concern ourselves with the study of the influence of various factors that may conceivably affect the efficiency with which rhodium is extracted by polyurethane foam.

1. A Brief Description of the Experiments

A commercially available open-cell, flexible polyurethane foam with a density of 0.0244 $g.cm^{-3}$ and which had been produced by polymerization of a trigol with a molecular weight of 3600 {13% poly(ethylene oxide) + 87% poly(propylene oxide) content in random distribution} and an 80:20 ratio of 2,4- and 2,6-toluene diisocyanate was obtained.

Batch experiments were performed using a progression of reaction vessels. These reaction vessels are illustrated and described in more detail in the experimental Section, Chapter 7. Initially, a water-jacketed cylinder which relied on the passage of nitrogen from the bottom inlet to the Bunsen valve outlet at the top for the constant agitation of the solution was used. This apparatus, which we shall refer to as Apparatus A, gave the following problems. A drop in the nitrogen pressure occasionally occurred, leading to an undesirable loss of solution through the sintered glass disc. In addition, this apparatus did not provide for sufficient "wetting" of the initially hydrophobic foam and consequently optimum foam-solution contact was not achieved.

An improved reaction vessel, referred to as Apparatus B, was designed. This consisted of a flat bottomed water-jacketed reaction vessel, for which the nitrogen inlet and outlet were contained in a rubber bung fitted to the top of the vessel. The solution was agitated by a magnetic stirrer. The reaction vessel was connected to a peristaltic pump which forced solution, as well as the small foam pieces, to regularly pass through the rollers of the peristaltic pump. In this way, regular squeezing of the foam occurred, yielding optimized foam-solution contact.

Although Apparatus B worked well, it allowed for the performance of a single experiment at any one time. Since each experiment spanned a considerable number of hours, collecting a series of data was very time consuming. Therefore, we resorted to batch experiments involving a series of stoppered bottles, shaken together in a waterbath equipped with a thermostat. This latter reaction vessel will be referred to as Apparatus C. When using Apparatus C, the polyurethane foam pieces were made less hydrophobic by swelling the material with a small quantity of

ethanol (the excess ethanol was removed by squeezing the foam between filter paper).

In the following discussion, the results are not necessarily reported in the chronological order in which the experiments were performed. Therefore, the apparatus used to obtain each set of results will be specified.

Briefly, the following experimental procedure was adopted. An aliquot of 1 ml of the bulk solution was withdrawn from the reaction vessel before foam addition, while the change in rhodium concentration was monitored by sampling the solution at selected intervals during the extraction process. After analysis by means of atomic absorption spectroscopy the quantity of rhodium and tin sorbed by the foam, was calculated by difference. All experiments were performed in a nitrogen atmosphere, to prevent the oxidation of tin(II) as far as possible.

For presentation of the results of the studies below, the following quantities were used. The percentage extraction, %E, refers to the percentage of the total amount of rhodium that had been extracted by the polyurethane foam from solution. A very useful quantity, $\mathbf{D'_m}$, represents the amount of rhodium sorbed per unit mass of foam in $mmol.g^{-1}$. In an extraction curve of $\mathbf{D'_m}$ versus time, the limiting value for $\mathbf{D'_m}$ is the maximum capacity, **C**, of the foam for rhodium under the relevant extraction conditions.

2. The Effect of Solution Conditions

2.1. The Role of Stannous Chloride in the Extraction of Rhodium

In the absence of stannous chloride, only a small amount of rhodium is sorbed by the foam. At room temperature less than 4.7% of the rhodium was extracted by 0.192 g of foam from a 2 M hydrochloric acid solution containing 76.41 $\mu g.ml^{-1}$ rhodium(III). The lack of affinity exhibited by the foam for the aquo-chloro complexes of rhodium(III), $[RhCl_n(H_2O)_{6-n}]^{(3-n)+}$ was reflected by the negligible change in the elemental (C, H, N) composition (by mass) of the foam after its exposure to the above-mentioned rhodium solution. The results of the elemental analysis were as follows:

	%C	%H	%N
Before exposure to the rhodium solution	61.15	8.9	4.85
After exposure to the rhodium solution	60.6	8.9	4.7

Addition of stannous chloride to a hydrochloric acid solution containing rhodium, dramatically enhanced the amount of rhodium extracted by the foam. A Sn:Rh ratio of 10:1 resulted in the extraction of 82.5% of the total amount of rhodium by 0.147 g of foam. Elemental analysis of the foam after extraction showed a significant drop in the weight percentage of carbon, hydrogen and nitrogen of the loaded foam, as shown below.

	%C	%H	%N
Before extraction	61.15	8.9	4.85
After extraction	40.6	6.2	3.15

It is evident that complexation of rhodium by trichlorostannato ligands, results in the formation of extractable rhodium species. Polyether type polyurethane foam, therefore, extracts anionic complexes with a certain degree of selectivity. Since polyurethane foam can be viewed as a type of "solid organic phase", the hydrophobicity of the anion might be expected to be a major criterion in determining the extractability of an anion. The larger $[Rh(SnCl_3)_nCl_{6-n}]^{3-}$ anions should certainly be more hydrophobic than the $[RhCl_n(H_2O)_{6-n}]^{+3-n}$ ions, which is reflected by the considerably higher extractability of the $[Rh(SnCl_3)_nCl_{6-n}]^{3-}$ anions.

2.2 The Effect of Varying Sn:Rh Ratios

Wyrley-Birch [1] concluded from a UV-visible spectrophotometric study of hydrochloric acid solutions of stannous chloride and rhodium, that a period of 16 hours was required to reach an apparent steady state. Hence, in this study of the effect of varying Sn:Rh ratios in the aqueous phase on the amount of rhodium extracted by polyurethane foam a 16 hour equilibration period was allowed before foam addition to the bulk solution. Using Apparatus A at room temperature polyurethane foam portions of a known mass (~ 0.15 g) were exposed to 100 ml of a 2 M hydrochloric acid solution containing 75 $\mu g.ml^{-1}$ rhodium and Sn:Rh ratios varying from 3:1 to 25:1.

Extraction was monitored with time. The rate of extraction was found to be slow, with the time required for maximum extraction increasing with increased Sn:Rh ratio. The maximum capacity, C, constituted a maximum in the extraction curve of D'_m versus time, after which some desorption occurred in the solutions with higher Sn:Rh ratios. The reasons for desorption are not clear. Possibly, slow oxidation of tin(II) occurred despite a constant nitrogen atmosphere. On the other hand,

trichlorostannato complexes of rhodium have been found to be kinetically labile [2]. Therefore, it is possible that after extraction, the chloro(trichlorostannato)-rhodium complexes reacted further within the foam phase to form species that were less favoured by the polyurethane foam.

The colour of the aqueous phases ranged from a bright yellow at a Sn:Rh ratio of 3:1 to a dark rust-red at 25:1. After extraction, the aqueous phases with low Sn:Rh ratios were pink, while the solutions with large excesses of tin(II) were bright yellow. The foam assumed a dark orange yellow colour after exposure to aqueous phases with low Sn:Rh ratios and a bright yellow colour after exposure to high Sn:Rh ratios.

Increasing the initial Sn:Rh ratios of the aqueous phase resulted in a steady increase in the amount of rhodium extracted by polyurethane foam. Further, an increase in the Sn:Rh ratio present on the foam after extraction was observed with an increase in the initial Sn:Rh ratios in the aqueous phase. The latter may indicate a higher extractability of rhodium species with a higher number of coordinated $SnCl_3^-$ ligands. The $[Rh(SnCl_3)_nCl_{6-n}]^{3-}$ species with higher values for n are larger and might be expected to be more hydrophobic, and in general to show a higher tendency to be extracted by organic phases. Tin(II) and rhodium were coextracted by polyurethane foam in the following ratios:

aqueous Sn:Rh ratio	3:1	6:1	10:1	15:1	20:1	25:1
ratios in which Sn and Rh are coextracted by polyurethane foam	3.1:1	3.6:1	4.2:1	5.3:1	5.4:1	4.5:1

It is evident that the ratios in which Sn and Rh are coextracted do not approach the value of an integer. It may thus be concluded that a distribution of species is sorbed

rather than a single complex anion. The results are summarized graphically in Figure 2.1.

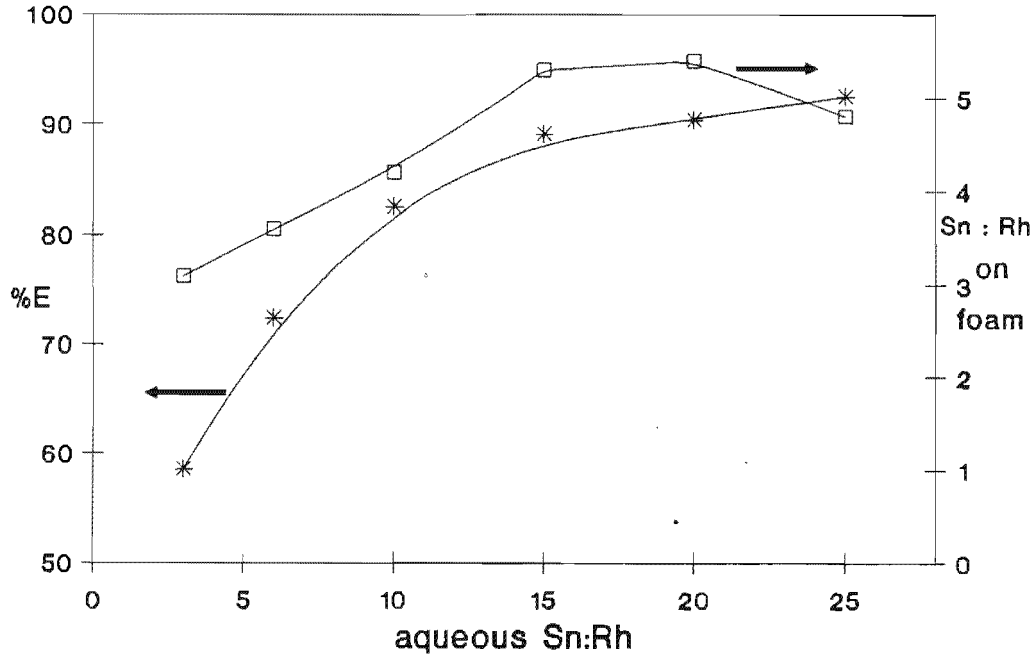

Figure 2.1 The effect of aqueous Sn:Rh ratios on the percentage extraction, %E, and on the ratios of Sn:Rh extracted by polyurethane foam. [HCl] = 2 M, [Rh] = 75 $\mu g.ml^{-1}$, mass of foam ~0.15 g.

In a similar study of the extraction of trichlorostannato complexes of platinum(II) [3,4], it was found that an increase in the initial Sn:Pt ratios of the aqueous phase, increased the amount of platinum extracted to a maximum value. A further increase in aqueous Sn:Pt ratios resulted in a decrease in extraction, to a limiting value, after which a steady level of platinum extraction was maintained.

In the above study of rhodium-extraction, no decrease had been observed in the amount of rhodium extracted with an increase in aqueous Sn:Rh ratios and we were interested in testing a larger range of Sn:Rh ratios. Hence, the study was repeated using Apparatus C, and the Sn:Rh ratios were varied from 3:1 to 200:1. The

extractions were performed at 40 °C using polyurethane foam portions of known mass of 0.0790 ± 0.0001g. The aqueous phase contained 2 M hydrochloric acid and an initial rhodium concentration of 75 $\mu g.ml^{-1}$. In a separate study discussed in Section 2.3 of this Chapter, the effect of the time allowed for equilibration of the aqueous phase prior to extraction was tested. No significant difference was found in the extent and the rate of rhodium-sorption between solutions that had not been allowed to equilibrate and those that had reached the apparent steady state equilibrium after 16 hours [1]. Hence, the equilibration of the aqueous phase was reduced to a period of 1 hour at 40 °C prior to extraction.

This experiment confirmed the steady increase in the extraction efficiency of polyurethane foam with increasing aqueous Sn:Rh ratios. Even with a Sn:Rh ratio of 200:1 no decrease in the amount of rhodium extracted by the foam was observed. The results of this study are illustrated in Figure 2.2. The UV-visible spectra of the solutions were recorded after extraction and the observed peak maxima are shown in Table 2.1.

Table 2.1 The peak maxima of the electronic spectra observed in the remaining aqueous phases after extraction.

aqueous Sn:Rh ratio	λ_{max} (nm)
3:1	~317, 475^{broad}
6:1	~300, 428
10:1	~300, 419
15:1	~300, 419
20:1	~300, 419
50:1	~300, 469
200:1	~300, 473

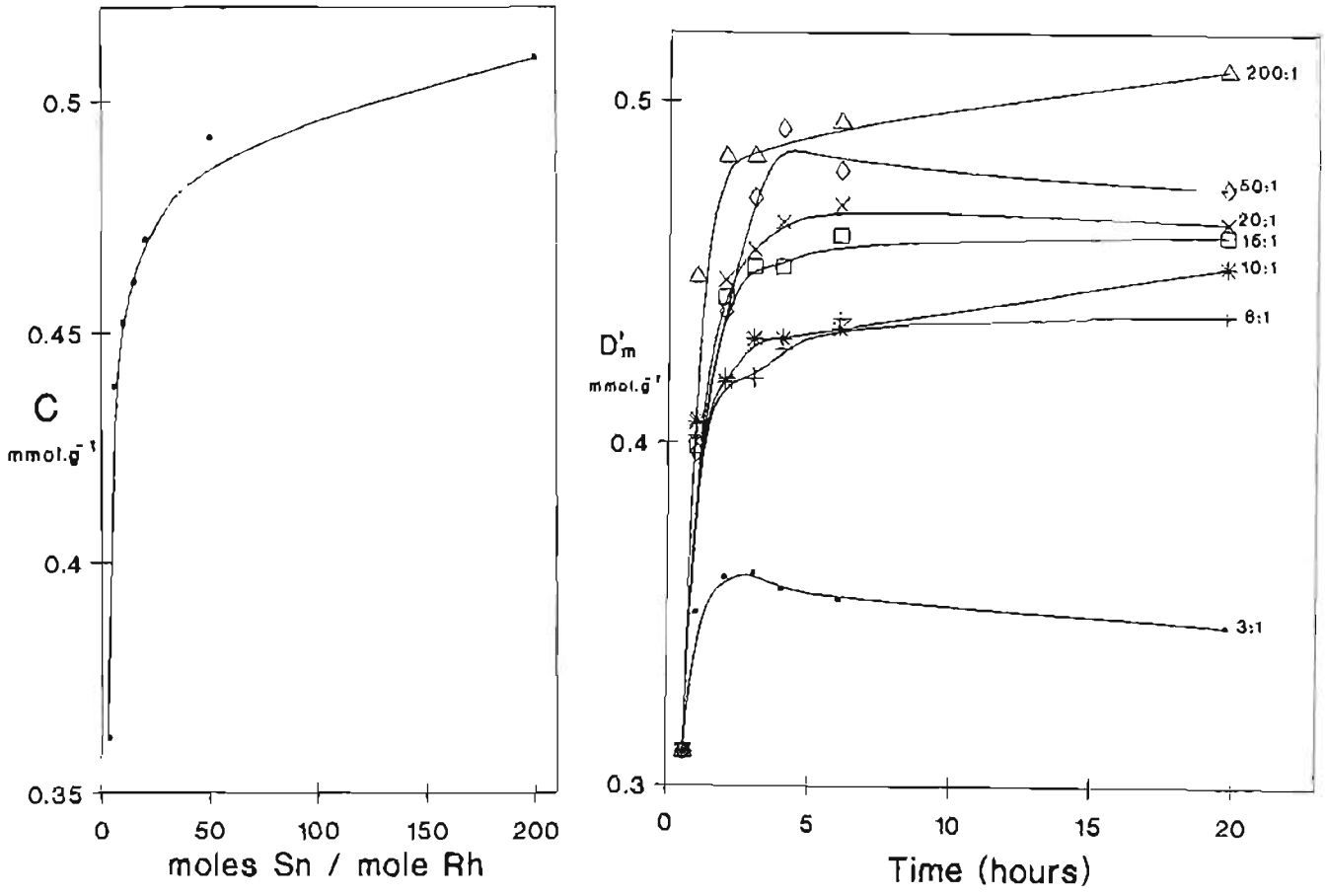

Figure 2.2 The effect of the Sn:Rh ratio in the aqueous phase on the distribution of rhodium between foam and 2 M HCl at 40 °C. [Rh] = 75 $\mu g.ml^{-1}$, 79 mg of foam.

Increased stannous chloride concentration should exert a definite influence on the nature of the trichlorostannato-rhodium complexes in solution. Thus increased Sn:Rh ratios in the aqueous phase, together with decreased Cl^-:$SnCl_2$ ratios, might be expected to favour octahedral complexes of the type $[Rh(SnCl_3)_nCl_{6-n}]^{3-}$ with larger values for n. In addition, the rate of formation of the purple trigonal bipyramidal Rh(I) complex, $[Rh(SnCl_3)_5]^{4-}$, has been found to be proportional to $[Rh][SnCl_3^-]^2[Cl^-]^{-2}$ [2]. Therefore, it is reasonable to expect that the favourable influence of high Sn:Rh ratios in the aqueous phase on the amount of rhodium sorbed by polyurethane foam is due mainly to the effect of higher $SnCl_3^-$ concentrations on the nature and the distribution of the chloro(trichlorostannato)-rhodium complexes present in solution at the time of extraction. This is borne out

by the higher Sn:Rh ratios determined for the species on the foam. A study of sorption of tin(II) in 2 M hydrochloric acid revealed that tin(II) was not significantly sorbed under these conditions. Hence, it may be concluded with reasonable certainty that all the tin(II) extracted is likely to be associated with rhodium, presumably as the $SnCl_3^-$ ligand. These results suggest that rhodium complexes with a larger number of coordinated $SnCl_3^-$ ligands are more readily extracted by the foam phase.

2.3 The Effect of the Equilibration of the Aqueous Phase

In view of the slow rate of equilibration observed by Wyrley-Birch [1], a 16 hour equilibration period was applied to the aqueous phases in previous experiments. However, this long equilibration period was experimentally tedious and time consuming. It was thus decided to test the effect of a 16 hour equilibration period on the extraction of rhodium. Duplicate experiments were performed with and without equilibration of the aqueous phase. Portions of 0.0791 ± 0.0002 g of the polyurethane foam were exposed to 2 M hydrochloric acid solutions containing 75 $\mu g.ml^{-1}$ rhodium and aqueous Sn:Rh ratios of 6:1. The study was performed at temperatures of 25 ± 0.2 °C and 40 ± 0.2 °C.

It is evident from Figure 2.3, that the difference in the rate and extent of sorption is negligible within an acceptable range of experimental error. Therefore, the sorption of rhodium appears not to depend markedly on the rate at which the various equilibria involving the chloro(trichlorostannato)-rhodium complexes are established. On this basis, it was considered reasonable to reduce the long equilibration time to between 30 minutes and 1 hour when carrying out further experimentation.

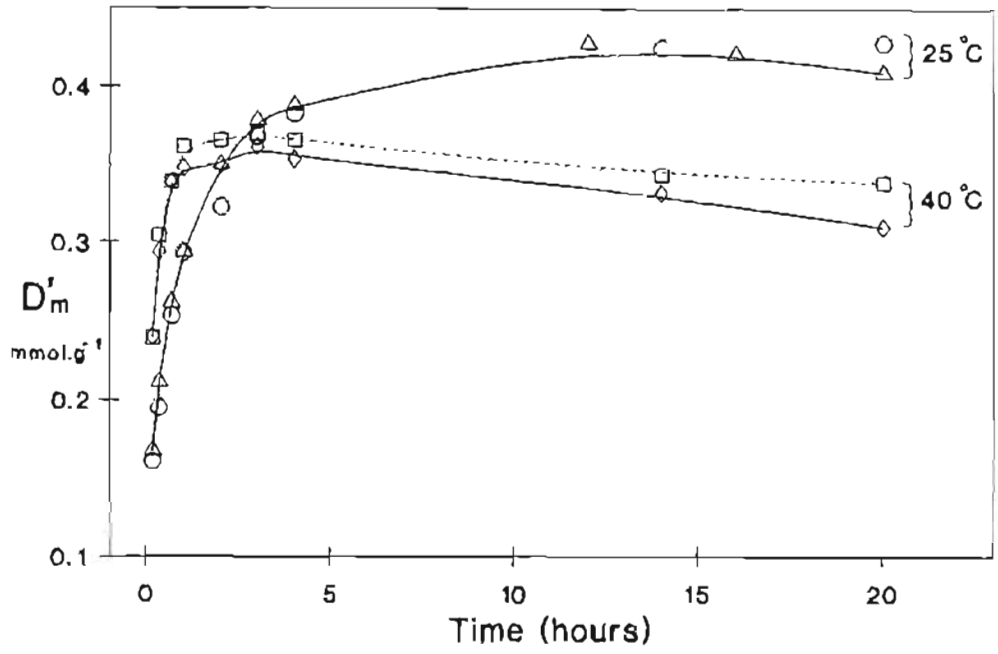

Figure 2.3 The effect of equilibration of the aqueous phase on sorption at T = 25 °C and 40 °C. [HCl] = 2M, aqueous Sn:Rh = 6:1, 79 mg of foam. (Δ , □ = no equilibration time, O ,◊ = 16 hour equilibration period.)

2.4 A Study of Reproducibility

In order to establish the reproducibility of the results obtained in the extraction experiments, extractions were monitored with time under identical conditions, from volumes of 150 ml and 200 ml of aqueous phase using Apparatus B ([HCl] = 4 mol.dm^{-3}, aqueous Sn:Rh = 6:1, temperature = 35 ± 0.5 °C, mass of foam = 0.0792 ± 0.0001g, equilibration period of 30 minutes). The values obtained for D'_m were compared to values that had been obtained previously for 100 ml of aqueous phase under similar conditions. A mean value for D'_m, as well as the standard deviation (s) and coefficient of variation (COV) were calculated. The results are shown in Table 2.2.

A reasonable reproducibility was achieved, with the COV ≤ 4.16%. A COV of 4% should be a reasonable estimate of the worst error, irrespective of the apparatus

used. The main sources of error are likely to be the transference of measured volumes of solution, dilutions, and calibration of the atomic absorption analysis process.

Table 2.2 Comparison of D'_m values observed for 3 separate experiments, for a reproducibility check.

	D'_m			mean D'_m		
time (hours)	100 ml aqueous phase	150 ml aqueous phase	200 ml aqueous phase		s	COV(%)
0.167	0.339	0.324	0.312	0.325	0.014	4.16
0.333	0.392	0.374	0.373	0.380	0.011	2.81
0.667	0.436	0.435	0.438	0.436	0.002	0.35
1.0	0.457	0.467	0.440	0.455	0.014	3.00
2.0	0.510	0.512	0.530	0.517	0.011	2.13
3.0	0.521	0.525	0.551	0.532	0.016	3.06
4.0	0.524	0.531	0.547	0.534	0.012	2.21
4.9	------	0.542	0.540	0.541	0.001	0.26
6.0	0.500	------	------	------	------	-----

2.5 The Effect of Temperature

Using Apparatus A, portions of 0.0792 ± 0.0002 g of foam were exposed to 100 ml of 2 M hydrochloric acid solution containing 75 $\mu g.ml^{-1}$ rhodium and an initial aqueous Sn:Rh ratio of 6:1, after the solution had been equilibrated at the desired temperature for 30 minutes. Figure 2.4 illustrates the effect of temperature on the sorption of rhodium.

It was found that elevated temperatures accelerated the initial rate of sorption, as well as the eventual desorption process previously observed. Furthermore, the

maximum capacity of the foam, C, decreases with increasing temperature, as is shown in Figure 2.5.

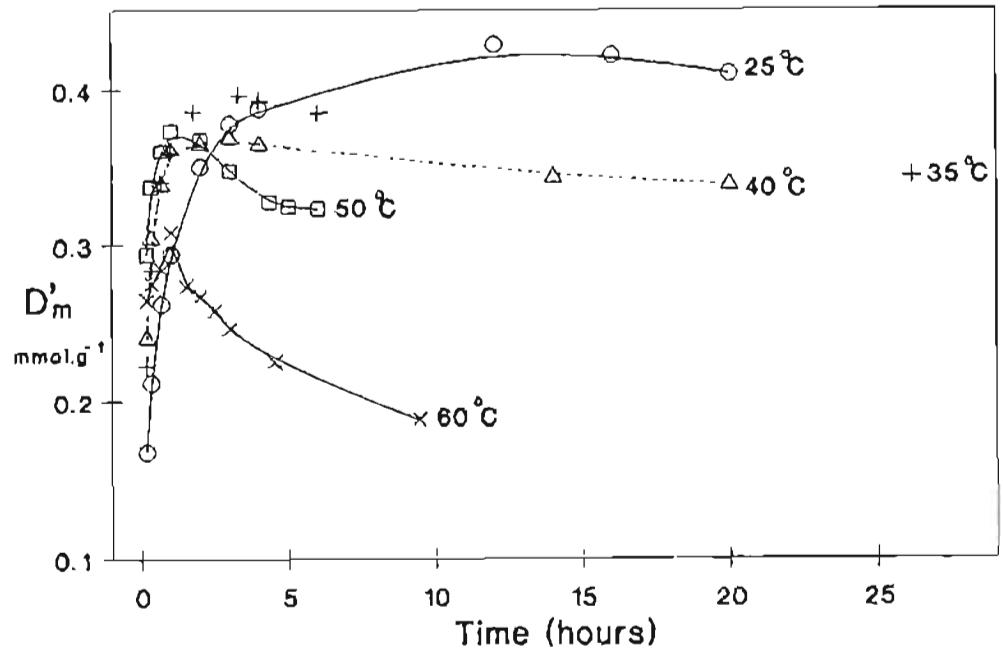

Figure 2.4 The effect of temperature on the distribution of chloro(trichlorostannato) complexes of rhodium between a 2 M hydrochloric acid solution and polyurethane foam (79 mg). Aqueous Sn:Rh = 6:1, 75 $\mu g.ml^{-1}$ rhodium.

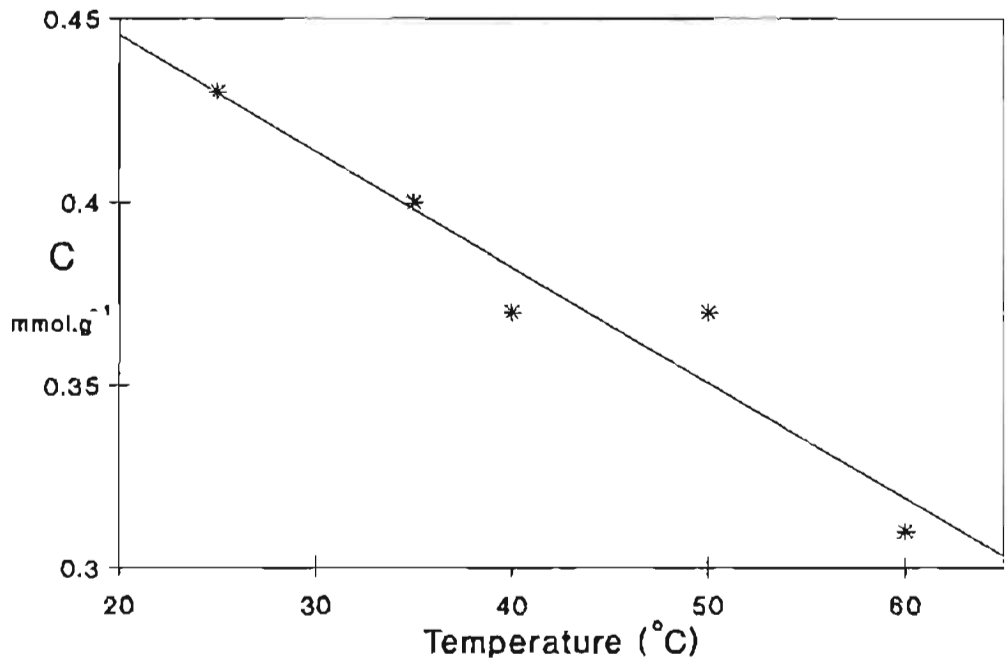

Figure 2.5 The effect of temperature on the maximum capacity. [HCl] = 2 M, aqueous Sn:Rh = 6:1, 79 mg of foam, 75 $\mu g.ml^{-1}$ rhodium.

The following series of partition equilibria are suggested to exist, each being influenced individually by temperature.

$$[Rh^{III}(SnCl_3)_nCl_{6-n}]^{3-}_{aq} \underset{}{\overset{K_{Di}}{\rightleftharpoons}} [Rh^{III}(SnCl_3)_nCl_{6-n}]^{3-}_{f} \qquad (1)$$

$$[Rh^{I}(SnCl_3)_5]^{4-}_{aq} \underset{}{\overset{K_{D7}}{\rightleftharpoons}} [Rh^{I}(SnCl_3)_5]^{4-}_{f} \qquad (2)$$

n = 1 to 6 and i assumes the same numerical value as n.

The subscripts aq and f indicate the aqueous and foam phases respectively.

A thermodynamic treatment of solvent extraction principles allows the derivation of equation 3 [5].

$$\frac{(a_A)_1}{(a_A)_2} = \exp \frac{\Delta U^o_A}{RT} = K^o_D \qquad (3)$$

therefore $\ln K^o_D = \Delta U^o_A / RT$ (4)

and $\ln K^o_D \propto 1/T$ (5)

where the subscripts 1 and 2 distinguish two immiscible liquids,

a_A = activity of solute A

ΔU^o_A = the difference in the constant U^o_A in solvents 1 and 2

R = gas constant

T = absolute temperature

K^o_D = the partition coefficient.

This equation implies a decrease in K°_{D} with increased temperature. Therefore, if sorption by polyurethane foam were governed by a solvent extraction mechanism a decrease could be expected in the amount of rhodium extracted by the foam with an increase in temperature. A similar trend may be predicted for any other mechanism according to the van't Hoff equation for chemical equilibria (see reaction 6) [6].

$$\log K = -(\Delta H^{\circ}/2.303RT) + \text{constant} \qquad (6)$$

where, K = reaction constant

ΔH° = heat of reaction

R = gas constant

T = absolute temperature.

According to the van't Hoff equation, $\log K \propto 1/T$ for a spontaneous, or exothermic, partition reaction ($\Delta H^{\circ} < 0$). An increase in temperature, therefore, would favour the endothermic reverse reaction, that is, the desorption reaction, and would result in the extraction of a smaller amount of rhodium by polyurethane foam.

Temperature has been found to influence the structure of the predominant chloro(trichlorostannato)-rhodium complexes present in solution [7,8]. Hence, Kimura reported the isolation of $[R_4N]_3[Rh(SnCl_3)_4Cl_2]$ from a hot solution, while the complex $[R_4N_3]_3[Rh(SnCl_3)_3Cl_3]$ was precipitated from a solution that had been cooled to -5 $^{\circ}$C for 20 hours [7]. The findings of Kimura were supported by those of Moriyama *et al.* [8], who found that the ^{119}Sn nmr signal of $[Rh(SnCl_3)_4Cl_2]^{3-}$ became large at 75 $^{\circ}$C, and decreased again upon cooling the probe to room temperature. If higher temperatures favoured the formation of species for which the foam had a smaller affinity, then the effect may also be manifested in a lower extraction efficiency.

Although elevated temperatures accelerate the initial rate of sorption, a period of one hour was required for maximum sorption, even at 60 °C. The latter phenomenon suggests that diffusion of the rhodium complexes through the polyurethane foam material plays a part in the rate determining step. Hence, an increase in temperature should increase the rate of diffusion, resulting in an increased rate of sorption.

An overall equilibrium of all the reactions involved in the distribution of the trichlorostannato-rhodium complexes between the aqueous solutions and polyurethane foam has apparently not been attained in the present system, since a steady value for D'_m is not reached. According to the van't Hoff equation (see reaction 6), a plot of log K versus 1/T should yield a linear relationship for a chemical reaction at equilibrium. In an attempt to apply the van't Hoff equation to our system the value of

$$K' = \frac{[Rh] \text{ on foam}}{[Rh] \text{ left in aqueous phase}}$$

was taken to be proportional to an overall reaction constant. The value for K' was calculated at maximum extraction, and plotted as a function of 1/T, see Figure 2.6.

At higher temperatures the curve appears linear, but severe deviation from linearity occurs at temperatures below 40 °C. This suggests that one cannot view the sorption process in terms of a simple overall equilibrium constant, and that kinetic factors such as diffusion plays a significant role, especially at lower temperatures.

The effect of temperature on the sorption of rhodium by polyurethane foam can not easily be rationalized, and an arbitrary optimum temperature was chosen purely for

practical reasons. Hence it was decided to perform the remainder of the experiments at 35 °C and 40 °C since at these temperatures the rate of desorption was slow, while the rate of sorption was considerably higher than that at 25 °C.

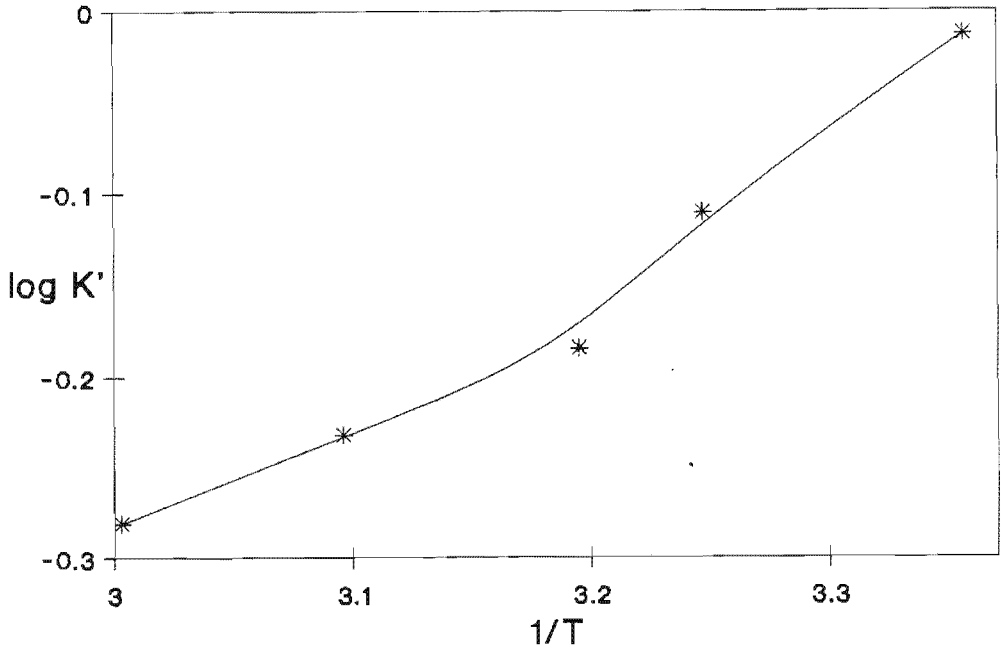

Figure 2.6 A plot of the relationship between log K' versus 1/T for the extraction of 75 $\mu g.ml^{-1}$ rhodium from 2 M hydrochloric acid solution (Sn:Rh = 6:1).

2.6 The Effect of Hydrochloric Acid Concentration

The effect of the concentration of hydrochloric acid on extraction was investigated at 34 ± 0.5 °C using Apparatus B. After a 30 minute equilibration period of the acidic aqueous phase containing 75 $\mu g.ml^{-1}$ rhodium and an initial Sn:Rh ratio of 6:1, portions of 0.0792 ± 0.0002 g of polyurethane foam were exposed to 100 ml of aqueous solution. The hydrochloric acid concentration was varied from 0.5 to 5.0 $mol.dm^{-3}$. (Bowen [9] had investigated the inertness of polyurethane foam, and had found the foam to remain unaltered by hydrochloric acid up to a concentration of 6 $mol.dm^{-3}$.)

A steady increase in the maximum foam capacity from a relatively low 0.36 mmol.g^{-1} at 0.5 M hydrochloric acid to a high value of 0.56 mmol.g^{-1} in 5.0 M hydrochloric acid, is illustrated in Figure 2.7. In addition, the figure shows a decrease in the Sn:Rh ratio in the foam phase with increasing hydrochloric acid concentration. The average Sn:Rh ratios determined for the sorbed species varied from 4.5:1 at 0.5 M hydrochloric acid to 3.4:1 at 5 M hydrochloric acid.

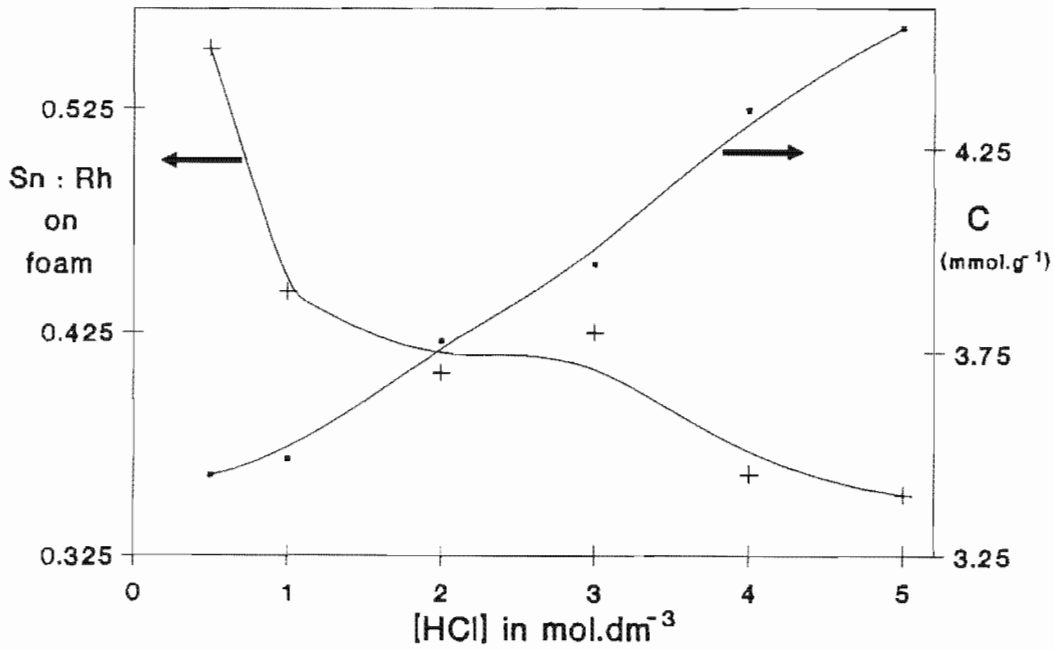

Figure 2.7 The influence of the hydrochloric acid concentration on the value of C and the Sn:Rh ratio of the species sorbed by the foam. (T = 34 °C, aqueous Sn:Rh = 6:1, 75 μg.ml^{-1} rhodium, 79 mg foam.)

Since in the present study the ionic strength of the solution was not kept constant, an explanation of the trend of increased extraction with increased hydrochloric acid concentration ought not to ignore the effect of ionic strength. Increased ionic strength is known to promote extraction in liquid-liquid extraction systems by decreasing the activity of the water and so decreasing the solvating power of the water [5]. If ionic strength were solely responsible for the steady increase in extraction observed with increased hydrochloric acid concentration, a similar trend would be

expected for the extraction from related systems. Brackenbury [10] investigated the extraction of platinum from hydrochloric acid solutions containing stannous chloride, and found extraction to reach a maximum at 0.8 M hydrochloric acid, after which extraction decreased with increasing concentrations. Therefore, factors other than ionic strength must be considered responsible for the observed increase in extraction with increased hydrochloric acid concentration of the present study.

It is not certain whether the increase in the amount of rhodium extracted with increased hydrochloric acid concentrations is due mainly to the activity of the hydronium ions, or due mainly to the activity of the chloride ions. Increased chloride ion concentration should increase the amounts of $SnCl_4^{2-}$ at the expense of the $SnCl_3^-$ concentration in solution, and perhaps lead to the increased extraction of the chloro complexes of tin(II). It was observed by Brackenbury [10] that although negligible amounts of tin(II) was extracted from 2 M hydrochloric acid solutions, approximately 6.4% (1.5 mg) of the total tin(II) was extracted from 4 M hydrochloric acid solutions. However, competitive sorption of the chloro-tin(II) species would be expected to result in a decreased rhodium-extraction as well as an increased ratio of Sn:Rh on the foam, which was not observed. Lower concentrations of $SnCl_3^-$ with respect to chloride ions should result in a higher proportion of $[Rh(SnCl_3)_nCl_{6-n}]^{3-}$complexes with lower values for n. For solutions containing higher hydrochloric acid concentrations, the lower Sn:Rh ratios estimated for the species on the foam, could be construed to be evidence in favour of such an effect. By such reasoning one might suggest that the foam material has a higher affinity for chloro(trichlorostannato)-rhodium complexes, $[Rh(SnCl_3)_nCl_{6-n}]^{3-}$, with lower values for n. Such an idea is in direct contradiction to the observations made in Section 2.2, where increased aqueous Sn:Rh ratios resulted in a considerable increase in extraction and in an increase in the Sn:Rh ratios of the species sorbed by the foam phase. It, therefore, seems that the overall effect of the

hydrochloric acid concentration is due mainly to the activity of the hydronium ions in solution. If a solvent extraction mechanism is predominant, an increased hydronium ion concentration would favour the formation of extractable species such as $H_3[Rh(SnCl_3)_nCl_{6-n}]$. An increase in the hydronium ion concentration would also favour extraction in terms of the cation chelation mechanism (increased chelation of H_3O^+ ions) as well as favouring a mechanism whereby extraction of anions is facilitated by protonation of the donor oxygen and nitrogen atoms.

2.7 The Effect of Alkali Metals

According to the proposal of the CCM (see Chapter 1, Section 3.5) made by Hamon *et al.* [11], cations are chelated by polyether portions of the polyurethane foam, thus creating cationic sites that facilitate the extraction of anions. The size of the cation was thought to play a major role in the relative affinity of the foam for a specific cation. A relatively high affinity for K^+ cations was observed [11], which was suggested to be due to the stability of the 18-membered spiral of poly(ethylene oxide) chains (as compared with the preferential chelation of K^+ by 18-crown-6).

Sorption experiments were carried out in the presence of Li^+, Na^+ and K^+ ions in order to establish the significance of the CCM in the extraction of chloro(trichlorostannato)-rhodium complexes. The order of increasing affinity of polyurethane foam for these cations in the presence of a constant anionic counter ion was found by Hamon *et al.* [11] to be $Li^+ < Na^+ < K^+$.

A preliminary study was made at 40 °C using Apparatus C. The aqueous phases, consisting of 75 $\mu g.ml^{-1}$ rhodium and a Sn:Rh ratio of 6:1 in a solution of 0.5 $mol.dm^{-3}$ HCl + 1.5 $mol.dm^{-3}$ MCl (M = H^+, Li^+, Na^+, K^+), were equilibrated at 40 °C for 1.7 hours. After this period portions of 0.0792 ± 0.0002 g of polyurethane

foam were shaken together with 100 ml of aqueous phase for 3.8 hours. The resultant order of increasing extraction efficiency after 3.8 hours was found to be $K^+(0.27) < Li^+(0.36) < Na^+(0.37) < H^+(0.41)$, where the value in parenthesis indicates D'_m in $mmol.g^{-1}$.

This study was repeated at 40 °C using Apparatus C, in which solutions of 2 $mol.dm^{-3}$ HCl, as well as 1 $mol.dm^{-3}$ HCl + 1 $mol.dm^{-3}$ MCl ($M = H^+, Li^+, Na^+, K^+$) were prepared, each containing 75 $\mu g.ml^{-1}$ rhodium and an aqueous Sn:Rh ratio of 10:1. Extraction by 0.0792 ± 0.0002 g portions of foam from 100 ml of solution was monitored for 6.3 hours. Two sets of experiments were performed. In set (a) solutions were equilibrated for 30 minutes at room temperature prior to foam addition, while in set (b) the aqueous phase was heated to 90 °C for one hour before the foam was added. The results are illustrated in Figure 2.8.

In the first three hours similar trends were observed for the two sets of experiments, where the amount of rhodium extracted increased in the presence of the various cations in the order $K^+ < Na^+ < Li^+ < H^+$. A similar effect of the alkali metal cations on the extraction of rhodium from thiocyanate medium has been reported previously [12]. Since this trend is opposite to that reported by Hamon *et al.* [11] in support of the CCM, the authors [12] concluded that the CCM did not significantly contribute to the extraction of the rhodium complexes.

The effect of alkali metal cations on D'_m after 6.3 hours is not simple to interpret. The apparent order of increasing extraction efficiency for set (a) (equilibrated at room temperature) is $K^+ < Li^+ < Na^+ < H^+$, which is the order observed in the preliminary investigation involving an equilibration period of 1.7 hours at 40 °C. Set (b), where the aqueous phase had been heated to 90 °C before extraction,

apparently shows the alkali metal cations to increase the extraction of rhodium in the order $K^+ < Na^+ < H^+ < Li^+$.

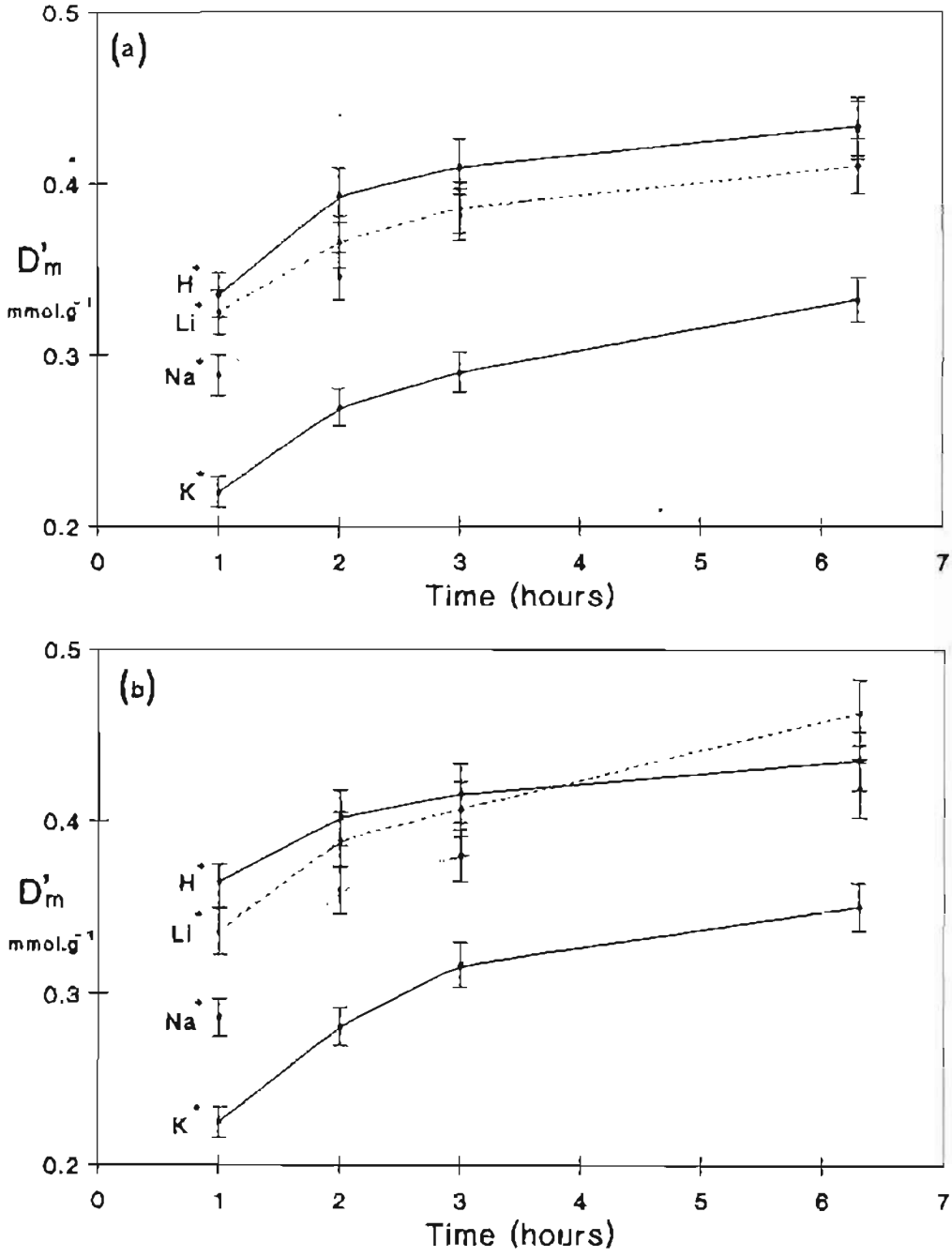

Figure 2.8 The effect of cations on the distribution of rhodium between polyurethane foam and acidic aqueous phase in 1 M HCl + 1 M MCl. [Rh] = 75 $\mu g.ml^{-1}$, Sn:Rh 10:1, 79 mg of foam, T = 40 °C. Set (a) : aqueous phases were equilibrated at room temperature for 30 minutes, and Set (b) : aqueous phases were equilibrated to 90 °C for one hour prior to extraction.

In an attempt to determine the significance of the difference in the values calculated for D'_m, error bars of $D'_m \pm 4\%$ were added to the plotted values in Figure 2.8 (the largest COV observed in the reproducibility study of Section 2.4 of this chapter was ~ 4%). Since the error bars of the D'_m values for H^+, Na^+ and Li^+ overlap to a large extent, no difference in their effect on the extraction of rhodium could be distinguished with certainty. However, the values of D'_m in the presence of K^+ are consistently lower, suggesting a significant inhibiting effect of K^+ on the extraction of rhodium in this system. The above results indicate that the presence of the cations K^+, Na^+ and Li^+ affect the values of D'_m, and that the extraction of rhodium in the presence of these cations increases in the order: $K^+ < Na^+ \leq Li^+ \leq H^+$.

The inhibiting effect of K^+ on the extraction of Rh in this system is contrary to the proposals made by Hamon *et al.* [11] in their formulation of the CCM. Although previous authors [12,13] have ascribed any deviation from the trends observed by Hamon *et al.* [11] to insignificance of the CCM in their extraction systems, such dismissal of the CCM is not necessarily justified. In the absence of the cation chelation mechanism, we would expect negligible amounts of alkali metals to be sorbed by the foam phase. If, for instance, a solvent extraction mechanism were to predominate, the species most likely to be extracted from acidic solutions would be $H_3[Rh(SnCl_3)_nCl_{6-n}]$ and $H_4[Rh(SnCl_3)_5]$, (having previously established that the chloro complexes of tin(II) are not significantly extracted from 2 M hydrochloric acid medium). After acid decomposition, atomic absorption spectroscopic analysis of the foam phase involved in the set (b) experiment with 1 M KCl + 1 M HCl, showed that 0.46 $mmol.g^{-1}$ of K^+ had been coextracted with 0.35 $mmol.g^{-1}$ of rhodium. The presence of K^+ in the foam strongly suggests that a measure of cation chelation takes place. However, if it is assumed that rhodium is sorbed as a triply

charged anion of the type $[Rh(SnCl_3)_nCl_{6-n}]^{3-}$, then the amount of K^+ found in the foam accounts for about 44% of the extracted rhodium.

It appears then that the extraction of the rhodium complexes occurs by more than one mechanism. It is possible that the extraction mechanism/s might vary with a change in solution conditions. If each mechanism resulted in the extraction of a different amount of rhodium, the total amount of rhodium extracted by the foam under a specific set of conditions would depend on which mechanism predominated under those conditions.

It might be argued that the presence of K^+ in the aqueous phase might facilitate the extraction of tin(II), although it is not normally extracted from 2 M hydrochloric acid. If the foam possessed a finite set of "sites" at which the extraction of metal complexes occurred, such competitive sorption might be responsible for the depression in rhodium sorption observed in the presence of potassium. Competitive sorption of tin(II) would lead to an increase in the ratios in which Sn and Rh are sorbed by the foam. However, the experimental results are not consistent with this idea. Determination of the Sn:Rh ratios for the species that had been sorbed by the foam involved in the set (b) experiments, yielded average values of 4.46 ± 0.08 for the solution with 2 M HCl and 4.07 ± 0.16 for the solution with 1 $mol.dm^{-3}$ HCl + 1 $mol.dm^{-3}$ KCl. Hence, the effect on extraction of the cations investigated is not likely to be related to the competitive sorption of chloro-tin species.

The extractions of rhodium achieved by set (a) and set (b) experiments are compared in Figure 2.9. For the majority of the samples analyzed, the extraction efficiency for the two sets did not differ significantly. The latter observation supports the conclusion reached in Section 2.3 of this Chapter that the equilibration

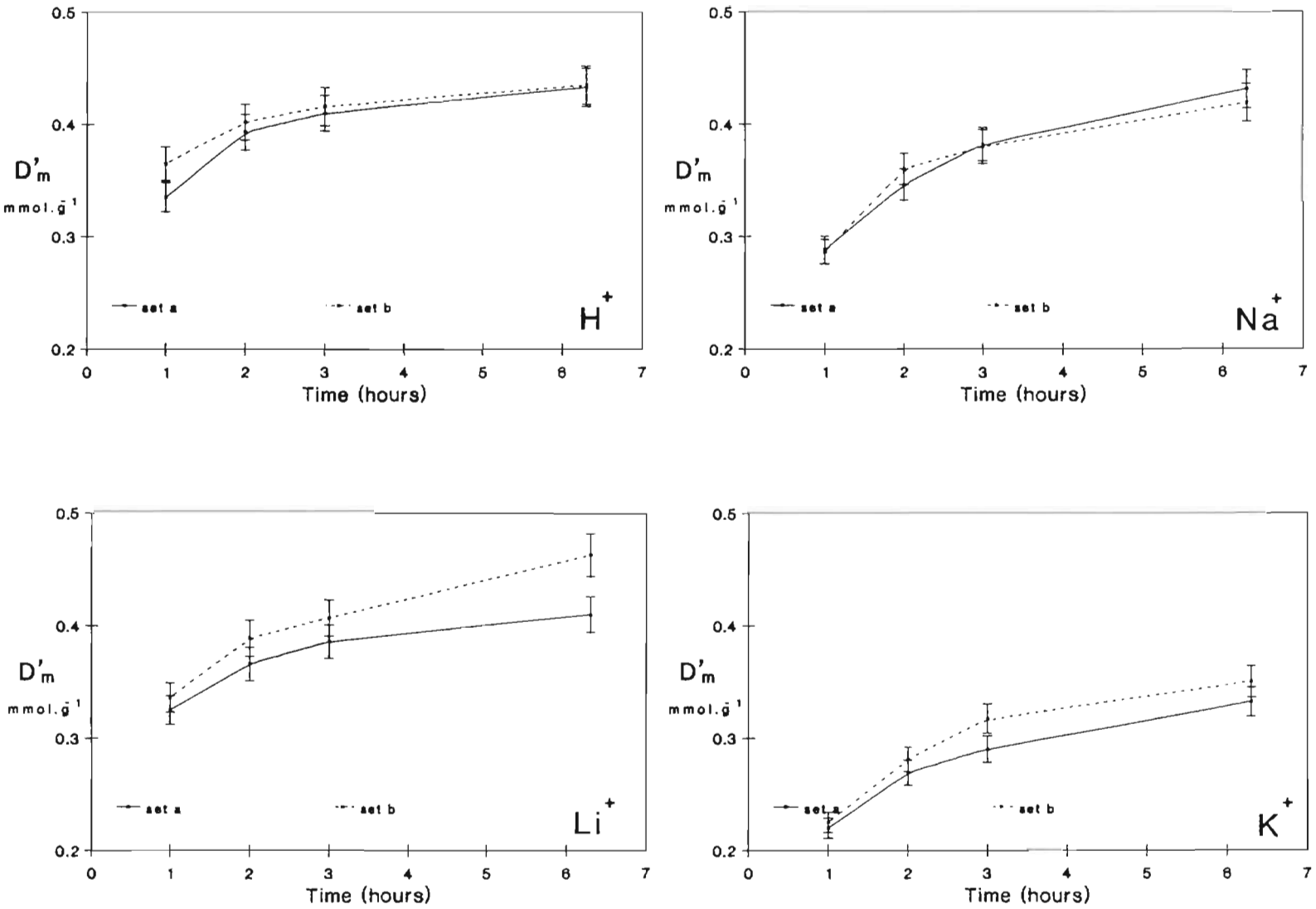

FIGURE 2.9 Comparison of set (a) and set (b) experiments to determine the effect of equilibration of the aqueous phase.

of the aqueous phase prior to extraction negligibly affected the amount of rhodium sorbed. It is not possible to explain the relatively large difference in extraction observed for the Li^+ samples at 6.3 hours (D'_m for set (a) = 0.41 and for set (b) = 0.46 $mmol.g^{-1}$).

3. Discussion

From the above studies, the effect of the solution conditions upon the extraction of rhodium by polyurethane foam has been established, making the choice of optimum conditions possible.

Interpretation of the results in order to understand the mechanism of extraction is not simple. Our results have indicated that more than one mechanism is likely to exist. There certainly is compelling evidence in support of a measure of cation chelation taking place. In Section 2.7 of this Chapter, the finding that 0.46 $mmol.g^{-1}$ of K^+ had been coextracted with 0.35 $mmol.g^{-1}$ of the rhodium complexes was discussed. The amount of coextracted K^+ could account for only approximately 44% of the extracted rhodium if all the rhodium was extracted as a triply charged anion. Therefore, the remainder of the rhodium was either extracted by cation chelation of H_3O^+ cations or by an alternate undetermined mechanism.

The occurrence of protonation of the donor nitrogen and oxygen atoms in the polyurethane foam at high hydrochloric acid concentrations cannot be discounted, especially if one considers the steady increase in the amount of rhodium extracted with increasing acid concentrations. In addition, there is the possibility of the foam acting as a type of solid solvent extractant. The formation of the yellow colour in an organic solvent on extraction of rhodium from hydrochloric acid solutions containing $SnCl_2$, irrespective of the colour of the aqueous phases, was discussed in

Chapter 1, Section 7. A similar yellow colour formation was observed on the extraction by polyurethane foam.

A ^{119}Sn nmr study of the yellow organic phase after liquid-liquid extraction of chloro(trichlorostannato) complexes of rhodium by 4-methylpentan-2-one by Koch *et al.* [14] revealed a distribution of species of the type $[Rh(SnCl_3)_nCl_{6-n}]^{3-}$ in the organic phase. In addition, it was shown that a hydrido complex anion, formulated to be $[RhH(SnCl_3)_4Cl]^{3-}$, was formed on extraction of the trichlorostannato complexes of rhodium. A yellow salt, found to be the hydrido complex $[R_4N]_3[HRh(SnCl_3)_5]$, has been precipitated from a 3 M hydrochloric acid solution [15]. The possibility exists, therefore, that similar hydrido complexes may be formed on extraction by polyurethane foam. The extraction of a distribution of rhodium complexes by polyurethane foam was indicated by the various ratios in which tin and rhodium were coextracted under the different solution conditions studied. Hence the importance of a speciation study of the rhodium complexes sorbed by polyurethane foam is highlighted.

Further empirical studies in which the solution conditions are extensively varied were thought not to be likely to lead to a better understanding of the extraction system. Our attention was focussed on the synthesis of a series of model urethane compounds of a more easily defined nature. The solubility of such compounds would allow a direct determination of the rhodium species that are extracted.

REFERENCES

1 J.M.WYRLEY-BIRCH,
M.Sc. Thesis, University of Cape Town, (1984)

2 S.IWASAKI, T.NAGAI, E.MIKI, K.MIZUMACHI AND T.ISHIMORI,
Bull. Chem. Soc. (Jpn.), **57** (1984) 386

3 K.R.KOCH AND I.NEL,
Analyst, **110** (1985) 217

4 K.F.G.BRACKENBURY, L.JONES AND K.R.KOCH,
Analyst, **112** (1987) 459

5 H.M.N.H.IRVING,
"Liquid-Liquid Extraction" from *"Treatise on Analytical Chemistry"*,
ed. by P.J.Elving, 2nd. ed., 5(1) (1982) 505

6 S.GLASSTONE AND D. LEWIS,
"Elements of Physical Chemistry", Macmillan and Company Limited,
London, (1960) p317

7 T.KIMURA,
Sci. Papers I.P.C.R. (Tokyo), **73** (1979) 31

8 H.MORIYAMA, T.AOKI, S.SHINODA AND Y.SAITO,
J. Chem. Soc. (Dalton Trans.), (1981) 639

9 H.J.M.BOWEN,
J. Chem. Soc., **A** (1970) 1082

10 K.F.G.BRACKENBURY,
M.Sc. Thesis, University of Cape Town, (1985)

11 R.F.HAMON, A.S.KHAN AND A.CHOW,
Talanta, **29** (1982) 313

12 S.J.AL-BAZI AND A.CHOW,
Talanta, **31** (1984) 431

13 A.S. KHAN AND A.CHOW,
Talanta, **30** (1983) 173

14 K.R.KOCH AND J.M.WYRLEY-BIRCH,
Inorg. Chim. Acta, **102** (1985) L5

15 D.P.KRUT'KO, A.B.PERMIN, V.S.PETROSYAN AND O.A.REUTOV,
Bull. Acad. Sci. USSR, Div. Chem. Sci. (Engl. Transl.), **12** (1984) 2553

CHAPTER 3

SYNTHESIS AND CHARACTERIZATION OF MODEL URETHANE COMPOUNDS

Introduction

The quest for a better understanding of the processes involved during polyurethane foam extraction is complicated by the insoluble, cross-linked nature of polyurethane foam. Techniques capable of analyzing the solid foam matrix are desirable for two reasons. Firstly, since the nature of the commercially available foam is largely unknown, characterization of the foam is necessary for meaningful conclusions about the mechanisms involved in the extraction of rhodium using polyurethane foam. Secondly, to identify the nature of the sorbed trichlorostannato-rhodium complexes, direct analysis of these metal species on the foam would be most reliable. Previous authors [1] have drawn conclusions about the sorbed species by analysis of the eluent employed for recovery of the metal complexes from the polyurethane foam. However, one cannot be certain that the complexes emerge unchanged during the elution process. The latter is especially true for complexes which are as kinetically labile as those under investigation. However, analysis of the insoluble solid foam matrix was difficult with the techniques available to us.

The possibility of making use of analytical services elsewhere was considered. Hence, solid-state nmr spectra with and without cross-polarization (CP) were recorded of the polyurethane foam before and after sorption (see Figure 3.1).

The cross-polarized spectrum of the foam before sorption exhibited very broad lines and a low signal-to-noise ratio. Without cross-polarization (CP) the signal-to-noise ratio and the resolution improved tremendously. However, not all the resonances were visible in the latter spectrum. Only resonances arising from the structural groups with relatively high mobility, (that is, polyether chains) could be observed. The spectrum of polyurethane foam after metal sorption showed the signals arising

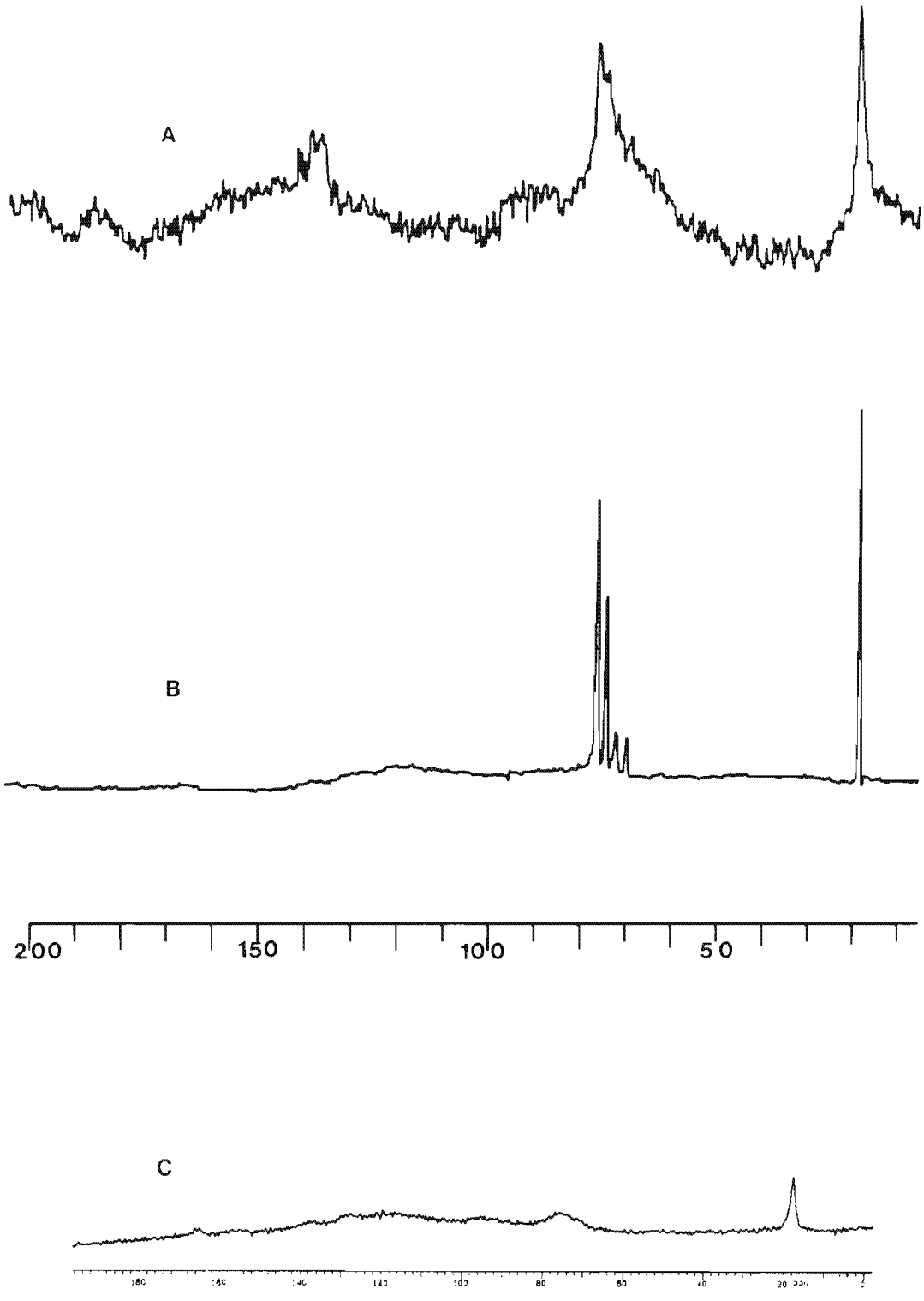

FIGURE 3.1 Solid state ^{13}C nmr spectra of polyurethane foam before (A and B) and after (C) sorption. A = cross polarized, B, C = no cross polarization. (Solid state spectra were run by Dr. J. Kelm of the "Bundesanstalt für Materialprüfung" in Berlin.)

from the polyether {poly(ethylene oxide) and poly(propylene oxide)} chains to be extremely broadened, to the extent of almost being indistinguishable from the background noise. Only the resonances from the freely rotating tolyl-methyl groups are clearly resolved. The latter spectrum indicates strong interaction between the poly(ethylene oxide) and poly(propylene oxide) groups and the extracted metal species, since the severe broadening of the ^{13}C resonances are most probably due to a loss of mobility on interaction.

The potential for obtaining further information on the sorption mechanism and sorbed species by solid-state nmr did not seem sufficiently great to pursue this avenue of analysis. Hence, a direct study of the extraction mechanism and the nature of the sorbed species was not practical.

In an attempt to overcome these difficulties a number of compounds were synthesized to model portions of the polyurethane foam. These model urethanes were soluble in organic solvents, allowing their direct analysis by nmr. In addition, polyurethane foams of known isocyanate index were synthesized from an 80:20 isomer ratio of 2,4- and 2,6-toluene diisocyanate (TDI) and a polyol consisting wholly of poly(propylene oxide). The isocyanate index is an indication of the stoicheiometric ratios of the isocyanate (NCO) and hydroxyl (OH) groups involved in foam formation [2]. An index of 100 indicates equimolar amounts of NCO and OH groups, while an index of 105 indicates 5% excess of NCO and an index of 90 a 10% deficiency of NCO (that is, a 10% excess of OH). Since increasing indexes imply increasing concentrations of nitrogen containing groups (which includes an increase in the degree of cross-linking and an increase in the number of $-NH_2$ relative to -OH terminated chains) a study of the extraction by foams of different indexes should elucidate the existence and extent of nitrogen donor atom involvement in extraction. A comparison of the extraction of trichlorostannato

complexes of rhodium achieved by polyurethane foams prepared from a 100% poly(propylene oxide) polyether with extraction by foams with a 13% poly(ethylene oxide) + 87% poly(propylene oxide) polyether content, (used in Chapter 2) should reveal the effect of the poly(ethylene oxide) content relative to that of poly(propylene oxide). Regrettably, exhaustive attempts to produce a stable foam from a polyol with 80% poly(ethylene oxide) and 20% poly(propylene oxide) content failed (as is discussed in the experimental section).

1. Composition of Model Urethanes

Oligoethylene glycols of various chain lengths were "urethane terminated" by reaction of the hydroxyl groups with phenyl isocyanate to give the series of diurethane molecules illustrated in Figure 3.2. These diurethane molecules bear a close resemblance to the open-chain oligoethers, generally referred to as podands [3]. These "open-chain crown compounds" or podands have been defined by Weber and Vögtle [3] to "include all ligands which possess the characteristics of an open-chain oligoether or which consist of chains bearing heteroatoms in a particular array". Hence, we shall refer to the diurethane molecules as diurethane podands.

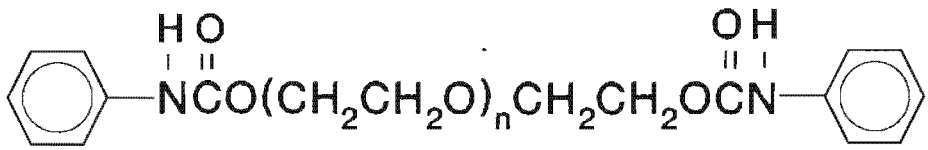

FIGURE 3.2 Diurethane podands (n = 2, 3, 7-8).

Simple, essentially unbranched linear polyurethanes were also synthesized by reaction of the above linear glycols with an 80:20 isomer ratio of 2,4- and 2,6-toluene diisocyanate (TDI) (see Figure 3.3). Care was taken to exclude water from

the reaction in order to further prevent cross-linking as well as foaming of the polymer.

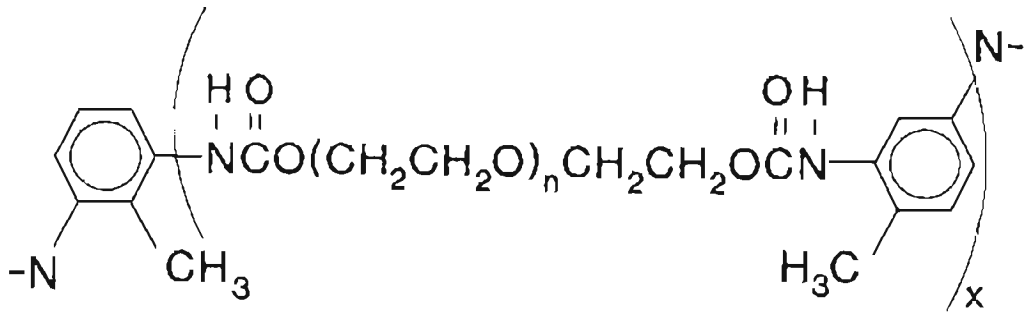

FIGURE 3.3 Linear polyurethanes (n = 2, 3, 7-8, 30-34, 130-170 and x = degree of polymerization).

The polyurethane molecular weight* was varied for the same glycol by variation of the isocyanate to hydroxyl ratio. In general, an NCO:OH ratio of 1:1 results in a much larger molecular weight (that is, a larger x value) than a 1:2 ratio.

The physical nature of the model urethanes which were synthesized, as well as the reactant glycols from which the urethanes were synthesized, is presented in Tables 3.1 and 3.2. The gum-like polyurethanes were warmed to facilitate their weighing when preparing solutions of the polyurethanes of known concentration. The approximate "melting" temperature ranges of these gum-like polyurethanes and the powder-like urethanes are also shown in the above-mentioned tables. Abbreviated names were devised for simplicity. For instance, Diϕ150U indicates a diurethane podand that had been synthesized from a glycol with a molecular weight of 150. Similarly, Pol400U(1:2) indicates a soluble, linear polyurethane that had been synthesized from a glycol with a molecular weight of 400. The value in parenthesis indicates the NCO:OH ratio that had been used for the synthesis.

*The term "weight" is commonly used in the polymer science literature, and is used with strictly the same meaning as the term "mass". Molecular weights of polymers usually carry the units Daltons or atomic mass units.

TABLE 3.1 Diurethane podands.

Reactant glycol	n	abbreviated podand name	physical nature	approx. "melting" temperature (°C)
triethylene glycol	2	Diϕ150U	powder	66 - 80
tetraethylene glycol	3	Diϕ194U	powder	64 - 69
PEG400	7-8	Diϕ400U	honey-like liquid	——

TABLE 3.2 Linear polyurethanes.

		(1:2)-polyurethanes		
reactant glycol	n	abbreviated polymer name	physical nature	approx. "melting" temperature (°C)
triethylene glycol	2	Pol150U(1:2)	hard clear gum	68 - 91
tetraethylene glycol	3	Pol194U(1:2)	hard clear gum	69 - 92
PEG400	7 - 8	Pol400U(1:2)	honey-like liquid	——
PEG1500	30 - 34	Pol1500U(1:2)	waxy opaque gum	42 - 45
		(1:1)-polyurethanes		
reactant glycol	n	abbreviated polymer name	physical nature	approx. "melting" temperature (°C)
triethylene glycol	2	*	——	
tetraethylene glycol	3	*	——	
PEG400	7 - 8	Pol400U(1:1)	hard clear gum	70 - 95
PEG1500	30 - 34	Pol1500U(1:1)	waxy opaque gum	40 - 41
PEG6000	130 - 170	Pol6000U(1:1)	waxy powder	58 - 60

PEG400, - 1500 and -6000 represent polyethylene glycols with average molecular weights of 400, 1500 and 6000, respectively.

n represents the poly(ethylene oxide) chain length (see Figures 3.2 and 3.3).

(1:2)- and (1:1)-polyurethanes represent linear polyurethanes that had been synthesized from NCO:OH ratios of 1:2 and 1:1 respectively.

* Pol150U(1:1) and Pol194U(1:1) were synthesized but hardened very quickly to form hard, practically unusable polymeric masses.

2. Characterization of the Model Urethanes

2.1 Elemental Analysis

The elemental composition determined for the urethanes are given in Tables 3.3 and 3.4. The expected values were calculated for the diurethane podands. Since Diϕ400U has an average value for the poly(ethylene oxide) chain length (that is, n = 7 - 8), a range of percentages expected for the carbon and hydrogen content are given. The linear, soluble polyurethanes, are not discrete, well-defined molecules. Hence, their elemental composition could not be calculated. However, the elemental composition determined by microanalysis, is presented in Table 3.4 for completion.

TABLE 3.3 Elemental analysis of the diurethane podands.

podands	calculated values			values found		
	%C	%H	%N	%C	%H	%N
Diϕ150U	61.9	6.2	7.2	61.8	6.3	7.4
Diϕ194U	61.1	6.5	6.5	60.0	6.3	6.4
Diϕ400U	56.4–60.2	6.9–7.5	4.4	59.3	7.2	4.9

TABLE 3.4 Elemental analysis of the linear polyurethanes.

polyurethane	%C	%H	%N
Pol150U(1:2)	61.8	6.3	7.4
Pol194U(1:2)	63.2	9.0	6.4
Pol400U(1:2)	53.3	8.1	2.8
Pol1500U(1:2)	59.9	10.3	0.8
Pol400U(1:1)	54.6	7.6	4.8
Pol1500U(1:1)	54.3	8.7	1.6
Pol6000U(1:1)	54.8	9.3	0.6

The higher nitrogen content of the (1:1)-polyurethanes, relative to the (1:2)-polyurethanes is consistent with the higher degree of polymerization expected for the (1:1)-polyurethanes.

2.2 Nuclear Magnetic Resonance Spectroscopy (nmr)

2.2 (i) ^{13}C nmr

The ^{13}C nmr spectra of the diurethane podands and the linear polyurethanes showed the characteristic resonances of the urethane, aromatic, and ethylene oxide functional groups, and their chemical shift values were consistent with chemical shift ranges published for these functional groups [4,5]. Typical proton-decoupled ^{13}C nmr spectra of the diurethane podands, (1:2)-polyurethanes and (1:1)-polyurethanes are shown in Figures 3.10 - 3.12. The tabulated chemical shift data for the urethanes are given in Tables 3.5 and 3.7. Figures 3.4 and 3.5 are general schematic representations of the diurethane podands and the linear polyurethanes. The numbering of the carbon atoms in Figures 3.4 and 3.5 pertain to all the podands and soluble linear polyurethanes in each series.

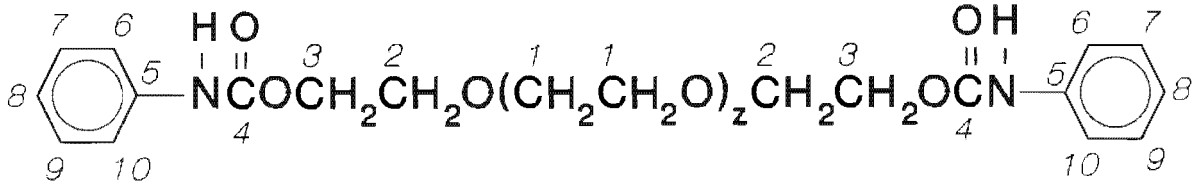

Diurethane Podand	z
Diϕ150U	1
Diϕ194U	2
Diϕ400U	6 - 7

FIGURE 3.4 General schematic representation of the diurethane podands, showing the numbering pertaining to their ^{13}C nmr spectra.

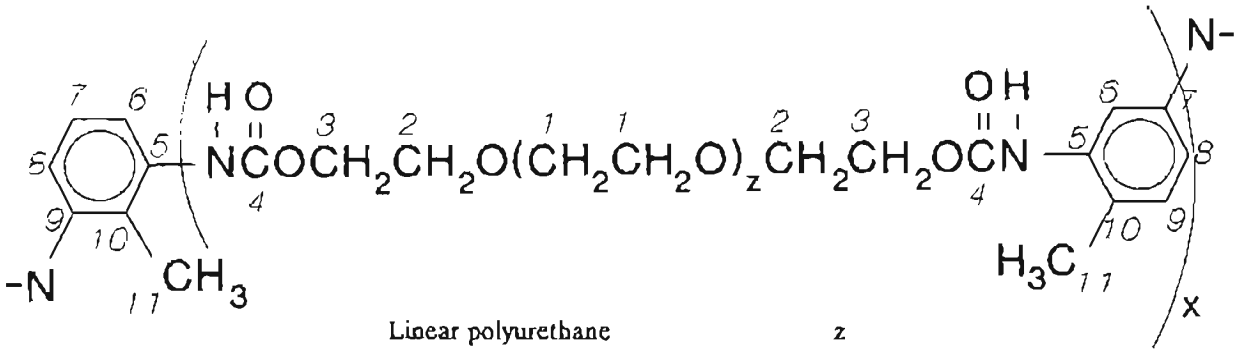

Linear polyurethane	z
Pol150U(1:2)	1
Pol194U(1:2)	2
Pol400U(1:2) and -(1:1)	6 - 7
Pol1500U(1:2) and -(1:1)	29 - 33
Pol6000U(1:1)	129 - 169

FIGURE 3.5 General schematic representation of the linear polyurethanes, showing the numbering pertaining to their ^{13}C nmr spectra (x = degree of polymerization).

Assignments were made of the major peaks only. The minor peaks (that is, < 5% of the average intensity), are regarded as having arisen from the presence of small amounts of impurities, and consequently are omitted from Tables 3.5 and 3.7.

(a) Diurethane Podands

Since the podands, that is Diϕ150U, Diϕ194U and Diϕ400U, differ only in the number of ethylene oxide groups, the spectra are very similar. The peak at approximately 70.4 ppm increases in intensity with increasing values for z, and is therefore assigned to C_1 (see Figure 3.4).

The ethylene oxide carbons of Diϕ150U (z = 1), occur in three different chemical environments and, as expected, three ethylene oxide resonances of similar intensity are observed. The peak at 70.72 ppm has been assigned to C_1 (see above). The

upfield position of the other ethylene oxide resonances (C_2 and C_3), may be due to magnetic anisotropy of the carbonyl double bond of the urethane group. The carbons directly adjacent to the urethane carbons would experience the largest effect and hence the most upfield peak at 64.21 ppm is assigned to C_3.

Diϕ194U has z = 2, and carbons C_1 occur in two chemical environments that differ very slightly, as is evident from the close proximity of the resonances (70.45 and 70.34 ppm). The central carbons (C_1) of the longer oligoethylene oxide chains of Diϕ400U have become indistinguishable. Due to the inherent chemical equivalence of the central carbons, the C_1 carbons approach magnetic equivalence, and the signals become fortuitously coincident.

The aromatic carbons were assigned with the aid of semi-quantitative ^{13}C nmr spectra and an attached proton test (APT), which is useful for distinguishing between CH_2 and quaternary carbons, and CH and CH_3 carbons.

(b) Linear Polyurethanes

The soluble, linear polyurethanes may be visualized as a combination of flexible oligo(ethylene oxide) portions interspersed with relatively rigid "flat" aromatic diurethane moieties. These linear polyurethanes may be expected to form random polymer coils in solution. Note that the term "linear polyurethanes" is used to denote non-cross-linked polyurethanes. The random polymer structure and statistical distribution of conformations of the linear polyurethanes are reflected in their nmr spectra. Unlike the fairly well defined chemical environments of each carbon of the diurethane podands, the functional groups of the polyurethanes do not occur in a single chemical environment. The position of a functional group along

the polymer backbone may influence the chemical shift of its carbons. In that respect, carbons in the proximity of a terminal hydroxyl group might be expected to resonate at a slightly different frequency relative to those in the center of the polymer. In addition, carbon atoms separated by several bonds strongly influence each other if they are spatially close [5]. Hence, the conformation of the polymer in solution may be expected to affect the chemical shift values, which in turn is anticipated to be dependent upon the nature of the solvent used in which these polymers are dissolved.

Certainly the different isomers of TDI (that is, an 80:20 isomer ratio of 2,4- and 2,6-toluene diisocyanate) give rise to different chemical environments. This is clearly evident from the significantly different chemical shifts of the methyl peaks (C_{11}), at 16.64 ppm and 11.73 ppm for Pol400U(1:2). The relative peak intensities of the two methyl peaks, reflect their 80:20 isomer ratio in the TDI starting material. Similarly, the different isomers may be expected to influence the chemical shifts of the urethane and aromatic carbons.

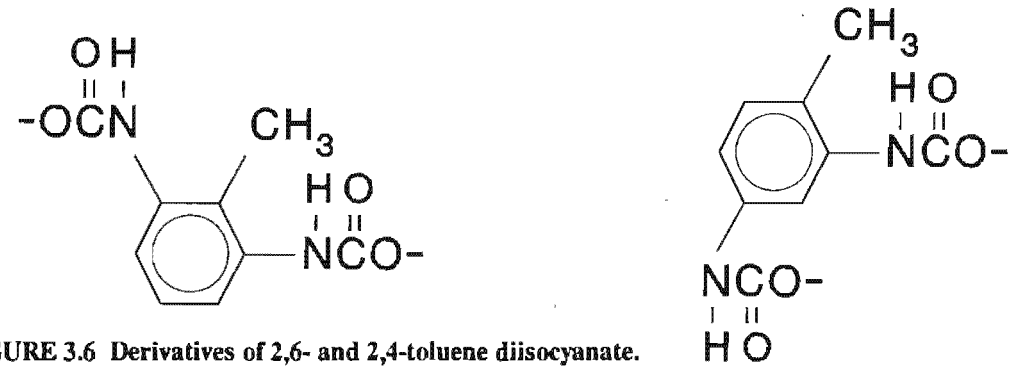

FIGURE 3.6 Derivatives of 2,6- and 2,4-toluene diisocyanate.

The longer polymer chain lengths, caused by longer oligo(ethylene oxide) chain lengths, appear to result in increased magnetic equivalence of the carbon atoms of the various moieties. Hence, fewer resonances are resolved in the ^{13}C nmr spectra of Pol400U(1:2) than for Pol150U(1:2) and Pol194U(1:2).

Another feature of the ^{13}C nmr spectra of the linear polyurethanes, is their relatively large line-widths. Partly, the peaks may appear broader due to unresolved resonances. However, the increased molecular weights of the polyurethanes, and their resultant increased correlation times (τ_c), may be expected to contribute to the increased line-widths of the linear polyurethane ^{13}C resonances. Qualitatively, the relationship between the relaxation times T_1 and T_2 and the correlation time τ_c [6] is illustrated in Figure 3.7.

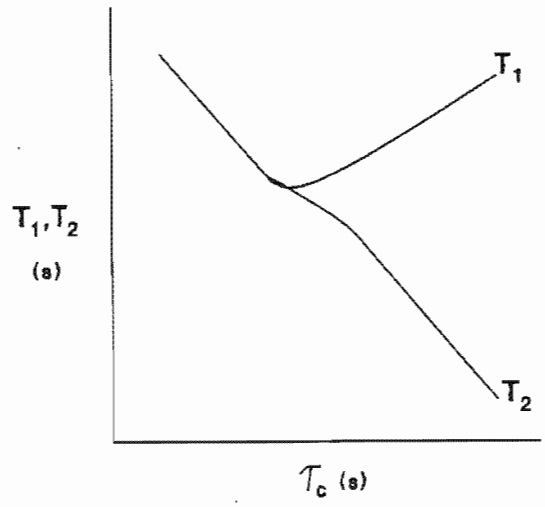

FIGURE 3.7 The effect of correlation time on T_1 and T_2.

The lower the rate of tumbling of the molecules, and the higher the correlation times, the smaller will be T_2. From the definition of T_2 processes,

$$1/\pi T_2 = \nu_{1/2} \qquad (1)$$

it follows that the smaller T_2 becomes, the broader will be the peaks [6].

The largest line-widths were observed for the aromatic carbons (C_5 to C_{10}). Possibly, one may ascribe this phenomenon to a lower mobility of the carbons of the

fairly rigid aromatic groups relative to the more flexible poly(ethylene oxide) groups and the freely rotating methyl groups.

2.2 (ii) ^{1}H nmr

The proton nmr spectra of the diurethane podands and the linear polyurethanes are complicated by poor resolution and second order effects which renders a detailed analysis of the spectra difficult. The chemical shifts are shown in Tables 3.6 and 3.8 with the numbering of the protons illustrated in Figures 3.8 and 3.9. The apparent multiplicities of the diurethane podand signals, and their average coupling constants have also been tabulated, to provide an approximate representation of the spectra.

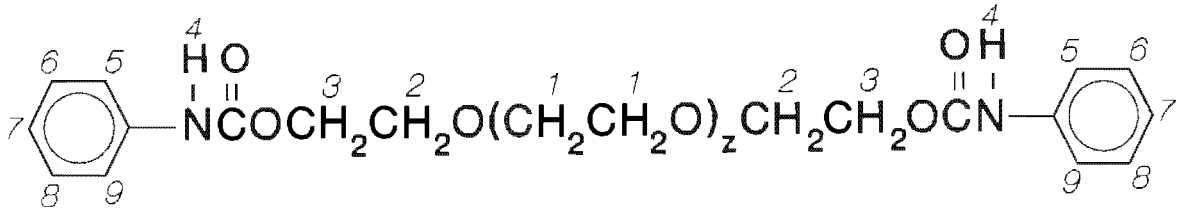

FIGURE 3.8 Numbering of the protons of the diurethane podands.
(For a definition of z, see Figure 3.4).

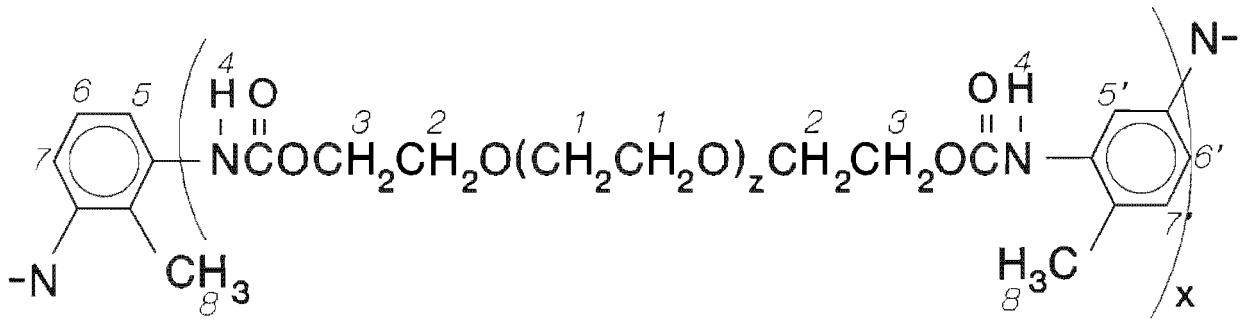

FIGURE 3.9 Numbering of the protons of the linear polyurethanes.
(For a definition of x and z, see Figure 3.5).

Typical proton spectra of each of a series of urethane compounds are shown in Figures 3.10 to 3.12.

Very poor resolution of the multiplicity of the peaks was observed for the linear polyurethanes. In addition the peaks were considerably broadened, and an increase in the number of signals arising from aromatic and urethane protons was observed. The multiplicity of these signals could not be distinguished.

The increased number of chemical environments and the line broadening observed for the polyurethanes relative to the podands can be explained using the same general arguments presented for the ^{13}C nmr spectra. The aromatic and urethane protons appear to be more sensitive to slight variations in the chemical environment, presumably due to their restricted mobility relative to the flexible oligoethylene groups. An increase in the polymer length with increasing oligoethylene chain length, results in an apparent decrease in the number of urethane and aromatic proton signals observed. Possibly, these protons approach magnetic equivalence with increasing polymer chain length. In addition, since it is difficult to distinguish the multiplicities, and we are only able to report the total number of peaks, the apparent decrease in signals observed may be due to poorer resolution of the multiplicities.

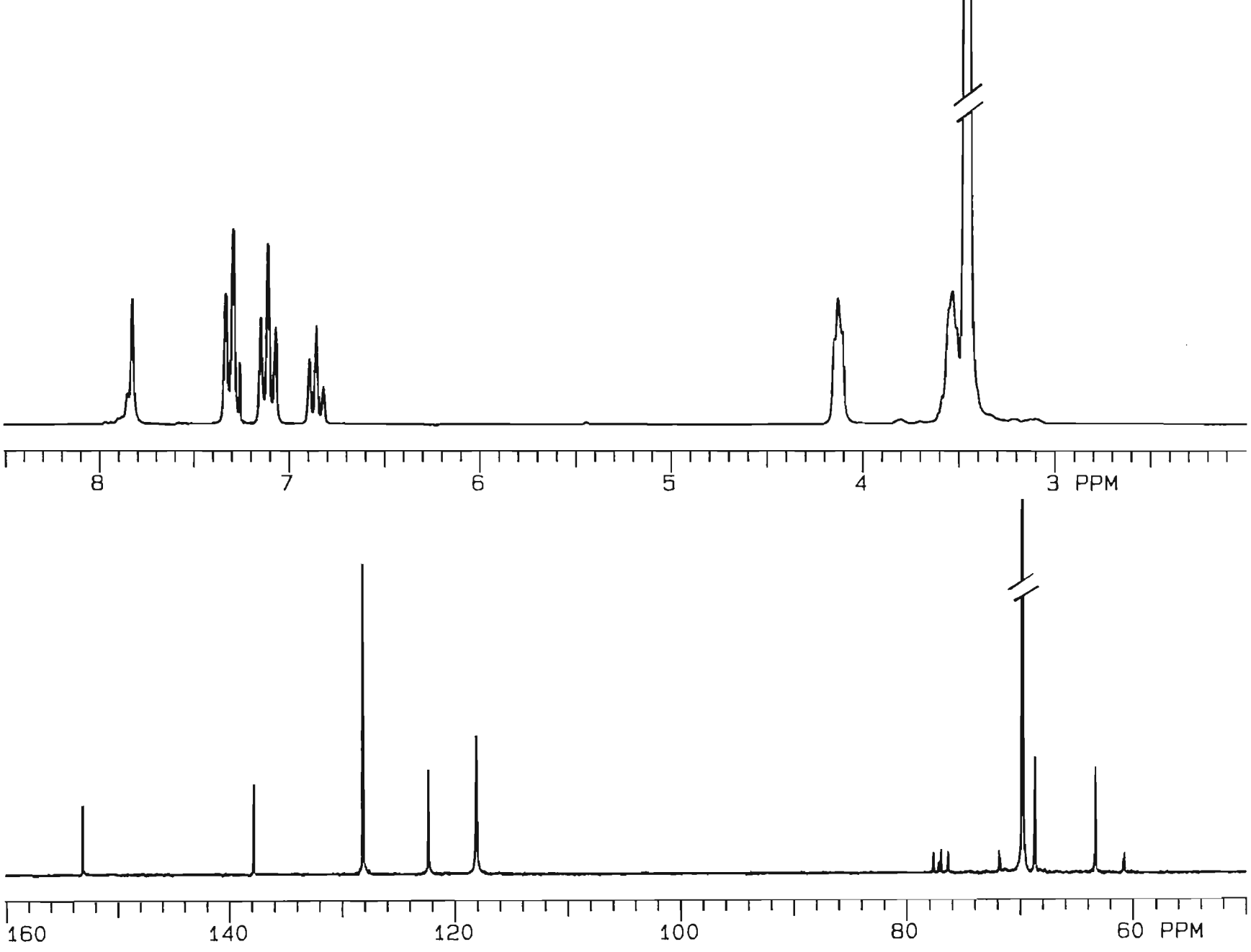

FIGURE 3.10 ^{1}H and ^{13}C nmr spectra of Diϕ400U ($CDCl_3$, Temp. = 30°C).

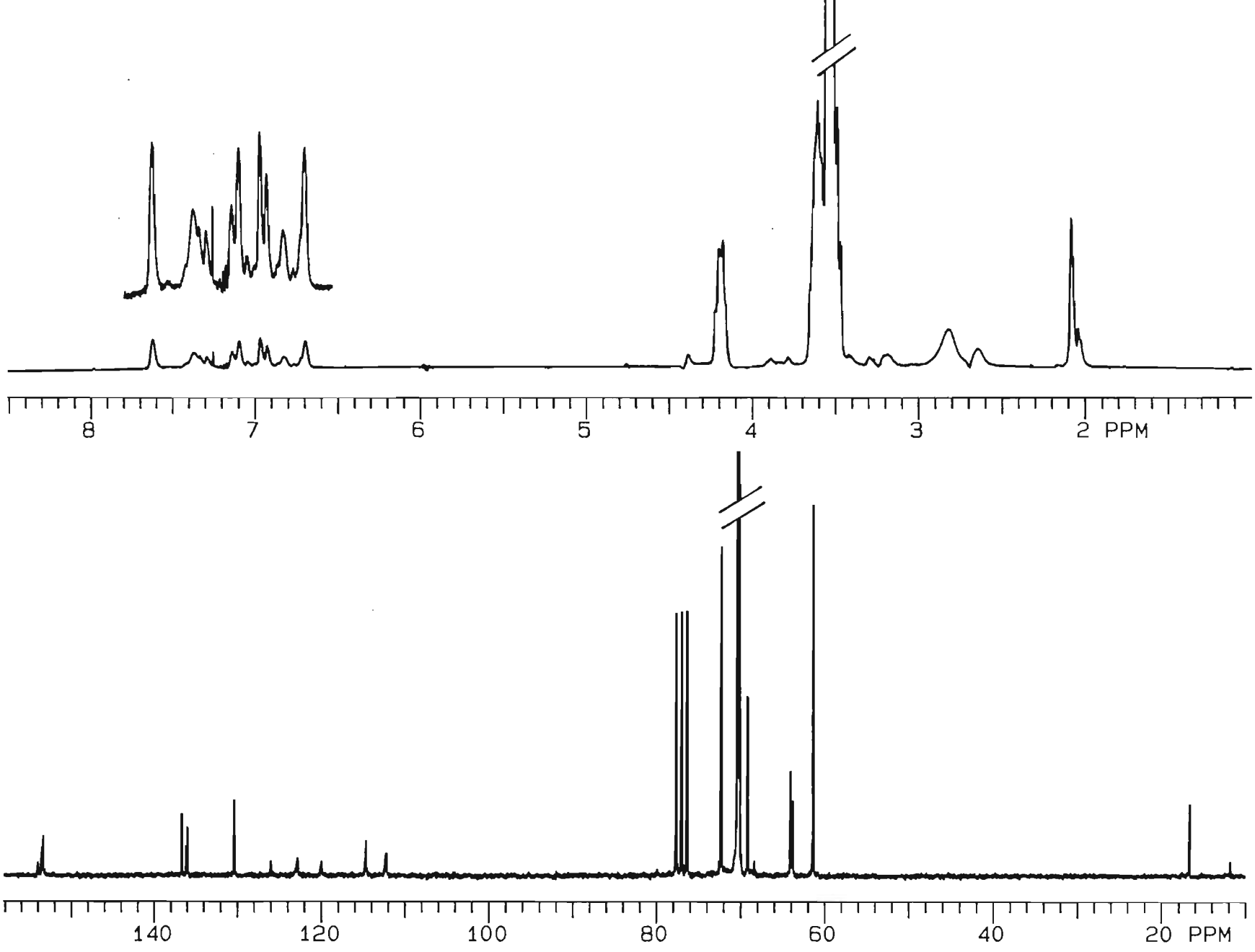

FIGURE 3.11 ^{1}H and ^{13}C nmr spectra of Pol400U(1:2) ($CDCl_3$, Temp. = 30°C).

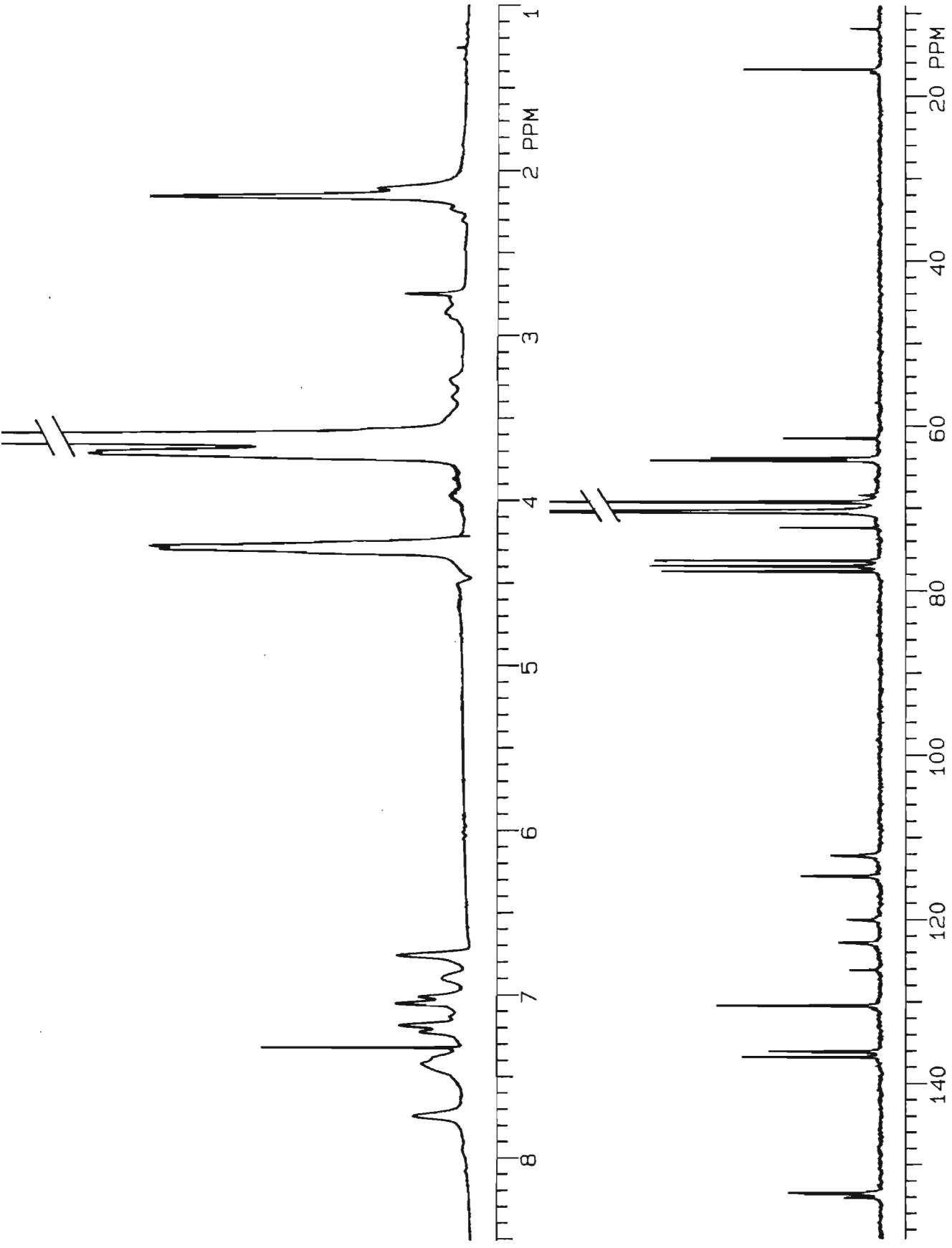

FIGURE 3.12 ^{1}H and ^{13}C nmr spectra of Pol400U(1:1) ($CDCl_3$, Temp. = 30°C).

Table 3.5 ^{13}C nmr chemical shift (ppm) data for the diurethane podands.

podand	C^1	C^2	C^3	C^4	C^5	C^6	C^7	C^8	C^9	C^{10}
Diϕ150U	70.72	69.58	64.21	153.54	137.84	118.70	128.97	123.38	128.97	118.70
Diϕ194U	70.45 70.34	69.38	63.88	153.52	137.97	118.56	128.81	123.12	128.81	118.56
Diϕ400U	70.35	69.25	63.91	153.45	138.00	118.53	128.75	123.03	128.75	118.53

Table 3.6 ^{1}H nmr data for diurethane podands.

podand	H^1	H^2	H^3	H^4	H^5	H^6	H^7	H^8	H^9
Diϕ150U	3.67 (s) 3.66 (sh)	3.73 (m)	4.30 (m)	7.12	7.36 (d)	7.25 (t)	7.02 (t)	7.25 (t)	7.36 (d)
		J_{av} = 4.59	J_{av} = 4.57		J = 8.61	J_{av} = 7.88	J_{av} = 7.22	J_{av} = 7.88	J = 8.61
Diϕ194U	3.62 (s)	3.67 (m)	4.26(m)	7.42	7.36 (d)	7.23 (t)	6.99 (t)	7.23 (t)	7.36 (d)
		J_{av} = 4.56	J_{av} = 4.59		J = 8.17	J_{av} = 7.37	J_{av} = 7.25		
Diϕ400U	3.62 (m)	3.70 (m)	4.29 (m)		7.40 (d)	7.27 (t)	7.02 (t)	7.27 (t)	7.40 (d)
	J_{av} = 2.70	J_{av} = 4.46	J_{av} = 3.76		J = 7.83	J_{av} = 7.88	J_{av} = 7.24	J_{av} = 7.88	J = 7.83

Chemical shift values in ppm. J_{av} = average coupling constant in Hz.
(s) = singlet or single resonance (t) = triplet (m) = multiplet characteristic of an AA'BB' spin system
(sh) = shoulder (d) = doublet

Table 3.7 ^{13}C nmr data for the linear polyurethanes.

	C^1	C^2	C^3	C^4	C^5 to C^{10}						C^{11}
Pol150U(1:2)	70.02 to 70.30 (2)	69.11 to 69.20 (2)	63.69 to 64.10 (3) 61.31* 72.25*	153.49 to 154.26 (7)	135.83 to 136.59 (5)	130.35	125.90	123.08 to 123.40 (2)	120.33	114.92 112.35 to 112.70 (3)	16.65 11.72
Pol194U(1:2)	70.17 to 70.46 (3)	69.45	63.92 to 64.19 (2) 61.47* 72.33*	153.48 to 154.14 (3)	135.97 to 136.78 (6)	130.46	126.08	122.87 to 123.07 (2)	120.20	114.71 to 114.81 (2) 112.36	16.76 11.84
Pol400U(1:2)	70.05 to 70.23 (2)	69.09	63.72 to 63.98 (2) 61.30* 72.26*	153.30 to 153.94 (3)	135.88 to 136.62 (3)	130.28	125.91	122.87	119.96	114.63 112.26	16.64 11.73
Pol1500U(1:2)	69.89 to 70.15 (2)	68.59† to 69.04 (2)	# # 61.18* 72.25*	# #	135.83 to 136.57 (3)	130.25	# #	# #	# #	# #	16.74 #
Pol400U(1:1)	70.23 to 70.40 (2)	69.25	63.91 to 64.18 (2) 61.52* 72.36*	153.39 to 154.02 (3)	136.02 to 136.72 (3)	130.46	126.14	122.79	120.00	114.70 112.17	16.77 11.85
Pol1500(1:1)	70.14 to 70.43 (2)	69.33 68.47†	63.92 to 64.17 (2) 61.55* 72.46*	153.35	136.09 to 136.71 (2)	130.58	126.40	#	119.68	114.31 111.46	17.00 12.03
Pol6000(1:1)	70.49	#	#	#	#	#	#	#	#	#	#

A chemical shift range (ppm) is given for each carbon with the number of signals in the range indicated in parenthesis.

The signals due to the aromatic carbons C^5 to C^{10} are listed but not specifically assigned.

* These signals possibly arise from terminal ethylene oxide resonances. However, the assignment is not unambiguous.

† not unambiguously assigned.

peaks are too small to measure.

Table 3.8 ^{1}H nmr data for the linear polyurethanes.

Polyurethane	H^1	H^2	H^3	H^4 - H^7	H^8
Pol150U(1:2)	3.63(s)	3.69(m)	4.26(m)	6.85 to 7.67 (~20 signals)	2.10 & 2.06
Pol194U(1:2)	3.63(s)	3.70(m)	4.27(m)	6.75 to 7.67 (~17 signals)	2.13 & 2.08
Pol400U(1:2)	3.62(s)	3.72(m)	4.28(m)	6.89 to 7.73 (~9 signals)	2.17 & 2.12
Pol1500U(1:2)	3.49(s)	3.69(m)		*	2.04
Pol400U(1:1)	3.63(s)	3.71(m)	4.29(m)	6.76 to 7.74 (~10 signals)	2.16 & 2.11
Pol1500U(1:1)	3.57(s)	3.65(m)	4.24(m)	6.65 to 7.73 (~12 signals)	2.16 & 2.11
Pol6000U(1:1)	3.62(s)				

Chemical shifts in ppm.

s = single resonance line.

m = unresolved multiplet.

* = The spectrum is dominated by an intense ethylene oxide peak. Hence all other resonances are difficult to measure.

2.3 Molecular Weight Determination

When faced with the task of determining the molecular weight of a polymer, one can approach the problem in two fundamentally different ways. Absolute methods may be employed to yield a direct estimate of the molecular weight. These methods usually require skill, as well as unrestricted time and funds. With the aid of secondary methods one can obtain comparisons between the molecular weights of different polymers, but the system has to be calibrated by reference to a system that has been studied by one of the absolute methods.

2.3 (i) Gel Permeation Chromatography (GPC)

(a) General Description of GPC

Gel permeation chromatography is a secondary method for the determination of molecular weight. It is essentially a fractionating process which separates molecules according to their size. A column is packed with finely divided solid particles which are permeated by pores of a selected average diameter. When a polymer solution with a wide molecular weight distribution is eluted through the column, the smaller molecules will diffuse through the pores or "tunnels" in the particles and will be delayed. The medium-sized particles might undergo partial diffusion through the openings of the pores and will be slowed to a lesser extent, while the large molecules will be swept along with the solvent front without delay. After calibration of the system in terms of the elution volume ($\mathbf{V_e}$) or retention time ($\mathbf{R_t}$), the number average and weight average molecular weight as well as the molecular weight distribution of the polymer, can be determined.

(b) Definition of Molecular Weight Averages

The number average molecular weight ($\bar{M}_n$) can be defined as the ratio of total polymer weight to the total number of polymer molecules [2].

$$\bar{M}_n = \frac{\sum_{i=1}^{\infty} W_i}{\sum_{i=1}^{\infty} n_i} \qquad (2)$$

or

$$\bar{M}_n = \frac{\sum_{i=1}^{\infty} n_i M_i}{\sum_{i=1}^{\infty} n_i} \qquad (3)$$

The weight average molecular weight ($\bar{M}_w$) is the sum of the weights of each species multiplied by the molecular weight of each corresponding species, divided by the polymer weight.

$$\bar{M}_w = \frac{\sum_{i=1}^{\infty} W_i M_i}{\sum_{i=1}^{\infty} W_i} \qquad (4)$$

or

$$\bar{M}_w = \frac{\sum_{i=1}^{\infty} n_i (M_i)^2}{\sum_{i=1}^{\infty} n_i M_i} \qquad (5)$$

$n_i M_i = W_i$

n_i = the number of moles of polymer molecules of the i^{th} species

M_i = the molecular weight of the i^{th} species

W_i = the total weight of the i^{th} species.

The viscosity average molecular weight ($\bar{M}_v$) is determined by measuring the solution viscosity and is related to the intrinsic viscosity by the Mark-Houwink-Sakurada equation:

$$[\eta] = K(\bar{M}_v)^a \qquad (6)$$

where $[\eta]$ = the intrinsic viscosity

K and **a** are constants characteristic of each polymer-solvent solution.

The viscosity average molecular weight lies between $\bar{M}_n$ and $\bar{M}_w$, but closer to $\bar{M}_w$ [7].

The ratio $\bar{M}_w/\bar{M}_n$ is commonly used as a measure of the breadth of the molecular weight distribution [8]. This ratio may be referred to as the dispersity (**D**) [9]. Hence,

$$D = (\bar{M}_w/\bar{M}_n) \qquad (7)$$

The smaller the value of **D**, the smaller the range of molecular weights present in the polymer sample. Hypothetical monodisperse polymers have **D** = 1, however the dispersities of monodisperse "living" polymers have been measured to be in the range 1.01 - 1.05 [8].

(c) Calibration in GPC

With reference to the calibration of the gel permeation chromatograph, it is important to bear in mind that in a good solvent, that is, a solvent in which the

polymer is highly soluble,* a polymer extends to maximize solvent to polymer contact, in contrast to the polymer coiling up in a bad solvent in order to minimize contact between the polymer and the solvent. From this fact, it becomes evident that for the same molecular weight, chemically different polymers in the same solvent can have a different hydrodynamic volume. Ideally, therefore, in order to reliably calibrate the relation between molecular weight and $\mathbf{R}_t$, the standards should be of the same polymer as the polymer samples being studied since the "sorting" mechanism is based on size and not on mass. In addition, each polymer standard should have such a narrow molecular weight range as to be essentially monodisperse. Often it is impractical to first fractionate a portion of the polymer under investigation into monodisperse standards, and then to determine the molecular weight of the standard fractions before constructing a calibration curve. Attention was focussed, therefore, on finding a universal calibration parameter that would be valid for most polymers.

Einstein's equation relating the relative viscosity of a colloid-containing solution to the volume fraction of a colloidal particle, led to the finding of the above-mentioned universal parameter. According to Einstein [10],

$$\eta_r = \eta/\eta_o = 1 + 2.5\phi_2 \qquad (8)$$

where η_r is the relative viscosity,

η the viscosity of the solution,

η_o the viscosity of the solvent, and

ϕ_2 the volume fraction of the spherical colloidal particle.

*A liquid will be a "good" solvent for a polymer if the molecules of the liquid chemically and physically resemble the structural units of a polymer. Thus cumene and ethylbenzene should be good solvents for polystyrene [7].

Polymer molecules may best be described as coils which randomly assume a statistical distribution of conformations. In dilute solution, these coils are disentangled from one another, and are completely solvated. The solvent saturated polymer coil, together with the adsorbed solvent molecules form a single entity, and resemble a molecular colloid. Hence, polymer solutions are correctly classified as colloidal-dispersions [7]. Therefore, Einstein's equation, describing colloidal solutions, may be applied to polymer solutions.

Equation 8 can be expressed in terms of the intrinsic viscosity as

$$[\eta] = \gamma(N_0 V/M) \qquad (9)$$

where N_0 is Avogadro's number,

M is the molecular weight,

V is the hydrodynamic volume of the molecule, and

γ is the Simha parameter (2.5 for spheres, and greater than 2.5 for non-spherical particles) [11]

Grubisic *et al.* [12] simplified Einstein's equation to

$$[\eta] = K(V/M) \qquad (10)$$

where $[\eta]$ is the intrinsic viscosity,*

V the hydrodynamic volume of the particles,

M their molecular weight, and

K a constant.

*Intrinsic viscosity is also known as the limiting viscosity number (recommended IUPAC nomenclature), or limiting viscosity index. However, "intrinsic viscosity" appears to be the term most abundantly used in the literature.

From $[\eta]\mathbf{M} = \mathbf{KV}$ *(11)*

it follows that $[\eta]\mathbf{M}$ is a direct measure of the hydrodynamic volume of the particles, and Grubisic *et al.* suggested the use of $\log[\eta]\mathbf{M}$ instead of logM for the calibration of the GPC system. These workers measured the GPC elution volumes and intrinsic viscosities of a number of polymer samples of different chemical nature and morphological structure, and determined their molecular weights by light scattering and osmometry. A good correlation was obtained when plotting $\log[\eta]\mathbf{M}$ against elution volume ($\mathbf{V_e}$), supporting the hypothesis that the viscometric hydrodynamic volume as characterized by $[\eta]\mathbf{M}$, determines retention in the gel chromatographic column.

(d) Universal Calibration for the Molecular Weight Determination of Linear Polyurethanes

In the present work, in order to estimate the molecular weight of the linear polyurethanes by gel permeation chromatography, monodisperse polystyrene standards were used. Polystyrene is a non-polar polymer, whereas the linear polyurethanes, comprising mainly poly(ethylene oxide) groups, are expected to be fairly polar. The dissimilarity of the standards and the samples suggests that it should be necessary to test the data to see which calibration technique will yield a reliable molecular weight determination. Hence, the intrinsic viscosities of selected linear polyurethanes were measured at 23 °C according to the method described by Colins *et al.* [8] to make a test of the universal calibration technique possible. Table 3.9 reports the results of the intrinsic viscosity measurements.

TABLE 3.9 Intrinsic viscosities measured for linear polyurethanes.

Polymer	$[\eta]$ (dl.g^{-1})	Standard deviation
Pol150U(1:2)	0.0392	0.002
Pol194U(1:2)	0.0840	0.003
Pol400U(1:2)	0.0459	0.004
Pol400U(1:1)	0.1160	0.003

The prohibitive cost of polystyrene standards necessitated the calculation of their intrinsic viscosities rather than to determine their viscosities experimentally. The intrinsic viscosities may be calculated from equation 6 - the Mark-Houwink-Sakurada equation,

$$[\eta] = K\bar{M}_v^{a}$$

where $[\eta]$ is the intrinsic viscosity

$\bar{M}_v$ the viscosity average molecular weight, and

K and a are the Mark-Houwink-Sakurada constants.

Boni *et al.* [11] reported that $K = 6.82 \times 10^{-3}$ ml.g^{-1} and $a = 0.766$ for polystyrene in tetrahydrofuran at 23 °C. These authors used the number average molecular weight ($\bar{M}_n$) in the place of the more accurate viscosity average molecular weight ($\bar{M}_v$). However, since polystyrene can be obtained in essentially monodisperse fractions, the error should not be large. All M averages should be equal for monodisperse polymers [7] where

$$D = \bar{M}_w/\bar{M}_n = 1$$

(e) Problems Encountered in Universal Calibration

In their discussion of the universal calibration technique, Boni *et al.* [11] point out that "the whole range of molecular weight-intrinsic viscosity data cannot be described by a single Mark-Houwink relationship", since polymer molecules with low molecular weights behave as if they are in a theta solvent where **a** = 0.5. Several authors [13,14] have similarly reported that in the very low molecular weight range, the Mark-Houwink equation for a theta solvent is applicable, namely,

$$[\eta]_\theta = \mathbf{K}_\theta \bar{\mathbf{M}}^{1/2} \qquad (12)$$

According to Boni *et al.* [11], errors of up to 50% from the true value of $\bar{\mathbf{M}}_\mathbf{n}$ could result from the use of high molecular weight Mark-Houwink constants for calculation of the molecular weights of polymers with low molecular weights.

In order to understand the concept of theta conditions, one must be aware of the two types of interactions experienced by the long chain molecules in solution, namely, "long-range" and "short-range" interactions.

Short-range interactions occur between atoms or groups separated only by a small number of valence bonds, and they result in the effectively constant bond angles and torques hindering internal rotations [15]. When the polymer experiences only short-range interactions, it is referred to as an "unperturbed" chain.

Long-range interactions are the interactions between non-bonded groups which are separated in the basic chain structure by many valence bonds. These interactions are identical in nature and in magnitude to van der Waal's forces between the parts of two different molecules. Long-range interactions give rise to the "excluded

volume effect", which can be pictured as an osmotic swelling of the random polymer coil by polymer-solvent interactions. A mathematical description would be

$$\langle S^2 \rangle = \alpha^2 \langle S^2 \rangle_0 \qquad (13)$$

where $\langle S^2 \rangle$ = the mean square radius of gyration of the molecule with the presence of both long- and short-range interactions,

$\langle S^2 \rangle_0$ = the mean square radius of gyration of the polymer chain in the absence of long-range interactions (that is, the unperturbed dimensions of the chain), and

α = the linear expansion factor, which is a function of the number of bonds in the chain.

The excluded volume effect vanishes under a special condition of temperature or solvent, (usually known as the Flory "theta" temperature or solvent), leaving the chain in its unperturbed state. Hence, under theta conditions the free energies of the polymer-polymer, polymer-solvent, and solvent-solvent interactions are all approximately equal.

The transition to $\mathbf{K}_\theta$ and $\mathbf{a} = 0.5$ in the Mark-Houwink-Sakurada equation, is found generally in the 50 000 - 30 000 molecular weight range [11]. Therefore, since the standards used in the present study range from 1350 to 50 000, we here are most likely dealing with polystyrene standards which occur in conformations usually prevalent under theta conditions.

(f) Universal Calibration under Theta Conditions

Several values of K_θ for polystyrene can be obtained from the literature. Therefore, a separate log[η]M versus R_t calibration curve for each of a number of K_θ values shall be established.

From each calibration curve, slightly different answers for the molecular weight determinations of the linear polyurethanes will be obtained. Therefore, an average molecular weight range would be obtained to characterize the linear polyurethanes as opposed to an absolute value for the average molecular weight.

The first K_θ value was taken from a discussion on the relationship between K and a by Aharoni [16]. The Mark-Houwink-Sakurada constants have been found to be related by the equation

$$\log K = C - Ba \qquad (14)$$

where C and B are constants typical of each polymer. Hence, under theta conditions when the polymeric chain is in its unperturbed state, and the intrinsic viscosity is described by the equation

$$[\eta]_\theta = K_\theta \bar{M}^{1/2}$$

log K_θ can be calculated from

$$\log K_\theta = C - B/2 \qquad (15)$$

It is apparent that K_θ is a characteristic quantity of each polymer and can be obtained from log **K** versus **a** plots. For polystyrene, the constants **C** and **B** are given as 0.86 and 3.97 respectively, resulting in a value for K_θ of 75 x 10^{-5} $dl.g^{-1}$.

An extrapolation method for estimating K_θ, using the Mark-Houwink-Sakurada constants for polymers in "good" solvents was presented by Chee [17]. The use of relationships well known in polymer hydrodynamic and intrinsic viscosity theory allowed the author to derive an equation to describe K_θ which is applicable to systems in the vicinity of the theta state, or to systems involving polymer fractions of relatively low molecular weights if "good" solvents are used. Mathematical manipulation of the equations results in a linear relationship between ln[2(1-**a**)**K**] and (**a** – ½). Extrapolation of the straight line yields K_θ as is evident from

$$\ln[2(1-a)K] = \ln K_\theta - \ln M_o(a - ½) \qquad (16)$$

Linear least squares treatment of the data points for polystyrene resulted in a value for K_θ of 0.083 $ml.g^{-1}$ or 83 x 10^{-5} $dl.g^{-1}$.

McCrackin [18] discussed Han's relationship between intrinsic viscosity and molecular weight, and proceeded to test the equation for 5 polymer-solvent systems. Han's theory stated that intrinsic viscosity is of the form $[\eta]_\theta = K_\theta \bar{M}^{½}$ for molecular weights less than a given molecular weight M_1, whereas for larger molecular weights the intrinsic viscosity increases more rapidly with molecular weight. In his study, McCrackin used the equation

$$[\eta] = K_\theta \bar{M}^{½} F(M/M_1) \qquad (17)$$

which is based upon the relationship derived by Han [19], and may be written as

$$[\eta]/[\eta]_o = F(M/M_1) \qquad (18)$$

The function $F(M/M_1) = 1$ for $M < M_1$, but for $M > M_1$

$$F(M/M_1) = \frac{4/3x^{1/2}\{x^{-2}(3 - 2/x) + 6x^{1/5}[5/11(1 - x^{-11/5}) - 5/16\,(1 - x^{-16/5})]\}}{\{2(1 - 1/3x) + 5/2(x^{2/5} - 1) - 5/7(x^{2/5} - x^{-1})\}} \qquad (19)$$

where $x = M/M_1$. The values of K_θ and M_1 for polystyrene in tetrahydrofuran (THF) were given by McCrackin as 0.0968 ml.g^{-1} and 11000 respectively. The curve described by Han's equation using these values, give an excellent fit to the plotted data from measurements of intrinsic viscosity of polystyrene in THF.

(g) Procedure Followed for Molecular Weight Determination of the Linear Polyurethanes by GPC

The retention times of the "monodisperse" polystyrene standards were determined by elution through the GPC columns under the same conditions used for the polyurethane samples. A typically narrow elution chromatogram for the standards is shown in Figure 3.13.

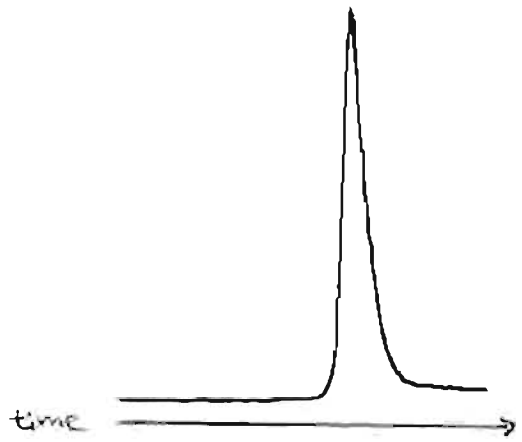

FIGURE 3.13 Elution chromatogram of polystyrene standard with M = 50 000.

The intrinsic viscosities of the series of polystyrene standards were calculated for each K_θ value obtained in the literature, using equation (12). A calibration curve of log[η]M versus R_t was constructed for each set of $[\eta]_\theta$ values. The results of the $[\eta]_\theta$ calculations and the data used for construction of the calibration curves are tabulated and shown in Table 3.10. A typical calibration curve is shown in Figure 3.14.

Table 3.10 The $[\eta]_\theta$ ($dl.g^{-1}$) **of polystyrene standards and data used for the calibration curves.**

		$[\eta]_\theta = 75 \times 10^{-5} \bar{M}^{1/2}$		$[\eta]_\theta = 83 \times 10^{-5} \bar{M}^{1/2}$		$[\eta]_\theta = 96.8 \times 10^{-5} \times \bar{M}^{1/2} F(M/M_1)$	
		ref. [16]		ref. [17]		ref. [18]	
M	R_t (min)	[η]	log [η]M	[η]	log[η]M	[η]	log[η]M
1350	18.52	0.0276	1.571	0.0305	1.615	0.0356	1.681
1830	18.21	0.0321	1.789	0.0355	1.813	0.0414	1.880
3300	17.70	0.0431	2.153	0.0477	2.197	0.0556	2.264
9500	16.28	0.0731	2.842	0.0809	2.886	0.0943	2.953
19750	15.49	0.1054	3.318	0.1166	3.362	0.1391	3.439
50 000	14.22	0.1677	3.924	0.1856	3.968	0.2578	4.110

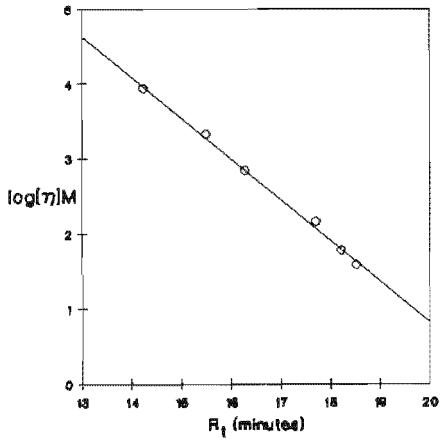

FIGURE 3.14 Calibration curve of log[η]M vs. R_t. $[\eta]_\theta$ of polystyrene standards calculated from $[\eta]_\theta = 75 \times 10^{-5} \bar{M}^{1/2}$ [16].

After elution of the linear polyurethane samples, the GPC data module (that is, the computerized data processor attached to the liquid chromatograph) divided the chromatogram into narrow "slices" and integrated the area under each slice. An example of a linear polyurethane chromatogram is shown in Figure 3.15.

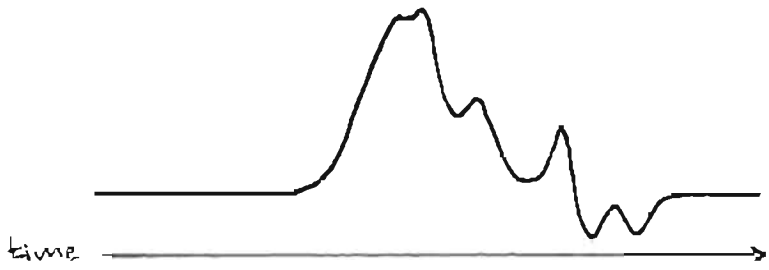

Figure 3.15 GPC chromatogram of Pol400U(1:2).

The data module also calculated the molecular weight averages and the dispersity of the polymer sample from a log**M** versus R_t calibration curve (that is, not a universal calibration curve) after the **M** and R_t values had been entered. The "slice" areas are necessary for calculation of the molecular weight averages. For instance, $\bar{M}_n$ is calculated as follows:

$$\bar{M}_n = \frac{\Sigma(\text{area}_i)}{\Sigma(\text{area}_i)/M_i} \qquad (20)$$

where area_i = the area of the i^{th} slice

M_i = the average molecular weight of the i^{th} slice

The molecular weight averages were manually calculated from the universal calibration curves mentioned above. For these calculations both the "slice" areas provided by the data module and the equations defined for $\bar{M}_n$ and $\bar{M}_w$ by the liquid chromatograph manual (see the experimental section) were utilized.

A definite resolution of species was evident in some of the chromatograms, especially in those of the (1:2)-polyurethanes (that is, polyurethanes that had been synthesized from a 1:2 NCO:OH ratio). Therefore, the molecular weight represented by each peak maximum of a chromatogram was evaluated and the corresponding degree of polymerization, x, was calculated.

(h) Results and Discussion of Molecular Weight Determination By GPC, Using a Universal Calibration Method

The results of the GPC molecular weight determinations are summarized in Table 3.11, which presents:

a) the molecular weight averages derived by the universal calibration method employing published $\mathbf{K}_\theta$ values for calculating the $[\eta]_\theta$ of the polystyrene standards,
b) the molecular weight averages obtained directly from the GPC data module, without universal calibration,
c) the molecular weights and degrees of polymerization, x, represented by each peak maximum,
d) the retention time of the reactant glycol from which the particular polyurethane had been synthesized.

The mean of the molecular weight averages obtained by the universal calibration method were calculated with a 95% confidence limit [20] and are tabulated in Table 3.12.

Table 3.11 Results of the molecular weight determinations by gel permeation chromatography.

		without universal calibration					with universal calibration													
		GPC Data Module					Ref.[16] ,K_θ = 75 x 10^{-5} dl/g					Ref.[17], K_θ = 83 x 10^{-5} dl/g					Ref.[18], K_θ = 96.8 x 10^{-5} dl/g				
Polyurethane	$R_{t(p)}$	$\bar{M}_n$	$\bar{M}_w$	D	M_p	x	$\bar{M}_n$	$\bar{M}_w$	D	M_p	x	$\bar{M}_n$	$\bar{M}_w$	D	M_p	x	$\bar{M}_n$	$\bar{M}_w$	D	M_p	x
Pol150U (1:2)	18.70	622	978	1.57	1118	3.0	466	784	1.68	858	2.2	516	867	1.68	950	2.5	569	977	1.72	1074	2.9
[η] = 0.0392 dl/g	18.98				844	2.1				604	1.4				669	1.6				749	1.8
(R_t of triethylene	19.38				505	1.1				366	0.7				405	0.8				448	0.9
glycol = 21.55 min.)	20.05				208	0.2				158	0				175	0.1				189	0.1
Pol194U (1:2)	17.80	1524	3015	1.98	2795	7.1	573	1601	2.79	1238	2.8	634	1772	2.79	13.70	3.2	714	2098	2.94	1595	3.8
[η] = 0.0840 dl/g	18.05				2196	5.4				905	1.9				1001	2.2				1156	2.6
(R_t of tetraethylene	18.43				1453	3.5				562	1.0				622	1.2				709	1.4
glycol = 21.32 min.)	18.90				894	1.9				312	0.3				345	0.4				387	0.5
	19.60				382	0.5				130	0				143	0				157	0
Pol400U (1:2)	18.56	625	1375	2.20	1301	1.6	414	1035	2.50	873	0.82	461	1146	2.49	967	1.0	503	1319	2.62	1098	1.2
[η] = 0.0459 dl/g	19.09				717	0.6				449	0.1				497	0.2				555	0.3
(R_t of PEG400	20.25				156	0				105	0				116	0				125	0
= 20.29 min.)																					
Pol400U (1:1)	16.33	4891	12344	2.52	9899	16.5	1648	11100	6.74	5661	9.2	1823	12284	6.74	6266	10.2	2106	15551	7.38	7653	12.6
[η] = 0.1160 dl/g	20.26				154	0				41	0				45	0				49	0
(R_t of PEG400																					
= 20.29 min.)																					
Pol1500U (1:2)	17.30	2068	3055	1.03	4411	1.7															
(R_t of PEG1500	18.26				1779	0.2															
= 18.46 min.)																					
Pol1500U (1:1)	16.00	6420	13030	2.03	12824	6.8															
(R_t of PEG1500	17.15				5028	2.1															
= 18.46 min.)	18.25				1798	0.2															
Pol6000U (1:1)	15.50	9159	10937	1.19	18819	3.0															
	16.22				10798	1.7															

$R_{t(p)}$, M_p, x refer respectively to the retention times, molecular weights and degrees of polymerization for the peak maxima that were resolved.

TABLE 3.12 The mean and the 95% confidence limits of the molecular weight averages calculated by universal calibration.

Polyurethane	$\bar{M}_n$	$\bar{M}_w$
Pol150U(1:2)	517 ± 128	876 ± 240
Pol194U(1:2)	640 ± 176	1823 ± 627
Pol400U(1:2)	459 ± 111	1167 ± 355
Pol400U(1:1)	1859 ± 574	12978 ± 5723

In considering the molecular weight averages of the polyurethane fractions shown in Table 3.11, the retention times of the fractions with the smallest molecular weights, {20.05 minutes for Pol150U(1:2) and 19.60 minutes for Pol194U(1:2)} do not correspond with the retention times of the reactant glycols (21.55 minutes for triethylene glycol and 21.32 minutes for tetraethylene glycol). The shorter retention times of the smallest molecular weight fractions imply that these fractions have larger molecular weights than the reactant glycols, and should represent at least x = 1. It would seem, therefore, that the GPC method employed, resulted in an underestimation of the molecular weight averages. The same considerations may be applied to Pol1500U(1:2) and Pol1500U(1:1).

The retention times of the smallest molecular weight fractions of Pol400U(1:2) and Pol400U(1:1), (20.25 minutes and 20.26 minutes respectively) are fairly similar to the retention time of the reactant glycol (20.29 for PEG400). Hence, it may be assumed that a significant amount of reactant glycol is present in both Pol400U(1:2) and Pol400U(1:1). $\bar{M}_n$ is highly sensitive to the presence of a small number fraction of low molecular weight material, while $\bar{M}_w$ is sensitive to small amounts by weight of high molecular weight fractions [8]. It may be expected, therefore, that the

presence of unreacted glycol of low molecular weight might negatively influence the value of $\bar{M}_n$. Thus, in addition to the underestimation mentioned above, the value of $\bar{M}_n$ for Pol400U(1:2) and Pol400U(1:1) may further be expected to be too low.

It appears, therefore, that the molecular weight determination by GPC using the hydrodynamic volume correlation as the universal calibration method was not entirely successful. Possibly, one might ascribe the apparent failure to ill-defined intrinsic viscosities of the polystyrene standards which were not measured, but calculated. The published $\mathbf{K}_\theta$ values obtained for calculating the above-mentioned intrinsic viscosities were never in agreement [16-18]. In addition, although the polystyrene standards were of a relatively low molecular weight, it is possible that they did not exist entirely in the unperturbed state. In this regard, physical measurements of the intrinsic viscosities of the polystyrene standards for construction of the $\log[\eta]M$ versus $\mathbf{R}_t$ calibration curve may have resulted in a more accurate determination, and such measurements ought to have been undertaken. However, the prohibitive cost of these standards prevented this.

The most likely reason for the failure of the universal calibration method used in the present study was found in a report by Tung and Moore [21]. These authors refer to two reported exceptions to the hydrodynamic volume correlation. One exception was reported for polymers in theta or very poor solvents (no explanation was given). It would seem that our results are in keeping with this finding. Although tetrahydrofuran is not necessarily a poor solvent for polystrene or the soluble linear polyurethanes, the relatively low molecular weight polymers used in this work most probably behaved as if they were in theta solvents.

(i) Inclusion of Retention Data for the Reactant Polyethylene Glycols in a Plot of logM versus R_t

It was noticed that when the retention data for the polyethylene glycols (used as starting materials for the synthesis of the linear polyurethanes) was added to that of the polystyrene standards in a plot of logM versus $\mathbf{R_t}$, a relatively good linear correlation was obtained.

Since the polyethylene glycols are chemically similar to the polyurethanes, their inclusion into the logM versus $\mathbf{R_t}$ plot (as compared to a plot containing only polystyrene standards) should provide improved calibration for the determination of the molecular weight of the linear polyurethanes. Hence, the calibration curve which had been constructed from polystyrene as well as polyethylene glycol data was used and the molecular weight averages, as well as the molecular weights and degrees of polymerization represented by each peak maximum, were recalculated. The unprocessed data may be found in Appendix 1. Figure 3.16 and Table 3.13 report the calibration curve and the tabulated molecular weight results respectively. In Table 3.13 the results using a polystyrene/polyethylene glycol calibration curve are compared to the results obtained using only polystyrene standards (the latter results were obtained directly from the GPC data module which used a plot of logM versus $\mathbf{R_t}$ for calibration).

The inclusion of the polyethylene glycol data into the logM versus $\mathbf{R_t}$ plot altered the slope from –0.3630 to –0.3449. The polystyrene/polyethylene glycol calibration curve yielded more realistic results for the linear polyurethanes that had been synthesized from glycols with molecular weights of up to 400. As mentioned above (Section 2.3(i)*h*), no evidence of the glycol starting material was found in the

chromatograms of Pol150U(1:2) and Pol194U(1:2). Therefore, values for x of approximately 1 for the smallest molecular weight fractions of these polyurethanes are consistent with the observed absence of the glycol starting material.

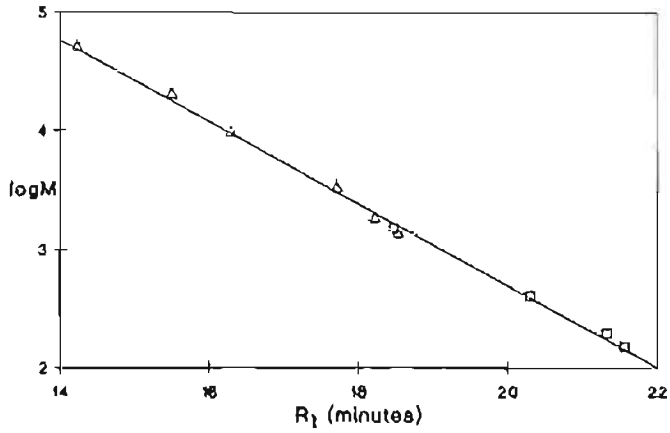

FIGURE 3.16 **A calibration curve of logM versus R_t constructed from polyethylene glycol and polystyrene standard retention data. (Δ = polystyrene standards, □ = polyethylene glycols.)**

Values of around 400 for the smallest molecular weight fractions of Pol400U(1:2) and Pol400U(1:1) are consistent with the observation that these polyurethanes contain a substantial amount of the reactant glycol. However, underestimation of the molecular weights of Pol1500U(1:2) and Pol1500U(1:1) {and, therefore, probably Pol6000U(1:1)} still appears to be evident, since the smallest molecular weight fractions have values for x of 0.3. These fractions (R_t = 18.25 and 18.26 min.) are unlikely to contain only the reactant glycol, since the retention time of PEG1500 was measured to be 18.46 minutes. It is not certain whether the presence of impurities in the glycols used for the synthesis of the polyurethanes caused a shift in the peak maximum, thus masking the presence of any reactant glycol that may be in the polyurethane sample.

Table 3.13 Results of molecular weight determinations using a plot of logM versus R_t for calibration.

		Polystyrene Standards					Polystyrene/Polyethylene Glycol Standards				
Polyurethane	$R_{t(peak)}$	$\bar{M}_n$	$\bar{M}_w$	D	M_{peak}	x	$\bar{M}_n$	$\bar{M}_w$	D	M_{peak}	x
Pol150U (1:2)	18.70	622	978	1.57	1118	3.0	1000	1235	1.23	1386	3.8
$[\eta]$ = 0.0392 dl/g	18.98				844	2.1				1109	3.0
(R_t of triethylene	19.38				505	1.1				808	2.0
glycol = 21.55 min.)	20.05				208	0.2				474	1.0
Pol194U (1:2)	17.80	1524	3015	1.98	2795	7.1	1976	3018	1.53	2832	7.2
$[\eta]$ = 0.0840 dl/g	18.05				2196	5.4				2322	5.8
(R_t of tetraethylene	18.43				1453	3.5				1717	4.1
glycol = 21.32 min.)	18.90				894	1.9				1182	2.7
	19.60				382	0.5				678	1.3
Pol400U (1:2)	18.56	625	1375	2.20	1301	1.6	1085	1581	1.46	1549	2.0
$[\eta]$ = 0.0459 dl/g	19.09				717	0.6				1017	1.1
(R_t of PEG400	20.25				156	0				405	0.0
= 20.29 min.)											
Pol400U (1:1)	16.33	4891	12344	2.52	9899	16.5	5176	11673	2.26	9098	15.2
$[\eta]$ = 0.1160 dl/g	20.26				154	0				402	0.00
(R_t of PEG400											
= 20.29 min.)											
Pol1500U (1:2)	17.30	2068	3055	1.03	4411	1.7	2328	3060	1.31	4212	1.6
(R_t of PEG1500	18.26				1779	0.2				1965	0.3
= 18.46 min.)											
Pol1500U (1:1)	16.00	6420	13030	2.03	12824	6.8	6541	12259	1.87	11823	6.2
(R_t of PEG1500	17.15				5028	2.1				4744	1.9
= 18.46 min.)	18.25				1798	0.2				1981	0.3
Pol6000U (1:1)	15.50	9159	10937	1.19	18819	3.0	8570	10119	1.18	17583	1.9
	16.22				10798	1.7				9926	0.6

$R_{t(peak)}$, M_{peak}, x refer respectively to the retention times, molecular weights and degrees of polymerization for the peak maxima that were resolved.

2.3 (ii) ^{1}H nmr

Quantitative ^{1}H nmr is a potentially useful tool for estimating an average chain length of the linear polyurethanes. This method provides the number average molecular weight ($\bar{M}_n$) [13], and will be shown to have more meaning for the (1:2)-polyurethanes (that is, polyurethanes synthesized from a 1:2 ratio of isocyanate to hydroxyl ratio), than their (1:1) counterparts, since certain simplifying assumptions can be made.

(a) ^{1}H nmr of (1:2)-Polyurethanes

The highly reactive nature of the isocyanate group, as well as the excess of glycol in the reaction mixture during synthesis of the polyurethanes, allows the reasonable assumption that almost all the polyurethane chains will terminate in hydroxyl groups. The linear polyurethanes can be presented, therefore, by the general formula shown in Figure 3.17.

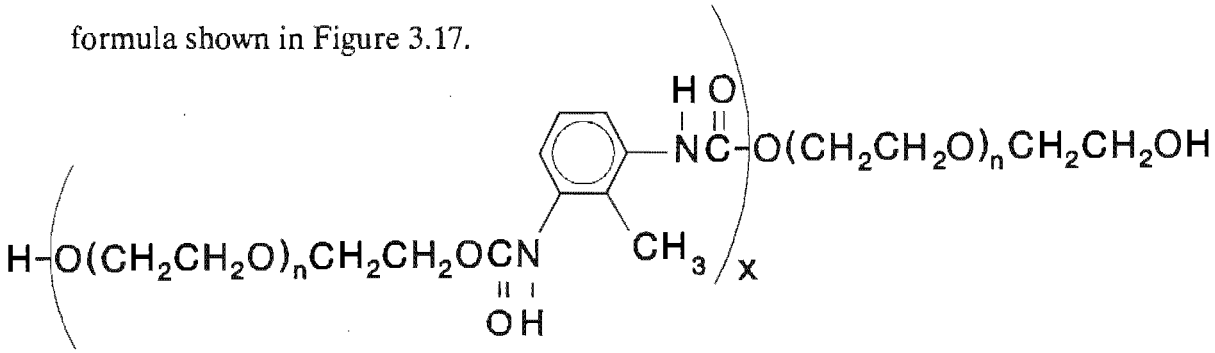

Figure 3.17 General formula for the (1:2)-polyurethanes. (Only the 2,6-toluene diisocyanate derivative is shown for simplicity.)

Since the number of tolyl-methyl protons (MP) increases linearly with the degree of polymerization, x, the ratio of ethylene oxide protons (EOP) to MP can be considered a measure of x.

Although the same argument may be used for the ratio of EOP to aromatic protons, the calculations were confined to the ratios of EOP:MP.

Theoretical values for the EOP:MP ratios were calculated and plotted for increasing values of x. The calculations and plots are contained in Appendix 3. The experimental and calculated ratios were compared to yield a corresponding value of x. To illustrate the determination of x and $\bar{M}_n$ by quantitative ^{1}H nmr, the graphical estimation for Pol400U(1:2) is shown in Figure 3.18.

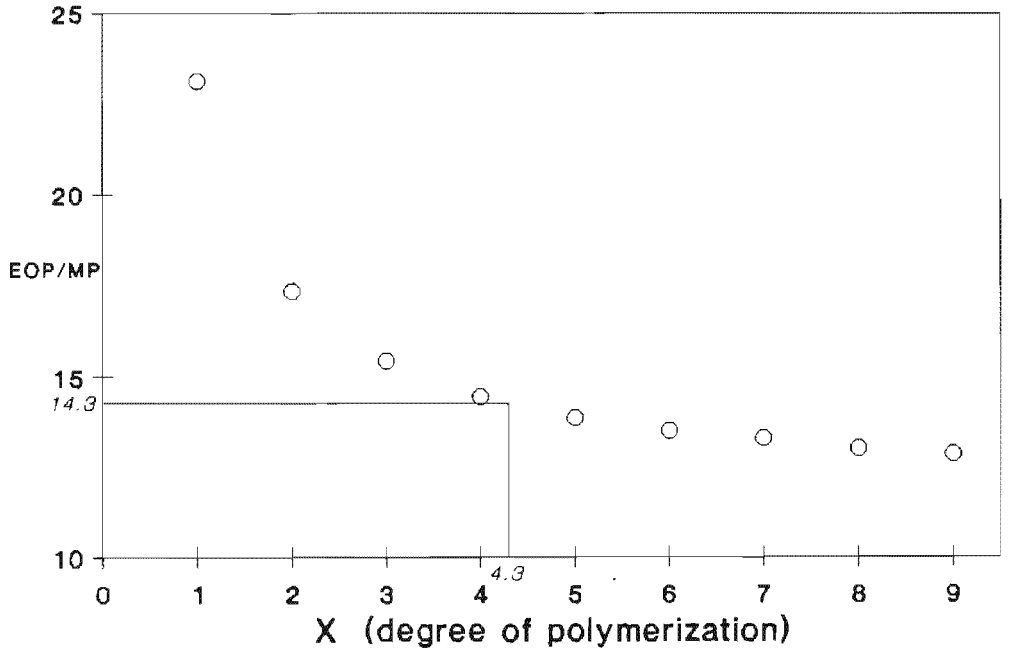

FIGURE 3.18 Graphical estimation of $\bar{x}$ and $\bar{M}_n$ of Pol400U(1:2) by quantitative ^{1}H nmr.

The experimentally determined EOP:MP ratio of 14.3 was translated to a value for x of 4.3 with the aid of the plot of theoretical EOP:MP ratios versus x. This value represents an average degree of polymerization, x, and corresponds to a number average molecular weight of 2868 (see Appendix 3 for the calculations).

The results for the molecular weight determinations of the (1:2)-polyurethanes by ^{1}H nmr are presented in Table 3.14.

Table 3.14 Average degree of polymerization, $\bar{x}$, and the $\bar{M}_n$ of (1:2)-polyurethanes as determined by ^1H nmr.

(1:2)-polyurethane	$\bar{x}_{nmr}$	$\bar{M}_n$
Pol150U(1:2)	2.8	1058
Pol194U(1:2)	4.5	1852
Pol400U(1:2)	4.3	2868

The proton nmr spectra for Pol1500U(1:2) were not suitable for these calculations, since the enormously intense resonances of the ethylene oxide protons resulted in dynamic range problems (due to the limited range of the A/D converter of the nmr spectrometer) in that the relatively weak methyl proton signals were poorly defined with a consequent large error in the relative integral ratios.

(b) ^1H nmr of the (1:1)-Polyurethanes

The prefix (1:1) indicates that equimolar quantities of isocyanate and glycol were present during synthesis of the polymers. In this case it is no longer reasonable to assume that all the polymer chains will terminate in hydroxyl groups. Considering the reactivity of the isocyanate group, it is feasible that a terminal toluene diisocyanate (TDI) group would "tail-bite" either,

a) another chain with a terminal hydroxyl group, resulting in an extended linear chain, or

b) the terminal hydroxyl group on the opposite end of the same chain in which the mentioned terminal TDI group occurs, resulting in the formation of a circular chain.

Any remaining terminal isocyanate group would have been converted to an amine by the purification step in which the polymer was washed with water in order to remove any unreacted glycol. The species likely to be formed are presented schematically in Figure 3.19. (Note: we shall confine our discussion to Pol400U(1:1) as adequate illustration of this class of linear polyurethanes.)

Synthesis of the macrocyclic coronands requires cyclization assistance (referred to as the template effect) by cation catalysis [3]. Hence, it is reasonable to assume that tail-biting to form a circular chain should be energetically and entropically unfavourable and negligible. Thus, we can propose three series of polymeric chains with the following general schematic formulae:

Series a: TH-(DU-PEO)$_x$-TA

Series b: TA-PEO-(DU-PEO)$_x$-TA

Series c: TH-(DU-PEO)$_x$-DU-TH

The theoretical EOP:MP ratio for *series a* is constant at 11.6. In contrast *series b* has an EOP:MP ratio of 5.8 for x = 0, the value increasing with increasing x, while *series c* begins with an EOP:MP ratio of 23.1 for x = 0, and the value decreases with increasing x (see Appendix 3 for the calculations).

From the nmr integration, an experimental EOP:MP ratio of 11.2 at 30 °C and 11.3 at 50 °C was obtained. The only meaningful interpretation would be to consider the spectrum originating wholly from *series b*. From a comparison of the EOP:MP ratios obtained with the theoretical values of *series b* a value of EOP:MP = 11.2 indicates x = 30.9 ($\bar{M}_n$ = 18475), whereas that of EOP:MP = 11.3 indicates x = 45.9 ($\bar{M}_n$ = 27079). We could therefore approximate 31 < x < 46.

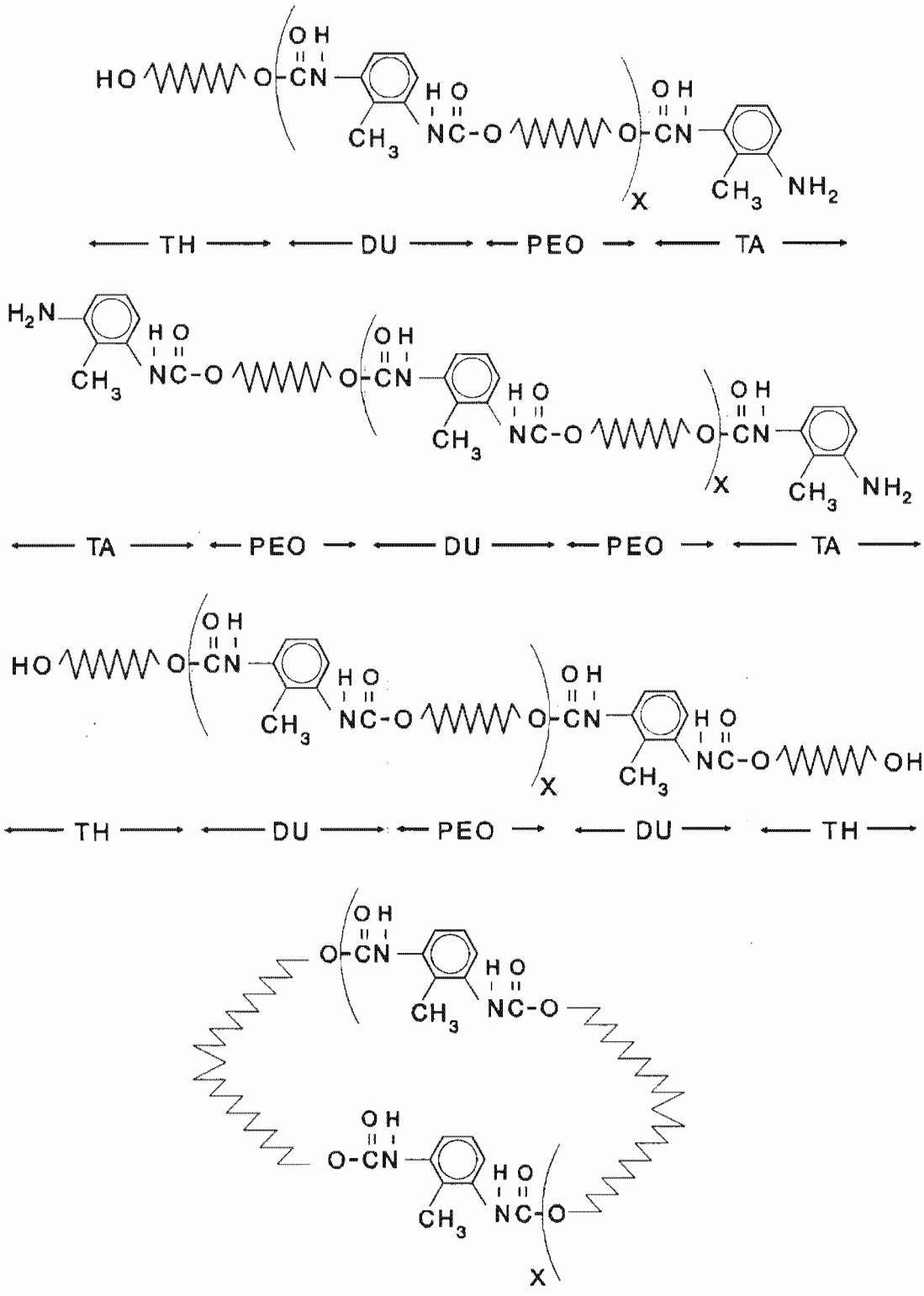

PEO = poly(ethylene oxide)

TH = terminal hydroxyl group

DU = diurethane group

TA = terminal amino group

Figure 3.19 Schematic representation of the (1:1)-polyurethane species that may be formed.

However a substantial amount of *series a* (with an EOP:MP ratio = 11.561 for all values of x) and of *series c* are both likely to have contributed to the overall EOP:MP value obtained from the ^{1}H nmr spectrum. The constant EOP:MP ratio for *series a* makes it of no practical use, while for *series c* the EOP:MP ratio value of 11.3 indicates that $x >>> 2000$ and $\mathbf{M} >>> 1.15 \times 10^6$. These enormously high values are unrealistic when compared to the GPC analyses where the peak maximum indicates $\mathbf{M} \sim 10\,000$.

It is evident, therefore, that no conclusive indication of the degree of polymerization may be adduced, and consequently the molecular mass of Pol400U(1:1) can not be obtained from the ^{1}H nmr spectrum.

2.3 (iii) Conclusion of the Molecular Weight Determination

An overview of the findings of the molecular weight determinations would facilitate a meaningful conclusion. Hence the results have been summarized in Table 3.15. Since the most reliable GPC results were obtained from a log**M** versus $\mathbf{R_t}$ calibration curve {which was constructed from the data of polystrene standards as well as poly(ethylene oxide) glycols}, only these GPC results are shown.

Very good agreement in the results obtained by GPC and by ^{1}H nmr was achieved for Pol150U(1:2) and Pol194U(1:2). Hence the molecular weight averages and the average degrees of polymerization ($\bar{x}$) determined for these two polyurethanes may be reported with confidence.

Table 3.15 Results of the molecular weight determinations.

	gel permeation chromatography		^{1}H nmr	
polyurethane	$\bar{M}_n$ ($\bar{x}$)	$\bar{M}_w$	$\bar{x}$	$\bar{M}_n$
Pol150U(1:2)	1000 (2.6)	1235	2.8	1058
Pol194U(1:2)	1976 (4.8)	3018	4.5	1852
Pol400U(1:2)	1085 (1.2)	1581	4.3	2868
Pol1500U(1:2)	2328 (0.5)	3060		
Pol400U(1:1)	5176 (8.3)	11673		
Pol1500U(1:1)	6541 (3.0)	12259		
Pol6000U(1:1)	8570 (0.4)	10119		

The relatively low molecular weights determined for Pol400U(1:2) by GPC can be ascribed to the presence of a substantial amount of the reactant glycol (which became evident from the chromatogram). Prior to the ^{1}H nmr determination, the polyurethanes were dissolved in chloroform and thoroughly washed with water. Therefore, the results obtained by the nmr method for Pol400U(1:2) should be a more accurate reflection of the molecular weight of that polyurethane. The GPC results should similarly be an underestimation of Pol400U(1:1), since the presence of PEG400 was also observed in the chromatogram of the latter polyurethane. From the GPC results, it is evident that the (1:1)-polyurethanes have significantly larger molecular weights than their (1:2)-counterparts. This finding is consistent with the larger intrinsic viscosity measured for Pol400U(1:1) ($[\eta]$ = 0.1160 dl.g^{-1}) relative to that measured for Pol400U(1:2) ($[\eta]$ = 0.0459 dl.g^{-1}). If one accepted the values for $\bar{M}_n$ and $\bar{x}$ as determined by ^{1}H nmr, and used the relative molecular weights of the (1:2)- and (1:1)-polyurethanes as determined by GPC, then $\bar{M}_n$ for Pol400U(1:1) may proportionately be estimated to be 13682 ($\bar{x}$ = 23). From our results (see Table 3.15) it appears that the (1:2)-polyurethanes have an average

degree of polymerization in the range 2 to 5. Since underestimation of the molecular weight of Pol1500U(1:2) is suspected, we may estimate a similar degree of polymerization for this polyurethane. Values for $\bar{x}$ of 2 to 5 correspond to a number average molecular weight range of 4850 - 9875 for Pol1500U(1:2). Therefore, the molecular weight averages ($\bar{M}_n$) of Pol1500U(1:1) may proportionately be estimated to be in the range 15050 – 30641 ($\bar{x}$ = 8 - 17). Although we could not claim to have determined the average molecular weights of all the linear polyurethanes accurately, we are nevertheless able to estimate the order of the magnitude of the number average molecular weights of Pol400U(1:1) and Pol1500U(1:2) and Pol1500U(1:1).

A final summary of the number average molecular weights, $\bar{M}_n$, and the average degree of polymerization, $\bar{x}$, including the "best" estimates for Pol400U(1:1), Pol1500U(1:2) and Pol1500U(1:1) is given in Table 3.16.

Table 3.16 A final summary of $\bar{M}_n$ and $\bar{x}$.

polyurethane	$\bar{x}$	$\bar{M}_n$
Pol150U(1:2)	2.7	1026
Pol194U(1:2)	4.7	1907
Pol400U(1:2)	4.3	2868
Pol1500U(1:2)	~2 - 5	~480 - 9875
Pol400U(1:1)	~23	~13682
Pol1500U(1:1)	~8 - 17	~15050 - 30641

It should be mentioned that it has become clear after the molecular weight determinations that the term oligourethanes would strictly be more correct than the term polyurethanes. However, the term polyurethanes, and the abbreviated

nomenclature, for example, Pol400U(1:2), shall be retained throughout this work for consistency.

REFERENCES

1 R.F.HAMON, A.S.KHAN AND A.CHOW,
Talanta, **29** (1982) 313

2 D.J.DAVID AND H.B.STALEY,
"Analytical Chemistry of the Polyurethanes", High Polymers,
16(III), John Wiley, (1969)

3 E.WEBER AND F.VÖGTLE,
"Host Guest Complex Chemistry/ Macrocycles",
Springer-Verlag, Berlin, (1985) p1

4 A.ŠEBENIK, U.OSREDKAR AND I.VIZOVIŠEK,
J. Macromol. Sci.-Chem., **A23** (1986) 369

5 F.W.WEHRLI AND T.WIRTHLIN,
"Interpretation of Carbon-13 NMR Spectra",
Hyden and Son, London, (1978)

6 J.W.AKITT,
"NMR and Chemistry", 2nd ed., Chapman and Hall, London, (1983)

7 H.R.ALLCOCK AND F.W.LAMPE,
"Contemporary Polymer Chemistry", Prentice-Hall, New Jersey, (1981)

8 E.A.COLINS, J.BAREŠ AND F.W.BILLMEYER,
"Experiments in Polymer Science", John Wiley, (1973)

9 Waters Liquid Chromatorgaph Manual

10 A.Einstein,
Ann. Physik, **19** (1906) 289

11 K.A.BONI, F.A.SLIEMERS and P.B.STICKNEY,
J. Pol. Sc., **Part A-2**(6) (1968) 1579

12 Z.GRUBISIC, P.REMPP and H.BENOIT,
Pol. Lettr., **5** (1967) 753

13 T.ALTARES, D.P.WYMAN AND V.R.ALLEN,
J. Pol. Sc., **Part A-2** (1964) 4533

14 U.BIANCHI, M.DALPIAZ AND E.PATRONE,
Makromol. Chem., **80** (1964) 112

15 M.KURATA AND W.H.STOCKMAYER,
Fortschr. Hochpolym.-Forsch., **3** (1963) 196

16 S.M.AHARONI,
J. Applied Pol. Sc., **21** (1977) 1323

17 K.K.CHEE,
Pol. Commun., **27** (1986) 135

18 F.L.MCCRACKIN,
Polymer, **28** (1987) 1847

19 C.C.HAN,
Polymer, **20** (1979) 1083

20 J.C.MILLER AND J.N.MILLER,
"Statistics for Analytical Chemistry",
John Wiley, Chichester, (1984)

21 L.H.TUNG and J.C.MOORE,
"Gel Permeation Chromatography" in *"Fractionation of Synthetic Polymers"*, ed. L.H.Tung, Marcel Dekker, New York, (1977), p585

CHAPTER 4

EXTRACTION BY THE MODEL URETHANE COMPOUNDS AND BY THE 100% POLY(PROPYLENE-OXIDE) BASED POLYURETHANE FOAM

1. Model Urethane Compounds

The urethane compounds characterized in Chapter 3 were intended to serve as models of the polyurethane foam, to simplify the study of the rhodium extraction process. Based on the reported extraction capabilities of the polyethylene glycols [1,2] it seemed likely that these model urethane compounds would extract metal complexes from aqueous solutions. However, the extent of the extraction capabilities of the model urethane compounds, as well as the dependance of their extraction capabilities on the nature of the individual urethane compounds, had not been tested experimentally. Therefore, it was decided to perform a preliminary investigation into the extraction of cobalt from thiocyanate medium using the above-mentioned urethane compounds. Cobalt was chosen initially because of its relatively low cost, and the relative simplicity of the extraction system. In the presence of excess thiocyanate, the aqueous cobalt containing solution contains mainly pink octahedral $[Co(NCS)_4(H_2O)_2]^{2-}$ anions. It has been fairly well established that the blue tetrahedral $[Co(NCS)_4]^{2-}$ species is extracted by organic solvents, as well as by polyurethane foam [3,4]. Following the preliminary investigation, we sought to study the more complex extraction of the trichlorostannato complexes of rhodium by the model urethane compounds. It was hoped that this study would facilitate a better understanding of the extraction of metal complexes, and in particular trichlorostannato-rhodium complexes, by polyurethane foam.

1.1 The Extraction of Cobalt from Thiocyanate Medium

These studies were performed by shaking organic solutions of the urethane compounds together with the cobalt thiocyanate containing aqueous phases in sealed test tubes. The cobalt concentration of the aqueous phase was (after

appropriate dilution of the aqueous phase with acetone or ethanol) then determined by visible photometric measurement of the blue colour at 620 nm. The amount of cobalt that had been extracted by the organic phase was calculated by difference.

1.1(i) The Extraction of Cobalt by Pol400U(1:2) from Thiocyanate Solutions Varying in Cobalt Concentration

The extraction of $[Co(NCS)_4]^{2-}$ by 0.120 ± 0.001 g of Pol400U(1:2) dissolved in 1 ml of acetone was studied using 2 M KSCN solutions containing 0.02 to 0.10 M $CoCl_2 \cdot 6H_2O$. The extraction of cobalt occurs by the spontaneous precipitation of the now poorly soluble polyurethane as a blue "gummy" substance, clearly containing the tetrahedral $[Co(NCS)_4]^{2-}$ complex.

This study demonstrated that Pol400U(1:2) possessed the capability of extracting relatively large amounts of $[Co(NCS)_4]^{2-}$ from neutral aqueous solutions. The results are illustrated in Figure 4.1.

An increase in $\mathbf{D'_m}$ (here defined as the amount of cobalt extracted per unit mass of urethane compound, in $mmol.g^{-1}$) is observed with increased concentration of cobalt in the aqueous phase, reaching a limiting value of 1.39 $mmol.g^{-1}$. Note that, although the samples and standards were subjected to identical treatment, the accuracy of the values for $\mathbf{D'_m}$ reported in this study are uncertain, since no correction was made for the partitioning of acetone between the aqueous phase and the polymer phase. A partitioning of acetone into the polymer phase will result in lowered absorbance values of the aqueous phase since the concentration of the acetone in the aqueous phase influences the intensity of the blue colour. However, the error would be approximately constant throughout the entire investigation since

the polymer concentration was kept constant and the variation in ionic strength due to the varying cobalt concentration is small in the presence of 2 M KSCN. Therefore, the observed trends are valid since the preliminary study was intended to be a semi-quantitative investigation.

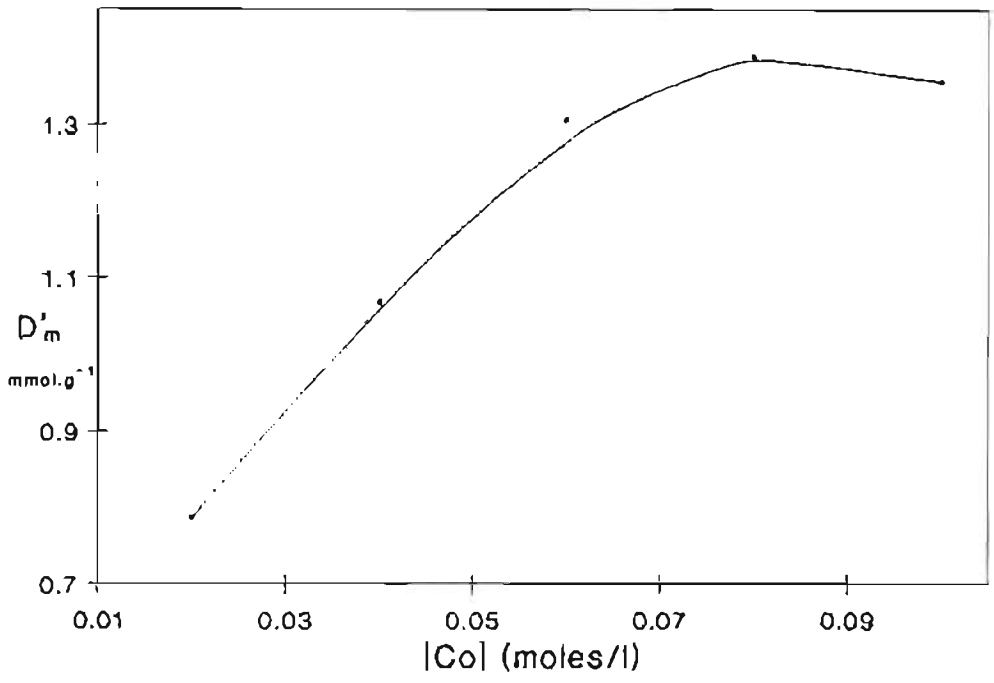

Figure 4.1 The effect of the initial aqueous cobalt concentration on the values for D'_m ($mmol.g^{-1}$).

1.1(ii) The Extraction of Cobalt from 2 M Thiocyanate Solutions by Varying Concentrations of Diϕ400U

The extraction of $[Co(NCS)_4]^{2-}$ by Diϕ400U dissolved in chloroform was studied. The concentration of Diϕ400U was varied from 0.01 to 0.10 $g.ml^{-1}$, while the aqueous phase comprised constant concentrations of $CoCl_2 \cdot 6H_2O$ (0.08 M) and KSCN (2 M) throughout the experiment. The results are illustrated in Figure 4.2.

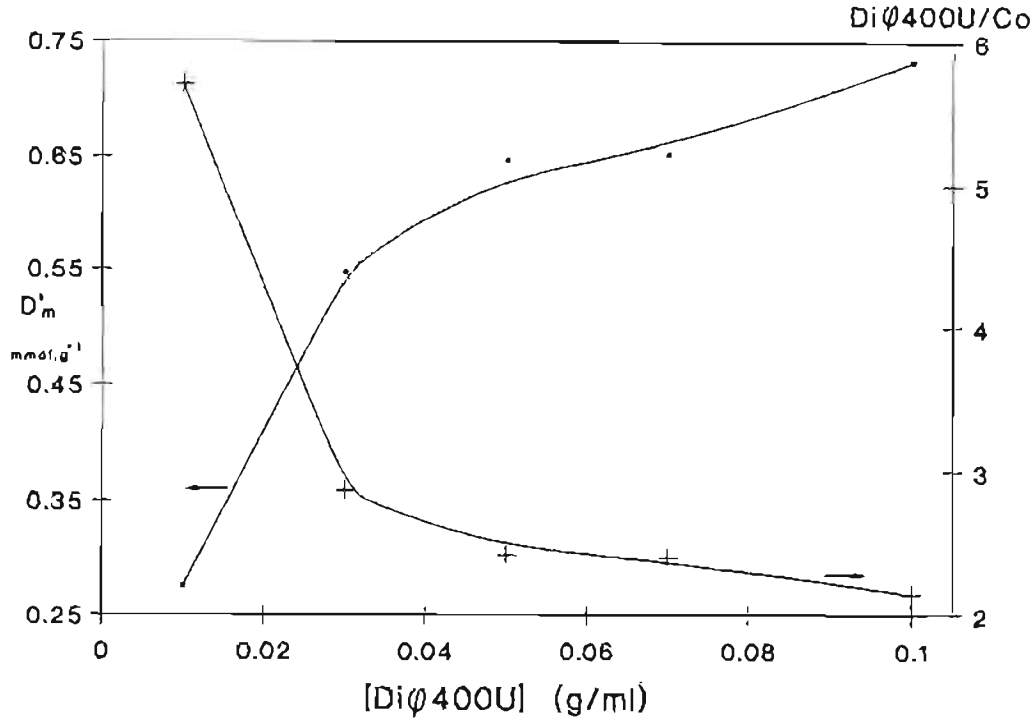

Figure 4.2 The effect of the Diϕ400U concentration on the partitioning of $[Co(NCS)_4]^{2-}$ between Diϕ400U and the aqueous phase.

Increased concentrations of Diϕ400U resulted in a steady increase in the values for D'_m, presumably due to a shift to the right in the partition reaction,

$$Di\phi400U + [Co(NCS)_4]^{2-} + 2K^+ \rightleftharpoons Di\phi400U[K_2Co(NCS)_4] \qquad (1)$$

The ratio of Diϕ400U to cobalt appears to approach a limiting value of 2. This observation is consistent with an extraction mechanism whereby each molecule of Diϕ400U chelates one K^+ cation. Hence two Diϕ400U cation chelates would facilitate the extraction of one $[Co(NCS)_4]^{2-}$ anion, and the partition reaction should probably be written more accurately as

$$2Di\phi400U + 2K^+ + [Co(NCS)_4]^{2-} \rightleftharpoons (KDi\phi400U)_2[Co(NCS)_4] \qquad (2)$$

1.1(iii) A Comparison of the Extraction Capabilities of Various Urethane Compounds

The extraction of cobalt by the diurethane podands, Diϕ150U, Diϕ194U and Diϕ400U, as well as by the soluble linear polyurethanes, Pol150U(1:2), Pol194U(1:2), Pol400U(1:2), Pol400U(1:1) and Pol6000U(1:1), from aqueous solutions containing 0.08 M $CoCl_2 \cdot 6H_20$ and 2 M KSCN was investigated. At the time of the study, the molecular masses of the polymers had not been determined. In an attempt to maintain equal concentrations of the urethane compounds the mass of each linear polyurethane used for the extraction was divided by the molar mass of its repeating unit, resulting in an approximate indication of the concentration of the repeating unit. Hence, extraction of cobalt was studied by using 0.2 $mol.dm^{-3}$ chloroform solutions of the diurethane podands, and by studying chloroform solutions of the linear polyurethanes with concentrations of the repeating units of approximately 0.2 $mol.dm^{-3}$. Due to the poor solubility of Pol6000U(1:1) a limiting concentration of 0.02 $mol.dm^{-3}$ of the repeating unit of Pol6000U(1:1) was used.

Two methods were used to illustrate the results of the present study (see Figure 4.3). Firstly, D'_m was plotted for each series of urethane compound against the value for n, the number of ethylene oxide units for each starting glycol. In addition, the percentage of the cobalt extracted from the aqueous phase (%E) per unit volume (2 ml) of the chloroform solutions of the urethane compounds was similarly compared for each urethane compound.

It becomes immediately evident that extraction by Diϕ150U and Diϕ194U (where n = 2 and 3, respectively, see Figure 3.2 of Chapter 3) is negligible, while a tremendously increased extraction capability of Diϕ400U (n = 7 - 8) is observed.

Therefore, there exists a critical value for n, below which significant extraction of metal complexes is not possible. Yanagida *et al.* [5] similarly reported that six to seven oxyethylene units seemed critical for the complexation of noncyclic poly(oxyethylene) derivatives with alkali metal ions. Qualitative tests showed that the cobalt complexes were solvent extracted from the solutions used in the present study by 4-methylpentan-2-one and, after acidification, by diethyl ether. However, even upon acidification, negligible extraction of cobalt by Diϕ150U and Diϕ194U was detected. From these results, we may conclude that extraction by the urethane compounds does not take place by a simple solvent extraction process, analogous to the extraction of metal species by diethyl ether. Instead, a mechanism is indicated, whereby chelation of cations by the poly(ethylene oxide) chains facilitate the extraction of anions.

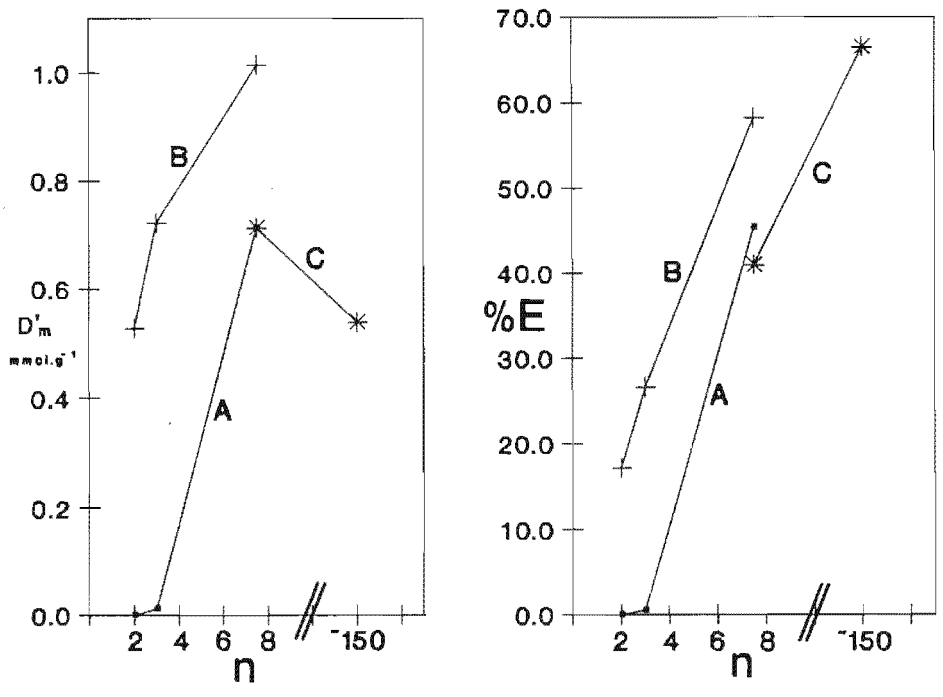

Figure 4.3 A comparison of the extraction capabilities of various urethane compounds. (A = diurethane podands, B = (1:2)-polyurethanes, C = (1:1)-polyurethanes).

Polymerization of tri- and tetraethylene glycol to form Pol150U(1:2) and Pol194U(1:2) (where n = 2 and 3 respectively, see Figure 3.3), results in linear polyurethanes with extracting powers several orders of magnitude higher than their diurethane podand counterparts. Hence, chain extension by the insertion of diurethane moieties gives rise to urethane derivatives of tri- and tetraethylene glycol with significant powers of extraction.

If the extraction efficiencies observed for the different (1:2)-polyurethanes are compared, a steady increase in extracting power is observed with increased oligoethylene chain length. The (1:1)-polyurethanes, that is Pol400U(1:1) (n = 7 - 8) and Pol6000U(1:1) (n = 130 - 170), also show an increased extracting power with increased oligoethylene chain length if one considers the percentage extraction observed. Pol6000U(1:1) shows a decreased value for $\mathbf{D'}_m$ relative to that for Pol400U(1:1). However, the mass of Pol6000U(1:1) used for the extraction was far greater than that used of Pol400U(1:1), (0.494 g/2 ml as opposed to 0.230 g/2 ml), even though only about 0.02 $mmol.g^{-1}$ of repeating unit was soluble for Pol6000U(1:1). Therefore, the decreased value for $\mathbf{D'}_m$ may largely be due to a far larger denominator in the equation

$$\mathbf{D'}_m = \frac{\text{mmol of cobalt}}{\text{mass of urethane compound}} \ (mmol.g^{-1})$$

for Pol6000U(1:1) and does not necessarily reflect a lower extracting power.

Chain extension by the insertion of diurethane moieties improved extraction in progressing from the diurethane podands to the (1:2)-polyurethanes. However, the improved extraction efficiency with an increased degree of polymerization appears to reach a limit, after which further chain extension has an inhibiting effect on

extraction. Hence, Pol400U(1:1) exhibited a significantly lower extracting power relative to Pol400U(1:2). A possible explanation for the latter phenomenon will be considered in the discussion {Section 1.1(v)}.

1.1(iv) A Comparison of Extraction from K^+ and Na^+ Containing Aqueous Phases

The above study {described in Section 1.1(iii)} was repeated for aqueous solutions containing 0.08 M $CoCl_2 \cdot 2H_2O$ + 2 M NaSCN, and the extraction achieved by the various urethane compounds was compared to the extraction achieved from the corresponding K^+ containing aqueous phases. See Figure 4.4.

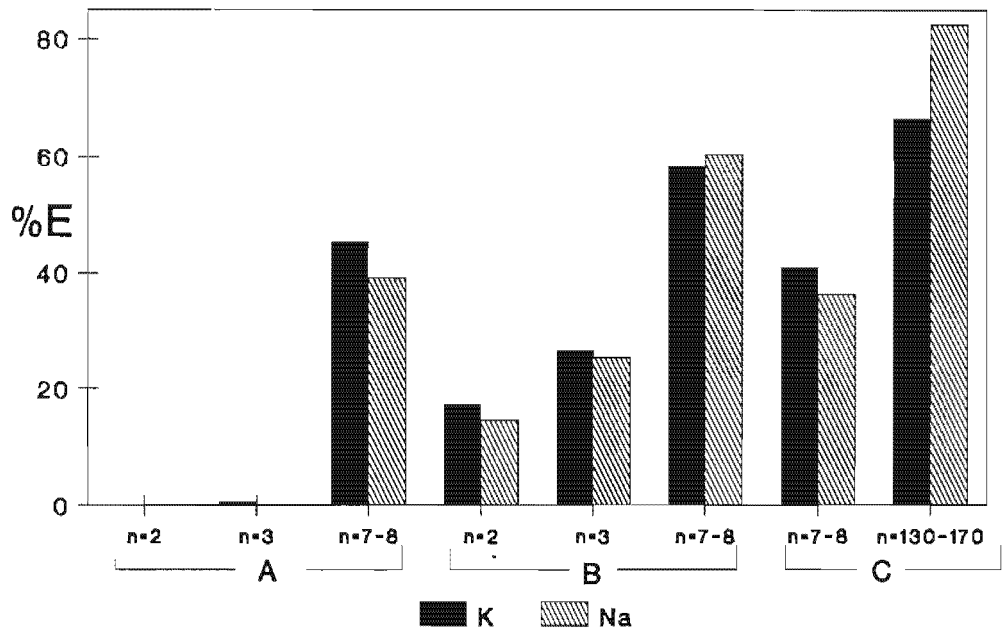

Figure 4.4 The effect of varying alkali cations on the extraction of $[Co(NCS)_4]^{2-}$ by urethane compounds. (A = diurethane podands, B = (1:2)-polyurethanes, C = (1:1)-polyurethanes).

No clear trend was observed for the effect on extraction of varying Na^+ relative to K^+ cations. Hence, if the extraction phenomenon is dominated by the chelation of a cation by the oligo(ethylene oxide) groups, it appears that K^+ and Na^+ are

essentially chelated equally well and that no discrimination based on ionic size of the alkali metal cations takes place.

1.1(v) Discussion of the Results of the Preliminary Investigation

The preliminary study of the extraction of cobalt has confirmed significant extraction capabilities of the soluble linear polyurethanes, and of the diurethane podands with $n \geq 7 - 8$. Hence, we have established that these urethane compounds may indeed be used as convenient models of polyurethane foam.

Due to the presence of linkages in the linear soluble polyurethane containing nitrogen donor atoms, one needs to consider the possibility of the involvement of these potential donor atoms in the extraction phenomenon of metal ions. Involvement of the nitrogen atoms in the extraction of metal ions is conceivable, either by direct coordination of these donor atoms to metal cations (eg. alkali metal cations), or by protonation of the nitrogen atoms. In both cases the formation of cationic sites would result in the extraction of anionic metal complexes. Since the preliminary extraction of cobalt was performed in the absence of acids, only chelation of alkali metals can be considered in this discussion.

Increased oligoethylene chain lengths would reduce the concentration of urethane linkages, so that it might be expected that a decreased extracting power would result with an increase in the oligoethylene chain length, if these urethane linkages were to play a significant role in the extraction process. However, the opposite is observed, which argues against a significant direct involvement of the urethane groups in the extraction of metal ions. It must be remembered though, that an intensive study

into the involvement of the urethane atoms in metal extraction was not performed and, therefore, such indirect evidence should be regarded with some caution.

The following observations indicate that extraction takes place by a cation chelation process involving the oligo(ethylene oxide) chains of the urethane compounds:

a) The Diϕ400U: cobalt ratio approaches a limiting value of two (two K^+ cations are chelated by Diϕ400U for the extraction of the doubly charged $[Co(NCS)_4]^{2-}$ anion),

b) Diϕ150U and Diϕ194U exhibited a negligible extraction capability (see below).

c) An increase in the oligoethylene chain length increased the extracting power of the urethane compounds.

It was reasoned above that extraction by the urethane compounds is not likely to occur significantly by a solvent extraction mechanism. One may ascribe the negligible tendency of Diϕ150U and Diϕ194U to extract $[Co(NCS)_4]^{2-}$ from the aqueous phase, simply to the fact that their oligoethylene chains are too short to effectively chelate the alkali metal cations. In addition, the electron withdrawing urethane moieties might be expected to reduce the electron density of the adjacent ethylene oxide groups, with a consequent reduction in the basicity of these ether-oxygen atoms. Such a reduced basicity of the nearly terminal oligoethylene heteroatoms is likely to have a dominantly negative influence on cation chelation by the short-chain Diϕ150U and Diϕ194U. It is also reasonable to consider the possibility of extraction by Diϕ150U and Diϕ194U as being effected by cooperative chelation of a metal cation by *two or more* of these diurethane podands. Evidently this does not occur, possibly due to an unfavourable entropic factor which is expected to favour dissociation of such chelates.

Although podand molecules with oligo(ethylene oxide) chain lengths for which n = 2 and 3 have been found inadequate for chelation {*cf.* the inability of Diϕ150U and Diϕ194U to extract $[Co(NCS)_4]^{2-}$}, linear polyurethanes with n = 2 and 3 do exhibit considerable extracting capabilities {*cf.* the extraction achieved by Pol150U(1:2) and Pol194U(1:2)}. The extended polyurethane chains presumably have sufficient flexibility to allow conformations of the polyurethane backbone which allow for cooperative chelation of a cation by various oligoethylene sections of the same polyurethane molecule. In the latter regard, entropy should not be as important a factor since the cooperative chelation involves different sections of a single polymer molecule.

The increase in extraction capability with increased oligoethylene chain length (*ie.* increasing values for n) of the (1:2)-polyurethanes and of the (1:1)-polyurethanes, might be ascribed to a greater stability of the cation-oligo(ethylene oxide) chelate. Possibly, longer oligoethylene sections are better able to encapsulate a cation making the demands on cooperative chelation between different oligoethylene sections of the same molecule smaller. This concept is illustrated in Figure 4.5.

Cooperative chelation between different oligoethylene sections of the same polymer molecule, may require conformations of the polyurethane that are energetically less favourable. Therefore, a reduced demand on cooperation might be expected to result in increased stability of the chelates and consequently an increased extracting power.

In the case of Pol6000U(1:1), it is conceivable that more than one cation may be accommodated in every oligoethylene chain section, allowing for sufficient charge separation to minimize electrostatic repulsion between the cations.

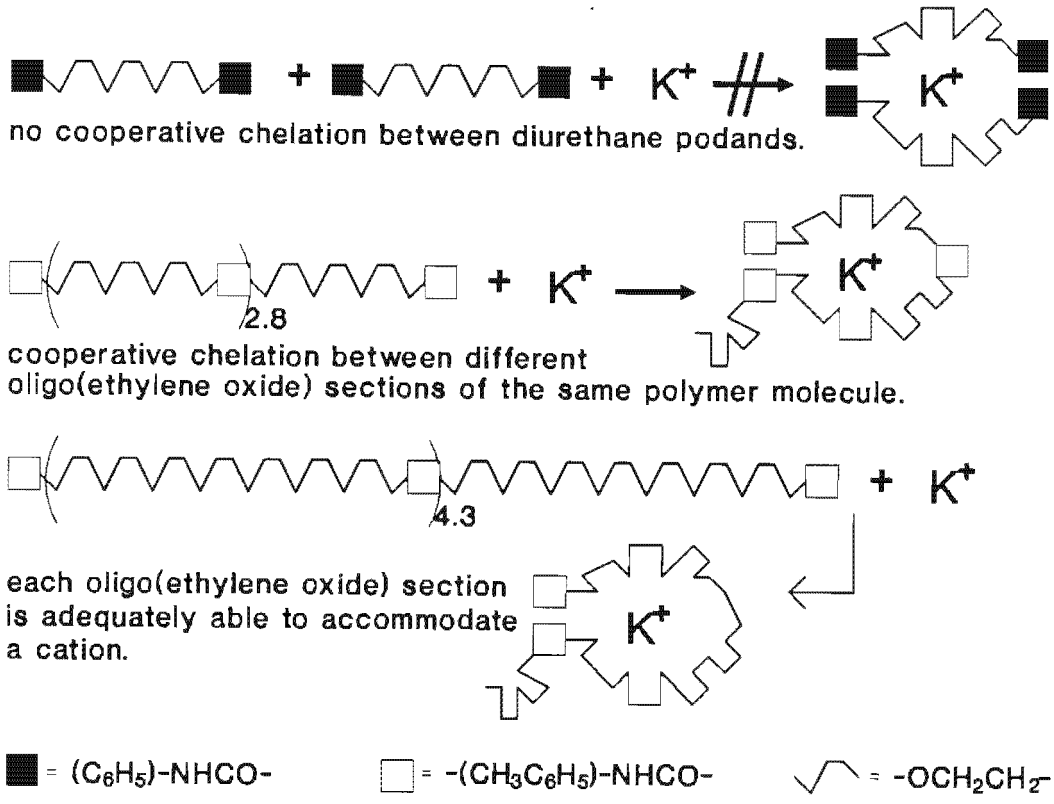

Figure 4.5 Illustration of the concept of cooperative chelation by the oligo(ethylene oxide) sections of the model urethane compounds.

In an attempt to explain the decrease in extraction capability observed in progressing from Pol400U(1:2) to Pol400U(1:1) one should consider the differences in their nature. These two polyurethanes both have n = 7 - 8, and they differ mainly in the degree of polymerization, x, as well as in the nature of the terminal groups. Due to the 1:2 NCO:OH ratio of the starting materials used in the synthesis of Pol400U(1:2), one may expect that this polymer should be terminated mainly by hydroxyl groups. In contrast, Pol400U(1:1) should contain a high proportion of terminal amine groups. Yanagida *et al.* [6] reported that upon interaction with strontium, a larger downfield shift of the nmr chemical shifts of the ethylene oxide protons was observed for polyethylene glycols, relative to that of the corresponding

glymes. These authors thus concluded that "the terminal hydroxyl groups are important to some extent in creating effective interaction with the strontium ion". Hence, it is possible that the larger extracting power of Pol400U(1:2) relative to Pol400U(1:1) is at least partially due to the higher proportion of hydroxyl terminated polyurethane chains.

The degree of polymerization, and hence the overall polyurethane chain length, may also be expected to influence the ability of the polyurethanes to extract metal ions. For Pol400U(1:2) $\bar{x} \sim 4.3$, while for Pol400U(1:1) $\bar{x} \sim 23$ (see Chapter 3). The increased degree of polymerization is accompanied by an increased concentration of diurethane moieties (see Figure 3.6). Since these moieties constitute relatively rigid sections of the polyurethane chain, an increased degree of polymerization might result in a loss of flexibility of the polyurethane chain. Such decreased flexibility might in turn be expected to detrimentally influence the ability of the polyurethane to chelate metal ions [7].

1.2 The Extraction of Trichlorostannato Complexes of Rhodium from Hydrochloric Acid Medium

The extraction of rhodium involved the partitioning of trichlorostannato-rhodium complexes between the hydrochloric acid medium and the urethane compounds in chloroform. These extractions were performed by shaking together equal volumes of the aqueous phase and the organic phase containing the urethane compound, under nitrogen in test tubes stoppered with inert silicone rubber stoppers. It was established in a preliminary study that a 30 minute shaking period was sufficient for the attainment of a steady state. The amount of rhodium extracted was calculated by difference after analysis of the aqueous phase by atomic absorption spectroscopy.

The samples and standards received identical treatment throughout the experiment. The resistance of the urethane compounds to acid hydrolysis was verified by comparison of the ^{13}C and ^{1}H nmr spectra before and after exposure to 6 M DCl. After recording the ^{13}C and ^{1}H nmr of Diϕ400U in $CDCl_3$, the Diϕ400U solution was shaken with 6 M DCl for 30 minutes, and the spectra were recorded again. No change was detected in either spectrum.

1.2(i) The Effect of Equilibration of the Aqueous Phase

Although it had been established that an equilibration period of 16 hours had a negligible effect on extraction by polyurethane foams, we sought to examine the effect of a longer period of equilibration on the extraction by the model urethane compounds. Hence, the extraction by Diϕ400U of rhodium from an aqueous phase which had been allowed to equilibrate for 4 days at 35 ^{o}C, was compared to extraction from the identical aqueous phase that had been equilibrated for 3.5 hours at 35 ^{o}C. Both aqueous phases contained 122.3 $\mu g.ml^{-1}$ rhodium, 3 M hydrochloric acid and a Sn:Rh ratio of 10:1. Chloroform solutions containing 0.0596 $g.ml^{-1}$ and 0.1011 $g.ml^{-1}$ Diϕ400U were used. The results are illustrated in Figure 4.6.

It is obvious from Figure 4.6 that an equilibration period of 4 days results in almost twice the amount of rhodium being extracted compared to solutions equilibrated for only 3.5 hours. These results indicate that extraction is strongly influenced by the distribution of the trichlorostannato-rhodium complexes present in solution at the time of extraction.

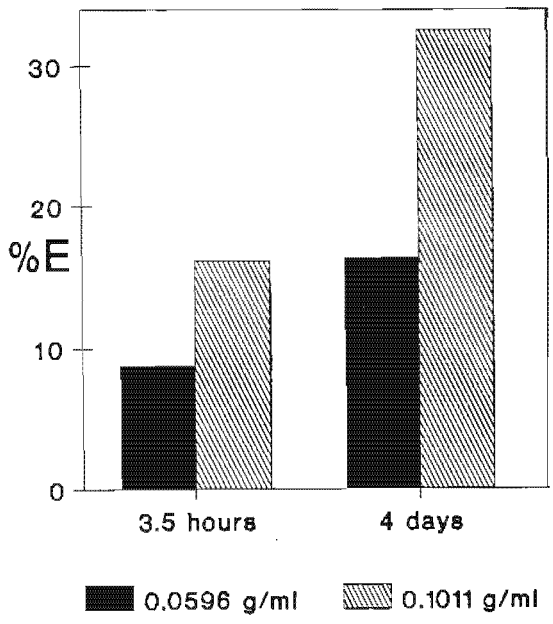

Figure 4.6 The effect of equilibration time on the extraction of rhodium by Diϕ400U. ([Rh] =122 μg. ml^{-1}, [HCl] = 3 M, and Sn:Rh = 10:1).

The electronic spectra of the aqueous phases were recorded after their respective equilibration periods, following dilution (5 x) with 1 M hydrochloric acid. Maxima at 424 nm and 437 nm were recorded for the aqueous phases subjected to 3.5 hours and 4 days equilibration respectively.

Although the nature of the species most favoured for extraction was not certain at this stage, a longer equilibration of the aqueous phase in the presence of excess tin(II) is thought to favour the formation of the purple, trigonal bipyramidal $[Rh(SnCl_3)_5]^{4-}$ species [8,9].

Iwasaki *et al.* [9] found that the purple species, $[Rh(SnCl_3)_5]^{4-}$, had an absorption maximum at 470 nm. Hence, after the appropriate equilibration periods, in the present study the absorbance at 470 nm of the aqueous phases was measured following dilution (5 x) with 1 M HCl, and were found to be 0.667 and 0.416 after 4 days and 3.5 hours respectively. Although a redistribution of species could occur on

dilution with HCl and the absorbance of other species in solution may overlap with the absorbance of $[Rh(SnCl_3)_5]^{4-}$, a significantly higher absorbance at 470 nm does provide evidence in support of a higher concentration of the purple species, $[Rh(SnCl_3)_5]^{4-}$. It might thus be concluded that the higher extraction efficiency observed after 4 days equilibration, was due to the higher concentration of $[Rh(SnCl_3)_5]^{4-}$ species in the aqueous phase.

1.2(ii) A Reproducibility Check

An important consideration in these experiments is the reproducibility of the results, without which little can be said about possible extraction mechanisms. Thus, extractions by Pol400U(1:2) and Pol1500U(1:1) were repeated using polyurethane concentrations of 0.0855 ± 0.0001 $g.ml^{-1}$ For each extraction, three aqueous phases, solution A (3.2 M HCl), solution B (3.2 M HCl + 0.2 M KCl) and solution C (0.5 M HCl + 2.5 M KCl), were freshly prepared. Each aqueous phase contained 150 $\mu g.ml^{-1}$ rhodium and a Sn:Rh ratio of 10:1, and was subjected to an equilibration period of 4 days at 35 °C before use. The results of the repeat experiments are compared in Table 4.1 below.

Table 4.1 Comparison of repeat experiments using solutions A, B and C and 0.0855 $g.ml^{-1}$ of Pol400U(1:2) and Pol1500U(1:1).

Sol.	Pol400U(1:2)						Pol1500U(1:1)					
	%E			$D'_m \times 10^2$ ($mmol.g^{-1}$)			%E			$D'_m \times 10^2$ ($mmol.g^{-1}$)		
	Exp.1	Exp.2	%diff.	Exp.1	Exp.2	%diff.	Exp.1	Exp.2	%diff.	Exp.1	Exp.2	%diff.
A	90.5	90.9	0.44	3.877	3.885	0.21	94.1	96.5	2.55	3.985	4.12	3.49
B	94.3	98.0	3.92	4.042	4.186	3.56	98.4	100.0	1.63	4.216	4.270	1.28
C	98.9	98.7	0.20	4.241	4.215	0.62	99.0	97.6	1.43	4.241	4.169	1.73

These results indicate that essentially similar results are obtained since the largest difference between $\mathbf{D'_m}$ and %E values of replicate extractions is about 4%.

1.2(iii) The Effect of Alkali Metal Cations and of the Type of Urethane Compound

Initially, the effect of K^+ on the extraction of trichlorostannato-rhodium complexes was studied. Chloroform solutions with concentrations of 0.2401 ± 0.0012 $g.ml^{-1}$ of Diϕ400U, all the (1:2)-polyurethanes, and Pol400U(1:1) and Pol1500U(1:1) were each shaken with the three freshly prepared aqueous phases A (3.2 M HCl), B (3.2 M HCl + 0.2 M KCl) and C (0.5 M HCl + 2.5 M KCl), allowing for equilibration of the aqueous solutions at 35 °C for 4 days, as described in Section 1.2(ii).

The amount of rhodium extracted by each urethane compound, as well as the Sn:Rh ratios in the extracted phase were determined (Figure 4.7 and Figure 4.8). It should be noted that, since equal masses of urethane compounds were used, the trends observed for $\mathbf{D'_m}$ parallel those of the percentage extraction (%E).

Considering only the extraction from aqueous phase A (3.2 M HCl, no KCl), the observations made in the preliminary cobalt extraction study concerning the effect of the oligo(ethylene oxide) chain length (n) and degree of polymerization (x), are confirmed. An increase in the oligo(ethylene oxide) chain length improves extraction, whereas a large increase in the degree of polymerization for the same polyurethane lowers the extracting power of the polyurethane {*cf.* extraction by Pol400U(1:1) relative to Pol400U(1:2) (both have n = 7 - 8) in Figures 4.7 and 4.3}. The latter phenomenon was not evident for Pol1500U(1:2) and Pol1500U(1:1). Both of these polyurethanes had quantitatively extracted the rhodium from the aqueous phase, suggesting that these systems had not reached their limiting extracting capacity. Therefore, any effects on extraction would be masked by virtue of the excess in which these polyurethanes occur.

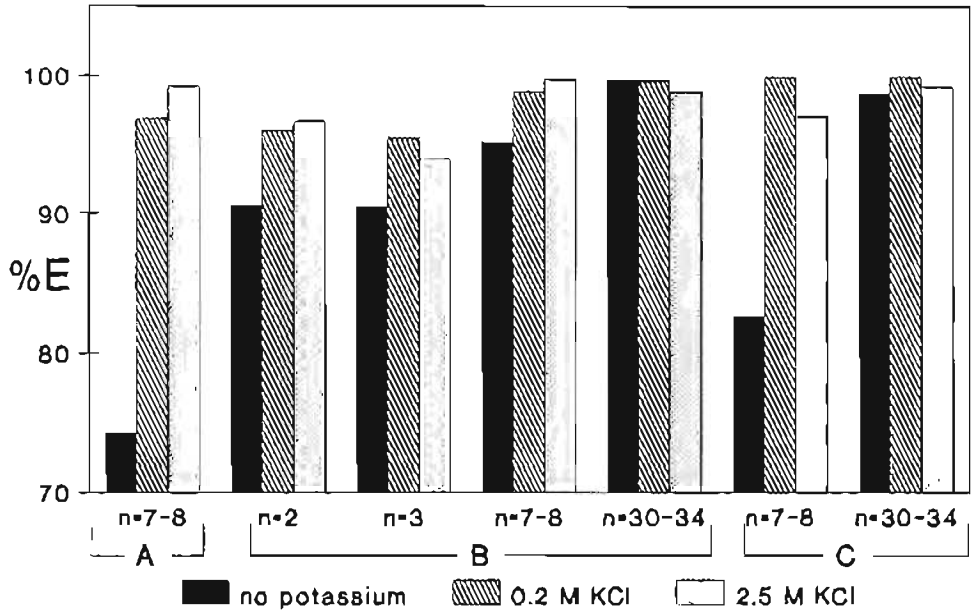

Figure 4.7 The effect of potassium on extraction by various urethane compounds. (Concentration of urethane = 0.2041 $g.ml^{-1}$). (A = diurethane podand, B = (1:2)-polyurethanes, C = (1:1)-polyurethanes. Aqueous phase composition : 150 $\mu g.ml^{-1}$ rhodium, $[Cl^-]$ = 3.2 ± 0.2 M, Sn:Rh = 10:1).

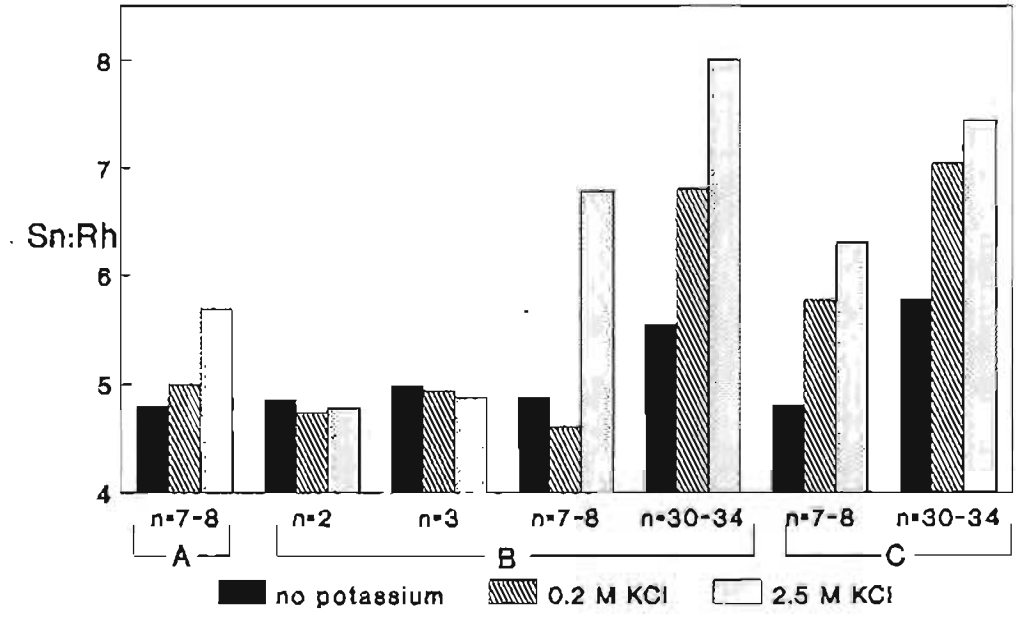

Figure 4.8 The effect of potassium on the ratios in which Sn and Rh are extracted by the urethane compounds. (A = diurethane podand, B = (1:2)-polyurethanes, C = (1:1)-polyurethanes).

Comparison of extraction from aqueous phases A, B and C reveals increased efficiencies from aqueous phases containing K^+ ions. The most dramatic increase in extraction was observed for Diϕ400U and Pol400U(1:1). The presence of only 0.2 M KCl increased extraction from 74.3 to 96.9% and from 82.7 to 99.3% respectively. While there was a significant difference in the amount of rhodium extracted from aqueous phases containing no alkali metal cations by Diϕ400U, Pol400U(1:2) and Pol400U(1:1) (having equal values for n) , this difference was not observed for extractions performed in the presence of K^+. Hence, extraction from solutions containing K^+ cations by these model urethane compounds (with n = 7 - 8) was similar with the effect of achieving essentially quantitative rhodium extraction under such conditions.

The presence of high concentrations of K^+ ions caused a significant increase in the ratios of Sn:Rh extracted by the urethane compounds with n = 7 - 8. Sn:Rh ratios in the organic phase of up to 8:1 were observed for these systems, in which essentially quantitative extraction of rhodium had been achieved. Since the maximum number of $SnCl_3^-$ ligands that could possibly coordinate to rhodium, is six, these results indicate that coextraction of unassociated $SnCl_3^-$ and $SnCl_4^{2-}$ anions may be facilitated by potassium ions.

In order to study the effect of the presence of K^+ ions on extraction by Pol400U(1:2), Pol400U(1:1), Pol1500U(1:2) and Pol1500U(1:1) more closely, the above extraction conditions needed to be altered to prevent the quantitative extraction of rhodium. Hence, the above study was repeated with lower concentrations of the polyurethanes (0.0855 ± 0.0001 $g.ml^{-1}$, compared to the initial concentration of 0.2401 ± 0.0012 $g.ml^{-1}$). It is evident from Figure 4.9 that the overall extraction efficiency did not decrease substantially with a decrease in the

concentration of the extractant. This suggests that at the higher concentrations, the polyurethane-containing organic phase had not been saturated with metal ions, since between 90 - 99% of the total rhodium was still extracted from organic phases using lower polyurethane concentrations. Furthermore, similar extraction trends were observed for both concentrations of the linear polyurethanes.

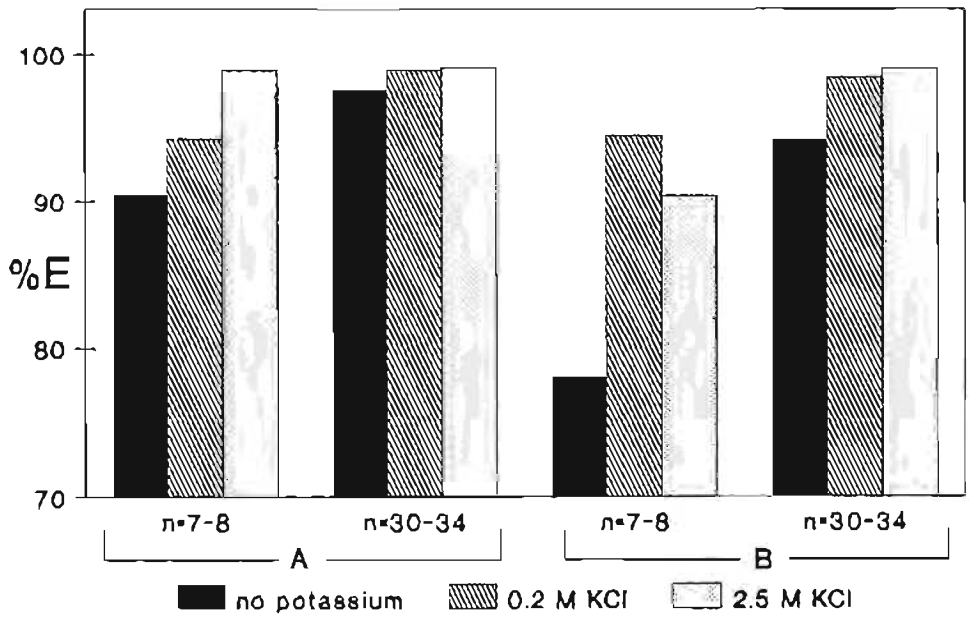

Figure 4.9 The effect of potassium on extraction. (Polyurethane concentration = 0.0855 g.ml^{-1}). (A = (1:2)-polyurethanes, B = (1:1)-polyurethanes. Aqueous phase composition : 150 μg.ml^{-1} rhodium, [Cl$^-$] = 3.2 ± 0.2 M, Sn:Rh = 10:1)

In the study using lower concentrations of linear polyurethane (0.0855 g.ml^{-1}), an increase in the ratios of Sn:Rh was again observed for increasing concentrations of K^+ ions (Figure 4.10), so confirming the observations made for the system in which higher polyurethane concentrations (0.2401 g.ml^{-1}) were used. The values of the Sn:Rh ratios are relatively lower for the lower polyurethane concentration systems, suggesting that relatively less unassociated $SnCl_3^-$ and $SnCl_4^{2-}$ had been extracted, presumably due to a smaller excess of the polyurethanes.

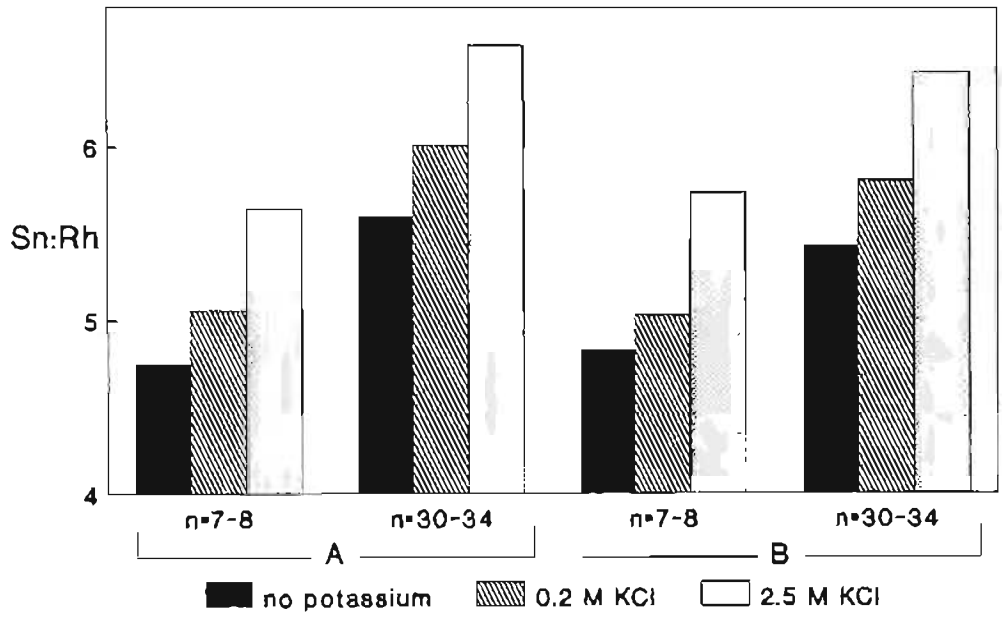

Figure 4.10 The effect of potassium on the ratios in which Sn and Rh are extracted by the polyurethanes. (A = (1:2)-polyurethanes, B = (1:1)-polyurethanes)

A comparative study of the influence of various alkali metal cations on extraction was undertaken. The effect of 0.2 mol.dm^{-3} MCl + 3.2 M HCl (where M = H^+, Li^+, Na^+, K^+) on the extraction of rhodium by 0.0853 ± 0.0001 g.ml^{-1} of Diϕ400U, Pol400U(1:2), Pol400U(1:1) and Pol1500U(1:1), was studied from aged (4 days at 35 °C) aqueous solutions containing 150 μg.ml^{-1} rhodium, with a Sn:Rh ratio of 10:1. (Since the addition of cesium to hydrochloric acid solutions containing rhodium(III) and tin(II) chloride resulted in the formation of a precipitate, it could not be used for the present study.)

A great many studies have shown that the chelation of alkali or alkaline-earth cations by crown ether-type macrocycles [10], as well as non-cyclic oligoethers (podands) [11], correlates with the ionic size of the cation. Therefore, in an attempt to demonstrate any such correlation, the results are presented as a plot of the %E

observed for each urethane compound against the ionic radius of the respective cations (see Figure 4.11). Pauling univalent radii [12] were used for Li^+, Na^+ and K^+. For comparison of the extraction achieved in the absence of alkali metals at constant ionic strength, an indication of the ionic radius of H_3O^+ was estimated by calculation of the van der Waals radius of H_3O^+. The calculations are based upon a published crystal structure [13] and are shown in Appendix 4.

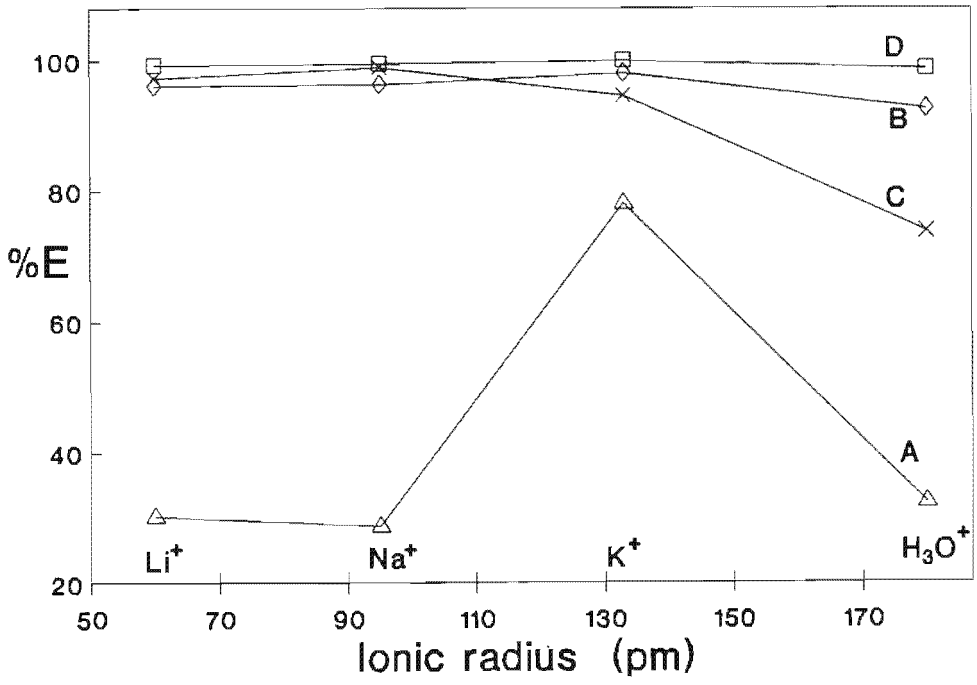

Figure 4.11 The effect of cations on extraction. ([urethane compound] = 0.0853 g.ml^{-1}, A = Diϕ400U, B = Pol400U(1:2), C = Pol400U(1:1), D = Pol1500U(1:1) ; Aqueous phase composition : 150 μg.ml^{-1} rhodium, Sn:Rh = 10:1, 3.2 M HCl and 0.2 M MCl).

The most striking effect is that of K^+ on the extraction by Diϕ400U. Whereas Diϕ400U extracted 30.2%, 28.7% and 32.3% of the total rhodium in the presence of Li^+, Na^+ and H_3O^+ respectively, 78.1% extraction was achieved in the presence of K^+ ions.

The high percentage extraction observed for the linear polyurethanes in this study suggests that these compounds had not reached their maximum extraction capacity. Hence any individual effect of the various cations might be masked by the excess of the linear polyurethanes in the extraction system. This experiment was repeated using lower concentrations of the linear polyurethanes (0.0201 ± 0.0001 $g.ml^{-1}$) Pol150U(1:2), Pol400U(1:2), Pol1500U(1:2), Pol400U(1:1) and Pol1500U(1:1). The aqueous phases described above were freshly prepared and aged at 35 °C for 4 days. The results are illustrated in Figure 4.12.

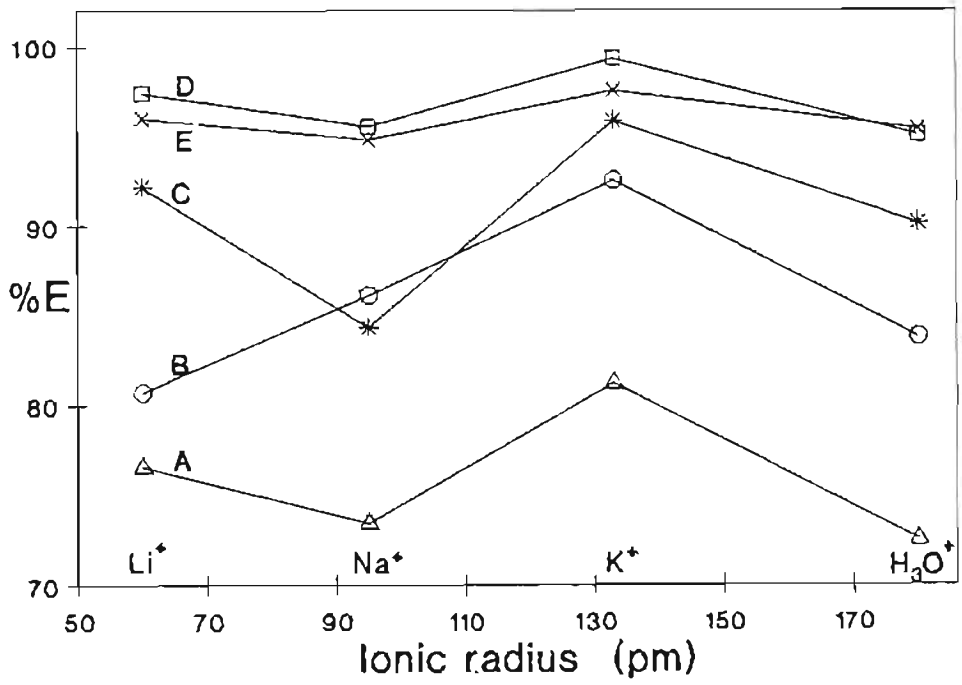

Figure 4.12 The effect of cations on extraction by the linear polyurethanes (0.0201 $g.ml^{-1}$) in chloroform. (A = Pol150U(1:2), B = Pol400U(1:2), C = Pol400U(1:1), D = Pol1500U(1:2), E = Pol1500U(1:1) ; Aqueous phase composition : 150 $\mu g.ml^{-1}$, Sn:Rh = 10:1, 3.2 M HCl and 0.2 M MCl).

For all the polyurethanes systems a maximum %E was observed for the K^+ containing aqueous phase. Rather unexpectedly, the second highest percentage of

rhodium extracted by all but one of the polyurethanes was from aqueous solutions containing Li^+.

These trends are difficult to rationalize. Since the order of the extraction efficiencies observed in the presence of H^+, Li^+, Na^+ and K^+ does not follow a simple trend paralleling ionic size, it seems evident that ionic size is not the only important factor which determines the extractability of the trichlorostannato-rhodium complexes. In addition, the effect of H^+ on the extraction of rhodium is not necessarily directly comparable to the effect of the alkali metal cations. It should be remembered that under constant ionic strength conditions, alkali metal cations can conceivably only result in the extraction of trichlorostannato-rhodium anions into the organic phase as a result of their ion-dipole interactions with the urethane compounds. In contrast, the proton ions can result in extraction, not only by chelation of H_3O^+ (or other hydrated species such as $H_5O_2^+$ [14]), but also by the possible protonation of donor atoms (O and N) of the polyurethane molecules, as well as by the formation of neutral extractable metal species such as $H_3[Rh(SnCl_3)_nCl_{6-n}]$.

It is interesting to note the different extraction behaviour of Pol400U(1:2) and Pol400U(1:1). At concentrations of 0.0853 $g.ml^{-1}$ the Pol400U(1:2) extracted 19% more rhodium from acidic solutions containing no alkali metals than did Pol400U(1:1) (see Figure 4.11). However, in the presence of the alkali metal cations (Li^+, Na^+, K^+), very similar extraction efficiencies were observed for both (essentially equal within a 4% error limit).

At very low concentrations of these polyurethanes (0.0201 $g.ml^{-1}$) the order of the extracting powers of Pol400U(1:2) and Pol400U(1:1) was reversed (see Figure 4.12).

Hence, in the absence of alkali metal cations, Pol400U(1:1) extracted more (6.4%) rhodium from the acidic solution than did Pol400U(1:2).

In the presence of Na^+ and K^+, Pol400U(1:2) and Pol400U(1:1) extracted similar amounts of rhodium. In contrast, the presence of 0.2 M Li^+ resulted in the extraction of 11.5% more rhodium by Pol400U(1:1). The order of decreasing extraction efficiencies found for low concentrations of Pol400U(1:2) and Pol400U(1:1) (0.0201 $g.ml^{-1}$) in the presence of various cations differs as follows:

Pol400U(1:2) : K^+ (92.5) > Na^+ (86.1) > H^+ (83.8) > Li^+ (80.1)
Pol400U(1:1) : K^+ (95.9) > Li^+ (92.2) > H^+ (90.2) > Na^+ (84.3)

where the values in parenthesis are the %E achieved in the presence of the respective cations.

Another noteworthy observation is that the Sn:Rh ratios found in the organic phase for the polyurethanes at low polyurethane concentrations (0.0201 $g.ml^{-1}$) did not exceed 5:1. Average Sn:Rh ratios of 4.55 ± 0.16, 4.44 ± 0.13, 4.64 ± 0.07 and 4.34 ± 0.18 were observed for solutions containing H^+, Li^+, Na^+ and K^+, respectively. In contrast, extractions carried out with higher concentrations of polyurethanes resulted in Sn:Rh ratios of up to 8:1 in the organic phase in the presence of K^+ ions (see Figure 4.8). These results indicate that at low polyurethane concentrations (*i.e.* at concentrations not constituting an excess of the linear polyurethanes) trichlorostannato-rhodium complexes are preferentially extracted over any chloro complexes of tin(II).

1.2(iv) The Effect of the Urethane Compound Concentration

It was noted above that Pol400U(1:2) had a consistently higher extraction capability relative to Pol400U(1:1), except at very low concentrations of these linear polyurethanes (0.0201 $g.ml^{-1}$) in which Pol400U(1:1) extracted relatively more rhodium from solution. This observation highlighted the influence of the concentration of the urethane compounds on extraction. It was thought that the concentration effect could be related to the effective size of the polyurethane molecule. Hence, the distribution ratio, D, achieved for various concentrations of each of Diϕ400U, Pol400U(1:2) and Pol400U(1:1) was represented graphically. D = $[Rh]_o/[Rh]_{aq}$ where the subscripts *o* and *aq* indicate the organic (or urethane compound) and aqueous phases, respectively. The results were taken for extractions performed from aqueous phases in which the Sn:Rh ratios were 10:1, hydrochloric acid concentrations were about 3 M, and with no alkali metals present.

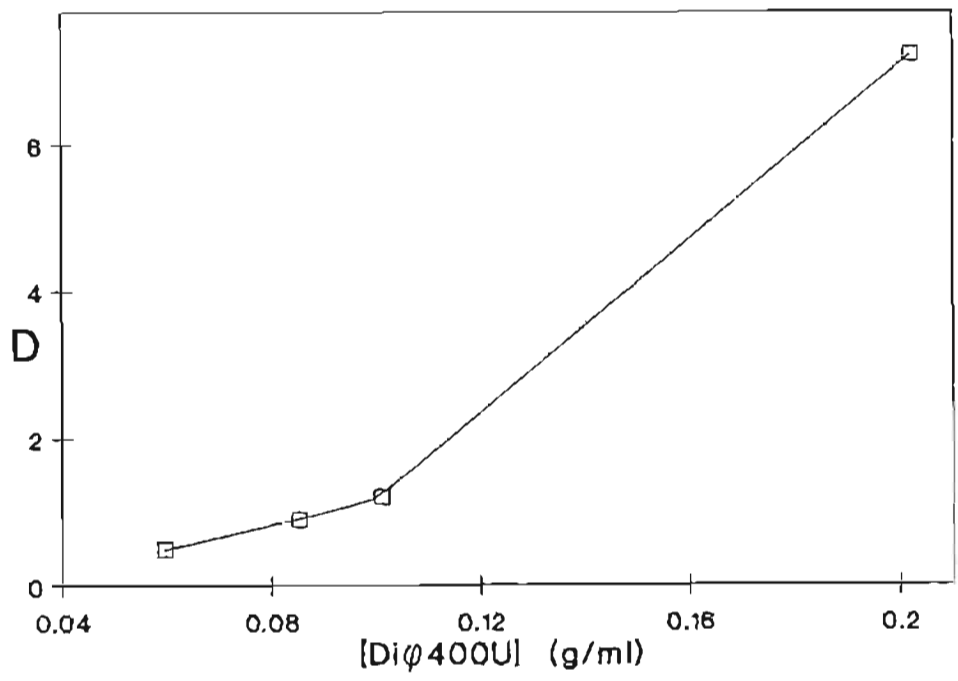

Figure 4.13 The effect of the concentration of Diϕ400U on the distribution ratio, D.

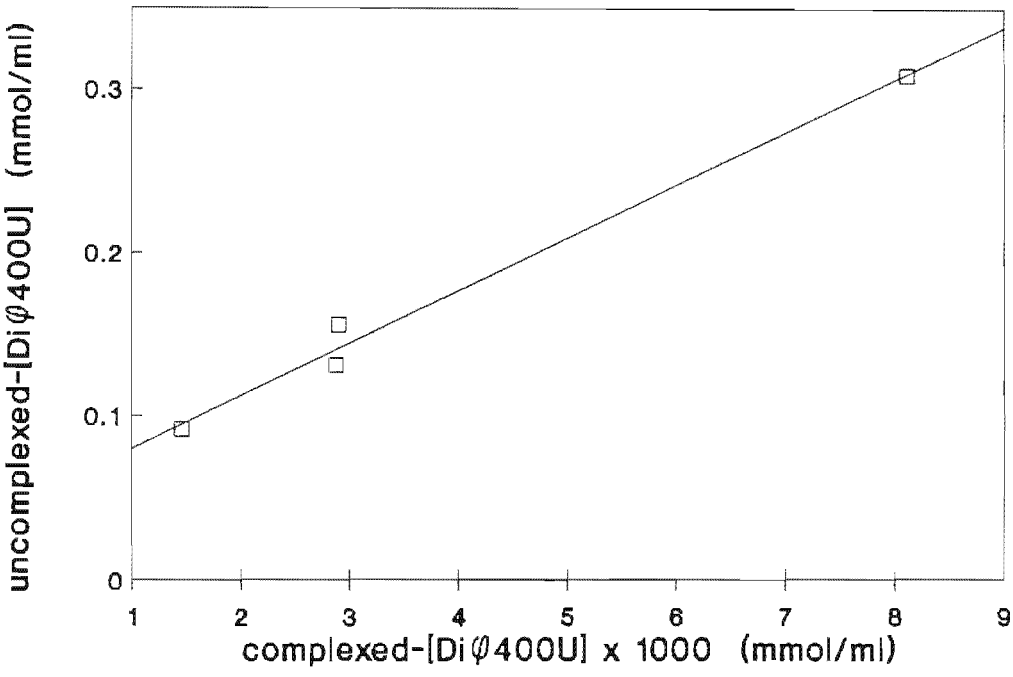

Figure 4.14 The relationship between uncomplexed Diϕ400U and complexed Diϕ400U.

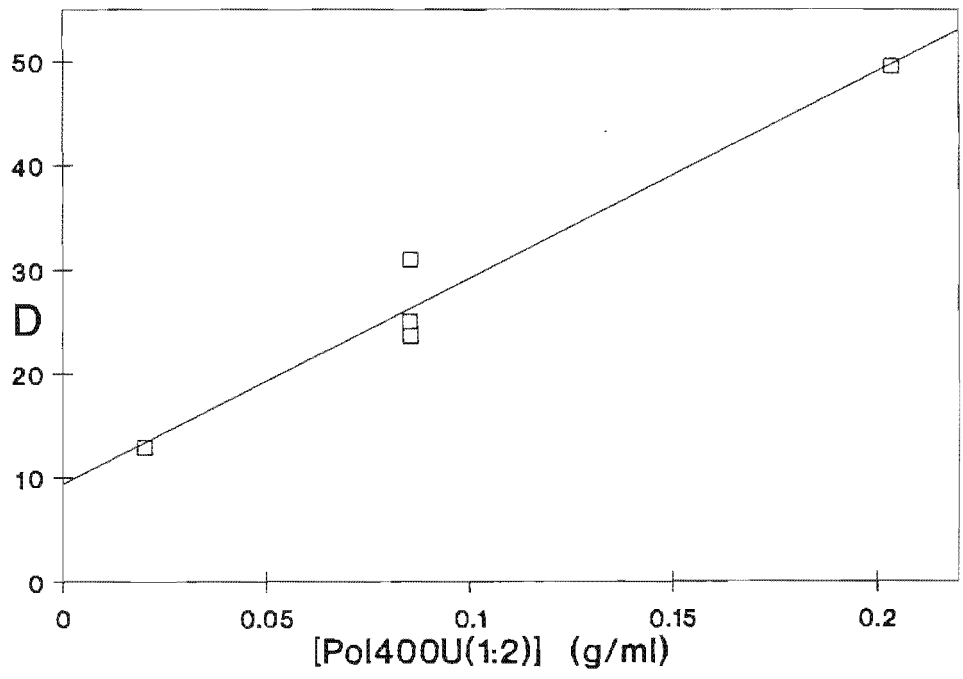

Figure 4.15 The effect of the concentration of Pol400U(1:2) on the distribution ratio, D.

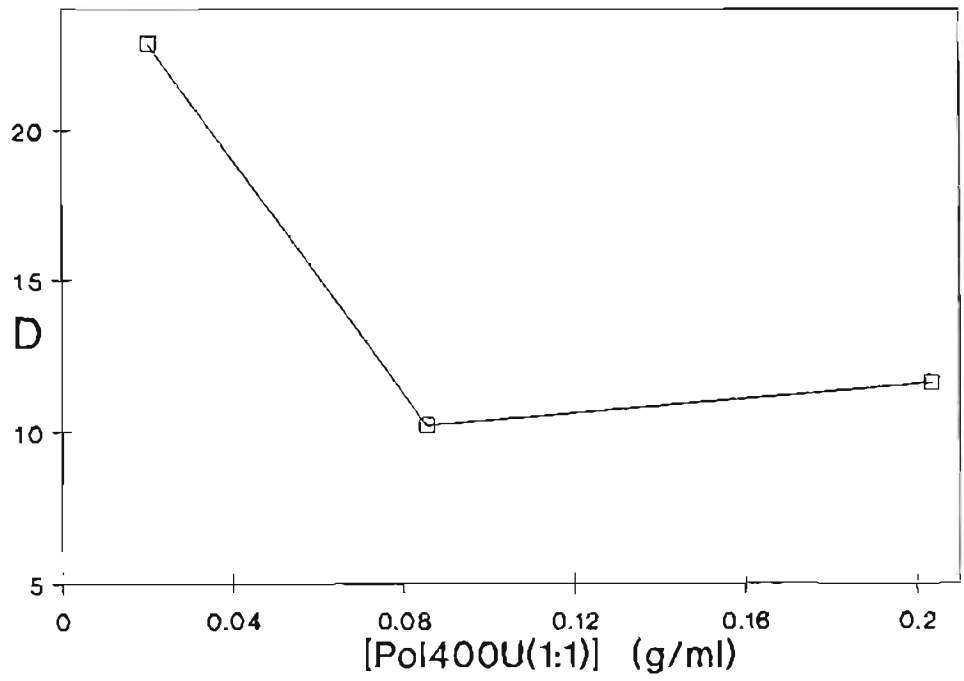

Figure 4.16 The effect of the concentration of Pol400U(1:1) on the distribution ratio, D.

Figures 4.13 and 4.15 clearly show a steady increase in the extraction efficiencies obtained with increasing concentrations of Diϕ400U and Pol400U(1:2). A relatively linear isotherm representing the increase in the concentration of uncomplexed Diϕ400U with an increase in the concentration of the complexed Diϕ400U, is shown in Figure 4.14. Remarkably, for the longer chain Pol400U(1:1) (*ie.* larger values for x) there is an initial decrease in the extraction efficiency with increased polyurethane concentration (see Figure 4.16). After a minimum in the value for D, a more gradual increase in the curve is again observed.

It is tempting to speculate about the meaning of the above trends observed for Pol400U(1:1). In dilute solution, the polymer molecules are relatively "disentangled" from one another [15] and are surrounded by solvent molecules. On complex formation, the polyurethane is likely to undergo conformational change in order to assume an appropriate orientation to allow the necessary interaction with

the alkali metals [7]. An increase in the concentration of the polyurethane molecules might be expected to result in a solution of molecules that are no longer "disentangled". These molecules will, therefore, interact with one another by, for example, hydrogen bonding. The *inter*molecular polyurethane interactions may conceivably hinder the necessary conformational changes of the polyurethanes, and in this way inhibit the chelation of cations. A lowering of macromolecular complex stability has been reported for a decrease in the set of conformations that a macromolecule is able to generate [7]. The lower macromolecular complex stability will be manifested in lower values for **D**. The gradual increase after the minimum in the extraction curve (shown in Figure 4.16) of the distribution ratios with increased polyurethane concentration, is again due to an increase in the number of molecules present, even though their extracting powers are limited.

Since Pol400U(1:2), and particularly Diϕ400U, are small in molecular size, relative to Pol400U(1:1), higher concentrations of the former two urethane compounds should be possible before *inter*molecular urethane compound interactions limit the conformational flexibility needed for efficient complex formation.

1.2(v) The Effect of the Sn:Rh Ratio in the Aqueous Phase

Extraction efficiencies from aqueous phases containing Sn:Rh ratios of 10:1 and 5:1 were compared for 0.0855 ± 0.0001 $g.ml^{-1}$ of Pol400U(1:2), Pol400U(1:1), Pol1500U(1:2) and Pol1500U(1:1). The aqueous phases had been equilibrated for 4 days at 35 °C, and contained 150 $\mu g.ml^{-1}$ rhodium, 0.5 M HCl and 2.5 M KCl. The results are presented in Table 4.2.

Table 4.2 The effect of the Sn:Rh ratio in the aqueous phase on the extraction of rhodium.

	Aqueous Sn:Rh ratio = 10:1		Aqueous Sn:Rh ratio = 5:1	
linear polyurethane	%E	Extracted Sn:Rh ratios	%E	Extracted Sn:Rh ratios
Pol400U(1:2)	98.9	5.65:1	80.9	4.03:1
Pol400U(1:1)	90.3	5.74:1	58.9	4.09:1
Pol1500U(1:2)	99.1	6.58:1	88.8	4.29:1
Pol1500U(1:1)	99.0	6.43:1	91.3	4.72:1

The generally lower amount of rhodium extracted from solutions with Sn:Rh ratios of 5:1 is consistent with the findings of a similar study using polyurethane foam (see Chapter 2). The total tin(II) concentration in the aqueous phase is expected to affect the distribution of the trichlorostannato-rhodium complexes in solution, as well as the rate of formation of the $[Rh^{I}(SnCl_3)_5]^{4-}$ complex, which has been found to be proportional to the square of the $SnCl_3^-$ concentration [9]. Hence, the larger amount of rhodium extracted by the soluble linear polyurethanes from aqueous solutions containing a Sn:Rh ratio of 10:1 may be explained by a higher proportion of rhodium complexes having a greater number of coordinated $SnCl_3^-$ ligands. That is, the results indicate that complexes of the type $[Rh(SnCl_3)_nCl_{6-n}]^{3-}$ with higher values for n, as well as $[Rh(SnCl_3)_5]^{4-}$, are favoured for extraction by the linear polyurethanes.

The latter idea is supported by the electronic spectra of the aqueous phases after equilibration and after a 5 times dilution with 1 M HCl. Maxima were recorded at 456 nm and 430 nm for Sn:Rh ratios of 10:1 and 5:1, respectively. The respective absorbances recorded at 470 nm (the absorption maximum ascribed to absorbance by the purple $[Rh(SnCl_3)_5]^{4-}$ species) were 0.914 and 0.550, respectively.

The coextraction of larger amounts of tin(II) chloride from aqueous solutions containing a ten fold excess of Sn(II) with respect to rhodium, yielding higher ratios of Sn:Rh in the organic phase, is consistent with the above proposal that rhodium complexes coordinatively saturated with $SnCl_3^-$ ligands are more favourably extracted. The coextraction of Sn and Rh in ratios of >6 by Pol1500U(1:2) and Pol1500U(1:1) from aqueous solutions containing Sn:Rh ratios of 10:1 indicates that under these conditions (where essentially quantitative extraction had occurred) unassociated $SnCl_3^-$ and $SnCl_4^{2-}$ are coextracted to a certain extent. The latter phenomenon was similarly observed in Section 1.2(iii).

1.2(vi) The Effect of the Hydrochloric Acid Concentration

The influence of hydrochloric acid on polyurethane *foam* is of considerable interest. It is evident from Figure 2.7 that a steady increase in the extraction of rhodium was observed with an increase in the hydrochloric acid concentration. Due to the difficulty of interpreting the influence of the hydrochloric acid concentration on the extraction of rhodium by polyurethane *foam*, it was of interest to examine the effect of the hydrochloric acid concentration on extraction by the model *urethane compounds*. Hence, extractions in which the aqueous hydrochloric acid concentrations were varied from 0.7 M to 5 M were undertaken. The aqueous phases were equilibrated for 4 days at 35 ^oC and contained 150 $\mu g.ml^{-1}$ rhodium and Sn:Rh ratios of 10:1. For this study, 0.0201 ± 0.0001 $g.ml^{-1}$ Pol150U(1:2), Pol400U(1:2), Pol400U(1:1), Pol1500U(1:2) and Pol1500U(1:1) were used.

Figure 4.17 clearly illustrates that an increased amount of rhodium is extracted by the linear polyurethanes with increased hydrochloric acid concentration, which

compares well with the results observed for the polyurethane foam extractions. (See Chapter 2, Section 2.6).

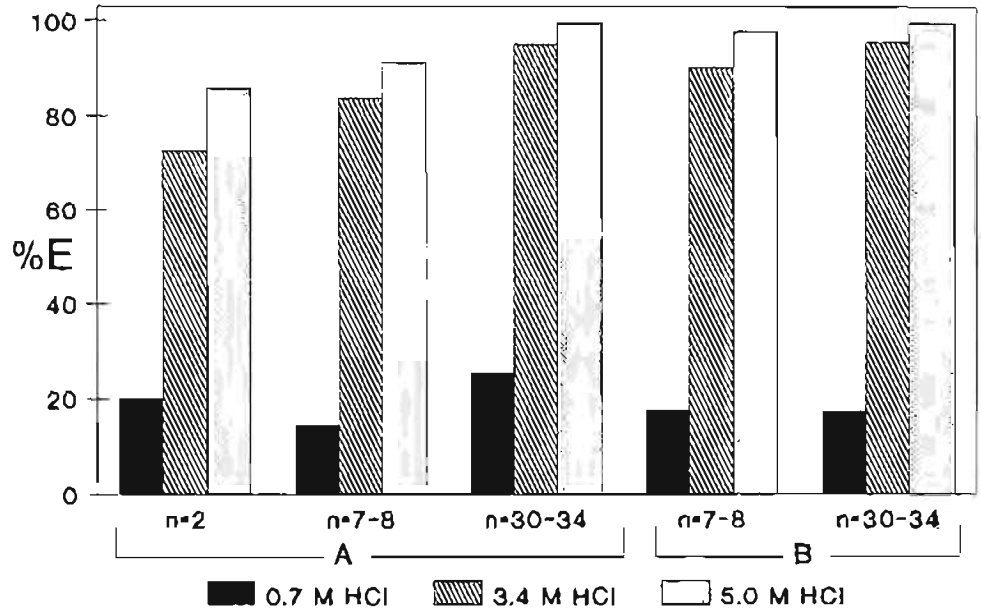

Figure 4.17 **The effect of hydrochloric acid on extraction by the linear polyurethanes. ([polyurethane] = 0.0201 g.ml^{-1}, A = (1:2)-polyurethanes, B = (1:1)-polyurethanes ; Aqueous phase composition : 150 μg.ml^{-1} rhodium, Sn:Rh = 10:1).**

As was mentioned in Chapter 2, an increase in the chloride ion concentration should increase the amount of $SnCl_4^{2-}$ at the expense of the $SnCl_3^-$ concentration. This is illustrated by the following set of equilibria:

$$SnCl_2 + Cl^- \rightleftharpoons SnCl_3^- \qquad (3)$$

$$SnCl_3^- + Cl^- \rightleftharpoons SnCl_4^{2-} \qquad (4)$$

The $SnCl_3^-$ concentration is influential in determining the distribution of the chloro(trichlorostannato) complexes of rhodium, as shown by the following series of equilibria.

$$[RhCl_6]^{3-} + SnCl_3^- \rightleftharpoons [Rh(SnCl_3)Cl_5]^{3-} + Cl^- \quad (5)$$

$$[Rh(SnCl_3)Cl_5]^{3-} + SnCl_3^- \rightleftharpoons [Rh(SnCl_3)_2Cl_4]^{3-} + Cl^- \quad (6)$$

$$[Rh(SnCl_3)_2Cl_4]^{3-} + SnCl_3^- \rightleftharpoons [Rh(SnCl_3)_3Cl_3]^{3-} + Cl^- \quad (7)$$

$$[Rh(SnCl_3)_3Cl_3]^{3-} + SnCl_3^- \rightleftharpoons [Rh(SnCl_3)_4Cl_2]^{3-} + Cl^- \quad (8)$$

$$[Rh(SnCl_3)_4Cl_2]^{3-} + SnCl_3^- \rightleftharpoons [Rh(SnCl_3)_5Cl]^{3-} + Cl^- \quad (9)$$

$$[Rh(SnCl_3)_5Cl]^{3-} + SnCl_3^- \rightleftharpoons [Rh(SnCl_3)_6]^{3-} + Cl^- \quad (10)$$

Although a very complex distribution of aquo-chloro complexes of rhodium is known to exist in acidic solution [16,17], for simplicity, only the chloro complex, $[RhCl_6]^{3-}$ is considered for the reaction with stannous chloride.

The reactions responsible for the formation of $[Rh(SnCl_3)_5]^{4-}$ have not been formulated conclusively, but possible routes were suggested by Iwasaki *et al.* [9]. One of these is shown by equation 11.

$$[Rh(SnCl_3)_3Cl_3]^{3-} \underset{Cl^-}{\overset{L^-}{\rightleftharpoons}} [Rh(SnCl_3)_4Cl_2]^{3-} \underset{Cl^-}{\overset{L^-}{\rightleftharpoons}} [Rh(SnCl_3)_5Cl]^{3-} \underset{Cl^-}{\overset{L^-}{\rightleftharpoons}} [Rh(SnCl_3)_6]^{3-}$$

$$[Rh(SnCl_3)_6]^{3-} \xrightarrow{rds} [Rh(SnCl_3)_5]^{4-} + Sn(IV)Cl_3^+ \quad (11)$$

rds = rate determining step, $L^- = SnCl_3^-$

It is evident that an increase in the chloride ion concentration would result in a shift to the left of the equilibria depicted by equations 5 - 11. Thus increased chloride ion concentrations would favour higher concentrations of the rhodium complexes of the type $[Rh(SnCl_3)_nCl_{6-n}]^{3-}$ with lower values for n. However, some evidence has been found which indicates that both $[Rh(SnCl_3)_nCl_{6-n}]^{3-}$ species with higher values for n and $[Rh(SnCl_3)_5]^{4-}$ are more extractable than the corresponding rhodium complexes with a smaller number of coordinated $SnCl_3^-$ ligands. {See Section 1.2(i)

and 1.2(v) of this Chapter and Section 2.2 of Chapter 2}. Therefore, the increase in the amount of rhodium extracted with increased hydrochloric acid concentrations is probably not due to an increase in the chloride ion concentration.

An alternative explanation is that the effect of an increase in the hydrogen ion concentration may be expected to increase the amount of rhodium extracted by one or all of the following methods:

a) the formation of a higher proportion of neutral extractable species such as $H_3[Rh(SnCl_3)_nCl_{6-n}]$ and $H_4[Rh(SnCl_3)_5]$,
b) the increased protonation of donor oxygen and nitrogen atoms present in the urethane compounds,
c) the increased chelation of H_3O^+ by the oligo(ethylene oxide) section of the urethane compounds.

Therefore, although while not certain whether the hydrochloric acid concentration affects extraction by action of the chloride ions, or by the hydrogen ions or both, it appears that the effect of the hydrogen ion concentration dominates. It is difficult to delineate what ionic strength effects play a part, since salts were not added to maintain a constant ionic strength when varying the HCl concentration. The presence of salts in solution would make it difficult to determine whether any observed effect should be ascribed to the change in the HCl concentration or due to a change in the concentration of the other cations in solution.

1.2(vii) Discussion of the Extraction of Rhodium by the Model Urethane Compounds

A discussion of the results of the investigation into the extraction of rhodium by the urethane compounds should address two important questions.

1) Was any evidence obtained from which one could deduce which rhodium complexes were most abundantly extracted by the urethane compounds ?
2) Is one able to draw meaningful conclusions regarding the mechanism by which the rhodium complexes are extracted ?

As regards the rhodium species favoured for extraction by the urethane compounds, a high extractability of $[Rh(SnCl_3)_5]^{4-}$ and $[Rh(SnCl_3)_nCl_{6-n}]^{3-}$ with higher values for n has been indicated. A comparison of the extraction of rhodium achieved from solutions that had been equilibrated at 35 °C for 4 days to that from solutions that had been equilibrated at 35 °C for only 3.5 hours, showed that approximately twice the amount of rhodium had been extracted after a 4 day equilibration period {see Section 1.2(i) of this Chapter}. UV-visible spectrophotometric analysis of the aqueous solutions immediately prior to extraction revealed considerably higher absorbances at 470 nm for the solutions that were equilibrated for 4 days. Absorbance at this wavelength has been ascribed by Iwasaki *et al.* [9] to the purple trigonal bipyramidal species $[Rh(SnCl_3)_5]^{4-}$. An increase in the concentration of the purple species in solution with an increased equilibration period is consistent with the findings of Kimura [8], who found that equilibration at 35 °C for several days was required for the formation of the purple solution. Hence, significant evidence has been found in support of an increase in the concentration of $[Rh(SnCl_3)_5]^{4-}$ resulting in the extraction of larger quantities of rhodium. Therefore, a high

extractability of the purple species $[Rh(SnCl_3)_5]^{4-}$ is indicated. In Section 1.2(v) of this Chapter it was shown that a higher concentration of tin(II) in the aqueous phase results in the extraction of a larger amount of rhodium, and the concomitant coextraction of tin, to yield higher ratios of Sn:Rh in the organic phase. A similar observation was made in a study using polyurethane foam (see Chapter 2, Section 2.2). In the polyurethane foam study it was ascertained that negligible extraction of chloro-tin(II) complexes occurred under the conditions of the study. Hence, it was concluded that all the coextracted tin(II) would be associated to the rhodium. In view of the results of the investigations using polyurethane foam, as well as the urethane compounds, it is reasonable to deduce that the $[Rh(SnCl_3)_nCl_{6-n}]^{3-}$ species with higher values for n are also favoured for extraction. The ionic size and polarizability of the anion plays a dominant role in determining the extractability of an anion.

Regarding the mechanism by which metal ions are extracted by urethane compounds, strong evidence has emerged in support of a "cation chelation" mechanism. The latter is dealt with in the discussion of the preliminary investigation {Section 1.1(v) of this Chapter} and shall not be repeated here. However, if one considers the effect of the various alkali metal cations on the extraction of rhodium (see Section 1.2(iii) of this Chapter), it is evident that the details of the extraction system remains poorly understood. When comparing the effects of the various cations on extraction a simple trend which parallels that of ionic size is not observed. Instead rather unexpectedly, the presence of Li^+ resulted in the second highest quantity of rhodium being extracted. (K^+ resulted in the highest extraction efficiency, see Figure 4.12). It is possible that due to the high charge to size ratio of Li^+, strong hydration of Li^+ might play a role in the effect of Li^+ on the extraction of rhodium by the various urethane compounds. However,

the hydration of Li^+ may be expected to be greatly reduced in the presence of 3.2 M hydrochloric acid. In addition, it is difficult to explain the apparent anomaly of Pol400U(1:2), for which the extracting efficiency decreased in the presence of the alkali metals in the order $K^+ > Na^+ > Li^+$. (It should also be remembered that no clear trend was observed in the preliminary investigation when comparing the effects of K^+ and Na+ on the extraction of $[Co(NCS)_4]^{2-}$ by the various urethane compounds.)

It became evident in Section 1.2(iv) that the amount of rhodium extracted by the various urethane compounds was influenced by the degrees of freedom of the urethane molecule to assume whichever conformations were needed for the chelation of cations. At low concentrations of the soluble linear polyurethanes (0.0201 $g.ml^{-1}$), Pol400U(1:1) extracted rhodium with a larger efficiency than did Pol400U(1:2). This is not surprising when considering the larger molecular mass, and hence size, of the former molecule {$\bar{M}_n \sim 13682$ and $\bar{x} \sim 23$ for Pol400U(1:1) compared to $\bar{M}_n = 2868$ and $\bar{x} = 4.3$ for Pol400U(1:2)}. However, at higher concentrations (> 0.08 $g.ml^{-1}$), Pol400U(1:1) extracted rhodium less efficiently, while Pol400U(1:2) extracted relatively more rhodium. The latter phenomenon is tentatively ascribed to *inter*molecular interactions between the Pol400U(1:1) molecules at high polyurethane concentration (eg. H-bonding involving the O and N donor atoms). If a change in the conformation of the urethane molecule were required for the effective chelation of a cation, it would be necessary to break these *inter*molecular interactions. Since energy would be required for the latter, one might expect a restriction in the number of conformations available for cation chelation by Pol400U(1:1), this being manifested in a lower extracting power. It is also possible that a loss of flexibility of the polyurethane chains, due to the incorporation of a large number of the relatively rigid diurethane moieties, has a

negative influence on the extracting power of Pol400U(1:1) at higher urethane concentrations.

In the latter consideration, one might expect a smaller difference in the extracting powers of Pol1500U(1:2) and Pol1500U(1:1), since the effect of the rigid diurethane sections may be expected to be reduced relative to the very long oligoethylene sections of the polyurethane chain (the number of ethylene oxide groups, n = 30 - 34, see Figure 3.3). On the other hand, one might expect both of these polyurethanes, and particularly Pol1500U(1:1), to be subject at higher concentrations of the polyurethane molecule to the restrictions imposed by the number of conformations available for chelation. Essentially quantitative extraction of rhodium was achieved by both Pol1500U(1:2) and Pol1500U(1:1) under the conditions used in this work. Therefore, no significant difference in their extraction behaviour could be detected.

It has become evident that many factors exist which influence the efficiency with which rhodium is extracted by the various urethane compounds, and that it is difficult to give a complete picture at this stage. However, the importance of the following factors have been demonstrated,

(1) the necessity of adequate oligomer chain length (either $n \geq 7 - 8$ or $x > 0$)
(2) the degree of flexibility of the linear polyurethane molecule
(3) the need for a high concentration of $[Rh(SnCl_3)_5]^{4-}$ (achieved by increasing the $SnCl_3^-$ concentration and/or the equilibration time of the aqueous phase)
(4) the need for a high concentration of hydrochloric acid (probably dependent on $[H^+]$).

1.3 More About the Extraction Mechanism

An important issue concerning the extraction mechanism is the question of the chelation of cations by the polyether sections of polyurethane foam. Evidence in support of the involvement of the polyether sections in the extraction process was found by the broadening of the poly(ethylene oxide) resonances in the solid state ^{13}C nmr spectrum of the foam after metal sorption (see the introduction to Chapter 3). In addition, after the extraction of rhodium-tin complexes from a K^+ containing hydrochloric acid solution, the analysis of the foam matrix revealed the coextraction of a substantial amount of potassium (see Chapter 2, Section 2.7). Further evidence in support of the chelation of cations by the oligo(ethylene oxide) chains is presented in this section.

1.3(i) ^{13}C nmr

After the extraction of $[RhH(SnCl_3)_5]^{3-}$ and some unassociated chloro-tin(II) complexes by Diϕ400U (identified by ^{119}Sn nmr, see Chapter 5), the ^{13}C nmr spectrum of the extracted phase was recorded. Figure 4.18 clearly illustrates that after the extraction process the single resonance arising from the central ethylene oxide carbons of uncomplexed Diϕ400U fragments into many peaks. This implicates the oligo(ethylene oxide) chains as major contributors towards the extraction of chloro(trichlorostannato)-rhodium complexes.

1.3(ii) ^{7}Li nmr

Conclusive proof of the coextraction of alkali metal cations would be the detection of such cations directly in the extracted phase. ^{7}Li nmr (spin = 3/2, natural

abundance = 92.58%) proved to be a useful tool for this purpose, allowing the semi-quantitative detection of any coextracted Li^+ ions.

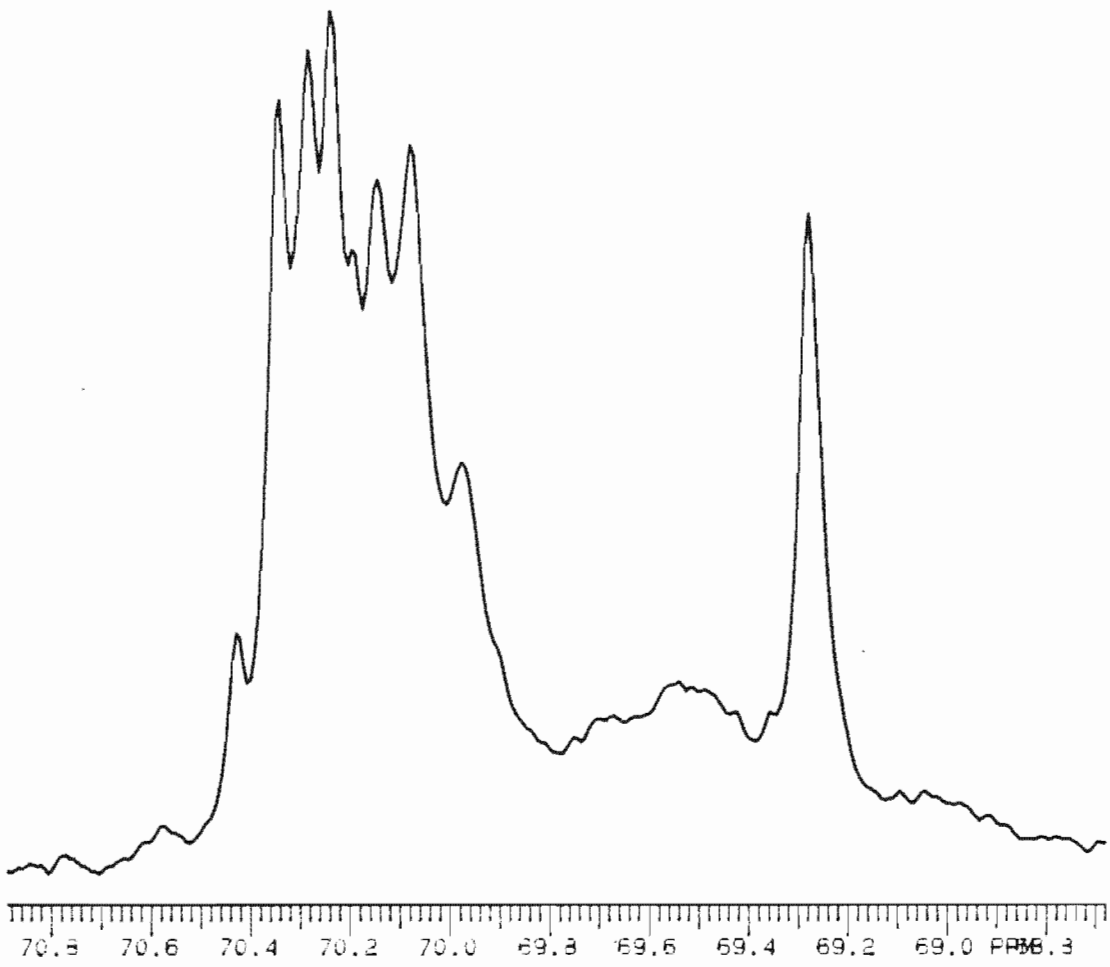

Figure 4.18 The change in the ^{13}C nmr signal of the central ethylene oxide carbons of Diϕ400U after extraction of $[RhH(SnCl_3)_5]^{3-}$ (compare with Figure 3.10, page 99).

Using chloroform solutions of Pol1500U(1:2), the chloro(trichlorostannato) complexes of rhodium were extracted from two solutions; one containing 0.2 M LiCl and 3.2 M HCl, the other containing 2 M LiCl and 1.4 M HCl. Both solutions contained 500 $\mu g.ml^{-1}$ rhodium and Sn:Rh ratios of 10:1. After separating the aqueous and organic phases by centrifuging the solutions, the aqueous phase (now devoid of any colour, hence suggesting quantitative extraction) was removed, and the organic phase was washed three times with a 1 M hydrochloric acid solution. The solubility of the Pol1500U(1:2) had decreased substantially on extraction, resulting in the separation of a "gummy" precipitate. This precipitate was solubilized by the addition of acetone to a final volume of 2 ml.

The presence of Li^+ in the extracted organic phase was shown conclusively by the appearance of a ^7Li nmr signal. The chemical shift position of the signal was very sensitive to the amount of acetone added to the extract, and it occurred in the range of 0.3 to 0.5 ppm relative to the external $Li^+(NO_3)^-$reference. After integrating the signal of three standards of known Li^+ concentration, as well as the integral of the reference signal, a linear calibration curve was constructed by plotting the integral ratios $I_{(standard)}/I_{(reference)}$ versus the concentration of each standard (see Figure 4.19). Comparison of the $I_{(sample)}/I_{(reference)}$ integral ratio to the calibration curve yielded the concentration of coextracted Li^+ in the extracted Pol1500U(1:2) phase. It was found that the Li^+ occurred mainly in the gummy precipitate.

Considering the complete removal of colour from the solution by the extraction process, it was reasonable to assume quantitative extraction of rhodium. Therefore, from the "known" concentration of rhodium in the organic phase, and the assumption that rhodium is extracted as a triply charged anion (this is verified in Chapter 5), one may calculate the concentration of positive charges required in the

organic phase to ensure electroneutrality. Thus it was determined that the concentration of the coextracted $^{7}Li^{+}$ in the organic phase accounted for 12% and 65% of the amount of cationic charge required for the extraction of rhodium from 0.2 M and 2 M LiCl solutions, respectively. However, it should be remembered that the cationic charge required for the neutralization of any chloro-tin complexes that might be coextracted is ignored in the above calculations, and the results are semi-quantitative at best. However, this study conclusively demonstrated two important facts: In the presence of alkali metal cations (eg. Li^{+}) in the aqueous phase from which rhodium is extracted,

a) coextraction of the alkali metal cations occurs, indicating the chelation of cations by the oligo(ethylene oxide) chains (a conclusion which was made in conjunction with the ^{13}C nmr spectrum),

b) the amount of alkali metal cations coextracted does not entirely account for the amount of rhodium extracted, thus underlining the importance of hydrogen ions in the extraction process.

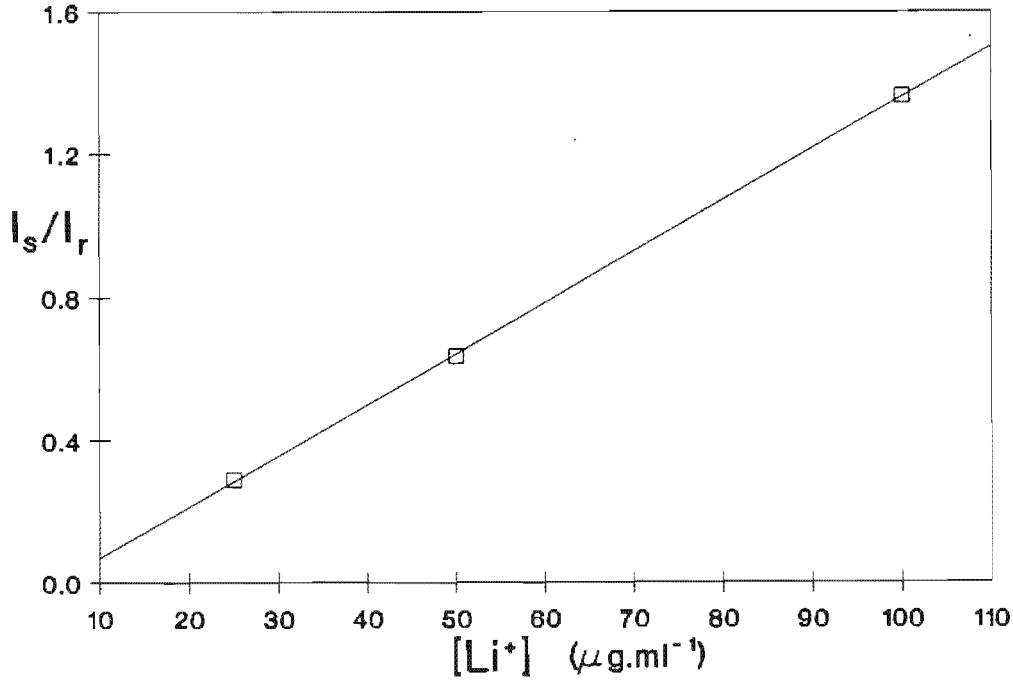

Figure 4.19 The calibration curve of $I_{(standard)}/I_{(reference)}$ versus the Li^{+} concentration used for the semi-quantitative determination of Li^{+} coextracted by Pol1500U(1:2).

2. 100% Poly(propylene oxide) Based Polyurethane Foam

An increase in the extracting power of polyurethane foam has been observed with an increase in the poly(ethylene oxide) (PEO) relative to poly(propylene oxide) (PPO) content [4]. Hamon *et al.* [4] ascribed this increased extraction to the ability of PEO chains to form helical conformations with inwardly directed oxygen atoms. Such a conformation was thought to be more efficient for the chelation of cations. Since PPO is not able to adopt such helical conformations (due to the steric hindrance of the methyl groups), a relatively higher proportion of PPO in the polyurethane foam is thought to result in a decreased extracting power.

To test the effect of the PEO content of polyurethane foam on the extraction of trichlorostannato complexes of rhodium, a comparison was made of the amount of rhodium extracted by the foam used in Chapter 2 (13% PEO + 87% PPO) to that extracted by the foam that had been produced from a polyol consisting wholly of PPO (100% PPO). The effect of a different isocyanate index was also tested (the meaning of an isocyanate index was explained in the introduction to Chapter 3). The synthesis of the 100% PPO based polyurethane foams is described in the experimental section (Chapter 7).

2.1 The Experiment

Portions of 0.0170 ± 0.0002 g of polyurethane foam together with 5 ml of aqueous phase in test tubes tightly sealed with inert silicone rubber stoppers, were shaken for 8 hours. The aqueous phase contained 150 $\mu g.ml^{-1}$ rhodium, a Sn:Rh ratio of 10:1, 3.2 M hydrochloric acid and 0.2 M MCl (where M = H^+, Li^+, Na^+ and K^+), and had been equilibrated at 35 °C for 4 days. The experiment was performed under nitrogen at constant temperature (20 °C). Small glass beads were added to the test

tubes in order to promote foam/solution contact, since it was thought that the agitating action of the beads during the shaking period should result in squeezing of the foam.

2.2 Results and Discussion

It is clear from Figure 4.20, that the foam with a 13% PEO content extracted almost twice the amount of rhodium than the highest amount extracted by a 100% PPO polyurethane foam. In addition, a higher isocyanate index evidently has an inhibiting effect on the extraction of rhodium.

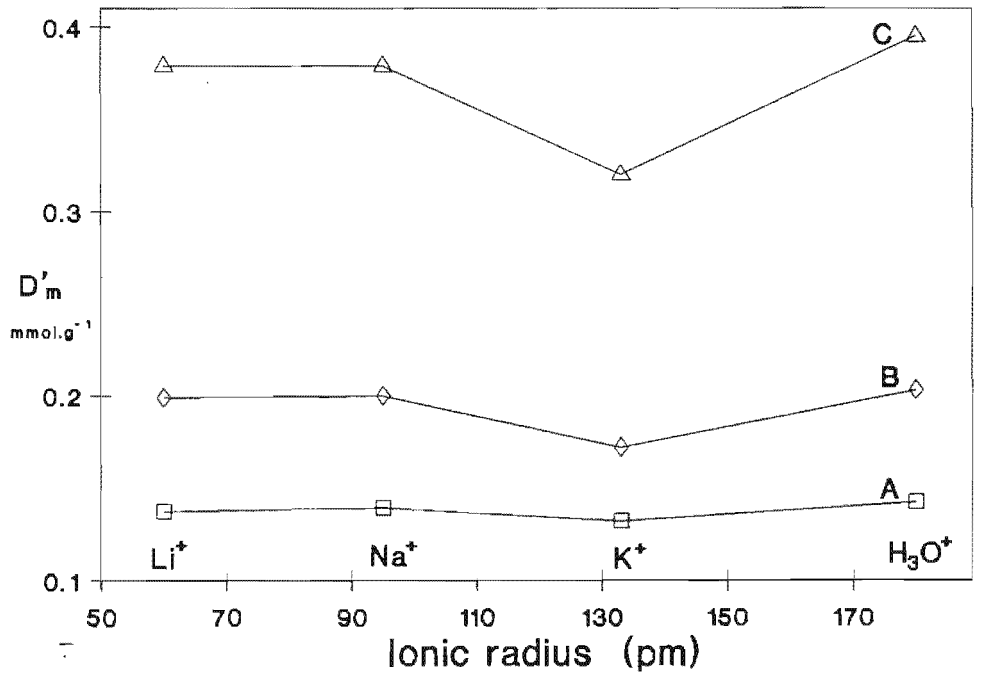

Figure 4.20 The effect of the PEO content, the isocyanate index and the presence of alkali metal cations on the extraction of rhodium. {150 $\mu g.ml^{-1}$ rhodium, Sn:Rh = 10:1, 3.2 M HCl and 0.2 M MCl ; A = 100% PPO foam (index 120), B = 100% PPO foam (index 90), C = 13% PEO + 87 PPO foam (index 107)}.

The effect of the various cations on the extraction of rhodium observed in the present study (*ie.* a general trend of $H^+ \geq Na^+ \sim Li^+ > K^+$ was observed), agrees well with the results of Chapter 2, Section 2.7). It is noteworthy that the effect of the cations on the extraction of rhodium is greatly reduced for the index 120 polyurethane foam where essentially similar amounts of rhodium were extracted under the conditions studied.

Before attempting to explain the difference in the extraction behaviour of the index 90 and index 120 polyurethane foams, one should be reminded of the difference in the nature of these two polyurethane foams. During the synthesis of the index 120 polyurethane foam, a 20% excess of isocyanate was used, resulting in a higher proportion of terminal amine groups, a higher proportion of urethane groups and other nitrogen containing groups, a higher degree of polymerization, as well as crosslinking. In contrast, the index 90 polyurethane foam has a 10% excess of hydroxyl groups and a lower proportion of nitrogen containing linkages, resulting in a higher proportion of hydroxyl terminated chains and a smaller degree of polymerization and crosslinking.

The decrease in the amount of rhodium extracted for an increase in the isocyanate index suggests that the nitrogen atoms do not contribute significantly towards the extraction process.

It was deduced from the study of the model urethane compounds {see Section 1.2(iv) and 1.2(vii)}, that any restriction on the flexibility of the linear polyurethane molecules necessary to assume the conformations needed for the chelation of cations, would have a negative influence on the amount of rhodium extracted. It is possible that this factor is of similar importance in determining the efficiency with

which rhodium is extracted by polyurethane foam. Hence, the higher proportion of relatively rigid groups such as the diurethane moieties, and the higher degree of crosslinking of the index 120 polyurethane foam, might be expected to restrict conformation changes of the polyether chains of the index 120 foam to a larger extent than for the index 90 foam. According to the explanations offered above, one would then expect a lower extracting power of the index 120 foam relative to the index 90 foam.

A similar reasoning may be used to explain the superior extracting powers of the polyurethane foam with a 13% PEO content. The steric hindrance of the methyl groups of the PPO chains in itself may be expected to restrict conformation changes of the polyether chains. Hence, the incorporation of PEO sections into the polyurethane foam should increase the flexibility of the polyether chains, with a concomitant increase in the number of conformations available for the chelation of cations.

The effect of the alkali metal cations on the extraction of rhodium is less easy to rationalize. Ionic size is evidently not the only factor of importance here. Potassium ions have an inhibiting effect on the extracting power of polyurethane foams, with the largest effect being observed for the polyurethane foam with a 13% PEO content. In view of the increased extraction by the model urethane compounds in the presence of K^+ ions, the K^+ induced depression of the extraction by polyurethane foam should be related to the nature of the foam. The negligible depression by K^+ ions of the extraction of rhodium by the index 120 polyurethane foam (100% PPO), supports the idea that the effect of K^+ is related mainly to the nature of the polyurethane foam.

The K^+ induced depression of the extraction of rhodium by polyurethane foam is thought not to be due to competitive sorption by chloro-tin complexes, since no large increase was observed in the ratios in which Sn and Rh were coextracted. Table 4.3 is a summary of the ratios of coextracted Sn and Rh for the different foams under the various conditions.

Table 4.3 The ratios in which Sn and Rh were coextracted by the various foams.

	3.2 M HCl			
Polyurethane foam	+ 0.2 M LiCl	+0.2 M NaCl	+ 0.2 M KCl	+ 0.2 M HCl
100% PPO index 90	5.09:1	4.83:1	5.50:1	5.16:1
100% PPO index 120	4.96:1	4.67:1	5.25:1	5.28:1
13% PEO + 87% PPO index ~107	5.20:1	4.56:1	4.92:1	4.83:1

REFERENCES

1 T.SOTOBAYASHI, T.SUZUKI AND K.YAMADA,
Chemistry Letters (Chem. Soc. Jpn.) (1976) 77

2 T.SOTOBAYASHI, T.SUZUKI AND S.TONOUCHI,
Chemistry Letters (Chem. Soc. Jpn.) (1976) 585

3 H.M.N.H. IRVING, "Liquid-Liquid Extraction", from
"Treatise on Analytical Chemistry", 2nd ed.,PT. 1, **VOL 5** (1982) 505
John-Wiley & Sons, Edited by P.J.Elving

4 R.F.HAMON, A.S.KHAN AND A.CHOW,
Talanta, **29** (1982) 313

5 S.YANAGIDA, K.TAKAHASHI AND M.OKAHARA,
Bull. Chem. Soc. (Jpn), **50** (1977) 1386

6 S.YANAGIDA, K.TAKAHASHI AND M.OKAHARA,
Bull. Chem. Soc. (Jpn), **51** (1978) 1294

7 S.L.DAVYDOVA AND N.A.PLATE,
Coord. Chem. Rev. **16** (1975) 195

8 T.KIMURA,
Sci. Papers I.P.C.R., **73** (1979) 31

9 S.IWASAKI, T.NAGAI, E.MIKI, K.MIZUMACHI AND T.ISHIMORI,
Bull. Chem. Soc. (Jpn), **57** (1984) 386

10 C.J.PEDERSEN,
J. Amer. Chem. Soc., **89** (1967) 7017

11 B.TÜMMLER, G.MAASS, F.VÖGTLE, H.SIEGER, U.HEIMANN AND E.WEBER,
J. Amer. Chem. Soc., **101** (1979) 2588

12 J.E.HUHEEY,
"Inorganic Chemistry", Harper & Row, New York, 2nd. ed., (1978)

13 E.KROGH ANDERSEN AND I.G.KROGH ANDERSEN,
Acta Cryst., B31 (1975) 379

14 F.A.COTTON AND G.WILKINSON,
"Advanced Inorganic Chemistry: A Comprehensive Text",
4th Ed., Wiley-Interscience, New York, (1980), p232

15 H.R.ALLCOCK AND F.W.LAMPE,
"Contemporary Polymer Chemistry", Prentice-Hall, New Jersey, (1981), p379

16 D.A.PALMER AND G.M.HARRIS,
Inorg. Chem., **14** (1975) 1316

17 C.CARR, J.GLASER AND M.SANDSTRÖM,
Inorg. Chim. Acta, **131** (1987) 153

CHAPTER 5

A SPECIATION STUDY

Introduction

The rhodium complexes that exist in aqueous acidic solutions containing stannous chloride have been relatively well characterized. Six-coordinate rhodium(III) complexes $[R_4N]_3[Rh(SnCl_3)_nCl_{6-n}]$ (with n = 2, 3 and 4) have been isolated by Kimura [1] from yellow solutions. In addition, the isolation of "some interesting complexes", a yellow and a violet salt from a purple solution was reported [1]. A published crystal structure [2] of the violet salt identified the complex as $[Rh(NH_3)_6]_3[Rh(SnCl_3)_4(SnCl_4)][SnCl_6].4H_2O$, where the anionic rhodium complex was trigonal bipyramidal. Kimura [1] was not able to identify the yellow salt, but the reported infrared band at 1940 cm^{-1} and the solution behaviour on dilution with HCl or LiCl coincided with the behaviour of a yellow salt isolated from 3 M solutions by Krut'ko *et al.* [3]. This latter yellow salt was precipitated with the bulky tetrabutyl- and tetraethylammonium cations, and was identified as the $[R_4N]_3[RhH(SnCl_3)_5]$ hydrido complex by ^{119}Sn and ^1H nmr spectroscopy [3]. The infrared stretching frequency ν(Rh-H) was reported to be at 1940 cm^{-1}.

A ^{119}Sn nmr study by Moriyama *et al.* [4] identified the rhodium(III) complexes, $[Rh(SnCl_3)_nCl_{6-n}]^{3-}$ (with n = 1 - 5) that exist in aqueous hydrochloric acid solutions of $RhCl_3$ and $SnCl_2$. The distribution of the species was found to be sensitive to the molar Sn:Rh ratio, which was varied from 1:1 to 7:1. With a Sn:Rh ratio of 6:1 a doublet peak at 8.5 ppm in the ^{119}Sn nmr spectrum became dominant, and this was postulated to arise from the trigonal bipyramidal rhodium(I) species $[Rh(SnCl_3)_5]^{4-}$. Strong evidence for the reduction of rhodium(III) to rhodium(I) was found by the appearance of a tin(IV) resonance. Analysis of the spectrum revealed that one mole of $SnCl_2$ per mole of $RhCl_3$ was converted to tin(IV). The tin ligands of the rhodium complexes were found to undergo fast intramolecular scrambling. A

kinetic investigation [5] revealed that the rhodium(III) complexes were kinetically labile and that excess $SnCl_2$ reacts with chloro(trichlorostannato)rhodium(III) species in hydrochloric acid to yield a purple species assumed to be $[Rh(SnCl_3)_5]^{4-}$.

The trichlorostannato-rhodium complexes that exist in organic phases have not been studied in great detail. The dehydrogenation of propan-2-ol is catalyzed in the presence of $RhCl_3$ and $SnCl_2$ to yield acetone and dihydrogen [6,7]. A ^{119}Sn nmr examination of the catalyst solution identified not only the 6-coordinate chloro(trichlorostannato)rhodium(III) complexes [7] observed in aqueous solutions [4], but also the hydrido complex $[RhH(SnCl_3)_5]^{3-}$ [8]. Koch *et al.* [9] studied the 4-methylpentan-2-one (MIBK) extracts obtained from hydrochloric acid solutions containing $RhCl_3$ and various amounts of $SnCl_2$, by ^{119}Sn nmr spectroscopy. The MIBK phases were found to contain the complexes $[Rh(SnCl_3)_nCl_{6-n}]^{3-}$ with n = 3 and 5, as well as a rhodium(III) complex which was tentatively proposed to be $[Rh(SnCl_3)_5]^{2-}$ in which a solvent molecule was suggested to occupy the vacant coordination site. In addition, a rhodium-hydrido complex was identified and formulated as the chlorotetrakis(trichlorostannato)rhodium(III) hydrido anion, $[RhH(SnCl_3)_4Cl]^{3-}$.

The synthesis of the soluble urethane compounds as models of polyurethane foam has made a direct analysis of the extracted rhodium complexes possible. This Chapter reports the identification of the trichlorostannato complexes of rhodium that are extracted under various solution conditions by the model urethane compounds. In order to detect any preference for rhodium species that are specific to the urethane compounds, the speciation study of the rhodium complexes extracted by these model compounds was compared to an analogous study of the complexes that are extracted by MIBK and a liquid anion exchanger,

tricaprylmethylammonium chloride (Aliquat 336). MIBK was chosen for comparative purposes since it is an oxygen donor solvent that is known to solvent extract the trichlorostannato complexes of rhodium from hydrochloric acid solutions [9]. Aliquat 336 extracts anions solely by the formation of ion pairs. Hence, the "anion-exchanged" rhodium complexes should be a true reflection of the complexes in the aqueous phase that are available for extraction.

1. ^{119}Sn nmr

1.1 Overview

In general, nuclear magnetic resonance has proved to be a powerful technique for providing structural information of organic as well as inorganic species. ^{119}Sn (I = 1/2, natural abundance = 8.58%) nmr spectroscopy is particularly profitable for the elucidation of inorganic tin species. With respect to rhodium-tin complexes the following additional advantages were highlighted by Moriyama *et al.* [4]:

1) Evidence for the coordination of tin ligands to rhodium is obtained by the appearance of a doublet due to the spin coupling with ^{103}Rh (I = 1/2, natural abundance = 100%)
2) Due to spin coupling with the ^{117}Sn isotope (I = 1/2, natural abundance = 7.61%) rhodium complexes containing more than one tin ligand should yield satellite peaks which provide information on the structure and fluxional behaviour of the complex.
3) Nuclear magnetic resonance parameters, such as $\delta(^{119}Sn)$, $^{1}J(^{103}Rh\text{-}^{119}Sn)$, and $^{2}J(^{117}Sn\text{-}^{119}Sn)$ are useful in assigning the observed resonances to the complexes from which they arise.

These authors were able to show on a statistical basis that the value of the peak intensity ratio, $I_{(satellite)}/I_{(main)}$, was related to the number of $SnCl_3^-$ ligands associated with the rhodium atom [4]. Since only one set of main and satellite peaks was observed for each complex (despite the likelihood of more than one isomer of each complex being present) it was concluded that these rhodium-tin complexes exhibited fast intramolecular scrambling. The theoretical peak intensity ratios, as well as the ratios observed by Moriyama *et al.* [4], that assisted in their assignment of the resonances to the various rhodium complexes, are shown in Table 5.1.

Table 5.1 The theoretical and observed peak intensity ratios of the trichlorostannato-rhodium complexes [4].

$Rh(SnCl_3)_nCl_{6-n}$ n	$I_{(satellite)}/I_{(main)}$ calculated (observed)	$\delta(^{119}Sn)$ (ppm)
1	no satellites	-914.1
2	4.2 (4.2)	-628.6
3	8.3 (8.2)	-411.1
4	12.3 (11.6)	-204.3
5	16.3 (16.2)	-100.5
$[Rh(SnCl_3)_5]^{4-}$	16.3 (16.2)	+8.5

The electronic properties of the rhodium-tin complexes are highly sensitive to substitution of the tin ligand, as is evident from the wide variation in the tin-chemical shift $\{\delta(^{119}Sn)\}$ values observed by Moriyama *et al.* [4]. In the series of complexes $[Rh(SnCl_3)_nCl_{6-n}]^{3-}$ (n = 1 - 5), the values for $\delta(^{119}Sn)$ ranged from 914.1 ~~991.6~~ to −100.5 ppm, and deshielding of the ^{119}Sn nmr resonance occurs with an increase in the number of tin ligands coordinated to the central rhodium atom. In addition, an increase in the number of coordinated tin ligands results in a decrease in the one bond coupling constants, $^1J(^{103}Rh\text{-}^{119}Sn)$. A definite correlation between the tin chemical shifts and the rhodium-tin coupling constants was observed. In

general, the metal-ligand coupling constant has been observed to be a good measure of the strength of the metal-ligand σ-bond [10]. Hence, as mentioned by Moriyama *et al.* [4], the above-mentioned trend of $^{1}J(^{103}Rh\text{-}^{119}Sn)$ within the complexes $[Rh(SnCl_3)_nCl_{6-n}]^{3-}$ (n = 1 - 5) indicates that the rhodium-tin σ-bond strength decreases as the number of the $SnCl_3^-$ ligands increases. This view was supported by a correlation between $^{1}J(^{103}Rh\text{-}^{119}Sn)$ and $^{2}J(^{117}Sn\text{-}^{119}Sn)$ that was observed for the rhodium(III) complexes [4].

The nmr characteristics of the doublet observed at 8.5 ppm [4] did not form part of the correlation for the rhodium(III) complexes. This peak was thought to arise from a rhodium(I) complex, probably the trigonal bipyramidal $[Rh(SnCl_3)_5]^{4-}$. According to Moriyama *et al.*, the relatively large $^{1}J(^{103}Rh\text{-}^{119}Sn)$ for this resonance "may be associated with the low valency of rhodium for the complex $[Rh(SnCl_3)_5]^{4-}$".

Krut'ko *et al.* [3] described the ^{1}H-decoupled ^{119}Sn nmr spectrum of the hydrido complex, $[BuN]_3[RhH(SnCl_3)_5]$, in acetonitrile recorded at -40 °C. An independent publication by Yamakawa *et al.* [8] also reported the ^{119}Sn nmr spectrum of the same hydrido complex, with the octahedral structure illustrated in Figure 5.1.

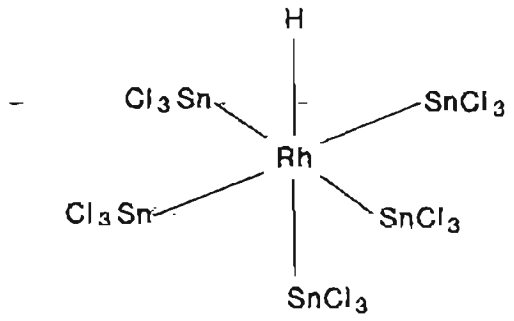

Figure 5.1 The octahedral structure of $[RhH(SnCl_3)_5]^{3-}$.

Intramolecular scrambling of the $SnCl_3^-$ ligands within the hydrido complex was not evident on the nmr time scale since separate resonances were detected for the axial and the equatorial $SnCl_3^-$ ligands. The axial ^{119}Sn ligand, δ_{axial} = 77,8 (91.0) ppm, was found to resonate downfield from the equatorial ^{119}Sn ligands, $\delta_{equatorial}$ = -13,7 (-1.2) ppm, where the chemical shifts reported by Yamakawa *et al.* [8] are quoted and those of Krut'ko *et al.* [3] are given in parenthesis. Since *trans*-coupling is usually much greater than *cis*-coupling [11,12], assignment of the low field resonance to the axial $SnCl_3^-$ moiety was made from the large $^2J(^1H\text{-}^{119}Sn)$ associated with this ^{119}Sn resonance and its relative resonance integral.

The ^{119}Sn resonance arising from the equatorial tin ligands is a doublet of doublets due to coupling with the ^{103}Rh and ^1H nuclei, and it is accompanied by 3 sets of satellites which are due to:

a) *trans* $^{117}Sn\text{-}^{119}Sn$ coupling of the equatorial tin ligands,

b) *cis* $^{117}Sn\text{-}^{119}Sn$ coupling of the equatorial ligands, and

c) *cis* $^{117}Sn\text{-}^{119}Sn$ coupling of the axial ligand to the equatorial ligands.

The doublet of doublets arising from the axial $SnCl_3^-$ ligand (coupled to the ^1H and ^{103}Rh nuclei) is accompanied by one set of satellites due to *cis* $^{117}Sn\text{-}^{119}Sn$ coupling [3,8].

The nmr parameters of the hydrido complex $[RhH(SnCl_3)_5]^{3-}$ as observed by Yamakawa *et al.* [8] and Krut'ko *et al.* [3] are compared in Tables 5.2 . When one considers the different values observed for $\delta(^{119}Sn)$ by these authors there appears to be a significant solvent effect upon the chemical shifts of the ^{119}Sn nmr resonances.

Table 5.2 Nmr data for $[RhH(SnCl_3)_5]^{3-}$ as observed by Yamakawa et al. [8] and Krut'ko et al. [3].

Parameter	Yamakawa *et al.*	Krut'ko *et al.*
$\delta(^{119}Sn)$	$77.8_{(ax)}$	$91.0_{(ax)}$
	$-13.7_{(eq)}$	$-1.2_{(eq)}$
$\delta(^{1}H)$	-10.5	-13.1
$^{2}J(^{1}H\text{-}^{119}Sn)$	$58.6_{(eq)}$	$60_{(eq)}$
	$1146_{(ax)}$	$1110_{(ax)}$
$^{2}J(^{117}Sn\text{-}^{119}Sn)$	$25506_{(trans,\ eq\text{-}eq)}$	$25420_{(trans,\ eq\text{-}eq)}$
	$1975_{(cis,\ eq\text{-}eq)}$	$1992_{(cis,\ eq\text{-}eq)}$
	$1762_{(cis,\ ax\text{-}eq)}$	$1772_{(cis,\ ax\text{-}eq)}$
$^{1}J(^{103}Rh\text{-}^{119}Sn)$	$596_{(eq)}$	$592_{(eq)}$
	$532_{(ax)}$	$524_{(ax)}$
$^{1}J(^{103}Rh\text{-}^{1}H)$	9.5	10

where eq = equatorial and ax = axial, δ in ppm and J in Hz.

It would seem that the rhodium hydride observed in MIBK extracts by Koch *et al.* [9] was not the $[RhH(SnCl_3)_4Cl]^{3-}$ anion proposed, but is really the same species as that reported by Yamakawa *et al.* [8]. Koch *et al.* [9] report a chemical shift of -14,6 ppm, which coincides with that reported by Yamakawa *et al.* for the equatorial ^{119}Sn resonance. In addition, the coupling constants reported by Koch *et al.* [9] are in agreement with the corresponding coupling constants that were previously observed for $[RhH(SnCl_3)_5]^{3-}$ [3,8]. Failure to detect the axial resonance as well as the satellites due to *trans*- $^{2}J(^{117}Sn\text{-}^{119}Sn)$ coupling (^{2}J = 25506 Hz according to Yamakawa *et al.*), would explain their erroneous assignment of the hydrido complex as $[RhH(SnCl_3)_4Cl]^{3-}$. A different solvent system might alter the stereochemical rigidity of the hydrido complex. Intramolecular scrambling would make it more difficult to detect the separate resonances arising from the axial and equatorial ligands. (Krut'ko *et al.* [3] recorded the spectrum of $[RhH(SnCl_3)_5]^{3-}$ in CD_3CN at a temperature of -40 °C.) Hence, it is evident that in MIBK (the solvent used by

Koch *et al.* [9]) a degree of intramolecular scrambling occurs, whereas in isopropyl alcohol (used by Yakamawa *et al.* [8]) the hydrido molecule is stereochemically rigid.

Based on their isolation of the impure *trans*-$[IrHCl(SnCl_3)_4]^{3-}$, Yamakawa *et al.* [8] concluded that many more complexes of the type $[RhH_aCl_b(SnCl_3)_c]^{3-}$ (where a + b + c = 6) may be available. Although the rhodium hydride seems to be stable in organic phases, it appears to form in the aqueous phase only under severely acidic conditions. Krut'ko *et al.* [3] detected the $[RhH(SnCl_3)_5]^{3-}$ anion by ^{119}Sn nmr only in a hydrochloric acid solution saturated with gaseous HCl.

From the above, it has become clear that the organic extracts might contain a large variety of the trichlorostannato-rhodium complexes. Hence, a detailed ^{119}Sn nmr study of the rhodium complexes that are extracted from a variety of aqueous acidic solutions by the urethane compounds, MIBK and Aliquat 336, was undertaken.

1.2 Results

The only urethane compound that could be used practically for the ^{119}Sn nmr study was Diϕ400U. The inherent insensitivity of the nmr technique requires a relatively high concentration of the nucleus under investigation in the phase being studied. Since the solubility of the linear polyurethanes was significantly reduced upon interaction with the rhodium-tin complexes, a sufficiently high concentration of ^{119}Sn could not be attained. However, a high concentration of the Diϕ400U-rhodium extracts could be solubilized in acetone, making the Diϕ400U extracts suitable for examination by ^{119}Sn nmr.

The solution conditions of the aqueous phases from which the rhodium-tin complexes were extracted were varied by adjusting the Sn:Rh ratio, the hydrochloric acid concentration, and the potassium chloride concentration.

1.2 (i) Extracts from Aqueous Phases Containing Excess Stannous Chloride

(a) Diϕ400U Extracts

The predominance of the hydrido complex, $[RhH(SnCl_3)_5]^{3-}$, in the Diϕ400U extracts was striking. In the presence of excess Sn(II) (Sn:Rh > 6:1), only $[RhH(SnCl_3)_5]^{3-}$ and unassociated chloro-tin(II) {and sometimes small amounts of tin(IV)} complexes were detected in the Diϕ400U solutions, irrespective of the hydrochloric acid concentration or the presence of potassium chloride (see Figure 5.3). The resonances of the chloro-tin(II) species that were not associated to rhodium occurred within the chemical shift range of -26.6 to -95.6 ppm. In the majority of these spectra, separate resonances accompanied by their respective satellites were detected for the axial and equatorial tin ligands of $[RhH(SnCl_3)_5]^{3-}$, confirming the spectral pattern and stereochemical rigidity of the hydrido complex reported by both Yamakawa *et al.* [8] and Krut'ko *et al.* [3]. Only when the rhodium-tin complexes were extracted from 0.7 M HCl solutions containing no KCl could the resonance due to the axial ^{119}Sn ligand and the satellites due to ^{117}Sn-^{119}Sn coupling not be distinguished from the baseline because of the low signal to noise ratio. Under these conditions of low acid concentration (and relatively low ionic strength, in the absence of alkali metals), extraction of rhodium by the urethane compounds was found to be relatively inefficient (see Chapter 4, Section 1.2(vi)). Thus, with the low concentration of ^{119}Sn nuclei in the Diϕ400U after extraction from 0.7 M hydrochloric acid solutions, the relatively weak nmr signals and consequently the low signal to noise ratio are not surprising.

(b) MIBK Extracts

The spectral patterns observed for the various MIBK extracts are summarized in Figure 5.4. In the presence of excess tin(II), three different rhodium-tin species were extracted by MIBK from solutions containing a fixed Cl^- concentration with varying concentration of K^+ relative to H^+. The relative proportions of these complexes, whose signals occurred at -14.2 ppm, -54.5 ppm and -115.7 ppm, were dependent upon the hydronium ion concentration. The species at -14.2 ppm was identified by its chemical shift position and its $^1J(^{103}Rh\text{-}^{119}Sn)$ and $^2J(^1H\text{-}^{119}Sn)$ coupling constants to be the hydrido complex $[RhH(SnCl_3)_5]^{3-}$. The hydridic nature of the complex was further confirmed by decoupling experiments and by recording the proton nmr spectrum {$\delta(^1H)$ = -13.2 ppm and $^1J(^{103}Rh\text{-}^1H)$ = 9.6 Hz}. Although the satellites resulting from ^{117}Sn to ^{119}Sn coupling of the equatorial $SnCl_3^-$ ligands of $[RhH(SnCl_3)_5]^{3-}$ were distinguishable in the MIBK extracts, they were generally very broad and ill-defined, making the $^2J(^{117}Sn\text{-}^{119}Sn)$ coupling constants difficult to measure. The axial ^{119}Sn nmr resonances were visible only in the spectrum of the MIBK extract from 3 M hydrochloric acid, in which the hydrido complex, $[RhH(SnCl_3)_5]^{3-}$, predominated. In no spectrum of the MIBK extracts could the satellites due to *trans* ^{119}Sn to ^{117}Sn coupling be distinguished.

The nmr parameters of the species at -54.5 and -115.7 ppm, which were noted to be stereochemically non-rigid (since only one set of main peaks and satellites were observed), correlated well with a plot of $^1J(^{103}Rh\text{-}^{119}Sn)$ as a function of $\delta(^{119}Sn)$ for the series of complexes $[Rh(SnCl_3)_nCl_{6-n}]^{3-}$ (n = 1 - 5) in 3.0 M hydrochloric acid as found by Moriyama *et al.* (see Figure 5.2) [4]. This suggests that these complexes are rhodium(III) species. The integrated peak ratios, $I_{(satellite)}/I_{(main)}$, were found to be 12.4% and 8.4% for the resonances at -54.5 and -115.7 ppm respectively.

These values agree well with the theoretical values calculated for four (12.3%) and three (8.3%) coordinated $SnCl_3^-$ ligands. However, the nmr coupling and shift parameters of these complexes do not coincide with those assigned to $[Rh(SnCl_3)_4Cl_2]^{3-}$ and $[Rh(SnCl_3)_3Cl_3]^{3-}$ by Moriyama *et al.* [4] (see Table 5.3).

Table 5.3 A comparison of the nmr characteristics of the complexes found in MIBK with those identified by Moriyama *et al.* [4] .

		Moriyama *et al.* [4]		
n	I_s/I_m	$\delta(^{119}Sn)$	$^1J(^{103}Rh\text{-}^{119}Sn)$	$^2J(^{117}Sn\text{-}^{119}Sn)$
3	8.2%	-411.1	718	2804
4	11.6%	-204.3	590	2158
		MIBK extracts		
n	I_s/I_m	$\delta(^{119}Sn)$	$^1J(^{103}Rh\text{-}^{119}Sn)$	$^2J(^{117}Sn\text{-}^{119}Sn)$
3	8.4%	-115.7	551	1910
4	12.4%	-54.5	519	1673

$I_s/I_m = I_{(satellite)}/I_{(main)}$, δ in ppm and J in Hz.

It should be remembered that the series of complexes $[Rh(SnCl_3)_nCl_{6-n}]^{3-}$ characterized by Moriyama *et al.* [4] were recorded in aqueous solutions whereas in this work the rhodium-tin complexes are being examined in organic phases. It is difficult to state at this stage whether the difference in the nmr characteristics of the complexes (with δ = -54.5 and -115.7 ppm) in MIBK with those of $[Rh(SnCl_3)_4Cl_2]^{3-}$ and $[Rh(SnCl_3)_3Cl_3]^{3-}$ identified by Moriyama *et al.* [4] is due to a strong solvent effect, or whether we are observing different rhodium-tin(II) species. It is possible that substitution of one or more of the chloro ligands by the oxygen donor solvent (MIBK) molecules takes place. A similar suggestion was proposed by Yamakawa *et al.* [8] who examined a catalyst solution containing $RhCl_3.3H_2O$ and $SnCl_2.2H_2O$

(after catalytic dehydrogenation of propan-2-ol to acetone) by ^{119}Sn nmr spectroscopy, and observed a signal at δ = -118.0 ppm with $^{1}J(^{103}Rh\text{-}^{119}Sn)$ = 557 Hz and $^{2}J(^{117}Sn\text{-}^{119}Sn)$ = 1891 Hz. These authors found the number of coordinated $SnCl_3^-$ ligands to be four. Since the chemical shift and the coupling constants did not coincide with those of $[Rh(SnCl_3)_4Cl_2]^{3-}$ in 3 M hydrochloric acid, Yamakawa *et al.* [8] proposed that substitution of the chloro ligands by the 2-propoxy ligands occurred. It is noteworthy that the latter species observed by Yamakawa *et al.* occurring at -118.0 ppm has similar chemical shift and coupling constant parameters to the species observed in this work (see Table 5.3). This suggests that these two species are similar. However, there is a discrepancy in the assignment of the number of $SnCl_3^-$ ligands coordinated to the rhodium atom. Yamakawa *et al.* reported four coordinated $SnCl_3^-$ ligands, while in the present work the integrated peak ratios of the resonance at -115.7 ppm indicated three $SnCl_3^-$ ligands to be coordinated. It is uncertain at this stage whether the resonances in question arise from different rhodium-tin species (with four and three coordinated $SnCl_3^-$ ligands) or whether there is an error in the integrated peak ratios.

The rhodium(III) complexes may be formulated as $[Rh(SnCl_3)_nX_mCl_{6-(n+m)}]^{(3-m)-}$, where X is a ligating extractant molecule and $(n + m) \leq 6$. As mentioned above, the relative proportions of $[Rh(SnCl_3)_nX_mCl_{6-(n+m)}]^{(3-m)-}$ (with n = 3 and 4) and $[RhH(SnCl_3)_5]^{3-}$, appeared to be dependent upon the hydronium ion concentration in the aqueous phase. This phenomenon is clearly illustrated in Table 5.4, which summarizes the relative amounts of the three rhodium-tin complexes that are extracted by MIBK from the various aqueous phases.

Table 5.4 The effect of $[H^+]$ on the relative amounts in which $[RhH(SnCl_3)_5]^{3-}$ and $[Rh(SnCl_3)_nX_mCl_{6-(n+m)}]^{(3-m)-}$ occur in MIBK (Sn:Rh in the aqueous phase = 10:1).

[HCl]	[KCl]	% $[RhH(SnCl_3)_5]^{3-}$	% $[Rh(SnCl_3)_4X_mCl_{2-m}]^{(3-m)-}$	% $[Rh(SnCl_3)_3X_mCl_{3-m}]^{(3-m)-}$
0.5	2.5	45.1	44.6	10.3
1.0	2.0	82.1	17.6	0.3
3.0	0.0	100	0	0

The results show that the increased hydronium ion concentration in the aqueous phase promotes the formation of the hydrido complex in the organic phase, which is consistent with an increase in the amount of coextracted HCl in the organic phase. It is noteworthy that approximately 37% of the total amount of ^{119}Sn detected in the MIBK extracts from 3 M hydrochloric acid solutions was unassociated tin(II) complexes, while no free $SnCl_3^-$ and $SnCl_4^{2-}$ was detected in the other extracts.

After recording the ^{119}Sn nmr spectrum of the MIBK extract from a 3 M hydrochloric acid solution in which $[RhH(SnCl_3)_5]^{3-}$ had been found as the only rhodium-tin complex, the extract was exposed to the atmosphere for 25 hours at 20 ^oC and the spectrum was re-recorded (see Figure 5.5). The predominant species was now the complex $[Rh(SnCl_3)_4X_mCl_{2-m}]^{(3-m)-}$ with a signal at -54.5ppm, while the signal (at -14.3 ppm) due to the hydrido complex, $[RhH(SnCl_3)_5]^{3-}$, was greatly reduced and considerably broadened. The relative proportions of the signals at -14.3 ppm and -54.5 ppm were 30.2% and 69.8% respectively. No resonance due to unassociated tin(II) species was detected since quantitative oxidation of the free tin(II) to tin(IV) had presumably occurred. {The ^{119}Sn nmr resonances of the chloro-tin(IV) complexes ($SnCl_4$, $SnCl_5^-$ and $SnCl_6^{2-}$) occur in the chemical shift range upfield of -500 ppm}. This suggests that the resonance at -54.5 ppm is due to

a complex formed upon decomposition of the hydrido complex, possibly due to oxidation of the $SnCl_3^-$ ligands (the extract had been exposed to air for 25 hours). Thus we tentatively propose that decomposition of the hydrido complex in MIBK occurs as follows:

$$[RhH(SnCl_3)_5]^{3-} + 3HCl \rightarrow [Rh(SnCl_3)_4(MIBK)Cl]^{2-} + 2H_2 + Sn(IV)Cl_5^- \quad (1)$$

(c) Aliquat 336 Extracts

The largest variation in the extracted rhodium complexes was observed using the liquid anion exchanger Aliquat 336 in $CDCl_3$ (see Figure 5.6). When extractions were made from aqueous solutions containing low hydrochloric acid concentrations (from 0.7 M hydrochloric acid solutions and from 0.5 M hydrochloric acid solutions containing 2.5 M KCl), only the purple trigonal bipyramidal rhodium(I) complex $[Rh(SnCl_3)_5]^{4-}$ and chloro-tin(II) complexes were detected in the nmr spectrum. It is interesting that this rhodium(I) complex was not detected in the comparable Diϕ400U and MIBK extracts (using similar aqueous phase compositions). Instead, the hydrido complex was prominent in the spectra of these oxygen-donor extracts despite low acid conditions during the extraction process. The ^{119}Sn nmr spectrum of the Aliquat 336 phase after extraction from 0.5 M hydrochloric acid solutions, is compared to those of Diϕ400U and MIBK in Figure 5.7. The coextraction of HCl by Diϕ400U and MIBK is likely, whereas Aliquat 336 constitutes an $(R_4N)^+Cl^-$ ion pair in chloroform, which does not provide the means for HCl extraction into the organic phase. This suggests that the stability of the trigonal bipyramidal complex in Aliquat 336 is due to the absence of coextracted acid, whereas the hydrochloric acid present in the MIBK and Diϕ400U phases results in the protonation of the trigonal bipyramidal (purple) species to form the hydrido complex $[RhH(SnCl_3)_5]^{3-}$. To test

this proposal, a few drops of a 5% v/v solution of CF_3COOH (in $CDCl_3$) were added to the Aliquat 336 extract made from a solution of 0.5 M HCl with 2.5 M KCl, which had been shown to contain $[Rh(SnCl_3)_5]^{4-}$ as the only rhodium-tin complex. The colour changed immediately from a deep purple-red to bright yellow. Examination of the solution by ^{119}Sn nmr revealed the predominance of the hydrido complex $[RhH(SnCl_3)_5]^{3-}$, with small amounts of two complexes resonating at -112.7 ppm $\{^1J(^{103}Rh\text{-}^{119}Sn) = 550$ Hz$\}$ and at -144.3 ppm $\{^1J(^{103}Rh\text{-}^{119}Sn) = 617$ Hz$\}$. In addition, the unassociated tin(II) resonance had shifted from -53.3 ppm to -163.7 ppm. These results provide compelling evidence in support of the proposal that the hydrido complex is formed by the protonation of the trigonal bipyramidal rhodium(I) complex as shown below:

$$[R_4N]_4[Rh(SnCl_3)_5] + CF_3COOH \rightleftharpoons [R_4N]_3[RhH(SnCl_3)_5] + [R_4N][CF_3COO]$$

Extractions from 3 M hydrochloric acid solutions resulted in Aliquat 336 solutions containing mainly the hydrido complex with some coextracted chloro-tin(II) complexes and trace amounts of a rhodium-tin complex that resonates at -116.31 ppm $\{^1J(^{103}Rh\text{-}^{119}Sn) = 544$ Hz$\}$. Presumably in the presence of high concentrations of acid in the aqueous phase, protonation of $[Rh(SnCl_3)_5]^{4-}$ occurs at the aqueous-organic interphase.

An interesting spectrum was observed for the Aliquat 336 extracts from 5 M hydrochloric acid solutions. In addition to the strong signal at -14.1 ppm due to $[RhH(SnCl_3)_5]^{3-}$, another hydrido complex was observed at -92.5 ppm, as confirmed by decoupling experiments. The satellites due to the ^{117}Sn to ^{119}Sn coupling could regrettably not be distinguished from the baseline because of the poor signal to noise ratio. However, the magnitude of the coupling of ^{103}Rh and ^1H to ^{119}Sn were measured to be $^1J(^{103}Rh\text{-}^{119}Sn) = 667$ Hz and $^2J(^1H\text{-}^{119}Sn) = 104$ Hz. It is likely

that, due to the high chloride concentration in the solutions from which it was extracted and in view of the analogous iridium complex $[IrH(SnCl_3)_4Cl]^{3-}$ identified by Yamakawa *et al.* [8], this complex may be formulated to be $[RhH(SnCl_3)_4Cl]^{3-}$.

1.2(ii) Extracts from 3 M Hydrochloric Acid Solutions with a 4:1 Molar Sn:Rh Ratio

(a) Diϕ400U Extracts

Four rhodium-tin complexes were observed in the spectra that covered the chemical shift range from + 100 ppm to -900 ppm (Figure 5.3). It was interesting to note that under conditions in which the Sn:Rh ratio in the aqueous phase was < 6:1, no coextraction of rhodium-unassociated chloro-tin(II) species was evident.

The ^{119}Sn resonance arising from the hydrido complex $[RhH(SnCl_3)_5]^{3-}$ at -13.7 ppm was again prominent. The remaining three complexes, which appear to undergo fast intramolecular scrambling, are thought to be rhodium(III) complexes since their chemical shift and coupling constant data lie on a line relating $^1J(^{103}Rh\text{-}^{119}Sn)$ with $\delta(^{119}Sn)$ for the complexes $[Rh(SnCl_3)_nCl_{6-n}]^{3-}$ (n = 1 - 5) as described by Moriyama *et al.* [4] (see Figure 5.2). The nmr parameters of these complexes are shown in Table 5.5.

Table 5.5 Nmr parameters of the non-hydridic rhodium(III) complexes in Diϕ400U (Sn:Rh in the aqueous phase = 4:1).

$\delta(^{119}Sn)$ (ppm)	$^1J(^{103}Rh\text{-}^{119}Sn)$ (Hz)	$^2J(^{117}Sn\text{-}^{119}Sn)$ (Hz)
-218.4	590	*
-270.4	665	*
-429.3	729	2772

* The satellites could not be distinguished from the baseline noise.

The predominant species in the Diϕ400U extract resonated at -429.3 ppm. Integration of this resonance revealed an integrated $I_{(satellite)}/I_{(main)}$ peak ratio of 8.0%, indicating three $SnCl_3^-$ ligands associated to the central rhodium atom. In addition, the chemical shift and coupling constant values agree reasonably well with those assigned to the trichlorotris(trichlorostannato)rhodate(III) anion, $[Rh(SnCl_3)_3Cl_3]^{3-}$ {$\delta(^{119}Sn)$ = -411.1 ppm ; $^1J(^{103}Rh\text{-}^{119}Sn)$ = 718 Hz and $^2J(^{117}Sn\text{-}^{119}Sn)$ = 2804 Hz} [4]. Hence the strong signal at -429.3 ppm is assigned to the complex $[Rh(SnCl_3)_3Cl_3]^{3-}$. From the spectral pattern of one set of main peaks and satellites, one may conclude either that the $[Rh(SnCl_3)_3Cl_3]^{3-}$ anion exists exclusively as the *fac*-isomer (predicted to be thermodynamically more stable by Kimura [1] by virtue of the π-acceptor ability of $SnCl_3^-$), or that the *fac-* and *mer-*isomers are indistinguishable due to the fast intramolecular scrambling of the $SnCl_3^-$ ligands.

(b) MIBK Extracts

From the low signal intensity in the nmr spectrum it was evident that a very low concentration of the rhodium-tin complexes was extracted by MIBK under the present conditions. The hydrido complex $[RhH(SnCl_3)_5]^{3-}$ constituted a significant proportion of the extracted rhodium-tin complexes. In addition, resonances arising from four other rhodium(III) complexes were observed (Figure 5.4). These species were assigned to be rhodium(III) complexes by the correlation of their nmr data with the plot of $^1J(^{103}Rh\text{-}^{119}Sn)$ versus $\delta(^{119}Sn)$ for the series of complexes $[Rh(SnCl_3)_nCl_{6-n}]^{3-}$ (n = 1 - 5) as characterized by Moriyama *et al.* [4] (Figure 5.2). The number of coordinated $SnCl_3^-$ ligands could not be determined for these complexes since the $^{117}Sn\text{-}^{119}Sn$ satellites could not be detected due to the poor

signal to noise ratio. The chemical shifts and $^1J(^{103}Rh\text{-}^{119}Sn)$ values for the non-hydridic complexes are summarized in Table 5.6.

Table 5.6 $\delta(^{119}Sn)$ and $^1J(^{103}Rh\text{-}^{119}Sn)$ values for the non-hydridic complexes in MIBK.

$\delta(^{119}Sn)$ (ppm)	$^1J(^{103}Rh\text{-}^{119}Sn)$ (Hz)
-355.7	729
-368.4	729
-372.5	733
-608.3	830

The close proximity of the signals between -355.7 and -372.5 ppm and their similar $^1J(^{103}Rh\text{-}^{119}Sn)$ coupling constants might suggest that these rhodium-tin complexes are very similar in nature. The possibility of distinguishing separate resonances for the *fac*- and *mer*-isomers of $[Rh(SnCl_3)_3Cl_3]^{3-}$ should not be ignored. Fast intramolecular scrambling of the $SnCl_3^-$ ligands would render the ^{119}Sn nuclei magnetically equivalent resulting in a single resonance. Therefore, these isomers could only be distinguished by nmr if they were stereochemically rigid. In the latter case one would expect a single resonance (doublet) with its corresponding splitting pattern to arise from the *fac*-isomer by virtue of the magnetic equivalence of these nuclei. In contrast, the *mer*-isomer should give rise to two resonances in a 2:1 intensity ratio since the ^{119}Sn nuclei *trans* to one another are magnetically inequivalent to the ^{119}Sn nucleus *trans* to a chloride. Although, in general, the chloro(trichlorostannato)rhodium complexes have been found to undergo fast intramolecular scrambling [4], it is possible that under certain conditions the complexes are stereochemically rigid. The signal at -372.5 ppm has an intensity of roughly half that of the resonances at -355.7 and -368.4 ppm. Thus the possibility of observing stereochemically rigid *fac*- and *mer*-isomers of $[Rh(SnCl_3)_3Cl_3]^{3-}$ remains

a valid consideration. However, in the absence of further evidence such as that information which may be obtained from satellites due to ^{117}Sn to ^{119}Sn coupling, this suggestion must remain speculative.

(c) Aliquat 336 Extracts

The ^{119}Sn nmr spectrum of the Aliquat 336 extract from a 3 M hydrochloric acid solution containing a molar Sn:Rh ratio of 4:1 proved to be of great interest and is shown in Figure 5.8. Three hydrido complexes were identified by decoupling experiments. A relatively high concentration of the hydrido complex at –92.5 ppm was detected, in addition to a smaller amount of $[RhH(SnCl_3)_5]^{3-}$ {$\delta(^{119}Sn)$ = –15.3 ppm} and trace amounts of a hydrido complex resonating at –211.9 ppm. The signal at –92.5 ppm had been previously observed in Aliquat 336 extracts from 5 M hydrochloric acid solutions with Sn:Rh ratios of 10:1, and it was thought to arise from the complex $[RhH(SnCl_3)_4Cl]^{3-}$. Under the present conditions of extraction (Sn:Rh = 4:1, 3 M HCl) the higher concentrations of the hydrido complex resonating at –92.5 ppm allowed the detection of the satellites resulting from the ^{117}Sn to ^{119}Sn coupling. Repeated integration of these satellites yielded $I_{(satellite)}/I_{(main)}$ peak ratios of 6.9% to 11.6%, indicating between three and four coordinated $SnCl_3^-$ ligands. Although the number of coordinated $SnCl_3^-$ ligands could not be established conclusively by the integrated peak ratios, if one considers the close proximity of its resonance to that of $[RhH(SnCl_3)_5]^{3-}$ (δ = –15.3 ppm), the resonance at –92.5 ppm most likely arises from $[RhH(SnCl_3)_4Cl]^{3-}$. In addition, an analogous iridium complex $[IrH(SnCl_3)_4Cl]^{3-}$ has been characterized in propan-2-ol solutions by Yamakawa *et al.* using ^{119}Sn nmr spectroscopy [8]. From the nmr evidence identification of the species as the *trans* isomer of $[RhH(SnCl_3)_4Cl]^{3-}$ is inferred, with the $SnCl_3^-$ ligands undergoing fast intramolecular scrambling. The

value of the $^2J(^1H\text{-}^{119}Sn)$ coupling constant (105 Hz) is of the order of magnitude expected for ^{119}Sn and ^1H nuclei oriented *cis* to one another {compare $^2J(^1H\text{-}^{119}Sn)$ coupling constants of the equatorial and axial ^{119}Sn nuclei of $[RhH(SnCl_3)_5]^{3-}$: $^2J(^1H\text{-}^{119}Sn)_{eq}$ = 60 Hz and $^2J(^1H\text{-}^{119}Sn)_{ax}$ = 1116 Hz}. If the complex $[RhH(SnCl_3)_4Cl]^{3-}$ were stereochemically rigid, one would expect two sets of satellites of equal intensity with *trans* $^2J(^{117}Sn\text{-}^{119}Sn)_{(eq\text{-}eq)}$ at least an order of magnitude larger than *cis* $^2J(^{117}Sn\text{-}^{119}Sn)_{(eq\text{-}eq)}$. The respective $^2J(^{117}Sn\text{-}^{119}Sn)$ coupling constants for the stereochemically rigid *trans*-$[IrH(SnCl_3)_4Cl]^{3-}$ were $30225_{(eq\text{-}eq)}$ and $2145_{(eq\text{-}eq)}$ for *trans* and *cis* respectively [8].

Finally for the third hydrido species, it was suspected that the hydrido complex resonating at –211.9 ppm might be the satellites arising from ^{117}Sn to ^{119}Sn coupling of *trans* oriented $SnCl_3^-$ ligands of a stereochemically rigid $[RhH(SnCl_3)_4Cl]^{3-}$. However, one would expect an identical set of satellites symmetrically downfield from the hydrido signal at –92.5 ppm. The absence of this duplicate set of satellites and the larger $^1J(^{103}Rh\text{-}^{119}Sn)$ coupling constant of the hydrido resonance at –211.9 ppm led to the conclusion that the $SnCl_3^-$ ligands of the hydrido complex *trans*-$[RhH(SnCl_3)_4Cl]^{3-}$ were undergoing fast intramolecular scrambling and that the resonance at –211.9 ppm arose from a separate hydrido complex. The nmr parameters measured for the hydrido complexes are shown in Table 5.7.

The rhodium-tin species most abundantly extracted by Aliquat 336 under these conditions (3 M HCl, Sn:Rh = 4:1), resonated at –442.9 ppm. The integrated peak ratio, $I_{(satellite)}/I_{(main)}$, was found to be 8.2%, indicating three $SnCl_3^-$ ligands coordinated to the central rhodium atom. The nmr parameters of the resonance at –442.9 ppm are similar to those of $[Rh(SnCl_3)_3Cl_3]^{3-}$, found to be the predominant species in the Diϕ400U phase after extraction under similar conditions. It is

interesting to note that the addition of one drop of CF_3COOH, resulted in a shift in the resonance at –442.9 ppm to a chemical shift of –421.4 ppm. The chemical shift value as well as the coupling constants {$^1J(^{103}Rh\text{-}^{119}Sn)$ = 721 Hz and $^2J(^{117}Sn\text{-}^{119}Sn)$ = 2758 Hz} were now nearly identical within experimental uncertainty to those of $[Rh(SnCl_3)_3Cl_3]^{3-}$ observed in the Diϕ400U extract. Hence, the resonance at –442.9 ppm may be assigned to the complex $[Rh(SnCl_3)_3Cl_3]^{3-}$. (Again, the spectral pattern either indicates a *fac*-isomer or a stereochemically non-rigid species of which the *fac*- and *mer*-isomers cannot be distinguished due to fast intramolecular scrambling). Further addition of CF_3COOH not only resulted in a large downfield shift but it also appeared to fragment the resonance to give rise to smaller resonances in close proximity to the major signal which now occurred at –368.9 ppm. The nmr parameters of the latter resonance resembled those of a rhodium-tin species observed in the MIBK extracts from 3 M hydrochloric acid solutions containing a Sn:Rh ratio of 4:1. Integration of the satellites of the major resonance still indicated three associated $SnCl_3^-$ ligands after it had shifted to –368.9 ppm. From these observations, it has become evident that the nmr characteristics of a particular rhodium-tin complex may be significantly affected by the nature of the solvent (eg. by the polarity or dielectric constant). It is possible on addition of CF_3COOH that the weaker resonances that appeared in close proximity of the major resonance at –368.9 ppm (thought to be $[Rh(SnCl_3)_3Cl_3]^{3-}$) arose from complexes in which at least one of the coordination sites about the central rhodium atom is occupied by CF_3COO^-.

The spectral pattern of the Aliquat 336 extract is presented in Tables 5.7 and 5.8. Table 5.7 shows all resonances observed, including those of the complexes present in trace amounts. Table 5.8 presents the nmr characteristics of the rhodium-tin complexes after the addition of CF_3COOH to the Aliquat 336 extract.

Table 5.7 Nmr parameters of the rhodium-tin complexes in Aliquat 336 extracts from 3 M hydrochloric acid solutions with molar Sn:Rh ratios of 4:1.

$\delta(^{119}Sn)$ (ppm)	$^{1}J(^{103}Rh\text{-}^{119}Sn)$ (Hz)	$^{2}J(^{117}Sn\text{-}^{119}Sn)$ (Hz)	$^{2}J(^{1}H\text{-}^{119}Sn)$ (Hz)
Hydrido complexes			
-15.3	590	*	59 (mi)
-92.5	666	2398	105 (ma)
-211.9	740	*	103 (t)
Non-hydridic rhodium(III) complexes			
-219.1	584	*	- (t)
-271.7	698	*	- (t)
-371.4	660	*	- (t)
-442.9	731	2518	- (p)
-705.5	815	*	- (mi)
-727.3	tin(IV) species		

where (p) = predominant species ; (ma) = major species ; (mi) = minor species ; (t) = species in trace amounts ; * = the satellites could not be distinguished from the baseline noise.

Table 5.8 Nmr parameters of the rhodium-tin complexes in Aliquat 336 extracts after the addition of CF_3COOH.

$\delta(^{119}Sn)$ (ppm)	$^{1}J(^{103}Rh\text{-}^{119}Sn)$ (Hz)	$^{2}J(^{103}Rh\text{-}^{117}Sn)$ (Hz)	$^{2}J(^{1}H\text{-}^{119}Sn)$ (Hz)
one drop of CF_3COOH			
-14.7	590	*	(t)
-205.8	609	*	(t)
-272.6	663	*	(t)
-421.4	721	2758	(p)
-705.5	#	#	(mi)
after further additions of CF_3COOH			
-12.2	592	*	(mi)
-194.1	594	*	(t)
-274.1	665	*	(mi)

Table 5.8 (....continued)

$\delta(^{119}Sn)$ (ppm)	$^1J(^{103}Rh\text{-}^{119}Sn)$ (Hz)	$^2J(^{103}Rh\text{-}^{117}Sn)$ (Hz)	$^2J(^1H\text{-}^{119}Sn)$ (Hz)
-308.1	670	*	(t)
-355.1	720	*	(m)
-368.9	726	2948	(p)
-413.3	717	*	(t)
-587.9	806	*	(mi)

# indicates that the spectral window only extended to 700 ppm, and the effect of CF_3COOH on this peak could not be detected.

(p) = predominant species ; (ma) = major species ; (mi) = minor species ; (t) = species in trace amounts ; * = the satellites could not be distinguished from the baseline noise.

1.2 (iii) The Spectral Pattern of $[RhH(SnCl_3)_5]^{3-}$

Whereas the ^{119}Sn nmr spectra of the stereochemically *non*-rigid complexes are simplified by the magnetic equivalence of the rapidly scrambling $SnCl_3^-$ ligands, the spectral pattern of the stereochemically *rigid* $[RhH(SnCl_3)_5]^{3-}$ warrants a more detailed description due to its interesting complexity. The ^{119}Sn nuclei of this complex occur in two different magnetic environments, which are illustrated in Figure 5.1. A typical ^{119}Sn nmr spectrum of $[RhH(SnCl_3)_5]^{3-}$ as observed in Diϕ400U and Aliquat 336 is shown in Figure 5.9, and the splitting pattern is illustrated qualitatively in Figure 5.10.

The axial ^{119}Sn resonance occurs at 78.7 ppm while the four magnetically equivalent equatorial $SnCl_3^-$ ligands resonate at -14.1 ppm. The ^{119}Sn nuclei under observation form part of an extensively coupled system which may be denoted as an ADXYZ system. Their resonances are split by coupling with ^{103}Rh (natural abundance = 100%) and ^1H (natural abundance = 99.99%).

Further first-order splitting by ^{117}Sn (natural abundance = 7.61%) gives rise to three sets of satellites (doublets of doublets) which are symmetrically arranged about the peaks of the main equatorial ^{119}Sn resonance (a doublet of doublets). These satellites occur due to :

a) *trans* ^{117}Sn-^{119}Sn coupling of the equatorial tin ligands (situated at the extreme ends of the spectrum shown in Figure 5.9, $^{2}J(^{117}Sn\text{-}^{119}Sn)_{(trans,\ eq\text{-}eq)}$ = 25334 Hz)

b) *cis* ^{117}Sn-^{119}Sn coupling of the equatorial ligands (which are situated at the foot of the main peaks with $^{2}J(^{117}Sn\text{-}^{119}Sn)_{(cis,\ eq\text{-}eq)}$ = 1973 Hz), and

c) *cis* ^{117}Sn- ^{119}Sn coupling of the equatorial ligands to the axial ligand (situated at the foot of the main peaks with $^{2}J(^{117}Sn\text{-}^{119}Sn)_{(cis,\ ax\text{-}eq)}$ = 1759 Hz).

The axial ^{119}Sn ligand should be accompanied by one set of satellites due to coupling with equatorial ^{117}Sn ligands. These satellites are distinguishable in the spectrum shown in Figure 5.9. In addition, an added multiplicity of these satellites is evident, which are not symmetrically placed around the major resonances. Similarly, the satellites accompanying the equatorial ^{119}Sn resonance exhibit an added multiplicity which is once again not symmetrical.

The latter satellites about the equatorial as well as the axial ^{119}Sn resonances may be assigned to ^{119}Sn *cis* coupled to ^{119}Sn. One may expect to observe this $^{2}J(^{119}Sn\text{-}^{119}Sn)_{(cis,\ eq\text{-}ax)}$ coupling based upon the magnetic inequivalence of the equatorial and axial ligands. Krut'ko *et al.* [3] reported weak signals (not shown in their paper) which they assign to the ABX system arising from second order $^{119}Sn_{(eq)}$-$^{119}Sn_{(ax)}$ coupling. However, the authors did not report the observed value of $^{2}J(^{119}Sn\text{-}^{119}Sn)_{(cis,\ eq\text{-}ax)}$. Furthermore, the additional satellites observed in the present work are comparable in intensity to the satellites arising from ^{117}Sn to ^{119}Sn coupling.

The coupling constant expected for the ^{119}Sn to ^{119}Sn coupling may be calculated from the observed value for $^{2}J(^{117}Sn\text{-}^{119}Sn)_{(cis,ax\text{-}eq)}$ and the ratio of the gyromagnetic constants of the ^{119}Sn and ^{117}Sn nuclei [13]. Thus,

$$\frac{^{2}J(^{119}Sn\text{-}^{119}Sn)}{^{2}J(^{117}Sn\text{-}^{119}Sn)} = \frac{\gamma(^{119}Sn)}{\gamma(^{117}Sn)}$$

therefore, $$\frac{^{2}J(^{119}Sn\text{-}^{119}Sn)}{1759} = \frac{-9.9756}{-9.5319}$$

and $^{2}J(^{119}Sn\text{-}^{119}Sn) = 1841$ Hz.

The chemical shift of the axial and equatorial ^{119}Sn nuclei were observed to occur at +78.7 and −14.1 ppm respectively, which corresponds to a frequency separation of 6922 Hz and

$$(\nu_A - \nu_B)/J_{AB} = 3.76$$

First order analysis of nmr spectra is usually considered applicable when $(\nu_A - \nu_B)/J_{AB} > 7$ [13]. Therefore, from the ratio of $(\nu_A - \nu_B)/J_{AB}$ for the axial and the equatorial ^{119}Sn nuclei, one may expect a degree of second order distortion of the spectrum of those species containing ^{119}Sn nuclei simultaneously in the axial and equatorial positions.

In order to simplify the ^{119}Sn nmr spectrum and thus facilitate the measurement of $^{2}J(^{119}Sn\text{-}^{119}Sn)_{(cis,\ ax\text{-}eq)}$, a proton decoupled spectrum of a Diϕ400U extract containing $[RhH(SnCl_3)_5]^{3-}$ was recorded. The equatorial resonance of this spectrum is shown in Figure 5.11. The decoupling of the axial resonance was not

entirely successful resulting in a broad hump from which it was difficult to distinguish the axial resonance and its accompanying satellites. The satellites due to $^{2}J(^{117}Sn\text{-}^{119}Sn)_{(cis,\ eq\text{-}eq)}$ and $^{2}J(^{117}Sn\text{-}^{119}Sn)_{(cis,\ ax\text{-}eq)}$ are symmetrical about the main peak, and the coupling constant values (1981 and 1764 Hz, respectively) agree well with the values reported in the literature [8]. The additional satellites were separated by 1844 Hz, which agrees well with the calculated value (1841 Hz) for $^{2}J(^{119}Sn\text{-}^{119}Sn)_{(cis,\ ax\text{-}eq)}$. However, these satellites were not symmetrically arranged about the main peaks. Each of the left hand satellites is separated from its respective main peak by 800 Hz, while each of the right hand satellites is separated from its respective main peak by 1044 Hz. These satellites are not thought to be peaks from a different species, since the satellites on the left are separated by 594 Hz as are the right hand satellites. This frequency difference is identical to the value of $^{1}J(^{103}Rh\text{-}^{119}Sn)$ which separates the main peaks. Hence, these satellites are assigned to the *cis* $^{119}Sn_{(ax)}$ to $^{119}Sn_{(eq)}$ coupling with $^{2}J(^{119}Sn\text{-}^{119}Sn)_{(cis,\ eq\text{-}ax)}$ = 1844 Hz. The asymmetry is ascribed to second order perturbations due to a relatively small frequency separation of the coupling axial and equatorial ^{119}Sn nuclei. The intensity variations of the satellites about both the axial and the equatorial main peaks are consistent with second order trends (i.e. the intensities increase towards the midpoint between the axial and the equatorial resonances). Despite the large *trans* $^{2}J(^{117}Sn\text{-}^{119}Sn)$ coupling constant (25334 Hz), coupling between *trans* orientated ^{117}Sn and ^{119}Sn nuclei remains first order due to their large frequency separation $\{(\nu_A - \nu_B)/J_{AB} > 100$ at 74.608 MHz$\}$.

A computer-aided simulation of the spectrum expected for the complex $[RhH(SnCl_3)_5]^{3-}$ was performed in order to confirm the assignment of the non-symmetrical satellites to second order ^{119}Sn to ^{119}Sn coupling of the axial and equatorial ligands. The simulation programme DNMR5 [14] and the frequency and

coupling constant data from Table 5.9 were used. The simulated equatorial ^{119}Sn nmr spectrum, as well as the individual resonances (satellites) arising from the various couplings of the *cis* oriented Sn nuclei, are shown in Table 5.12. The non-symmetry of the satellites arising from $^{119}Sn_{(ax)}$ to $^{119}Sn_{(eq)}$ coupling is clearly evident in the combined and the sub-spectrum {Figure 5.12(b)}, confirming the second order perturbations predicted and confirming the value of $^2J(^{119}Sn\text{-}^{119}Sn)_{(cis,\ ax\text{-}eq)}$ = 1844 Hz.

Finally, an interesting observation was made which we are unable to explain. On re-recording the spectrum of a Diϕ400U extract that had been found to contain $[RhH(SnCl_3)_5]^{3-}$ exclusively and had aged for one week, a shoulder to the left of each of the left hand peaks of the main doublet of doublets was noticed. On cooling (to 0 °C) this shoulder became more pronounced, see Figure 5.13. Since these shoulders are separated by a frequency value (592 Hz) that is essentially equal to the one-bond coupling constant $^1J(^{103}Rh\text{-}^{119}Sn)$, it is likely to be related in some undetermined way to the hydrido complex, $[RhH(SnCl_3)_5]^{3-}$. It is interesting to note that this set of "shoulders" was also observed by Wyrley-Birch [15] in MIBK containing $[RhH(SnCl_3)_5]^{3-}$ as the predominant species, but no explanation was given.

1.3 Discussion

All the observed resonances and their nmr characteristics are summarized in Table 5.9, which also shows the extractant phase in which the signals were detected. The diversity of the spectral pattern not only bears witness to the existence of a large variety of rhodium-tin complexes, but underlines the sensitivity of the nmr characteristics to the nature of the extractant/solvent phase in which the complexes

are examined. It was shown that an increase in the polarity of the extractant phase (by the addition of CF_3COOH to the Aliquat 336 extract) resulted in a downfield shift of the resonance assigned to $[Rh(SnCl_3)_3Cl_3]^{3-}$ from -442.9 to -368.7 ppm. Spectral evidence suggests the existence of rhodium-tin complexes in which a donor molecule other than $SnCl_3^-$, Cl^- or H^- occupies a coordination site about the central rhodium atom. Upon exposing the extract to the atmosphere the appearance of the resonance at -54.5 ppm which was assigned to a complex with four $SnCl_3^-$ ligands coordinated to the rhodium atom, and the concomitant decrease in the resonance of $[RhH(SnCl_3)_5]^{3-}$, suggested the formation of the decomposition product $[Rh(SnCl_3)_4(MIBK)_mCl_{2-m}]^{(3-m)-}$ (where m = 1 or 2). Further, the addition of CF_3COOH to the Aliquat 336 extract containing $[Rh(SnCl_3)_3Cl_3]^{3-}$ not only resulted in the downfield shift of the resonance of this complex, but also resulted in the appearance of several other weaker resonances. It is possible that these weaker resonances arose from complexes in which CF_3COO^- acted as a ligand to rhodium.

Sensitivity of the resonances to solvent effects together with the possibility of either the solvent molecules or CF_3COO^- occupying at least one of the coordination sites about the central rhodium atom makes a definite assignment of the various signals difficult. The $I_{(satellite)}/I_{(main)}$ integrated peak ratios were used to determine the number of $SnCl_3^-$ ligands associated to the central rhodium atom. However, it should be mentioned that the accuracy of these ratios is not always certain. Experiments were performed to measure the T_1 relaxation times of the rhodium-tin complexes (T_1 ~ 0.09 s). Based upon these experiments, a sufficient delay time to prevent saturation of the resonances was utilized. However, these experiments were not repeated for each extract, and since each rhodium-tin complex might relax at a different rate, it is possible that the data acquisition conditions were not always optimized to ensure quantitative results in all cases. One example of a complex for

which the recorded nmr spectrum yielded inaccurate integrated peak ratios is the trigonal bipyramidal rhodium(I) complex, $[Rh(SnCl_3)_5]^{4-}$. This complex was found in two Aliquat 336 extracts, and integration of the peaks yielded $I_{(satellite)}/I_{(main)}$ ratios between 11.6% and 13.7%, which indicates four rather than five coordinated $SnCl_3^-$ ligands. Nevertheless, the assignment of the resonance to the species $[Rh(SnCl_3)_5]^{4-}$ was based upon the chemical shift values and the one- and two- bond coupling constants $\{^1J(^{103}Rh\text{-}^{119}Sn)$ and $^2J(^{117}Sn\text{-}^{119}Sn)\}$ which coincided with reported values for $[Rh(SnCl_3)_5]^{4-}$ [4].

The correlation of $^1J(^{103}Rh\text{-}^{119}Sn)$ with $\delta(^{119}Sn)$ has been used as an assignment technique by Moriyama *et al.* [4]. In their study of rhodium-tin complexes in hydrochloric acid solutions, these authors [4] assigned the resonance at -100.5 ppm to $[Rh(SnCl_3)_5Cl]^{3-}$ because the point for this resonance falls along the extrapolated line joining the points for $[Rh(SnCl_3)_nCl_{6-n}]^{3-}$ (with n = 1 - 4). Although in the present work such a correlation could not be used for the conclusive assignment of resonances to specific complexes, it was used as a confirmatory test in support of the classification of a resonance as that arising from a certain series of complexes. This was based upon the interesting observation that a plot of the one-bond coupling constant $\{^1J(^{103}Rh\text{-}^{119}Sn)\}$ as a function of the chemical shifts of all the resonances observed yielded two series of correlating data points. The first series of points constituted the resonances of the hydrido complexes, while the second series of points correlated well with the data points reported by Moriyama *et al.* [4] for the series of complexes $[Rh(SnCl_3)_nCl_{6-n}]^{3-}$ (n = 1 - 5). Hence, the near coincidence of a particular data point upon the second correlation curve was taken as evidence in support of the resonance arising from a rhodium(III) complex of the type $[Rh(SnCl_3)_nX_mCl_{6-(n+m)}]^{3-}$ (with $m \geq 0$, $(n + m) \leq 6$ and the charge = $(3\text{-}m)^-$ for neutral X) where X is a ligand other than $SnCl_3^-$, Cl^- or H^-. The data point for

$[Rh(SnCl_3)_5]^{4-}$ does not lie on either correlation line, a phenomenon ascribed to the low valency of the rhodium for this complex [4]. The plot of $^1J(^{103}Rh\text{-}^{119}Sn)$ as a function of $\delta(^{119}Sn)$ yielding two lines (for the hydrido complexes and the non-hydridic complexes), is shown in Figure 5.2.

Despite the large number of different ^{119}Sn nmr resonances observed, it became evident that very few complexes were extracted in high concentrations and that a definite pattern emerged for each extractant. Extractions made from solutions containing excess tin(II) chloride (Sn:Rh > 6:1) resulted in the exclusive presence of the hydrido complex $[RhH(SnCl_3)_5]^{3-}$ in the Diϕ400U phase. Under these conditions, exclusive extraction of $[Rh(SnCl_3)_5]^{4-}$ is thought to occur which is followed by the protonation of this complex to form $[RhH(SnCl_3)_5]^{3-}$. This hydrido complex was still present in Diϕ400U extracts that were made from aqueous phases containing Sn:Rh ratios of 4:1, but the predominant species here was the trichlorotris(trichlorostannato)rhodate(III), $[Rh(SnCl_3)_3Cl_3]^{3-}$, complex.

The hydrido complex $[RhH(SnCl_3)_5]^{3-}$ was also prominent in the MIBK extracts as was evident from its presence in every MIBK extract examined. However, two other species formulated as $[Rh(SnCl_3)_nX_mCl_{6-(n+m)}]^{(3-m)-}$ (with n = 3 and 4 and X = a solvent molecule) were also present in extracts made from aqueous phases containing relatively low concentrations (0.5 or 1.0 M) of hydrochloric acid. These complexes, especially $[Rh(SnCl_3)_4X_mCl_{2-m}]^{(3-m)-}$, were thought to be formed upon decomposition of $[RhH(SnCl_3)_5]^{3,-}$ since on standing the resonance of $[Rh(SnCl_3)_4X_mCl_{2-m}]^{(3-m)-}$ appeared at the expense of the $[RhH(SnCl_3)_5]^{3-}$ signal. At low tin(II) concentrations (Sn:Rh = 4:1), the predominant species resonated at –355.4 and –368.7 ppm. Although these species could not be specifically assigned in MIBK, they are thought to contain three coordinated $SnCl_3^-$ ligands {probably

$[Rh(SnCl_3)_3Cl_3]^{3-}$} by analogy to similar species observed in Aliquat 336. A species at -608.3 ppm was also observed (in trace amounts) which is tentatively assigned to be $[Rh(SnCl_3)_2Cl_4]^{3-}$ on the basis of its chemical shift (*cf.* Table 5.10).

The hydrido complex $[RhH(SnCl_3)_5]^{3-}$ was found to be relatively stable in Diϕ400U but less stable in MIBK. A Diϕ400U extract containing only $[RhH(SnCl_3)_5]^{3-}$ was allowed to stand for eleven days in a sealed nmr tube. The ^{119}Sn nmr spectrum was re-recorded after this period and revealed the predominance of the hydrido complex with only traces of other species at –54.5 and –115.1 ppm {previously assigned to $[Rh(SnCl_3)_nX_mCl_{6-(n+m)}]^{(3-m)-}$ with n = 3 or 4}. In contrast, a shorter standing period of only seven days (also in a sealed nmr tube) resulted in a significant change in the spectral pattern of an MIBK extract containing mainly $[RhH(SnCl_3)_5]^{3-}$ with traces of $[Rh(SnCl_3)_4X_mCl_{2-m}]^{(3-m)-}$. The spectrum of the aged MIBK extract revealed a predominance of $[Rh(SnCl_3)_4X_mCl_{2-m}]^{(3-m)-}$ and showed a weaker and broader signal of $[RhH(SnCl_3)_5]^{3-}$. It is also interesting to note that in MIBK a certain degree of motional behaviour by the $SnCl_3^-$ ligands of $[RhH(SnCl_3)_5]^{3-}$ was apparent. The spectral pattern of $[RhH(SnCl_3)_5]^{3-}$ was not as clearly defined in MIBK as it was both in Diϕ400U and Aliquat 336. The signals due to the axial $SnCl_3^-$ ligand and the *trans* ^{117}Sn to ^{119}Sn coupling of the equatorial $SnCl_3^-$ ligands were not always evident and the satellites about the equatorial ^{119}Sn resonances were broad and ill-defined. This is a problem because it can lead to erroneous spectral assignments.

In Aliquat 336, the hydrido complex $[RhH(SnCl_3)_5]^{3-}$ predominated only when extractions were made from solutions containing excess tin(II) and high hydrochloric acid concentrations. Extracts from 0.5 M HCl and 0.7 M HCl solutions contained exclusively the trigonal bipyramidal rhodium(I) complex, $[Rh(SnCl_3)_5]^{4-}$. In the

presence of 5 M hydrochloric acid with excess tin(II) another hydrido complex (thought to be $[RhH(SnCl_3)_4Cl]^{3-}$) was found to be present. Aqueous phases with low tin(II) concentrations (Sn:Rh = 4:1) yielded Aliquat 336 extracts containing predominantly $[Rh(SnCl_3)_3Cl_3]^{3-}$, relatively high concentrations of $[RhH(SnCl_3)_4Cl]^{3-}$, small amounts of $[RhH(SnCl_3)_5]^{3-}$ and a species resonating at -705.5 ppm (tentatively assigned to be $[Rh(SnCl_3)_2Cl_4]^{3-}$).

The results have shown that only rhodium-tin species containing at least three $SnCl_3^-$ ligands associated to the rhodium are readily extractable into the organic phase. The extractability of these complexes may qualitatively be linked to the size and polarizability of these trichlorostannato complexes of rhodium. Although the trigonal bipyramidal $[Rh(SnCl_3)_5]^{4-}$ was observed in Aliquat 336 extracts, it was never observed in the "oxygen-donor" organic phases. It is clear that MIBK and Diϕ400U coextract hydrochloric acid, which results in the rapid protonation of $[Rh(SnCl_3)_5]^{4-}$ to form the hydrido complex $[RhH(SnCl_3)_5]^{3-}$. The organic phase rapidly changes colour to bright yellow on extraction of rhodium from the purple aqueous phase by Diϕ400U and MIBK. This suggestion was further supported by a spectacular colour change from purple to yellow upon adding CF_3COOH to an Aliquat 336 extract containing only $[Rh(SnCl_3)_5]^{4-}$ with the consequent change in the nmr spectral pattern . The addition of CF_3COOH results in a spectrum in which the $[RhH(SnCl_3)_5]^{3-}$ species predominates. This hydrido complex appeared to predominate in the Diϕ400U and MIBK extracts, but was found to be more stable in Diϕ400U. However, the other hydrido complexes observed in Aliquat 336 were evidently not stable in the oxygen donor extractants since their presence was not observed in MIBK and Diϕ400U by ^{119}Sn nmr spectroscopy.

Although it is beyond the scope of this work, it should be mentioned that the nmr data may provide information about the electronic properties of the $SnCl_3^-$ ligand. It should be stressed at the outset, however, that any interpretation in this report regarding the electronic properties of $SnCl_3^-$ is based upon indirect evidence, and a detailed quantum mechanical study of the molecular orbitals involved (specifically their *s*-orbital contributions) was not carried out. Hence the following discussion should serve merely to highlight areas with potential for a more detailed interpretation.

A decrease in the $^1J(^{103}Rh\text{-}^{119}Sn)$ coupling constant with an increase in the number of $SnCl_3^-$ ligands may be interpreted as signifying a decrease in the σ-bond strength [4] and *s*-electron density of the coupling nuclei. This is consistent with the reported characteristics of $SnCl_3^-$ being a weak σ-donor and a strong π-acceptor [16] according to the following reasoning. The one bond coupling constant has been described by Pople and Santry [17] as follows:

$$J(AB) = \text{constant}\ \{\gamma_A\gamma_B\,[s_A(0)]^2\,[s_B(0)]^2\ \pi_{AB}\} \qquad (2)$$

Where γ_A and γ_B = the gyromagnetic ratios of nuclei A and B

$[s(0)]^2$ = the valence *s*-electron densities at the nuclei A and B, and

π_{AB} = the mutual polarizability.

Withdrawal of electrons from the rhodium atom by π-backdonation to $SnCl_3^-$ should influence the effective bond order of the rhodium-tin bond, and hence play a role in determining the magnitude of π_{AB}. It is conceivable that an increase in the number of $SnCl_3^-$ ligands results in competition for the rhodium d_π orbitals resulting in a smaller mutual polarizability between rhodium and tin, thus reducing the coupling constant, $^1J(^{103}Rh\text{-}^{119}Sn)$.

Protonation of the rhodium(I) complex $[Rh(SnCl_3)_5]^{4-}$ to form $[RhH(SnCl_3)_5]^{3-}$ is accompanied by a change in the geometry of the molecule. The dsp^3 hybridization of the five-coordinate rhodium(I) complex contains a higher percentage *s*-character than the d^2sp^3 hybridized octahedral complex $[RhH(SnCl_3)_5]^{3-}$. Therefore, the *s*-electron density on the rhodium nucleus is higher for the trigonal bipyramidal complex $[Rh(SnCl_3)_5]^{4-}$ and from ~~reaction~~ equation 2, a higher $^1J(^{103}Rh\text{-}^{119}Sn)$ is implied for this rhodium(I) complex. These predictions are consistent with the observed values of $^1J(^{103}Rh\text{-}^{119}Sn)$ for $[Rh(SnCl_3)_5]^{4-}$ (801 Hz) and $[RhH(SnCl_3)_5]^{3-}$ ($594_{(eq)}$ and $528_{(ax)}$ Hz).

Further, deductions may be made regarding the *trans* influence of the $SnCl_3^-$ ligands. If one considers the $^1J(^{103}Rh\text{-}^{119}Sn)$ coupling constants of the stereochemically rigid $[RhH(SnCl_3)_5]^{3-}$ complex, a weaker *trans* influence of the $SnCl_3^-$ ligand relative to H^- might be inferred. This is based upon the finding that the $^1J(^{103}Rh\text{-}^{119}Sn)$ coupling constant for the axial $SnCl_3^-$ *trans* to the hydride was smaller (528 Hz) than the corresponding coupling constant for $SnCl_3^-$ ligands in the equatorial plane that are *trans* to other $SnCl_3^-$ ligands (594 Hz). The $SnCl_3^-$ ligand was found to have a sizeable *cis* influence [18]. This *cis* influence of the axial $SnCl_3^-$ ligand, compared with an axial chloride ligand in the complexes $[Ru(SnCl_3)_6]^{4-}$ and *trans*-$[RuCl_2(SnCl_3)_4]^{4-}$, manifests itself in the form of a smaller *trans* two bond coupling constant, $^2J(^{117}Sn\text{-}^{119}Sn)_{trans}$, in the former complex. Hence, $^2J(^{117}Sn\text{-}^{119}Sn)_{trans}$ = 26914 Hz for *trans*-$[RuCl_2(SnCl_3)_4]^{4-}$ and 13034 Hz for $[Ru(SnCl_3)_6]^{4-}$. The *cis* influence, as well as the observed coupling constants {and the observed order of $^2J(^{117}Sn\text{-}^{119}Sn)_{trans} > {}^2J(^{117}Sn\text{-}^{119}Sn)_{cis}$} were explained in terms of the orbital characteristics of the specific occupied and unoccupied molecular orbitals in the Pople-Santry framework [18].

Table 5.9 A summary of all the trichlorostannato complexes of rhodium observed in this work.

Species. No.	$\delta(^{119}Sn)$ (ppm)	$^1J(^{103}Rh\text{-}^{119}Sn)$ (Hz)	$^2J(^{117}Sn\text{-}^{119}Sn)$ (Hz)	n	m		
	$[Rh(SnCl_3)_5]^{4-}$						
1	-9.9	801	3554	5	-		#(m)
	$[RhH(SnCl_3)_nCl_{5-n}]^{3-}$					$^2J(^1H\text{-}^{119}Sn)$	
2	$-14.1_{(eq)}$	$594_{(eq)}$	$1973_{(cis,\ eq\text{-}eq)}$ $25334_{(trans,\ eq\text{-}eq)}$ $\{^2J(^{119}Sn\text{-}^{119}Sn)_{(cis,\ ax\text{-}eq)} = 1844\ Hz\}$	5	-	$58_{(cis,\ eq)}$	‡(m), #(m), †(m)
	$+78.7_{(ax)}$	$528_{(ax)}$	$1759_{(cis,\ ax\text{-}eq)}$			$1115_{(trans,\ ax)}$	
3	-92.5	666	2398	4	-	105	#(m)
4	-211.9	740	*	?	-	103	#(t)
	$[Rh(SnCl_3)_nX_mCl_{6-(n+m)}]^{3-}$ (charge = $(3\text{-}m)^-$ if X is neutral) $m \geq 0$, $n + m \leq 6$						
5	-54.5	519	1679	4	?		‡(t), †(m)
6	-115.1	549	1910	3	?		†(m), ‡(t), §(mi)
7	-144.3	617	*	?	?		§(t)
8	-194.1	594	*	?	?		§(t)
9	-205.8	609	*	?	?		§(t)
10	-218.9	586	*	?	?		‡(mi), #(t)
11	-219.9	632	*	?	?		#(t)
12	-272.1	672	*	?	?		‡(mi), #(t), §(mi)
13	-355.4	724	*	?	?		†(m), §(mi)
13	-368.7	727	2948	3	0		†(m), §(m)
13	-421.4	721	2758	3	0		§(m)
13	-429.3	729	2770	3	0		‡(m)
13	-442.9	731	2518	3	0		#(m)
14	-587.9	805	*	?	?		§(mi)
15	-608.3	830	*	?	?		†(mi)
16	-705.5	815	*	?	?		#(mi)

where
* = satellites too small to observe
† = in MIBK
§ = in Aliquat 336 after the addition of CF_3COOH
? = value not determined
(mi) = minor species
‡ = in Diϕ400U
# = in Aliquat 336
(m) = major species
(t) = species present in trace amounts

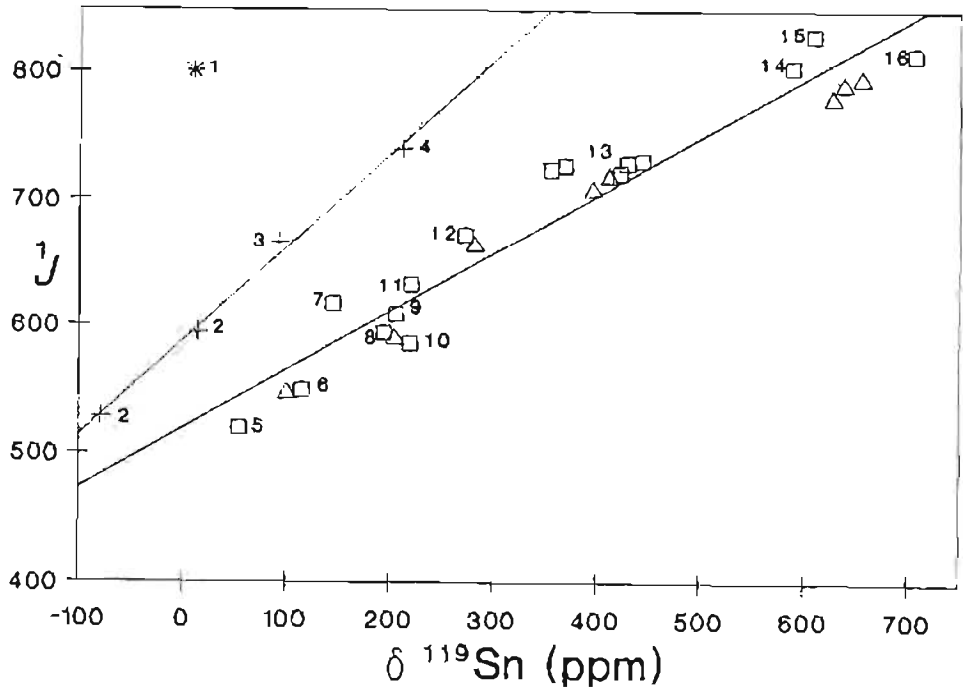

Figure 5.2 A plot of $^{1}J(^{103}Rh\text{-}^{119}Sn)$ as a function of $\delta(^{119}Sn)$. The numerical labels correspond with the species numbers in Table 5.9. (* = $[Rh(SnCl_3)_5]^{4-}$, + = $[RhH(SnCl_3)_nCl_{5-n}]^{3-}$, □ = $[Rh(SnCl_3)_nX_mCl_{6-(n+m)}]^{3-}$ m ≥ 0 and (n + m) ≤ 6, Δ = $[Rh(SnCl_3)_nCl_{6-n}]^{3-}$ reported by Moriyama *et al.* [4].)

Table 5.10 The ^{119}Sn nmr characteristics reported for $[Rh(SnCl_3)_nCl_{6-n}]^{3-}$ (n = 1-5) and $[Rh(SnCl_3)_5]^{4-}$ in 3 M HCl by Moriyama *et al.* [4].

Species	δ(ppm)	$^{1}J(^{103}Rh\text{-}^{119}Sn)$(Hz)	$^{2}J(^{117}Sn\text{-}^{119}Sn)$(Hz)
$[Rh(SnCl_3)Cl_5]^{3-}$	-991.6, -932.4, -914.1	864, 860, 850	none
$[Rh(SnCl_3)_2Cl_4]^{3-}$	-654.4, -637.0, -626.0	796, 791, 780	–, 3056, 3091
$[Rh(SnCl_3)_3Cl_3]^{3-}$	-411.1, -395.4	718, 708	2804, 2840
d	-281.4	664	2222
$[Rh(SnCl_3)_4Cl_2]^{2-}$	-204.3	590	2158
$[Rh(SnCl_3)_5Cl]^{3-}$	-100.5	547	1952
$Rh(SnCl_3)_5]^{4-}$	8.5	806	3634

d = structure unassigned (two coordinated Sn ligands)

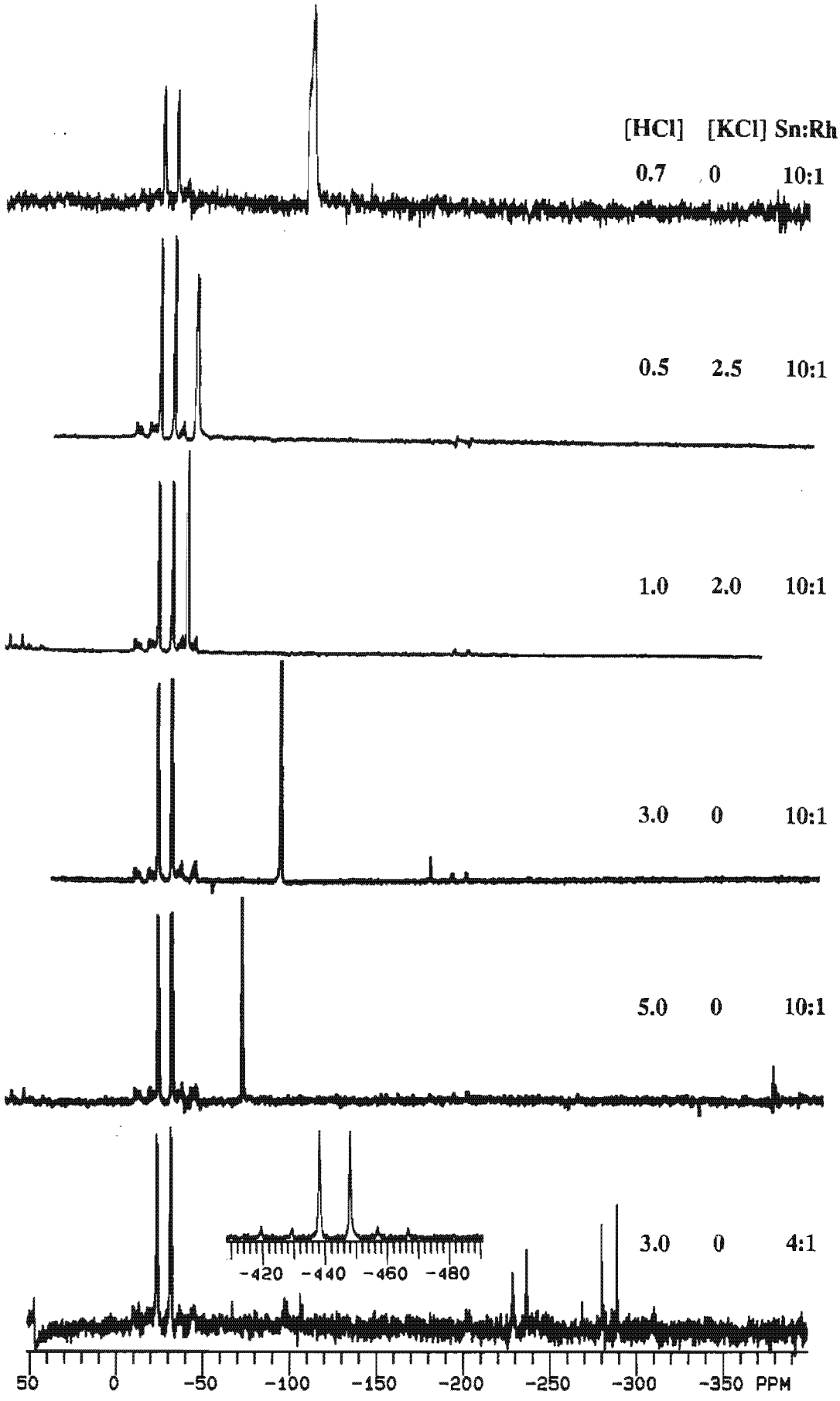

FIGURE 5.3 The ^{119}Sn nmr spectra recorded for the various Diϕ400U extracts. The solution conditions of the respective aqueous phases from which the extractions were made, are given.

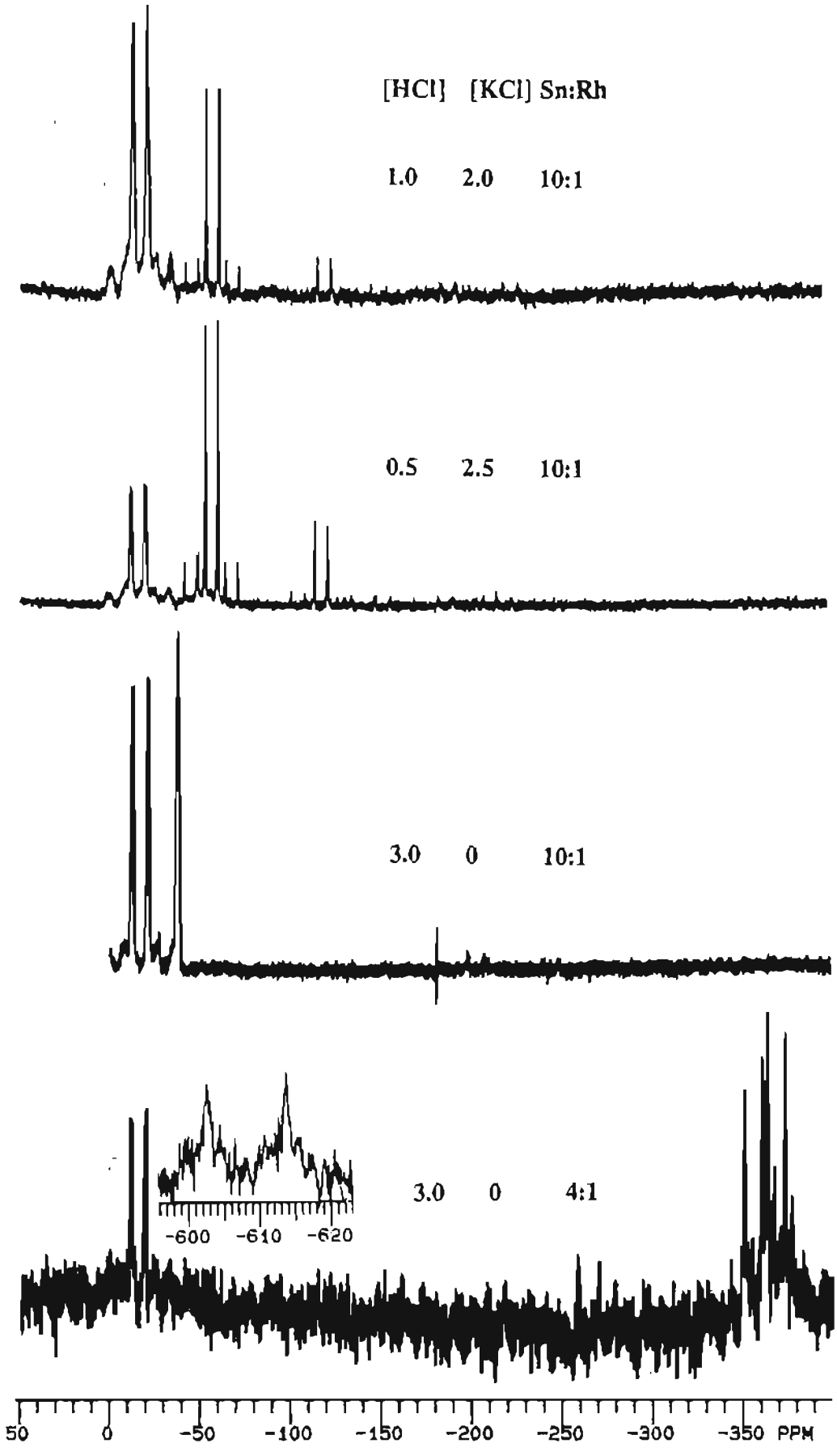

FIGURE 5.4 The ^{119}Sn nmr spectra of the various MIBK extracts. The solution conditions of the respective aqueous phases from which the extractions were made, are given.

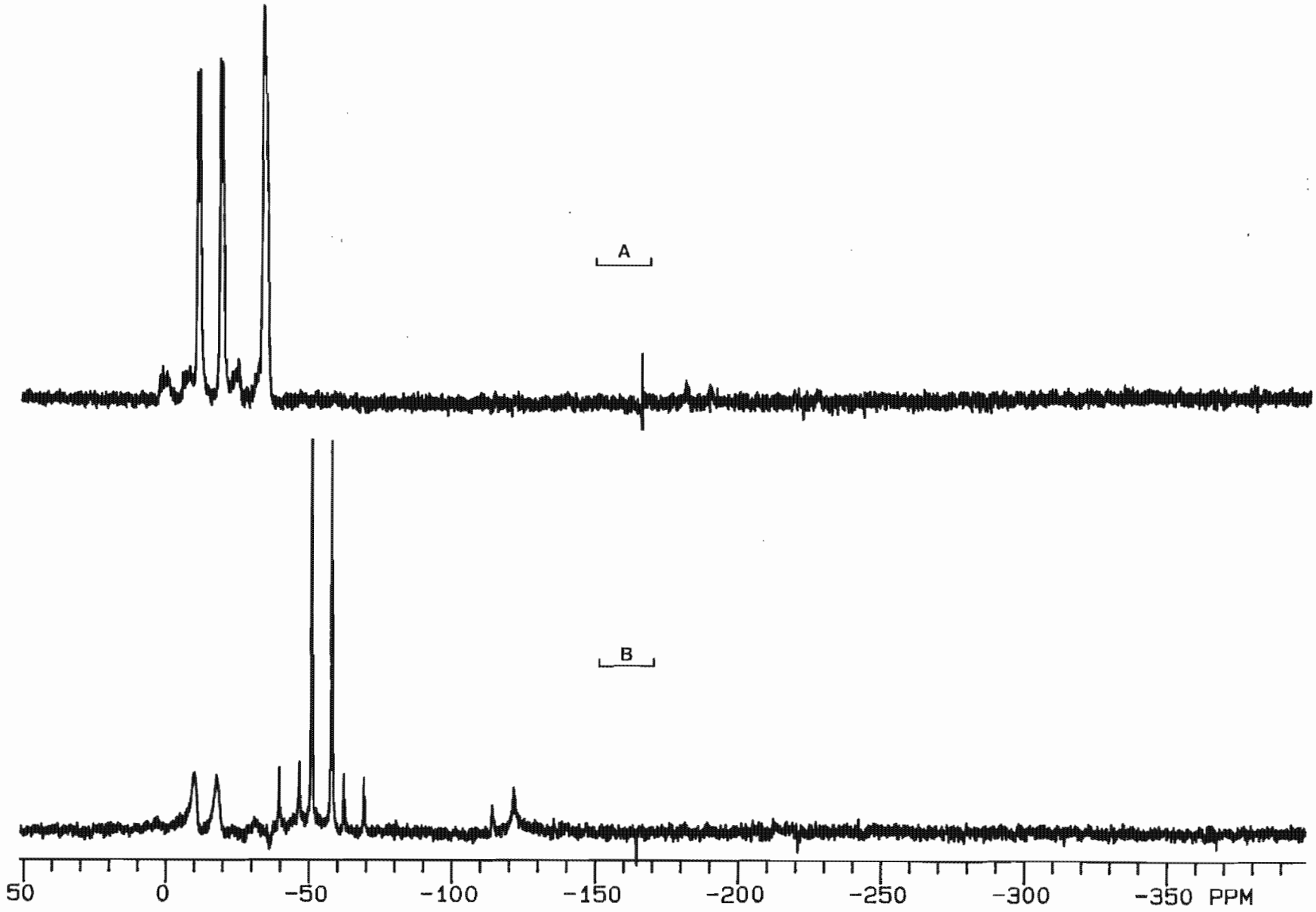

FIGURE 5.5 The change in the ^{119}Sn nmr spectral pattern of an MIBK extract on exposure to air for 25 hours at 20 °C (A = new extract, B = after exposure to air, aqueous phase composition: 3 M HCl, Sn:Rh = 10:1).

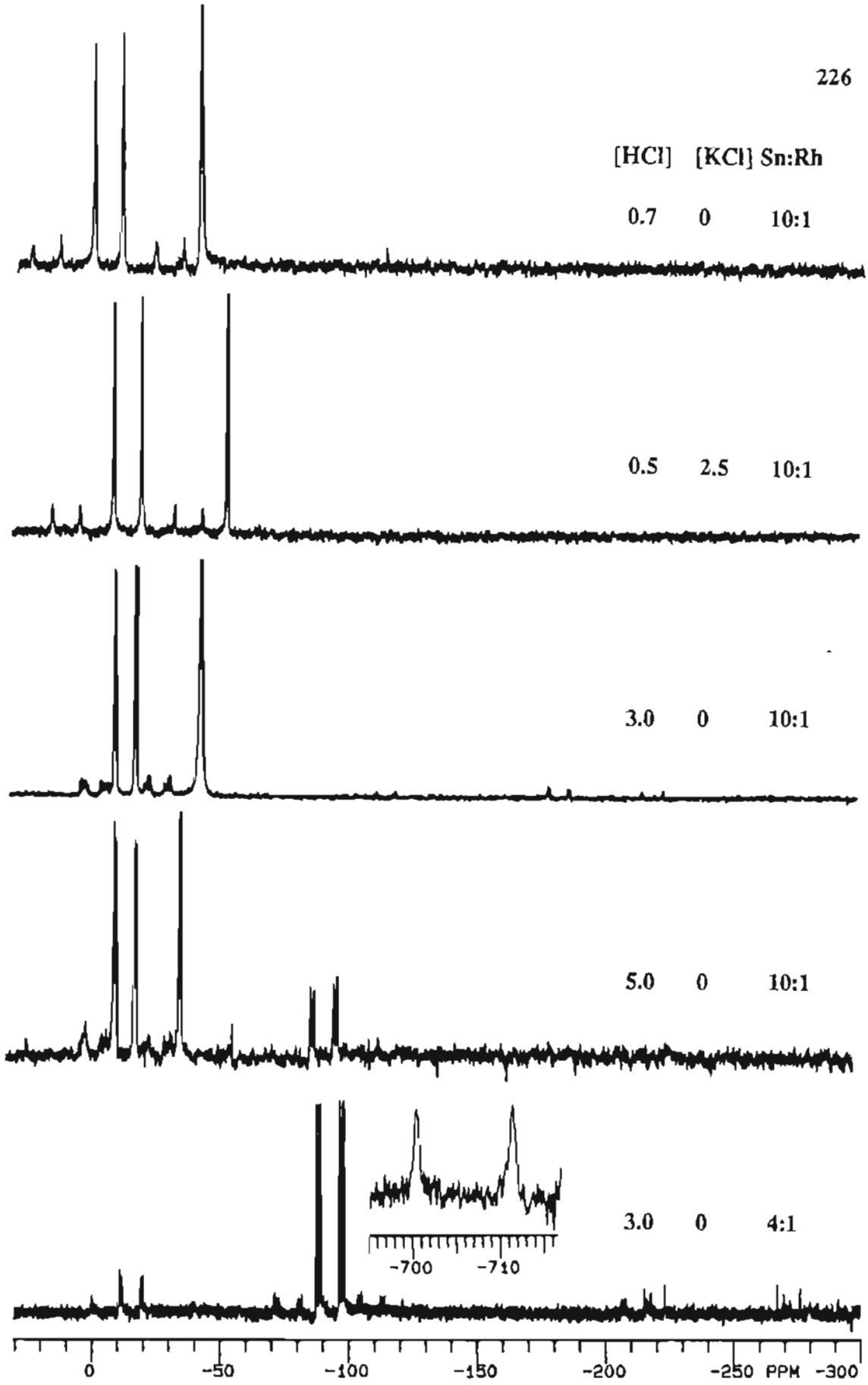

FIGURE 5.6 The ^{119}Sn nmr spectra recorded for the various Aliquat 336 extracts. The solution conditions of the respective aqueous phases from which the extractions were made, are given.

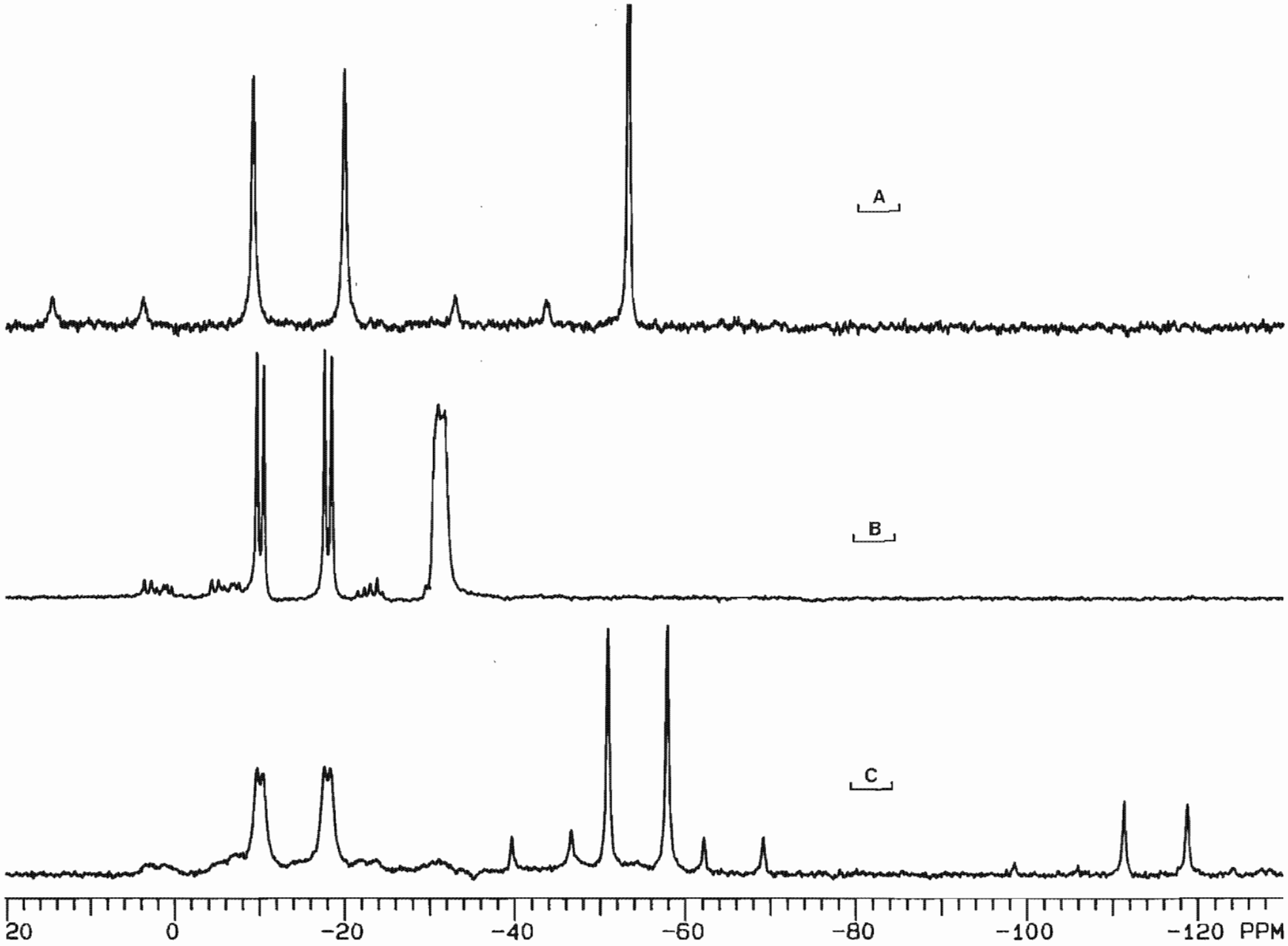

FIGURE 5.7 The ^{119}Sn nmr spectra of Aliquat 336 (A), Diϕ400U (B) and MIBK (C) phases after extraction from 0.5 M hydrochloric acid solutions containing 2.5 M KCl (Sn:Rh = 10.1).

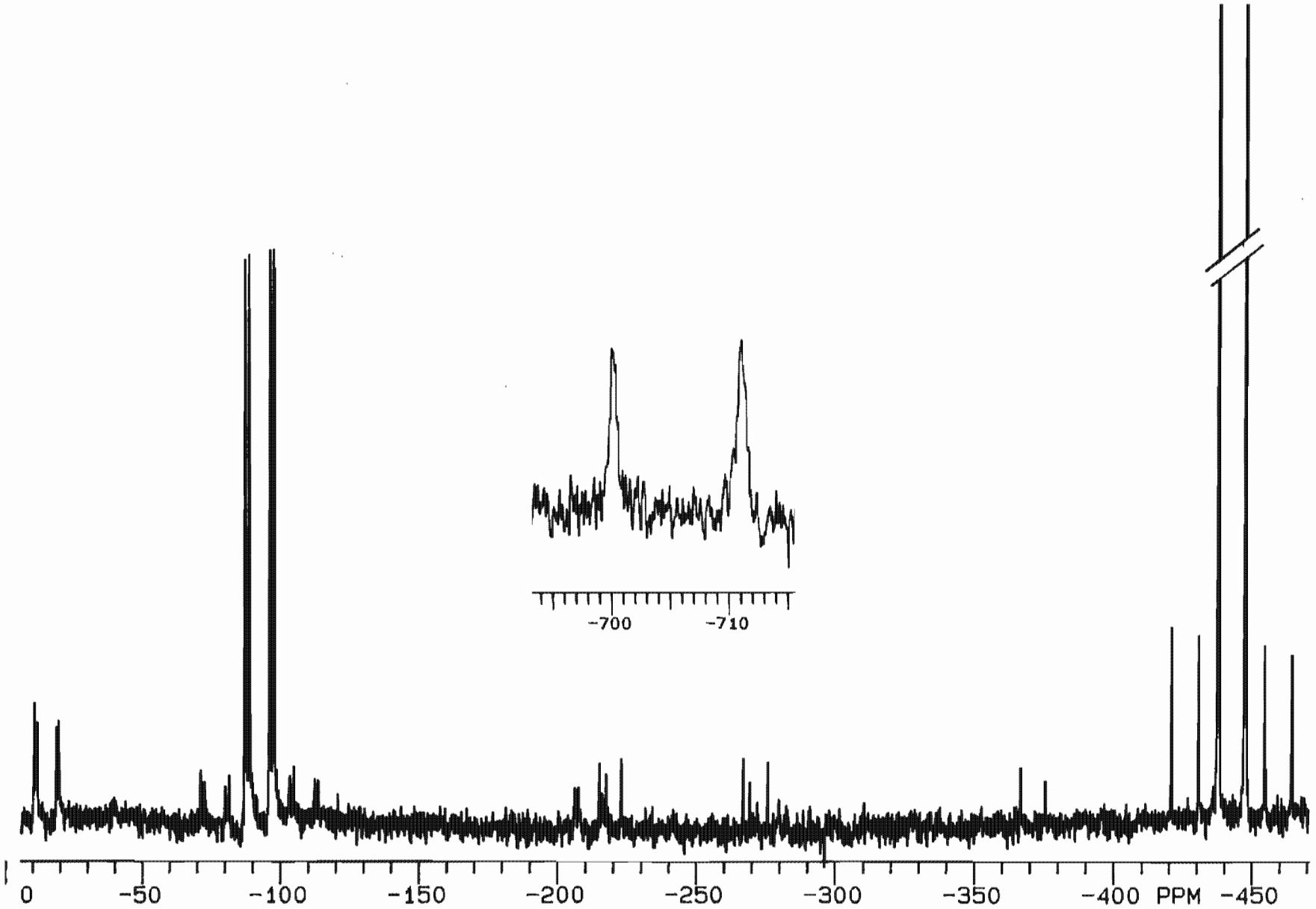

FIGURE 5.8 The ^{119}Sn nmr spectrum of the Aliquat 336 extract from a 3 M hydrochloric acid solution with a Sn:Rh ratio of 4:1.

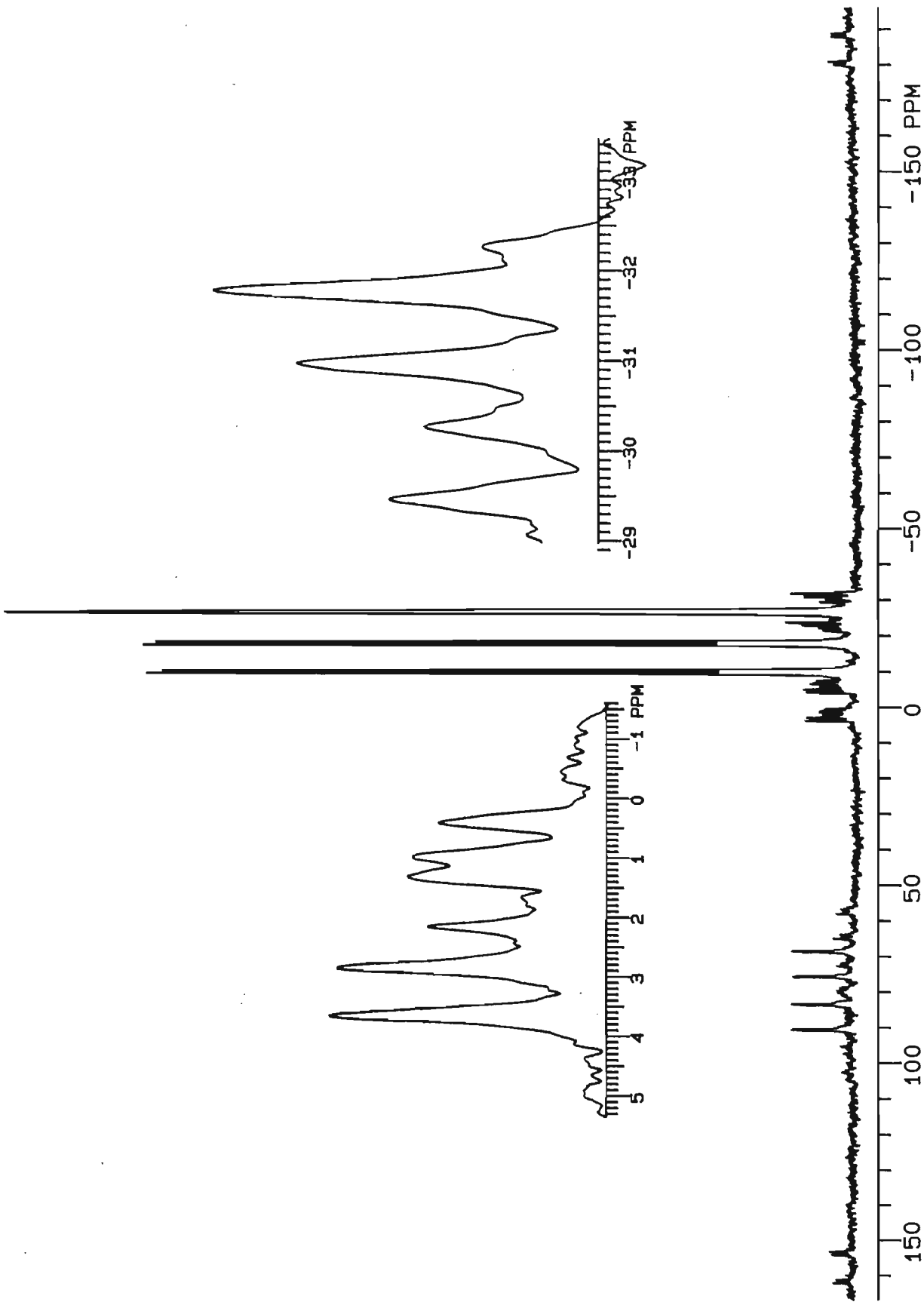

FIGURE 5.9 The ^{119}Sn nmr spectral pattern of the hydrido complex $[RhH(SnCl_3)_5]^{3-}$ in a Diϕ400U extract.

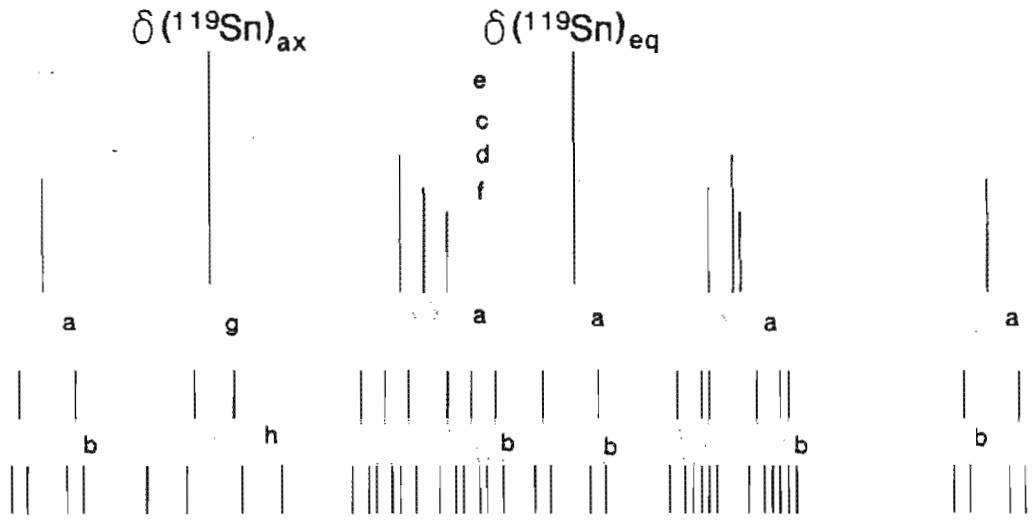

FIGURE 5.10 The splitting pattern of the ^{119}Sn nmr spectrum of $[RhH(SnCl_3)_5]^{3-}$ (not to scale). a = $^1J(^{103}Rh\text{-}^{119}Sn)_{(eq)}$, b = $^2J(^1H\text{-}^{119}Sn)_{(cis,\ ax\text{-}eq)}$, c = $^2J(^{117}Sn\text{-}^{119}Sn)_{(cis,\ eq\text{-}eq)}$, d = $^2J(^{117}Sn\text{-}^{119}Sn)_{(cis,\ ax\text{-}eq)}$, e = $^2J(^{117}Sn\text{-}^{119}Sn)_{(trans,\ eq\text{-}eq)}$, f = $^2J(^{119}Sn\text{-}^{119}Sn)_{(cis,\ ax\text{-}eq)}$, g = $^1J(^{103}Rh\text{-}^{119}Sn)_{(ax)}$, h = $^2J(^1H\text{-}^{119}Sn)_{(trans,\ ax\text{-}ax)}$.

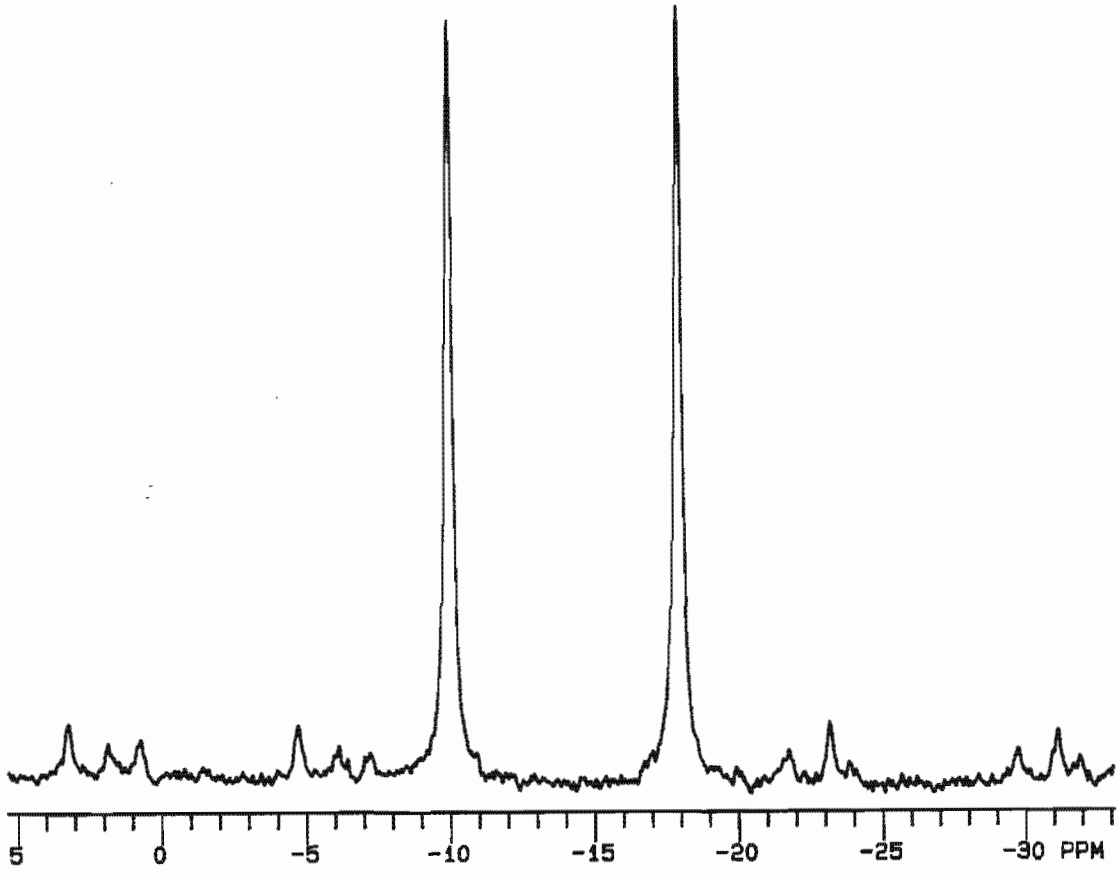

FIGURE 5.11 The ^1H-decoupled ^{119}Sn nmr spectrum of $[RhH(SnCl_3)_5]^{3-}$ (only the resonances due to the equatorial $SnCl_3^-$ ligands are shown).

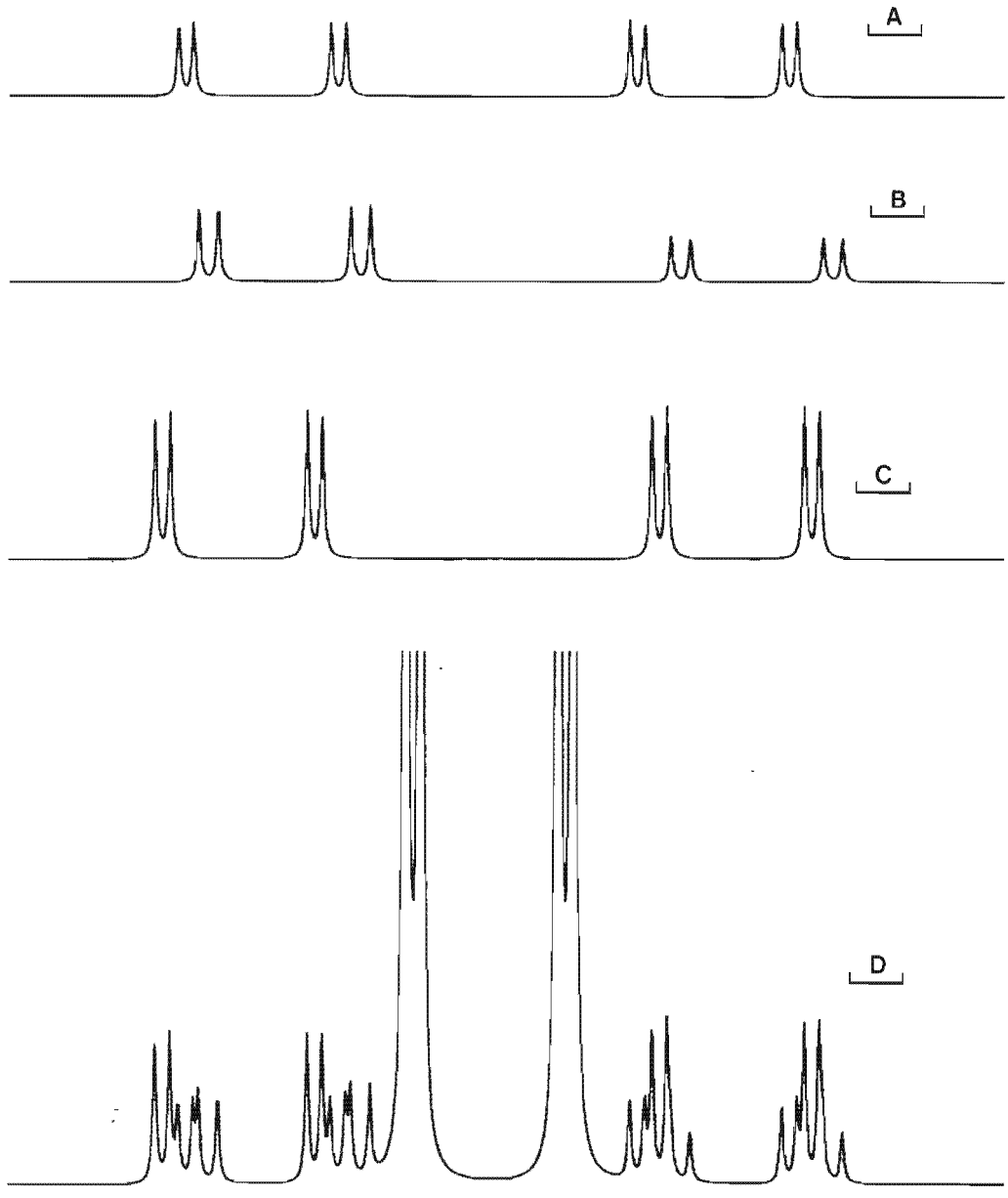

FIGURE 5.12 The computer simulated ^{119}Sn nmr spectra of the equatorial $SnCl_3^-$ resonances of $[RhH(SnCl_3)_5]^{3-}$ showing the coupling between the *cis* oriented $SnCl_3^-$ ligands. The combined and the subspectra of the various satellites are shown. A = $^2J(^{117}Sn\text{-}^{119}Sn)_{(cis,\ ax\text{-}eq)}$, B = $^2J(^{119}Sn\text{-}^{119}Sn)_{(cis,\ ax\text{-}eq)}$, C = $^2J(^{117}Sn\text{-}^{119}Sn)_{(cis,\ eq\text{-}eq)}$, D = combined spectrum.

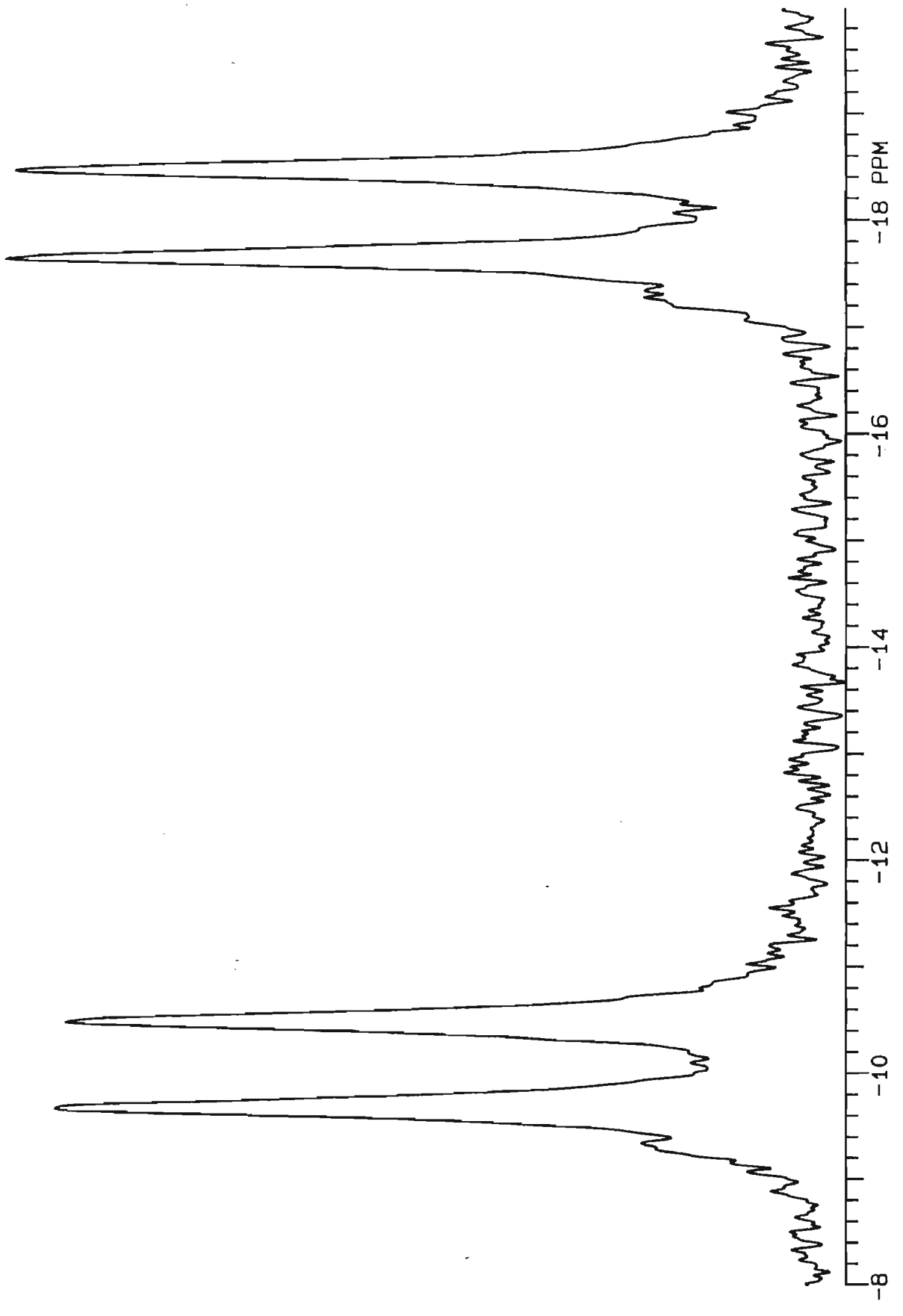

FIGURE 5.13 The ^{119}Sn nmr spectrum of $[RhH(SnCl_3)_5]^{3-}$ in a Diϕ400U extract, showing the shoulder to the left of the ^{119}Sn nmr peaks (Temp. = 0 °C).

2. A UV-Visible Spectrophotometric Study of the Protonation of $[Rh(SnCl_3)_5]^{4-}$

The above-mentioned ^{119}Sn nmr studies suggest that $[Rh(SnCl_3)_5]^{4-}$ is protonated to yield the hydrido complex $[RhH(SnCl_3)_5]^{3-}$. Krut'ko *et al.* [3] reported acidic properties of this hydrido complex in acetonitrile since deprotonation of $[RhH(SnCl_3)_5]^{3-}$ with the addition of dimethylformamide (DMF) as a base was confirmed by ^{119}Sn nmr. These authors [3] suggested the existence of a reversible protonation/deprotonation reaction involving $[Rh(SnCl_3)_5]^{4-}$ and $[RhH(SnCl_3)_5]^{3-}$.

It was decided to examine the reversibility of this reaction by a simple UV-visible spectrophotometric experiment. Iwasaki *et al.* [5] had found that the purple species, $[Rh(SnCl_3)_5]^{4-}$ showed a maximum absorbance at 470 nm. Hence, the concentrations of the complex $[Rh(SnCl_3)_5]^{4-}$ could be monitored by measuring the absorbance at this wavelength.

2.1 Results and Discussion

The UV-visible spectrum of a purple aqueous rhodium-tin solution was recorded relative to a hydrochloric acid solution (in which the concentrations of HCl and KCl were matched to that of the rhodium sample). A maximum absorbance observed at 470 nm was consistent with Iwasaki *et al.* [5].

The rhodium-tin complexes were extracted into an Aliquat 336 solution (in chloroform) and the absorbance at 470 nm was monitored with consecutive additions of CF_3COOH and DMF. Since the absorbance at 470 nm is proportional to the concentration of $[Rh(SnCl_3)_5]^{4-}$, a shift in the following reaction equilibrium:

$$[Rh(SnCl_3)_5]^{4-} + H^+ \rightleftharpoons [RhH(SnCl_3)_5]^{3-} \quad (3)$$

may be monitored. The results are illustrated in Figure 5.14.

The decrease in the absorbance at 470 nm with the addition of CF_3COOH suggests that the concentration of $[Rh(SnCl_3)_5]^{4-}$ was lowered by a protonation reaction, while the increase in the absorbance with the addition of DMF suggests a shift to the left of equation 3. Thus a reversible acid/base reaction is indicated. To confirm the reversibility of reaction 3, the experiment was repeated reversing the order of the acid/base additions (Figure 5.15). DMF was added first, resulting in an increase in absorbance, followed by the addition of CF_3COOH and a consequent decrease in the concentration of $[Rh(SnCl_3)_5]^{4-}$. A reversible reaction is clearly indicated in which the concentration of $[Rh(SnCl_3)_5]^{4-}$ may be altered at will by the addition of an acid or a base.

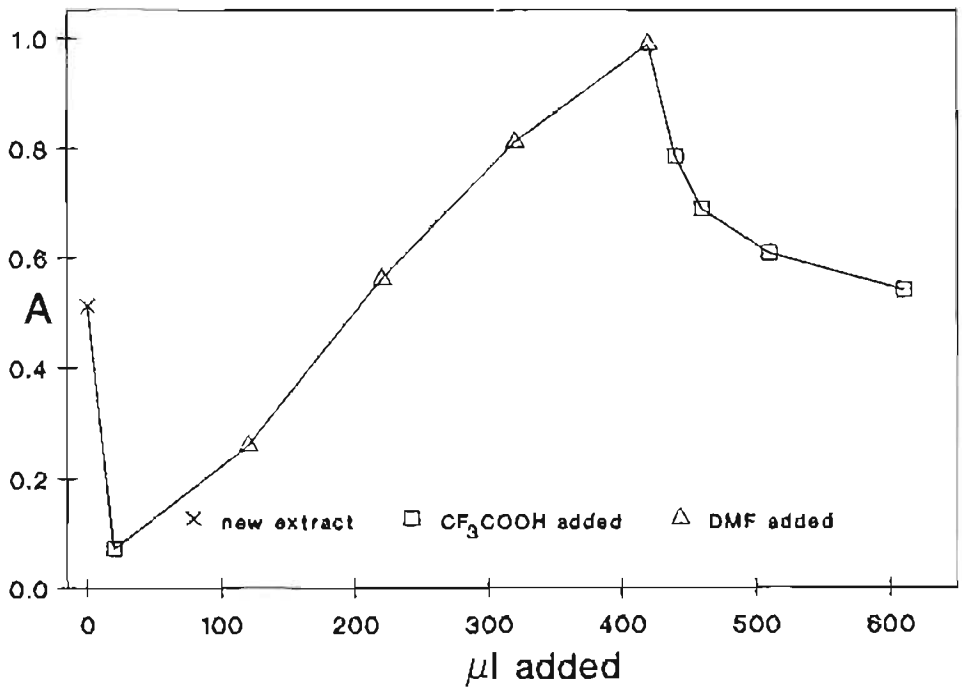

Figure 5.14 The change in the absorbance at 470 nm with the addition of CF_3COOH and DMF. The absorbance values were corrected for dilution.

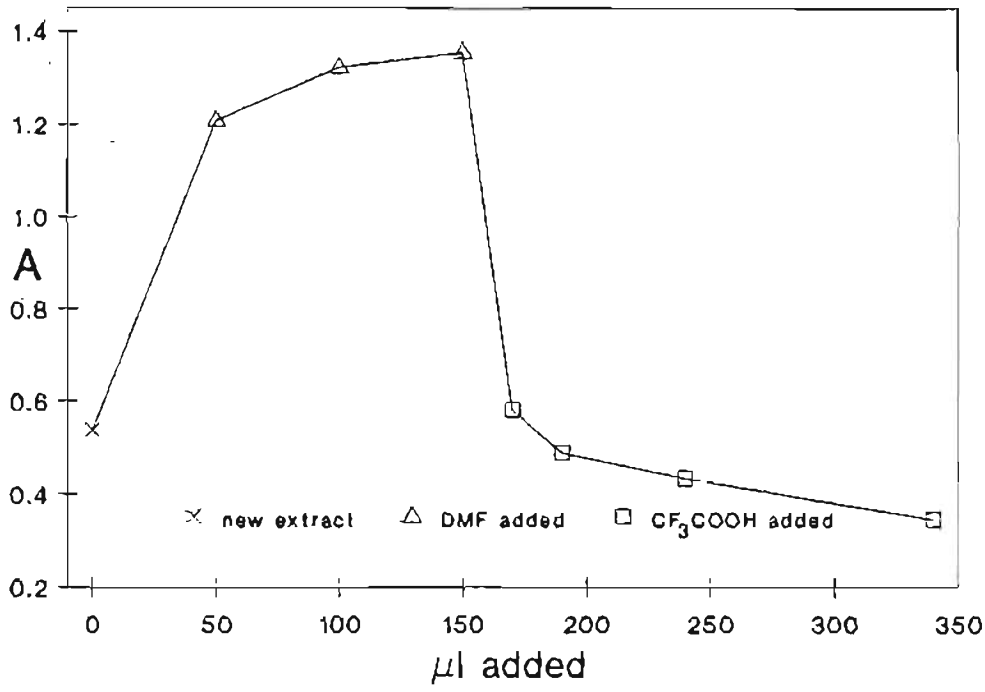

Figure 5.15 A repeat experiment showing the change in the absorbance at 470 nm with the addition of DMF and CF_3COOH. The absorbance values were corrected for dilution.

3. An Infrared Study of the Protonation of $[Rh(SnCl_3)_5]^{4-}$

Further proof of the reversible protonation reaction 3 would be to study the bond formation and bond scission of the rhodium-hydrido bond. Such a study could be performed by the observation of a change in the absorbance of ν(Rh-H) with the addition of an acid or a base.

The ν(M-H) of hydrido complexes of transition metals have been found to occur in the region 2300 to 1600 cm^{-1} [19]. Krut'ko *et al.* [3] reported a stretching frequency of 1940 cm^{-1} for the complex $[RhH(SnCl_3)_5]^{3-}$. The first task was to establish the frequency at which absorption occurred by the Rh-H bond of $[RhH(SnCl_3)_5]^{3-}$ in the Aliquat 336 extracts. These extracts were prepared using identical volumes of the same Aliquat 336 solutions (in chloroform) and aqueous phases that were nearly

identical in all respects except that one solution was partially deuterated (approximately 90%). The spectra are shown in Figure 5.16. The significant difference in the peak intensities of the peak at 1924 cm^{-1} for the two spectra, identified this frequency as the stretching frequency of the rhodium-hydrido bond ν(Rh-H). In addition to a large decrease in the intensity of ν(Rh-H) upon partial deuteration, one expects the concomitant appearance of a peak arising from ν(Rh-D). The expected stretching frequency of ν(Rh-D) was calculated to occur at approximately 1370 cm^{-1} (see Chapter 7). Regrettably, interference of solvent peaks (C-N bands absorb in this region) prevented the detection of ν(Rh-D).

The change in the absorbance at 1924 cm^{-1} with the addition of CF_3COOH as well as DMF is shown in Figure 5.17. The growth of the peak at 1924 cm^{-1} with the addition of CF_3COOH indicates an increase in the concentration of $[RhH(SnCl_3)_5]^{3-}$ due to a protonation reaction. It was ascertained by a prior investigation that CF_3COOH does not give rise to infrared bands that interfere with ν(Rh-H). The addition of a base (DMF) clearly results in the breaking of the rhodium to hydrogen bond since the peak at ν(Rh-H) = 1924 cm^{-1} disappears and the remaining spectral pattern in the surrounding frequency region coincides with that of DMF in the Aliquat 336 solution in the absence of any rhodium-tin complexes.

Compelling evidence is thus presented in support of a reversible acid/base reaction which determines the formation of $[RhH(SnCl_3)_5]^{3-}$ by the protonation of $[Rh(SnCl_3)_5]^{4-}$ (see reaction 3).

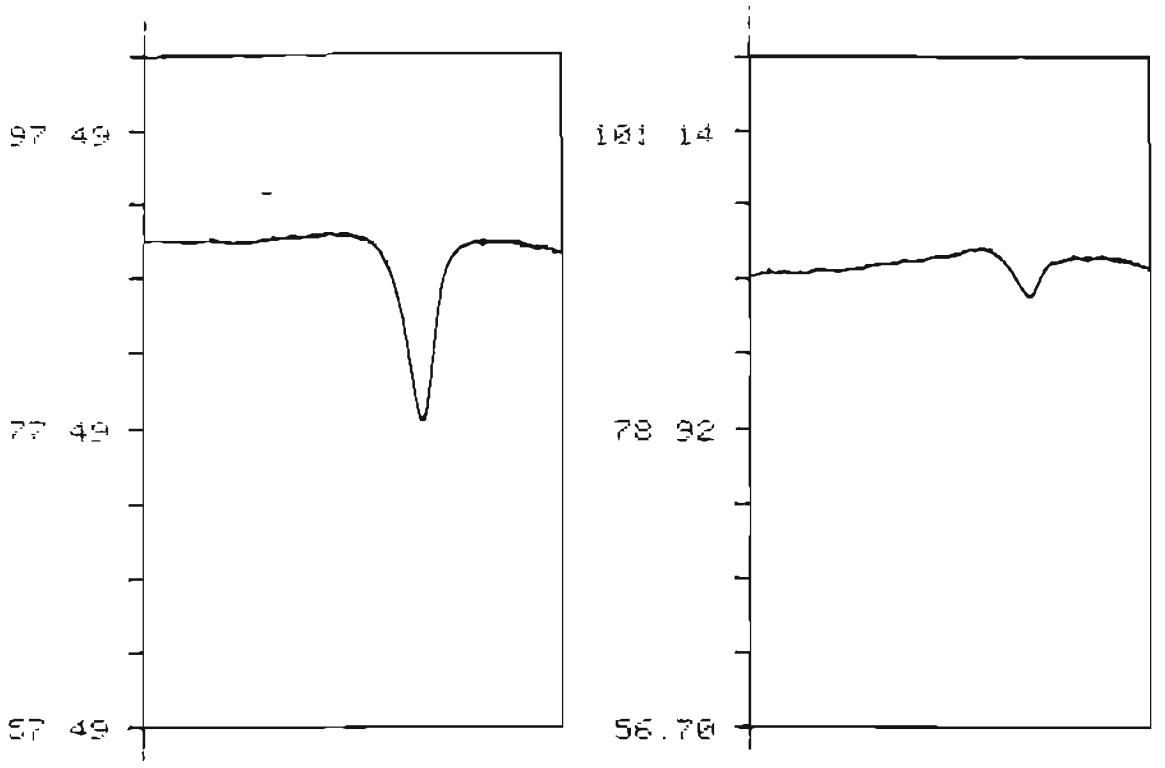

Figure 5.16 The decrease in the infrared absorption at 1924 cm^{-1} on deuteration of the Aliquat 336 extract containing $[RhH(SnCl_3)_5]^{3-}$, identifying the peak as ν(Rh-H).

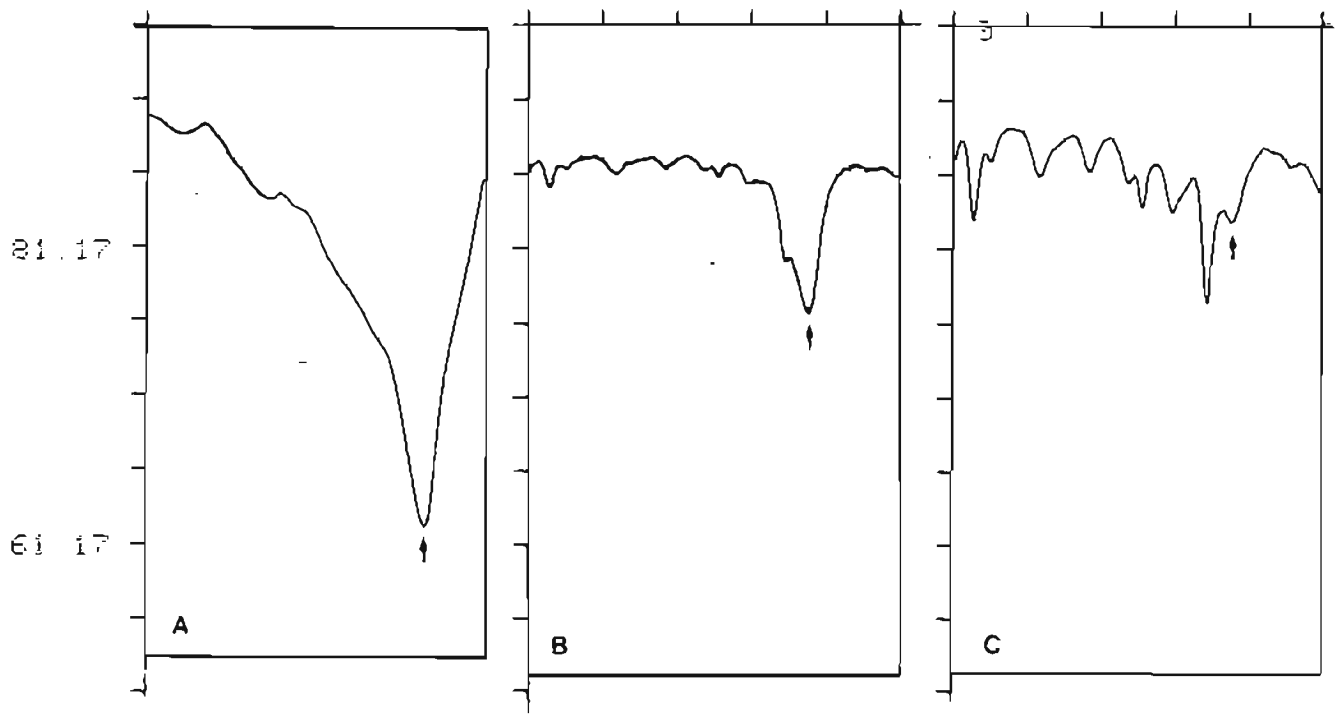

Figure 5.17 The change in the infrared absorption intensity at 1924 cm^{-1} (indicated by arrows) with the addition of CF_3COOH and DMF. (A = 20 μl CF_3COOH added, B = 60 μl DMF added, C = 100 μl DMF added.)

REFERENCES

1 T.KIMURA
Sci. Papers, I.P.C.R., 73 (1979) 31

2 T.KIMURA AND T.SAKURAI,
J. Solid State Chem., 34 (1980) 369

3 D.P.KRUT'KO, A.B.PERMIN, V.S.PETROSYAN AND O.A.REUTOV,
Izv. Akad. Nauk SSSR, Ser. Khim. (Engl Transl.), (12) (1984) 2553

4 H.MORIYAMA, T.AOKI, S.SHINODA AND Y.SAITO,
J. Chem. Soc. (Dalton), (1981) 639

5 S.IWASAKI, T.NAGAI, E.MIKI, K.MIZUMACHI AND T.ISHIMORI,
Bull. Chem. Soc. (Jpn.), **57** (1984) 386

6 H.B.CHARMAN,
J. Chem. Soc., (B) (1970) 584

7 H.MORIYAMA, T.AOKI, S. SHINODA AND Y.SAITO,
J. Chem. Soc. (Perkin II), (1982) 369

8 T.YAMAKAWA, S.SHINODA, Y.SAITO, H.MORIYAMA AND P.S.PREGOSIN,
Magn. Reson. in Chem., **23** (1985) 202

9 K.R.KOCH AND J.M. WYRLEY-BIRCH,
Inorg. Chim. Acta, **102** (1985) L5

10 T.G.APPLETON, H.C.CLARK AND L.E.MANZER,
Coord. Chem. Rev., **10** (1973) 335

11 M.KRETSCHMER AND P.S.PREGOSIN,
Inorg. Chim. Acta, **61** (1982) 247

12 H.MORIYAMA, P.S.PREGOSIN, Y.SAITO AND T.YAMAKAWA,
J. Chem. Soc. (Dalton Trans.), (1984) 2329

13 E.D.BECKER,
"High Resolution NMR : Theory and Chemical Applications",
2nd ed., Academic Press, (1980) New York

14 D.S.STEPHENSON AND G.BINSCH,
DNMR5, QCPE 11 (1978) 365

15 J.M.WYRLEY-BIRCH,
M.Sc. Thesis, University of Cape Town, (1984)

16 G.W.PARSHALL,
J. Amer. Chem. Soc., **88** (1966) 704

17 J.A.POPLE AND P.D.SANTRY,
Mol. Physics, **8** (1964) 1

18 T.YAMAKAWA, H.MORIYAMA, S.SHINODA AND Y.SAITO, *Inorg. Chem.*, **26** (1987) 3347

19 D.S.MOORE AND S.D.ROBINSON, *J. Chem. Soc. (Quart. Rev.)*, **12** (1983) 415

CHAPTER 6

GENERAL DISCUSSION AND CONCLUSION

General Discussion and Conclusion

Polyether-type polyurethane foam has been shown to be an efficient and convenient means for the recovery of rhodium from hydrochloric acid solutions containing stannous chloride. A maximum capacity of 0.51 mmol of rhodium per gram of foam was observed during extraction from an aqueous phase containing 2 M hydrochloric acid and a molar Sn:Rh ratio of 200:1. The effect of a variety of factors (*inter alia* temperature, Sn:Rh ratio, hydrochloric acid concentration) on the extraction of the trichlorostannato-rhodium complexes was established. From this study followed the development of an efficient method for the complete separation of rhodium from iridium [1]. If a higher capacity of the foam for rhodium is required, the extraction conditions may be further optimized. For instance, although it was shown in Chapter 2, Section 2.3 that an equilibration time of 16 hours prior to extraction did not significantly affect the rate and the extent of the extraction of rhodium by polyurethane foam, it was shown in Chapter 4, Section 1.2(i), that an equilibration time of 4 days significantly increased the amount of rhodium extracted by the soluble linear polyurethanes. Hence, the maximum capacity of polyurethane foam may possibly also be increased by a longer equilibration time of the aqueous phase prior to extraction. A convenient method for the recovery of metals is always a compromise between the "best" results and the most cost and time effective experimental conditions.

The increased extraction of rhodium with an increase in the equilibration time could only reasonably be related to the nature of the trichlorostannato complexes of rhodium in solution, and this provided the first indication of the rhodium species with the highest extractability. It was shown in Chapter 4, Section 1.2(i) that an increase in the equilibration period was accompanied by an increase in the

absorbance at 470 nm in the UV-visible spectrum of the aqueous phase. Hence, the favourable effect on the extraction of rhodium of a longer equilibration time at 35 °C, was linked to a higher concentration of the trigonal bipyramidal "purple species", $[Rh(SnCl_3)_5]^{4-}$. This was based upon the report by Iwasaki *et al.* [2] that $[Rh(SnCl_3)_5]^{4-}$ exhibited an absorption maximum at 470 nm, and was supported by the report by Kimura [3] who found that a long equilibration period (more than 10 days at 35 °C) was needed for the complete formation of the purple solution.

Compelling evidence in support of the above considerations was obtained from the ^{119}Sn nmr study of the rhodium-tin complexes extracted by the model urethane compound, Diϕ400U, MIBK, and the liquid anion-exchanger, Aliquat 336. Chloroform solutions of Aliquat 336 extracted only the trigonal bipyramidal $[Rh(SnCl_3)_5]^{4-}$ from aqueous phases containing low $[H^+]$ (0.5 and 0.7 M). On the other hand, under these conditions the hydrido complex, $[RhH(SnCl_3)_5]^{3-}$, was the only rhodium-tin complex evident in the Diϕ400U phase. Furthermore, in the presence of excess stannous chloride (Sn:Rh > 6:1) in the aqueous phase, the Diϕ400U extract contained $[RhH(SnCl_3)_5]^{3-}$ exclusively, irrespective of the hydrochloric acid or potassium chloride concentrations. It was shown by ^{119}Sn nmr and UV-visible and infrared spectrophotometric methods {Chapter 5, Sections 1.2(i)(*c*), 2. and 3.} that the hydrido complex $[RhH(SnCl_3)_5]^{3-}$ was formed by the reversible protonation of $[Rh(SnCl_3)_5]^{4-}$. Since the purple species, $[Rh(SnCl_3)_5]^{4-}$, is stable in Aliquat 336, it is significant that this species was never detected in the "oxygen-donor" extracts (Diϕ400U and MIBK). This observation may be ascribed to the coextraction of significant amounts of hydrochloric acid by Diϕ400U and MIBK resulting in the rapid protonation of $[Rh(SnCl_3)_5]^{4-}$ to produce $[RhH(SnCl_3)_5]^{3-}$ in the organic phase.

It seems clear that an increased concentration of $[Rh(SnCl_3)_5]^{4-}$ in the aqueous phase leads to the more efficient overall extraction of rhodium. In addition, an increase in the hydrochloric acid concentration results in a steady increase in the amount of rhodium extracted by polyurethane foam and the model urethane compounds. The latter effect may be linked to an increase in the amount of acid coextracted, resulting in a shift to the right of the protonation reaction (reaction 3, Chapter 5, Section 2.1) so yielding higher concentrations of $[RhH(SnCl_3)_5]^{3-}$ in the urethane phase. This suggestion that the beneficial effect of hydrochloric acid on the extraction of rhodium is due to its effect on the protonation reaction involving $[Rh(SnCl_3)_5]^{4-}$ is supported by the observation in the analogous platinum extraction system (where $[Pt(SnCl_3)_5]^{3-}$ is not protonated) in which the extraction of platinum by polyurethane foam increases with increasing hydrochloric acid concentration to a maximum at approximately 1 M, after which the extraction of platinum decreases with increasing hydrochloric acid concentration [4]. One could hold the view, therefore, that the $[RhH(SnCl_3)_5]^{3-}$ complex is the rhodium-tin species with the highest affinity for the urethane phase, and that, since it is formed by protonation of $[Rh(SnCl_3)_5]^{4-}$, an increase in the concentration of this rhodium(I) complex as well as the hydrochloric acid concentration would result in a more efficient extraction of rhodium by polyurethane foam. In the context of a favoured species for extraction by the urethane compounds and polyurethane foam, it is interesting to note that the hydrido complex, $[RhH(SnCl_3)_5]^{3-}$ was considerably more stable in Diϕ400U than in MIBK, and that the Diϕ400U phase appeared to provide an environment in which $[RhH(SnCl_3)_5]^{3-}$ was stabilized.

From the estimates of the ratios of Sn:Rh that were coextracted by polyurethane foam, the extraction of a distribution of species is indicated (the values of the Sn:Rh ratios on the foam did not approach integer values). The ^{119}Sn nmr study showed

that Diϕ400U extracted predominantly $[Rh(SnCl_3)_3Cl_3]^{3-}$ from aqueous solutions containing a Sn:Rh mole ratio of 4:1. Although under these conditions small amounts of two other species were detected, these were evidently present in very low concentrations. The extraction of other rhodium-tin complexes cannot therefore be excluded. Nevertheless, current evidence shows that mainly $[RhH(SnCl_3)_5]^{3-}$ and $[Rh(SnCl_3)_3Cl_3]^{3-}$ are extracted by Diϕ400U.

If one accepts the validity of Diϕ400U as a model for polyurethane foam in the speciation study, we may conclude that polyurethane foam extracts mainly $[RhH(SnCl_3)_5]^{3-}$ and $[Rh(SnCl_3)_3Cl_3]^{3-}$, and the values of Sn:Rh ratios of the species on the foam, which generally ranged from three to five, depend largely on the relative amounts in which these species are extracted. In this regard the qualitative observation made in Chapter 2, Section 2.2 might be relevant. It was noted that in the presence of low tin(II) concentrations, the foam phase assumed an orange-red colour on extraction. Similarly, the Diϕ400U extract from an aqueous phase containing Sn and Rh in a 4:1 ratio, and which was found to contain predominantly $[Rh(SnCl_3)_3Cl_3]^{3-}$, was an orange-red colour. In the presence of high initial tin(II) concentrations (Sn:Rh > 6:1), the foam turned bright yellow. High concentrations of tin(II) have been found to promote the rate of formation of the purple species $[Rh(SnCl_3)_5]^{4-}$. The extraction of rhodium by Diϕ400U and MIBK from purple aqueous solutions, resulted in a rapid colour change of the organic phase, to bright yellow. The yellow colour was observed in all the Diϕ400U extracts (from solutions containing Sn and Rh in a 10:1 ratio), which contained exclusively the hydrido complex $[RhH(SnCl_3)_5]^{3-}$. Thus the colour of the polyurethane foam on extraction is consistent with the results of the ^{119}Sn nmr study of the rhodium complexes extracted by the model urethane compound, Diϕ400U.

The mechanism by which the trichlorostannato complexes of rhodium are extracted by polyurethane foam is not a trivial question. The complexity of the system became increasingly evident during the course of this work, and further extensive investigation is needed before it will be fully understood. However, from the results of our studies using polyurethane foam, as well as the model urethane compounds, we are able to present a working model of the extraction system.

To begin with, the direct involvement of the polyether sections of polyurethane foam in the extraction of metal complexes has been confirmed, and we believe that these sections play a major role in the present extraction process. The solid state ^{13}C nmr spectrum showed severe broadening of the resonances arising from the polyether portions of polyurethane foam after the foam had been loaded with trichlorostannato complexes of platinum, suggesting that the polyether chains were associated with the metal complexes on the foam. In addition, the ^{13}C nmr spectrum of Diϕ400U showed an increase in the number of resonances arising from the central ethylene oxide groups after the extraction of the rhodium-tin(II) complexes. This indicated an increase in the number of chemical environments in which these carbons occurred, and implicated the poly(ethylene oxide) chains in the extraction process. These results are consistent with those of Hamon *et al.* [5] who found a shift of 30 cm^{-1} in the ethylene oxide infrared bands of polyurethane foam after the extraction of $[Co(NCS)_4]^{2-}$.

The role of the nitrogen containing linkages of polyurethane foam (for instance, urethane, urea, allophanate, biuret and anhydride groups) was not studied in any great detail. The increase in the extraction efficiency of the model urethane compounds with an increase in the oligo(ethylene oxide) chain length (and the concomitant decrease in the concentration of the urethane groups in these

compounds) suggests that the urethane linkages are not significantly involved in the extraction phenomenon of the rhodium complexes. Further, in the study of the 100% poly(propylene oxide) based polyurethane foams, it was found that the index 120 foam extracted less rhodium than did the index 90 foam. The index 120 foam contained a higher proportion of nitrogen linkages and was more highly cross-linked, arguing against the significant involvement of the nitrogen donor groups in the extraction process.

An important consideration in the study of the extraction mechanism, is the role of cations such as H_3O^+ and the alkali metal cations. The coextraction of alkali metal cations by both polyurethane foam and the soluble linear polyurethanes was confirmed. It was found that the polyurethane foam that had been used for the extraction of rhodium from K^+ containing solutions had coextracted 0.46 $mmol.g^{-1}$ of K^+. This accounted for 44% of the total number of positive charges required for the amount of rhodium extracted, assuming that the rhodium was extracted as a triply charged anion. A ^7Li nmr study of the Pol1500U(1:2) phase, after the extraction of rhodium complexes from acidic aqueous solutions containing 0.2 M and 2 M LiCl, positively confirmed the coextraction of some Li^+. The amount of Li^+ coextracted was strongly dependant upon the Li^+ concentration in the aqueous phase. The amount of Li^+ extracted from aqueous solutions containing 0.2 M LiCl accounted for only approximately 12% of the cationic sites required for the rhodium extracted, whereas from 2 M LiCl solutions approximately 65% of the cationic sites were formed by Li^+.

Since the amount of coextracted metal cations could not entirely account for the extraction of rhodium, the balance of the positive charge required to ensure

electroneutrality must have been derived from hydrogen ions. This could conceivably occur in one or more of the following ways:

a) chelation of H_3O^+

b) protonation of donor heteroatoms in the polyurethane matrix, or

c) the "solid solvent extraction" of neutral acidic species such as $H_3[RhH(SnCl_3)_5]$.

Thus in contrast to the findings of Hamon *et al.* [5], hydrogen ions were found to play a major role in the extraction of rhodium-tin complexes by polyurethane foam. The importance of the $[H^+]$ is demonstrated by the increase in the amount of rhodium extracted by both polyurethane foam and the model urethane compounds with increased hydrochloric acid concentration. In addition to its importance for the creation of cationic "sites" in the polyurethane phase, a high $[H^+]$ is also thought to favourably influence the extraction of rhodium by promoting the formation of the hydrido complex $[RhH(SnCl_3)_5]^{3-}$, which is thought to be the species favoured by the polyurethane foam phase.

Initially, it appears that the contribution of the alkali metal cations in the extraction of rhodium is less complex than that of the hydrogen ions. The evidence discussed above, showing the direct involvement of the polyether chains in the extraction process, suggests that chelation of cations by the polyether sections of polyurethane foam plays a major role in facilitating the extraction of anions. This suggestion is supported by the results discussed in Chapter 4, Section 1.1(iii) which showed the existence of a minimum oligo(ethylene oxide) chain length, below which negligible extraction of anionic metal complexes occurs. Consistent with this observation was the increase in the extraction efficiency of the soluble linear polyurethanes with an increase in the oligo(ethylene oxide) chain length {refer to Chapter 4, Sections 1.1(iii), 1.1(v) and 1.2(iii)}. It was also shown that the extraction of $[Co(NCS)_4]^{2-}$ by

the model urethane compounds could not be ascribed to a simple solvent extraction mechanism {Chapter 4, Section 1.1(iii)}.

Chelation of cations by the polyether chains of polyurethane foam was postulated by Hamon *et al.* [5] in their proposal of the cation chelation mechanism (CCM). These authors found that the alkali metal cations increased the amount of $[Co(NCS)_4]^{2-}$ extracted by polyurethane foam in an order which parallels the order of increasing alkali metal complex stability with dibenzo-18-crown-6. This idea was linked to the stability of PEO chains as 18-membered spirals [5,6], and the effect of cations on extraction was thought to be based upon their cationic size [5]. From these considerations followed the suggestion that the polyether portions of polyurethane foam form helical conformations with inwardly directed oxygen atoms surrounding the complexed cations. This reasoning is supported by several reports in the literature of the helical conformations of PEO and of the ability of PEO polymers to interact with alkali metal ions. The lower efficiency with which metal complexes are extracted by polyester based polyurethane foams relative to polyether based foams was explained by the CCM as being attributable to the inherent inability of polyesters to become helically orientated about a central axis. Similarly, the increased sorption of $[Co(NCS)_4]^{2-}$ by polyurethane foam containing increasing proportions of PEO relative to PPO was explained by a smaller tendency of PPO to adopt helical conformations due to steric restrictions of the methyl groups. The importance of the helical conformations of the polyurethane backbone is emphasized by Hamon *et al.* [5] who conclude "We thus believe that a helical arrangement of inwardly directed polyether oxygen atoms forms the basis of complexation between cations and the polymer". The CCM as proposed by Hamon *et al.* [5] contributed significantly towards a better understanding of the extraction of metal complexes by polyurethane foam, and the results of a great many workers

have been consistent with the predictions of the CCM (as is discussed in Chapter 1 Section 3.5). In view of the results of this work however, the emphasis on the helical conformation of the polyether sections of polyurethane foam for the efficient chelation of cations is an oversimplification. If one considers that the PEO content is generally smaller than 20% of the total polyether content of polyurethane foam, it is difficult to ascribe this relatively small proportion of helically oriented polyether chains to account for the significant increase in the extraction efficiency of polyurethane foam with increasing PEO content.

The apparent simplicity of the contribution of alkali metal cations towards the extraction process is deceptive. Although conclusive evidence for the extraction of alkali metal cations by both polyurethane foam and the model urethane compounds was found, the presence of alkali metal cations affected the extraction of the chloro(trichlorostannato)rhodium complexes by polyurethane foam and by the model urethane compounds in opposite ways. The depressive effect of K^+ on the extraction of the rhodium-tin complexes by polyurethane foam, as opposed to the increase in the amount of rhodium extracted by the model urethane compounds in the presence of K^+, is contrary to the predictions of the CCM and is difficult to explain. It is evident that the interaction of the alkali metal cations with the polyether chains of polyurethane foam and their effect on the extraction of rhodium is of a complex nature. At this stage it is only possible to conclude that the depressive effect of K^+ may be linked to the nature of the solid polyurethane foam matrix. This conclusion is underlined by the observation (Chapter 4, Section 2.2) that the polyurethane foam synthesized from a polyol consisting of 87% PPO + 13% PEO was far more sensitive to the depressive effect of K^+ on the extraction of rhodium than was the 100% PPO based polyurethane foam. In addition, the isocyanate index of the polyurethane foam was also found to influence the sensitivity

of the foam to the depressive effect of K^+ on the extraction of rhodium. Hence, the index 90 foam (100% PPO) showed a slight decrease in the extraction of rhodium in the presence of K^+, while a negligible decrease was observed for the index 120 foam (100% PPO).

Not only were the above polyurethane foams affected differently by the presence of alkali metal cations, but these foams also extracted rhodium with differing efficiencies. Hence, the amount of rhodium extracted by these respective polyurethane foams decreased in the order 87% PPO + 13% PEO > 100% PPO (index 90) > 100% PPO (index 120) (where the foams are distinguished by their polyol content and isocyanate index). This order of decreasing extraction efficiency may be linked to a corresponding order of decreasing flexibility of the respective polyurethane chains (discussed in Chapter 4, Section 2.2). This reasoning is supported by the results of Chapter 4, Section 1.2(iv), where the extracting power of Pol400U(1:1) was found to decrease with increasing concentration of this linear polyurethane to a minimum value for the distribution ratio describing the amount of rhodium extracted (Figure 4.16). This trend is thought to arise from *inter*molecular interactions at high concentrations (an increase in *intra*molecular interactions probably also occurs with increasing polymer concentration), which restricts conformation changes of the polyurethane chains. Such restrictions limit the number of conformations of the polyurethane for suitable chelation of cations, and so results in a decreased extracting power.

Our studies have not allowed us to pinpoint one predominant extraction mechanism to the exclusion of others. From the study of the model urethane compounds it appears that a "solid solvent extraction" type of mechanism does not contribute significantly towards the extraction of the trichlorostannato complexes of rhodium.

Ligand addition to the coordinatively saturated six-coordinate octahedral rhodium(III) complexes extracted by polyurethane foam is not likely to occur. However, the possibility of ligand exchange exists, and the formation of complexes of the type $[Rh(SnCl_3)_nX_mCl_{6-(n+m)}]^{3-}$ (where X is a ligating extractant molecule and the charge = $(3 - m)^-$ for neutral X) was postulated in Chapter 5, Section 1.2(i)(*b*). However, the ^{119}Sn nmr resonances of these species, where m was thought to be greater than 0, were only detected in aged (eleven days) Diϕ400U extracts, and then only in trace amounts. Hence, ligand exchange cannot be considered a major mechanism accounting for the extraction of the rhodium complexes. The two most likely mechanisms for the extraction of the trichlorostannato-rhodium complexes are the chelation of cations such as H_3O^+ by the polyether chains, and the protonation of the O and N donor atoms to create cationic sites, so resulting in the coextraction of the anionic rhodium complexes (note that no evidence for the involvement of nitrogen atoms was found, and the emphasis should lie on the oxygen atom involvement). The observed increase in the amount of rhodium extracted with an increase in the $[H^+]$ is consistent with both these proposed extraction mechanisms. It is probable that, within any particular extraction system rhodium is extracted by both protonation and cation chelation, and that the dominant mechanism is dictated by solution conditions and the nature of the polyurethane foam.

At this stage it would be expedient to list those factors identified by our studies as having a positive influence on the amount of rhodium extracted by polyurethane foam. These are:

1) a relatively high concentration of the trigonal bipyramidal rhodium(I) complex, $[Rh(SnCl_3)_5]^{4-}$ in the aqueous solution. (The concentration of $[Rh(SnCl_3)_5]^{4-}$ is increased by a high $SnCl_3^-$ concentration and an increased equilibration time.),

2) a high $[H^+]$, which is thought to be necessary for the creation of cationic sites as well as for the protonation of $[Rh(SnCl_3)_5]^{4-}$ to form the hydrido complex $[RhH(SnCl_3)_5]^{3-}$, which was found to be favoured by the urethane phase,
3) the flexibility of the polyether chains of polyurethane foam, which depends on the PEO content as well as the isocyanate index.

The Working Model

Since the heterogeneous microstructure of polyurethane foam should be taken into account, a model for the process responsible for the extraction of the rhodium-tin complexes by polyurethane foam (mainly $[RhH(SnCl_3)_5]^{3-}$ and $[Rh(SnCl_3)_3Cl_3]^{3-}$) requires the description of the solid polyurethane foam matrix as an irregular crosslinked network of polyurethane chains which are linked *via* nitrogen containing linkages. The oxygen-donor containing polyether sections of these polyurethane chains play a major role in the extraction of the trichlorostannato complexes of rhodium. Further, one may assume that a finite number of sites exist which are able to accommodate a cation (be it by protonation of, for instance, the $-CH_2-O-CH_2-$ groups, or by chelation of either H_3O^+ or alkali metal cations). The favourable interaction between cations and donor groups of the macromolecule may demand a conformational rearrangement of the polyurethane chains so that these polymer chains may assume appropriate orientations. The total number of sites available is thus expected to be dependent upon the flexibility of the polyurethane chains. The extraction of the rhodium-tin complexes may be thought to be accompanied, therefore, by conformation changes of the polyurethane chains, each change resulting in a polyurethane chain conformation which simultaneously allows the polyether-cation interaction and the coextraction of the bulky rhodium-tin anions. In this context, it may be postulated that sites of different energies of ion pair

formation exist, the site with the lowest energy resulting in the most favourable [polyether(cation^{+})]$_3$ [anion^{3-}] complex. The energy of each site might conceivably depend upon:

a) the extent of the necessary conformation change, and the flexibility of the polyurethane chain that is required to change its orientation

b) the energy required to break any *inter-* and *intra*-polyurethane chain interactions (such as hydrogen bonding involving the O and N atoms) that would inhibit the required polyurethane conformation changes,

c) the steric limitations imposed by surrounding portions of the polyurethane matrix on the extraction of bulky anions,

d) the separation from other cationic sites, and hence the electrostatic repulsion that may be experienced at a particular site.

Thus the foam matrix is proposed to contain a distribution of sites of different energies. It is conceivable that some individual sites might be more suited for a particular postulated extraction mechanism. For instance, it is probable that potential sites that occur near relatively rigid portions of the foam matrix (for instance, near crosslinkages and near the diurethane-tolyl groups) may disfavour cation chelation. Therefore, whereas the chelation of cations by such sections may be energetically unfavourable, these sections may become readily protonated. In contrast, a podand-like chelation of cations might prevail in those sites which occur in highly flexible portions of the polyurethane foam. The inherent energy of a particular site may conceivably depend upon the mechanism by which a cationic site is to be created. Thus, for example, a potential site within a relatively rigid portion of the foam matrix may be expected to have a lower energy for protonation, but a high energy value might be associated with a cation chelation mechanism. Although the present model does not emphasize a helical conformation, it is likely that a

helical conformation may occur in certain sections of the polyether chains, resulting in stable polyether-cation interactions. Since rhodium is extracted in the present system as a triply charged anion (mainly as $[RhH(SnCl_3)_5]^{3-}$ and $[Rh(SnCl_3)_3Cl_3]^{3-}$), each complex requires the creation of three cationic sites. It seems plausible that a complex may be associated with three cationic sites of differing energies that were created *via* different mechanisms.

Before concluding this work, it should be mentioned that although the study of the model urethane compounds contributed significantly towards a better insight into the extraction of rhodium by polyurethane foam, there are (inevitably) short-comings to the model. The heterogeneous nature of the crosslinked polyurethane matrix, incorporating a variety of nitrogen containing linkages, could not be duplicated by the model compounds. This short-coming was evident in the different extraction behaviour of these model urethane compounds and polyurethane foam in the presence of alkali metal cations. In addition, the ^{119}Sn nmr study was performed on acetone solutions of Diϕ400U. It is not known to what extent the presence of acetone might influence the nature of the rhodium-tin complexes present in these extracts. However, the parallel in the colours of the Diϕ400U extracts and polyurethane foam, lends support to the results of the speciation study. In this regard, it is of interest to note that the polarity of the polyurethanes has been found to be similar to that of acetone [see pg. 15].

To finally summarize the results of this work, we may conclude that the extraction of trichlorostannato complexes of rhodium must be considered to be the result of the creation of cationic sites within the foam matrix *via* several plausible mechanisms. The chelation of cations by the polyether sections, and the protonation of the oxygen donor groups are thought to predominate. Several rhodium-tin species , but mainly $[RhH(SnCl_3)_5]^{3-}$ and $[Rh(SnCl_3)_3Cl_3]^{3-}$, are extracted, depending on the aqueous phase composition.

REFERENCES

1 L.JONES, I.NEL AND K.R.KOCH,
Anal. Chim. Acta, **182** (1986) 61

2 S.IWASAKI, T.NAGAI, E.MIKI, K.MIZUMACHI AND T.ISHIMORI,
Bull. Chem. Soc. (Jpn.), **57** (1984) 386

3 T.KIMURA,
Sci. Papers I.P.C.R., **73** (1979) 31

4 K.R.KOCH AND I.NEL,
Analyst, **110** (1985) 217

5 R.F.HAMON, A.S.KHAN AND A.CHOW,
Talanta, **29** (1982) 313

6 W.L.MATTICE,
Macromolecules, **12** (1979) 944

CHAPTER 7

EXPERIMENTAL

1. Physical Methods

1.1 Atomic Absorption Spectroscopy (AAS)

The Varian Techtron 70 and the Perkin Elmer 5000 were used for the analysis of rhodium, tin and potassium. An air-acetylene flame was used throughout.

1.1(i) Determination of Rhodium

The rhodium absorbance was measured at 343.5 nm, which is the most sensitive resonance line with the lowest background noise. Maximum sensitivity was obtained by using strongly oxidizing air-acetylene mixtures (lean, blue flames). The spectrophotometer settings used for rhodium are given in Table 7.1.

Table 7.1 The spectrophotometer settings used during the analysis of rhodium.

	Perkin Elmer	Varian Techtron
Lamp current (mA)	5	5
Slit width (nm)	0.2	0.5
Wavelength (nm)	343.5	343.5

The presence of tin in aqueous acid solutions of rhodium was found to cause a depression of the rhodium absorbance signal [1]. Studies by Wyrley-Birch [1] showed that this interference of tin could be adequately suppressed by the presence of 0.2% lanthanum nitrate as a releasing agent. Hence, stock solutions of 20 000 $\mu g.ml^{-1}$ $La(NO_3)_3.6H_2O$ were made up in 1 M HCl, and were diluted 10 times on addition to the standards and samples to give a final La^{3+} concentration of 0.2%.

An increase in the hydrochloric acid concentration was found to decrease the absorbance of rhodium due to changes in the physical properties of the solutions, which affects the efficiency of transport and atomization of the analyte into the flame [1]. These effects result from lower sample flow rates, changes in solution density and viscosity, and different droplet size in the flame when working with concentrated acid solutions. Therefore, all samples and standards were diluted to volume (1-5 dilutions for Chapter 2, 1-10 dilutions for Chapter 4) with 1 M hydrochloric acid, and the acid concentrations of the samples and standards were matched at all times.

Further, the absorbance of rhodium is affected by dissolved organic solvents, which are known to enhance the sensitivity of the determination of the noble metals by AAS [2,3,4]. In addition, the presence of the easily ionizable alkali metal salts also enhance the absorbance of rhodium. The latter effect was verified by comparing the absorbance values of 15 $\mu g.ml^{-1}$ rhodium solutions in the absence of K^+ and in the presence of 18639 $\mu g.ml^{-1}$ K^+(the concentration that would result from a 1-10 dilution of a 2.5 M KCl solution). The results are shown in Table 7.2. These considerations emphasize the importance of carefully preparing matched matrix standards. Therefore, the standards and samples were subjected to identical procedures throughout (for example in chapter 4, the standards were shaken with chloroform to ensure similar levels of dissolved chloroform in the samples and standards).

Table 7.2 The effect of 18639 $\mu g.ml^{-1}$ K^+ on the absorbance signal of 15 $\mu g.ml^{-1}$ rhodium.

rhodium (343.5 nm)			
no K^+	0.421	0.424	0.425
18639 $\mu g.ml^{-1}$ K^+	0.563	0.557	0.561

Since deviations from linearity of the calibration curves often occur in AAS, empirical curves must be prepared [5]. Hence, calibration curves were constructed from a minimum of 5 standards throughout this work. Typical calibration curves are shown in figure 7.1.

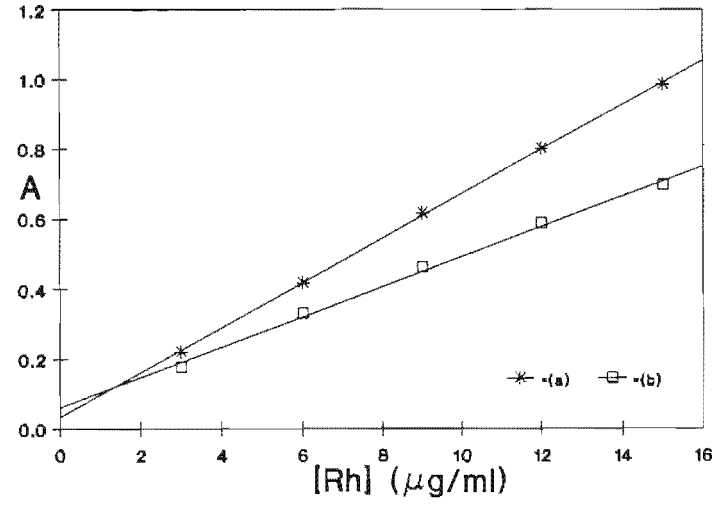

FIGURE 7.1 Rhodium calibration curves with 0.2% $La(NO_3)_3$ in (a) 1M HCl containing Sn and Rh in ratios of 15:1 after a polyurethane foam extraction experiment, and (b) in 1M HCl containing 1491 $\mu g.ml^{-1}$ K^+ and Sn and Rh in ratios of 10:1 after a model urethane extraction experiment.

1.1(ii) Determination of Tin

For the determination of tin in hydrochloric acid solutions, a strongly reducing (rich, yellow) air-acetylene flame was used. The tin absorbance measurements were made at 286.3 nm and at 224.6 nm. The former wavelength has the advantage of a more extensively linear calibration range, while the latter signal offers a greater sensitivity. No rhodium line occurs in the immediate spectral vicinity of the tin resonance at 224.6 nm [6] and it was shown by Wyrley-Birch that rhodium does not interfere with the determination of tin in aqueous acid solution using the signal at 286.3 nm [1]. However, increasing hydrochloric acid concentrations were found to

decrease the absorbance signal of tin. Similarly, the effect of alkali metals and dissolved organic solvents may also be expected to influence the tin absorbance signal. Therefore, care was taken to prepare matched matrix standards for the determination of tin. Typical calibration curves are shown in Figure 7.2. The spectrophotometer settings used for the analysis of tin are shown in Table 7.3.

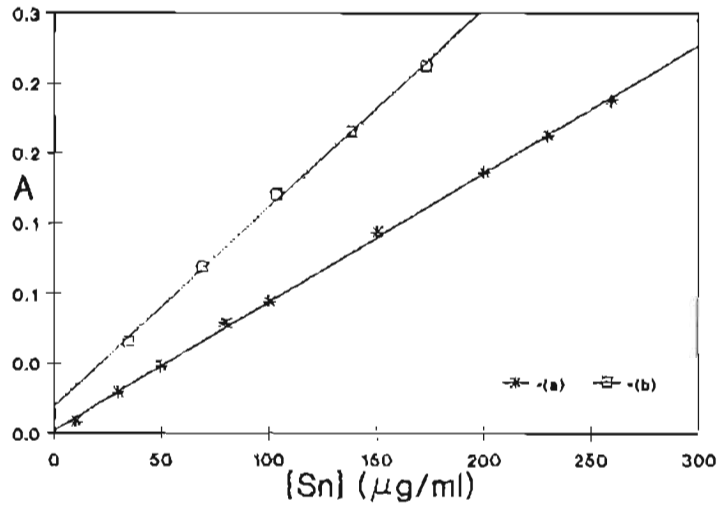

FIGURE 7.2 Tin calibration curves in the presence of 0.2% $La(NO_3)_3$ in (a) 1 M HCl containing Sn and Rh in a ratio of 15:1 after a polyurethane foam extraction experiment (286.3 nm), and (b) in 1 M HCl containing 1491 $\mu g.ml^{-1}$ K^+ after a model urethane extraction experiment (224.6 nm).

Table 7.3 The spectrophotometer settings used during the analysis of tin.

	Perkin Elmer	Varian Techtron
Lamp current (mA)	5	5
Slit width (nm)	0.7	0.2(0.5)*
Wavelength (nm)	286.3	286.3(224.6)†

*A larger slit width than recommended was used due to ageing of the photomultiplier.

† Alternate wavelengths were used, see text.

1.1(iii) Determination of Potassium

The amount of potassium coextracted with the trichlorostannato complexes of rhodium by polyurethane foam, was determined after nitric acid decomposition of the foam matrix. In order to prepare matched matrix standards, equal mass portions of clean polyurethane foam were similarly decomposed and spiked with 1000 $\mu g.ml^{-1}$ potassium nitrate solution (SpectrosoL, BDH Ltd.) to yield a range of potassium concentrations. The sample and standards received identical treatment. A preliminary experiment established relatively high levels of potassium to be present. Therefore, the less sensitive line at 404.4 nm was chosen for the potassium analysis. A 2 nm slit width and an oxidizing (lean, blue) air-acetylene flame was used. The calibration curve is shown in Figure 7.3.

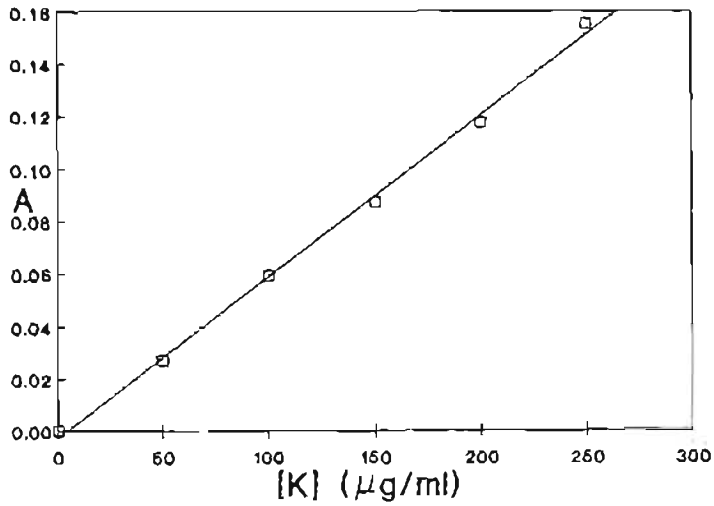

FIGURE 7.3 Calibration curve for the determination of potassium in acid-decomposed foam samples.

1.2 Elemental Analysis

Microanalyses were performed by Mr. W.R.T. Hemsted and Mr. P. Benincasa on a Heraeus Universal Combustion Analyzer model CHN-MIKRO.

1.3 Gel Permeation Chromatography

The molecular weights of the linear polyurethanes were determined by gel permeation chromatography. A detailed description of the experimental procedure is given in Section 2.2(iii) of this Chapter.

1.4 Infrared Spectra

The infrared spectra (2000 - 1100 cm^{-1}) of the Aliquat 336 extracts were recorded on a Perkin Elmer 983 spectrophotometer using fixed pathlength potassium bromide solution cells and nitrogen saturated chloroform as solvent. The quoted wavenumber accuracy of the spectrophotometer is ± 1 cm^{-1} for the 2000 - 1800 cm^{-1} region. The reproducibility is better than 0.1 cm^{-1}.

1.5 Nuclear Magnetic Resonance Spectroscopy

The ^{1}H, ^{13}C, ^{7}Li and ^{119}Sn nmr spectra were recorded on a Varian VXR-200 Fourier transform spectrometer operating at 200.0, 50.3, 74.6 and 77.7 MHz, respectively. The ^{1}H and ^{13}C chemical shifts (δ values) were measured relative to the internal solvent resonance ($CDCl_3$) and are reported in parts per million downfield from tetramethylsilane (TMS) using the following conversion factors.

^{1}H spectra $\quad \delta(TMS) = \delta(CDCl_3) - 7.27$

^{13}C spectra $\quad \delta(TMS) = \delta(CDCl_3) - 77.00$

The ^{7}Li chemical shifts were measured relative to $LiNO_3$ (SpectrosoL, BDH Ltd., diluted to approximately 500 $\mu g.ml^{-1}$) as an external standard, while the ^{119}Sn chemical shifts are given relative to tetramethyltin, also as an external standard (in a

capillary using D_2O for locking purposes). Negative signs are used for low frequency and positive signs for high frequency shifts. Unless otherwise specified, the nmr spectra were recorded at room temperature (ambient = 298K). Appropriate delay times were chosen on the basis of preliminary T_1 measurements of the various nuclei in representative samples. The number of transients depended on the concentration of the various nuclei in the samples (for the ^{119}Sn nmr spectra the number of transients ranged from 6000 to 60000).

1.6 UV-Visible Spectrophotometry

The electronic spectra were recorded on a Varian Superscan 3 ultraviolet and visible spectrophotometer in the absorbance mode using 10 mm and 1 mm quartz cells.

2. Specific Experimental Procedures

All chemicals and reagents used for experimental work were analytically pure. $RhCl_3.3H_2O$ was supplied by Aldrich Chemical Company, while $La(NO_3)_3.6H_2O$ was obtained from BDH Chemicals.

KIO_3 was dried at 100 °C for one hour and stored in a desiccator. KCl, NaCl and LiCl were dried under vacuum (0.1 mm Hg) for 16 hours prior to use.

High purity nitrogen was freed from residual oxygen by passing the gas through a chromous chloride solution [7] and distilled water before use. In cases where dry nitrogen was required, the gas was passed through concentrated sulphuric acid and then over KOH pellets. Hydrochloric acid was deoxygenated by passing nitrogen through it for 30 - 45 minutes. The concentration of the nitrogen saturated

hydrochloric acid was accurately determined directly before use by standardizing with sodium tetraborate.

A mixture of A and B grade glassware was used. Weighings were performed on a Mettler four decimal balance. The larger masses required for the polyurethane synthesis were weighed on Mettler 3 and 2 decimal balances.

2.1 Procedures Employed within Chapter 2

Double distilled water, initially boiled for 30 - 45 minutes to remove the dissolved oxygen, was cooled and saturated with nitrogen and was stored in a glass aspirator fitted with an argon inlet. This water was used for the preparation of all aqueous solutions.

Sheets of polyether polyurethane foam were obtained from Flexaire Foams, South Africa. These sheets were first cut into cubes (~1 cm^3), washed with Tepol detergent and then thoroughly rinsed. The cubes were subsequently soaked in 0.5 M hydrochloric acid for 72 hours, followed by thorough rinsing with deionized water until the rinsing water was neutral to pH indicator paper. Finally the foam cubes were allowed to stand in acetone overnight and then dried in an oven at 50 ^{o}C. A similar cleaning procedure was recommended by Al-Bazi *et al.* [8]. To prevent discolouration due to UV-radiation, the foams were stored in the dark.

The apparatus used to conduct the polyurethane foam extraction experiments had to fulfill certain requirements. Firstly, sufficient agitation of the solution was needed to ensure that the foam was continuously brought into contact with fresh solution. Secondly, the ease with which Sn(II) is oxidized to Sn(IV) demands that the

solutions be purged with nitrogen and the experiment be conducted under nitrogen. As discussed in Chapter 2, Section 1. a number of different reaction vessels were used. Diagrammatic representations of apparatus A, apparatus B and apparatus C are shown in Figures 7.4 - 7.6.

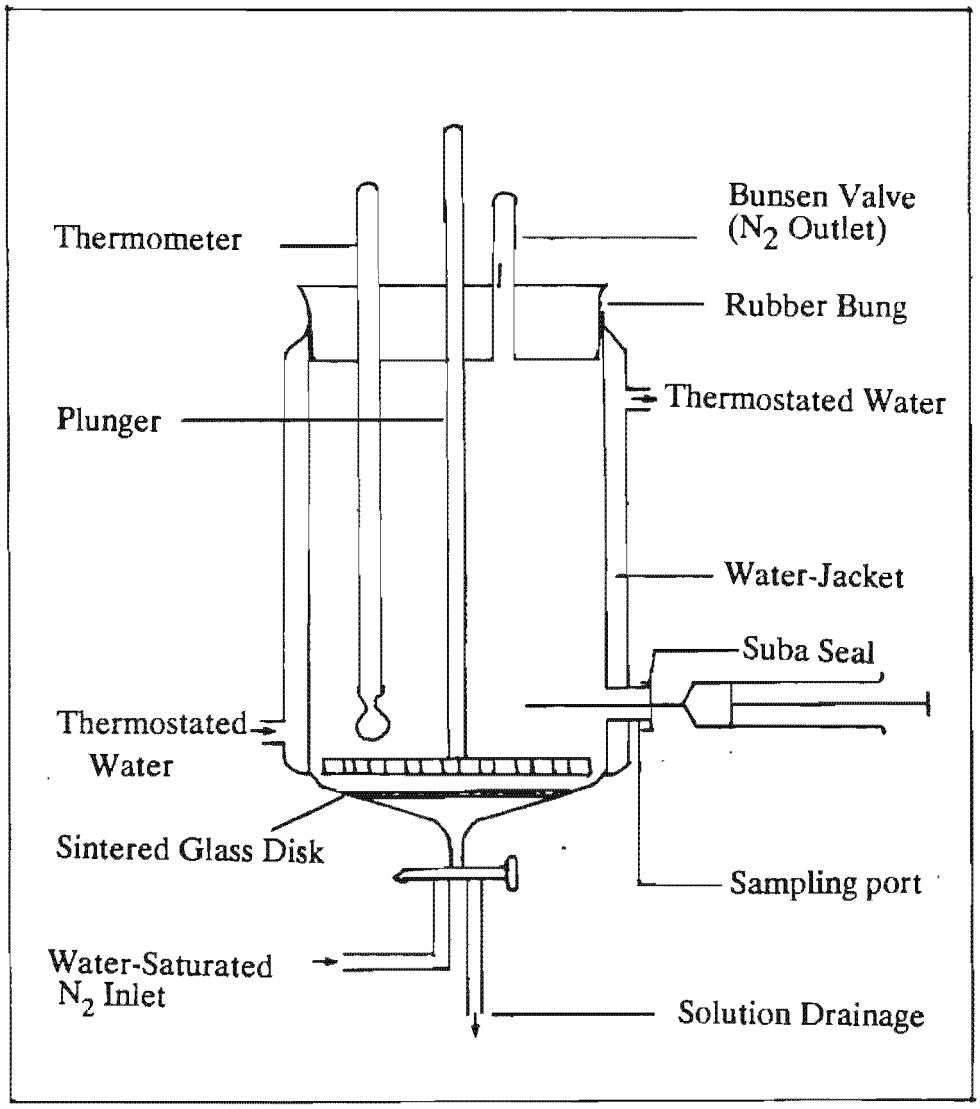

Figure 7.4 Diagrammatic representation of Apparatus A.

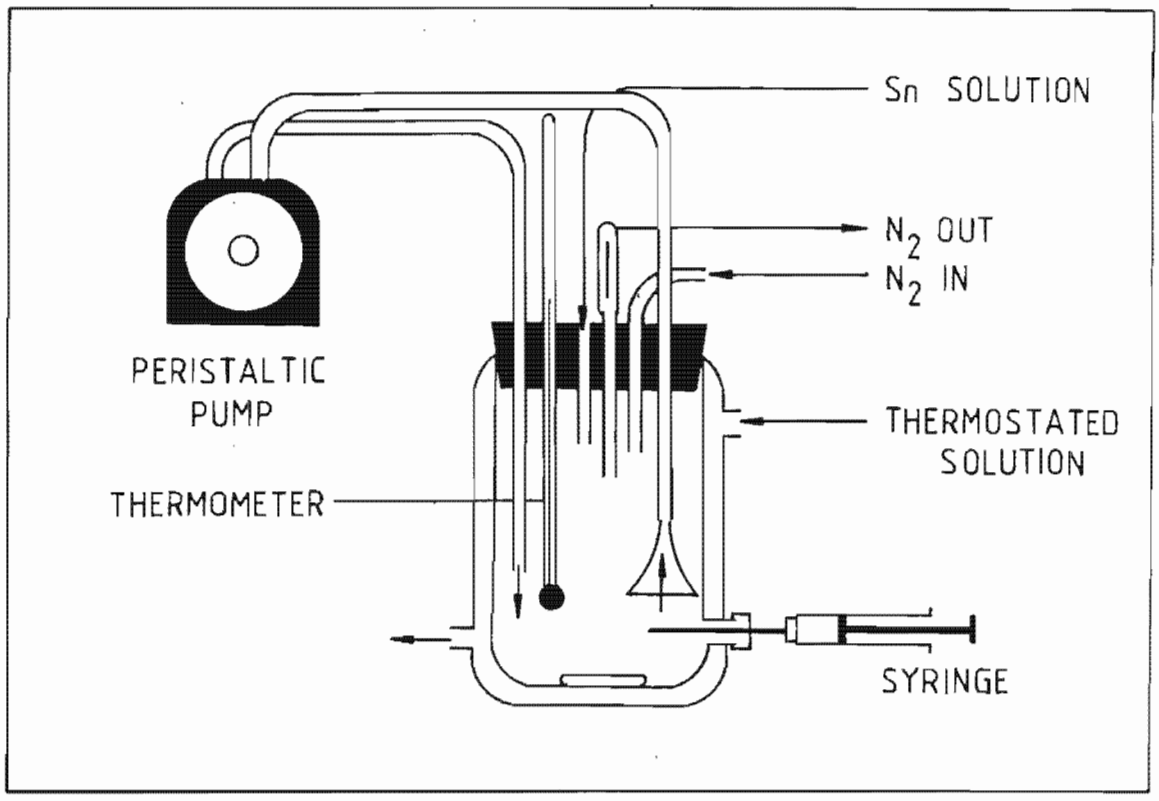

Figure 7.5 Diagrammatic representation of Apparatus B.

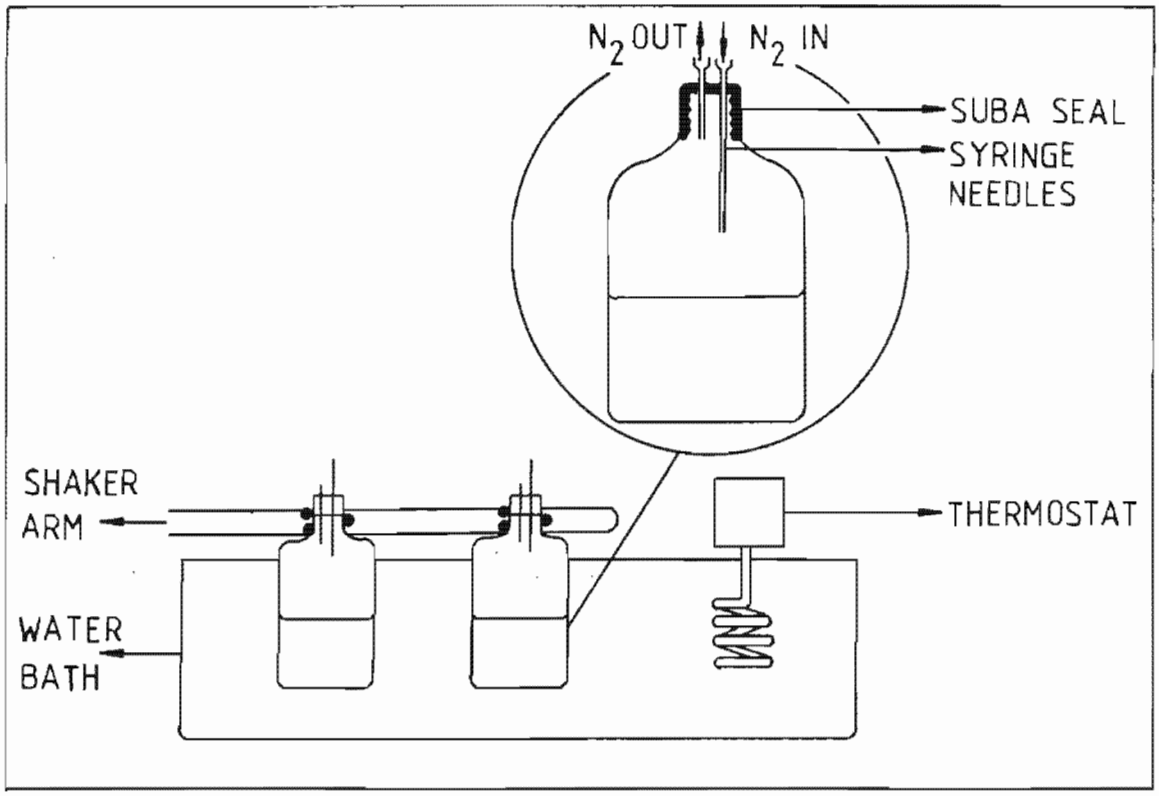

Figure 7.6 Diagrammatic representation of Apparatus C.

All rhodium and tin solutions were prepared in nitrogen flushed containers using deoxygenated solvents. The rhodium solution was added to the reaction vessel and again purged with nitrogen for 15 minutes. Then the calculated volume of tin(II) solution of known concentration was added to produce the required Sn:Rh ratio. The exact concentration of divalent tin in the tin solution was determined by iodometric titration, using a few ml of an immiscible solvent (carbon tetrachloride) to detect the disappearance of the last trace of iodine [7]. After the addition of tin(II), the solution was allowed to equilibrate at the set temperature for the desired equilibration time before the addition of polyurethane foam. Before the addition of the foam an accurately measured aliquot (precision Hamilton syringe) of 1 ml of the aqueous rhodium-tin solution was withdrawn to act as the blank. Further 1 ml aliquots were periodically withdrawn after foam addition in order to monitor the extraction of rhodium with time. After atomic absorption analysis of the blank and samples, the amount of rhodium and tin extracted at the various intervals was calculated by difference. The calculations took into account the amount of rhodium extracted during sampling and the respective D'_m and %E values were corrected for the amount of rhodium and tin that had been "lost" at the time of sampling.

For the direct analysis of the foam phase, the polyurethane foam was decomposed in a Kjeldahl apparatus. The foam pieces were boiled in 6-7 ml of concentrated nitric acid, during which time the foam material broke down and dissolved. The volume of this solution was reduced to near dryness. Then approximately 5 ml of hydrochloric acid was added and boiled to further reduce the volume. This solution was quantitatively transferred to volumetric flasks and made to volume as required.

2.2 Procedures Employed within Chapter 3

2.2(i) Synthesis of Model Urethane Compounds

Triethylene glycol, tetraethylene glycol, PEG400, PEG1500, PEG6000 and phenyl isocyanate (>98% purity) were supplied by BDH laboratory chemicals division. The glycols were dried by overnight evacuation at 0.5 mm Hg. An 80:20 isomer ratio of 2,4- and 2,6-toluene diisocyanate (TDI) was kindly donated by Flexair Foams, Cape Town and by Dow Chemical Company, Johannesburg. The TDI was decanted into smaller bottles (~100 ml capacity) under dry nitrogen in a glove box to protect the bulk of the chemical from atmospheric water. Dichloromethane was purified by a standard washing and distilling procedure [9], and was stored over 4Å molecular sieve. Prior to use all glassware was dried by flaming and then cooled under an atmosphere of nitrogen. All reactions were performed under an atmosphere of dry nitrogen. The melting-temperatures of the urethane compounds were determined on a Reichert Thermovar hot-stage microscope and are uncorrected.

(a) Diurethane Podands

Excess glycol was used for the synthesis of the podands to ensure quantitative reaction of the phenyl isocyanate, since the excess glycol could easily be removed from the water immiscible podands by washing the product with water. Phenyl isocyanate of known mass (~30 g) was dissolved in dichloromethane (~30 ml) in a three-necked round bottom flask. A dichloromethane solution (~70 ml of dichloromethane) of the required glycol (~5% in excess) was slowly added dropwise into the phenyl isocyanate solution from a fitted pressure equalized separating funnel. The reaction mixture was vigorously stirred for approximately 20 hours,

using a magnetic bar stirrer. Finally, the product was washed several times with water, and dried under vacuum at 80 °C, aliquots of ethanol being periodically added to enhance removal of water as an azeotrope.

(b) Soluble Linear Polyurethanes

The glycol of known mass (~50 g) was dissolved in dichloromethane (~50 ml) in a round bottom flask. A dichloromethane solution of TDI of the desired mass was quantitatively transferred to a pressure equalized separating funnel. The TDI solution was then allowed to drip slowly into the glycol solution while stirring vigorously. The reaction mixture was stirred continuously for approximately 20 hours, after which the product was washed with water and dried at 80 °C under vacuum.

2.2(ii) Preparation of Polyurethane Foam

Polyols containing 100% poly(propylene oxide), as well as 20% poly(propylene oxide) + 80% poly(ethylene oxide), were donated by Dow Chemical Company, Johannesburg. TDI, a silicone surfactant and 2 catalysts (a tertiary amine and stannous octoate) were donated by Flexaire Foams, Cape Town. Precautions were taken to protect TDI from moisture as described in Section 2.2(i). The TDI was standardized directly prior to use by the method recommended by the American National Standards Institute [10].

The apparatus used for foam formation was as follows:

a) a full-face gas mask attached to an air-cylinder (sensitization towards isocyanate had occurred),

b) an overhead stirrer located within a fume cupboard,

c) 500 ml paper cups,

d) conventional bread tins lined with wax paper, into which the rising foam mixture was poured,

e) an oven at 70 °C for curing of foams,

f) a soxhlet extractor for cleaning of the foam before extraction experiments were performed.

(a) Definition of Terms and Example Calculations.

The reactions responsible for polyurethane foam formation are described in Chapter 1, Section 2. The relevant definitions of terms and calculations used, are described below [11].

Functionality: The number of chemically active atoms or groups per molecule for the considered reactions. This is an average value for polymers.

Equivalent weight: The weight of compound or polymer per active group for a specific reaction. This is an average value for polymers.

$$E = \bar{M}_n / f \qquad (1)$$

where E = equivalent weight

$\bar{M}_n$ = number average molecular weight

f = functionality

$$\text{Total Equivalents} = \frac{\text{Total Sample Weight}}{\text{Equivalent Weight}} \qquad (2)$$

For polyols or OH-terminated prepolymers

$$E = \frac{56.1 \times 1000}{\text{OH No.}} \qquad \text{OH No. = hydroxyl number} \qquad (3)$$

$$\bar{M}_n = \frac{56.1 \times 1000 \times f}{\text{OH No.}} \qquad f = \text{functionality} \qquad (4)$$

Hydroxyl number: The number of milligrams of KOH equivalent to the active functions (hydroxyl content) of 1 g of the compound or polymer.

$$\text{Isocyanate Index} = \frac{\text{NCO equivalents}}{\text{OH equivalents}} \times 100 \qquad (5)$$

An example calculation of the required mass of TDI for a given mass of polyol, is given below. Consider the following formulation:

	Parts by weight
Polyol (with OH No. = 47.5)	100
tertiary amine catalyst	0.7
stannous octoate catalyst	0.66
silicone surfactant	1.1
water	4.55
TDI	?

First, the total hydroxyl equivalents are calculated.

$$\text{For the Polyol: } E = \frac{56.1 \times 1000}{\text{OH No.}} = \frac{56100}{47.5} = 1181.05$$

Total equivalents from equation (2) = $\frac{100}{1181.05}$ = 0.0847 for the polyol

For water: $E = \frac{M_n}{f} = \frac{18}{2} = 9.0$

Total equivalents = $\frac{4.55}{9.0}$ = 0.506 for water

In this formulation the polyol and water are the only hydroxyl contributors. Therefore, the total hydroxyl equivalents = 0.0847 + 0.506 = 0.5907

For an isocyanate index of 100, 0.5907 equivalents of isocyanate are required (see equation 5).

The equivalent weight of TDI is calculated from,

$$E = \frac{M_n}{f} = \frac{174}{2} = 87$$

The mass of TDI required for 0.5907 equivalents of isocyanate can be calculated from equation 2.

$$\text{Hence } 0.5907 = \frac{\text{total sample weight}}{87}$$

Therefore, the total mass of TDI required for an Index 100 foam, is 51.39 g.

Index 90 would require 0.9 x 51.39 = 46.25 g TDI.

Index 120 would require 1.2 x 51.39 = 61.67 g TDI.

The polyols obtained from Dow Chemical Company were trigols and had the following specifications (brand names have been omitted as requested by the chemical company).

Polyether content	M	OH No.
100% poly(propylene oxide)	3000	56
20% poly(propylene oxide) + 80% poly(ethylene oxide)	4800	36

M = molecular weight

(b) Procedure Followed

Polyurethane foams of index 90 and 120 were prepared from 100% poly(propylene oxide) polyol by the following procedure. A stock was prepared by mixing the polyol, stannous-octoate, the tertiary amine catalyst and the silicone surfactant in the desired ratios. The correct mass of the stock was weighed into a paper cup. The desired volume of water was then added. After approximately 4 seconds stirring, the calculated mass of TDI was added followed by approximately 7 seconds of stirring. At this stage the reaction mixture was already rising due to gas evolution. The rising mixture was poured into the bread tins lined with wax paper. When the foam had risen, the bubbles/cells became dodecehedral in shape, with most of the polymer in the struts that support the foam and very little in the thin membranes that make up the cell walls. At the full rise time, the cell walls are unable to contain the gas pressure. They rupture, and the polymer contracts into the struts to form an open cell polyurethane foam. The completely risen foam was cured at 70 °C for

approximately two hours. Higher temperatures were not used since allophanate and biuret linkages break down at temperatures higher than 110 °C.

In order to check the mixing efficiency of the overhead stirrer, a small quantity of red dye was added to the paper cup prior to the addition of 100 g of polyol. The colour was homogeneously dispersed within seconds of stirring.

The relative amounts of stannous octoate, tertiary amine, silicone surfactant and water had to optimized. Stannous octoate catalyses the isocyanate-hydroxyl reaction and therefore controls polymerization. The tertiary amine catalyst catalyses the isocyanate-water reaction. Hence, it is responsible for the blowing reaction and, to a certain extent, polymerization. The silicone surfactant assists in nucleation (bubble formation) by lowering the surface tension of the polymer mixture. It also induces film elasticity (stabilizes the foam during its rise) and prevents coalescence or collapse of the cells. The gas evolution and the polymer growth must be matched so that the gas is trapped efficiently and the polymer has sufficient strength at the end of the gas evolution to maintain its volume without collapse or gross shrinkage. A correct balance of catalysts is also needed to ensure rupture of the cell walls to produce open-cell flexible foams. The amount of water must be adjusted to suit the foam formation, since too many gas bubbles may weaken the cells. The isocyanate index should be limited to the range 90 - 120 to prevent collapse and ensure an open cell polyurethane foam [12].

The following foam formulation was found to be adequate:

	Parts by weight
100% poly(propylene oxide) polyol	100
tertiary amine	0.25
silicone surfactant	0.30
stannous octoate	0.22
water	3.5

For index 90 and 120, the masses of TDI required were 38.280 and 51.040 parts by weight, respectively.

Regrettably, all attempts at obtaining a stable polyurethane foam from the 80% poly(ethylene oxide) + 20% poly(propylene oxide) polyol were unsuccessful. A suitable formulation was not found for which the total collapse of the foam did not occur.

The foams were cut into cubes of approximately 1 cm^3. Thereafter,the cubes were soaked in 1 M HCl for 24 hours, rinsed with distilled water until the latter was neutral to pH-paper, and soxhlet extracted with ethanol for 12 hours. The cubes were air dried at approximately 50 ^{o}C and stored in the dark.

2.2(iii) Gel Permeation Chromatography (GPC)

Two styra-gel columns of 500 Å and 10^4 Å were used in series on a Waters Liquid Chromatograph with the facility to switch into GPC mode. A differential refractometer model R401 was chosen as the detector, since the chromatogram

obtained from the refractometer appeared to reveal more information than that obtained from the UV-visible spectrophotometric detector. See Figure 7.7.

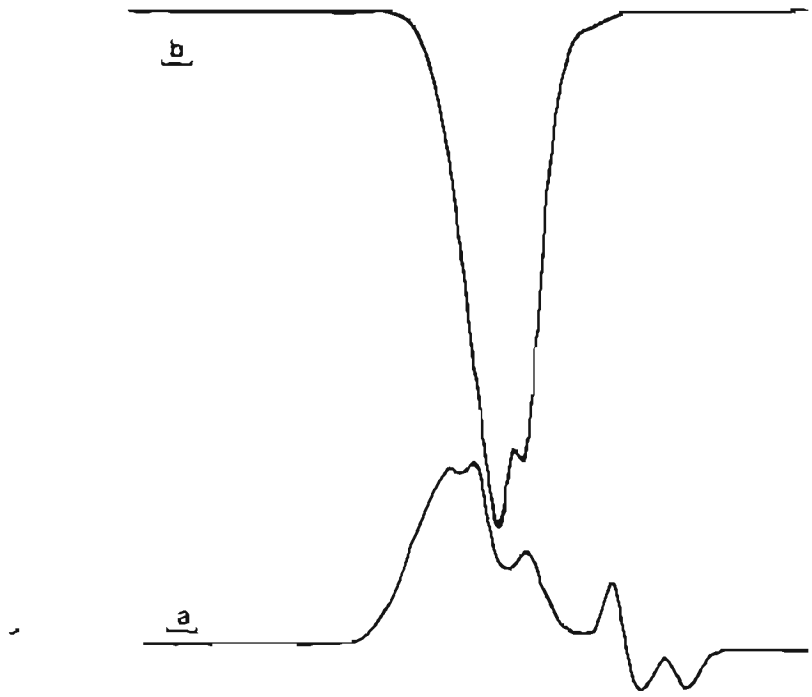

Figure 7.7 Comparison of the chromatograms obtained by the refractometer (a), and by the UV-visible spectrophotometer (b).

For calibration, polystyrene standards from Polymer Laboratories (Ltd.) were used. Samples and standards were dissolved and eluted with HPLC-grade tetrahydrofuran from millipore. Twenty microlitre aliquots of 2% (m/v) solutions of the samples and standards were injected into the liquid chromatograph using a Hamilton syringe.

The retention times and molecular masses of the standards were loaded into the data module to establish a calibration curve. The molecular mass information given by Polymer Laboratories (Ltd.) for each standard is listed in Table 7.4. Preliminary

liquid chromatographs of the sample polymer solutions were used to aid in the choice of standards. The standards with the highest and lowest retention times should encompass the samples with retention times at the extremes of the calibration curve.

Table 7.4 Molecular mass data supplied by Polymer Laboratories (Ltd.)

$\bar{M}_n$	$\bar{M}_w$	$\bar{M}_v$	M_{peak}	$\bar{M}_w/\bar{M}_n$
1350				< 1.18
1830				< 1.15
3300				< 1.11
9500				< 1.06
19165	19850		19750	
51150		47400	50000	

After the molecular masses and retention times of the standards had been entered into the microprocessor, the data module calculated a least squares fit to a third order polynomial. To describe the curve, the coefficients D_0 to D_3 for the following equation are calculated:

$$M = D_0 + D_1R_t + D_2(R_t)^2 + D_3(R_t)^3 \qquad (6)$$

The instruction manual [13] describes the calibration procedure as follows: "In order to calculate molecular weight averages, the polymer peak is cut into slices. Each slice has a retention time and an area. The retention time is used to determine the average molecular weight eluting during the slice. The average molecular weight for each slice is determined using the calibration curve. The area of each slice is directly related to the weight of a particular molecular weight fraction in the whole

polymer. The areas are determined by drawing a baseline from the beginning of the polymer peak to the ending baseline level. The area and the average molecular weight of each slice is used to calculate the molecular weight averages $\bar{M}_n$, $\bar{M}_w$ and $\bar{M}_z$. The formulae used are:

$$\bar{M}_n = \frac{\Sigma(\text{area}_i)}{\Sigma(\text{area}_i)/M_i} \qquad (7)$$

$$\bar{M}_w = \frac{\Sigma(\text{area}_i M_i)}{\Sigma(\text{area}_i)} \qquad (8)$$

$$\bar{M}_z = \frac{\Sigma(\text{area}_i M_i)^2}{\Sigma(\text{area}_i / M_i)} \qquad (9)$$

where area_i = the area of the i^{th} slice

M_i = the average molecular weight of the i^{th} slice."

We shall concern ourselves only with $\bar{M}_n$ and $\bar{M}_w$.

The calibration table which allowed the estimation of the molecular weight of the linear polyurethanes is represented in Table 7.5.

Table 7.5 Calibration table established from polystyrene standards.

Molecular weight	1350	1830	3300	9500	19750	50000
logM	3.130	3.262	3.519	3.978	4.296	4.699
Retention times (R_t)	18.52	18.21	17.70	16.28	15.49	14.22

The coefficients D_0 to D_3 for the polynomial describing the calibration curve, were as follows:

$$D_0 = 0.231922 \times 10^{2}$$
$$D_1 = -0.306166 \times 10^{1}$$
$$D_2 = 0.180132$$
$$D_3 = -0.395786 \times 10^{-2}$$

The standard error of estimate was given as 0.660545×10^{-1}, and the correlation coefficient was given as 0.994460.

Universal calibration was achieved with the aid of K_θ constants obtained from the literature [14-16]. For each K_θ value, the intrinsic viscosity of each polystyrene standard was calculated from the relationship $[\eta]_\theta = K_\theta \bar{M}^{1/2}$, and a calibration curve of $\log[\eta]M$ versus retention time (R_t) was constructed. From the calibration curve, the R_t of each slice of the polyurethane chromatograph yielded $\log[\eta]M$, by linear regression. Since the $[\eta]$ of the linear polyurethanes had been predetermined, M was easily calculated. $\bar{M}_n$ and $\bar{M}_w$ were calculated from equations 7 and 8 as described by the HPLC instruction manual. The raw data are shown in Appendix 1.

2.2(iv) Intrinsic Viscosity Measurements

An Ubbelohde glass viscometer suspended in a water bath at 23 ± 0.05 °C was used to measure the intrinsic viscosities of the 4 selected polyurethanes. The viscometer was thoroughly cleaned and dried with a stream of filtered dry nitrogen before use. The polymers were dissolved in high quality (Univar) tetrahydrofuran (THF), to give 10 ml of an approximately 10% (m/v) stock solution (the concentration was

accurately known). All solutions and solvents were filtered through a glass fibre filter attachment fitted to a Hamilton syringe before being transferred to the viscometer. After the efflux time of THF had been measured to give t_o, and the viscometer dried as described, the polymer stock solution was filtered and transferred to the viscometer. An accurately known volume of THF was then added, rinsing down any polymer that may have remained on the side of the large tube, to give a minimum volume of 25 ml. Efficient mixing was obtained by passing nitrogen through the solution in the viscometer for a few seconds, causing bubbles which sufficiently agitated the solution. After each dilution, 20 - 30 minutes were allowed for temperature equilibration before measuring the next set of efflux times. All the tubes of the viscometer were stoppered during this equilibration interval to minimize evaporation. Each efflux time was the mean of at least five measurements.

The viscosities of solution (η) and solvent (η_o) are related to the corresponding efflux times by

$$\eta = Ctd - Ed/t^2 \qquad (10)$$

$$\eta_o = Ct_od_o - Ed_o/t_o^2 \qquad (11)$$

t = efflux time of the polymer solution $\quad$ t_o = efflux time of the solvent

d = density of the polymer solution $\quad$ d_o = density of the solvent

C and E are constants for the particular viscometer used. For dilute solutions, d and d_o are substantially equal [17], and for efflux times of around 100 seconds, the second terms are negligible. Therefore, the relative viscosity (η_r) can be calculated from

$$\eta_r = \eta/\eta_o \approx t/t_o \qquad (12)$$

The intrinsic viscosity, $[\eta]$, can be calculated from

$$[\eta] = \lim_{c \to 0}(\ln\eta_r)/c = \lim_{c \to 0} \eta_{sp}/c \qquad (13)$$

where η_{sp} is the specific viscosity,

c is the concentration in $g.dl^{-1}$, and

the quantities $(\ln\eta_r)/c$ and η_{sp}/c are the inherent viscosity, η_{inh}, and the reduced viscosity, η_{red}, respectively.

The common names for the various viscosities are used to remain consistent with the polymer science literature. The recommended IUPAC names, although more logical, have been adopted to a lesser extent. The common and IUPAC names are listed in Table 7.6 [17].

Table 7.6 A list of common and IUPAC names for the various definitions of viscosity.

Common name	IUPAC name
relative viscosity	viscosity ratio
specific viscosity	-----
reduced viscosity	viscosity number
inherent viscosity	logarithmic viscosity number
intrinsic viscosity	limiting viscosity number

Hence, $(\ln\eta_r)/c$ and η_{sp}/c were plotted versus c to yield two nearly equal y-intercepts at c = 0. The mean of the two y-intercepts was taken as the intrinsic

viscosity. Note that efflux times larger than 97.5 seconds were obtained, allowing for the reasonable disregard of the second term in equations 1 and 2.

The viscosity of polymer solutions is dependant upon the shear rate within the viscometer [17,18] which can lead to significant error for values of $[\eta]$ above 2 - 3. Since we obtained values for intrinsic viscosity below $[\eta]$ = 2, we did not attempt to correct for the rate of shear.

As an example, the results and calculations for Pol400U(1:1) are presented below. The efflux times of Pol150U(1:2), Pol194U(1:2), and Pol400U(1:2) can be found in Appendix 2. Efflux times (seconds) at various concentrations ($g.dl^{-1}$) of Pol400U(1:1) are listed in the table below.

Table 7.7 Efflux times (t), mean efflux times ($\bar{t}$) and the coefficient of variation (COV) measured for THF solutions of Pol400U(1:1).

concentration ($g.dl^{-1}$)	Efflux times, t (s)						$\bar{t}$	COV (%)
0 (THF)	97.37	97.44	97.47	97.38	98.22	97.72	97.60	0.34
2.376	128.47	128.78	128.31	128.25	128.87		128.34	0.26
1.980	122.59	122.60	122.19	122.44	122.66		122.50	0.15
1.485	115.75	115.72	116.00	115.63	115.88		115.78	0.14
0.990	108.59	109.44	109.72	109.50	109.41	109.31	109.33	0.35
0.660	105.38	105.29	105.41	105.60	105.56		105.45	0.12
0.495	103.50	103.50	103.63	103.39	103.53		103.51	0.08

The inherent viscosities and reduced viscosities were calculated from the efflux times at the various concentrations, as follows:

$$\eta_{inh} = (\ln\eta_r)/c = \ln(t/t_o) \times 1/c \quad \text{in dl.g}^{-1} \qquad (14)$$

$$\eta_{red} = \eta_{sp}/c = t - t_o/t_o \times 1/c \quad \text{in dl.g}^{-1} \qquad (15)$$

The results are given in Table 7.8.

Table 7.8 η_{inh} and η_{red} calculated at various concentrations of Pol400U(1:1)

concentration ($g.dl^{-1}$)	η_{inh}	η_{red}
2.376	0.1152	0.1325
1.980	0.1147	0.1288
1.485	0.1150	0.1254
0.990	0.1146	0.1214
0.660	0.1172	0.1218
0.495	0.1188	0.1223

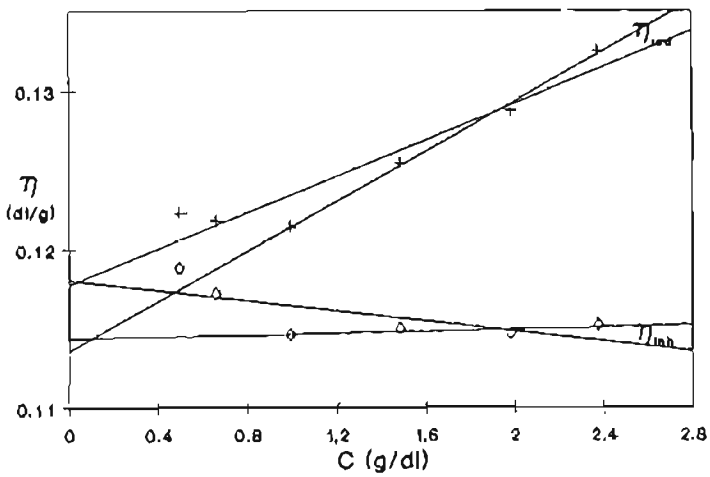

Figure 7.8 A plot of ln η_{inh} versus c and η_{red} versus c for Pol400U(1:1).

If only the four "best points" are considered, that is those at higher concentrations forming a straight line, the two y-intercepts are 0.1143 and 0.1135 for $(\ln\eta_r)/c$ and η_{sp}/c respectively. This would give an intrinsic viscosity of 0.1139 from the average value of the two y-intercepts. However, when all six measurements are considered

$(\ln\eta_r)/c$ and η_{sp}/c have y-intercepts of 0.1181 and 0.1178 respectively. Hence the intrinsic viscosity would have a value of 0.1180. We assumed this variation in $[\eta]$ to represent the error in our determinations. Hence we took $[\eta]$ = 0.1160 ± 0.0029, or 0.1160 ± 2.5 % $dl.g^{-1}$

2.2(v) ^1H nmr for the Determination of Molecular Weight

When recording the proton nmr of linear polyurethanes the presence of unreacted starting material would reflect EOP/MP ratios that are not representative of the degree of polymerization. Due to the high reactivity of the isocyanate group, it is reasonable to assume that the amount of unreacted toluene diisocyanate in the polymer mixture is negligible. Therefore, it is only necessary to separate unreacted glycol from the polymer mixture. The water solubility of ethylene oxide glycols rendered this an easy task. The polyurethane was dissolved in chloroform, shaken up with aliquots of distilled water in a separating funnel and the clear polymer containing chloroform layer was separated from the water layer. (Sometimes a third white emulsified layer formed between the chloroform and water, which would break up with time.) The water washing procedure was repeated three to four times before the chloroform solution was passed through a column of extrulet for drying. The chloroform was removed under rotor-vacuum, after which the polymer was dried under vacuum (~0.1 mm Hg) at ~80 °C for at least three hours. The ^1H nmr spectra of $CDCl_3$ solutions of the linear polyurethanes were recorded at 30 °C. After integration of the relevant resonances, the EOP/MP ratios were calculated. These ratios are given in Appendix 3.

2.3 Procedures Employed within Chapter 4

2.3(i) Procedure for Section 1.1 (i)

Portions of 0.120 ± 0.001g Pol400U(1:2) were dissolved in 1 ml of acetone (accurately measured with a Hamilton syringe). Aliquots of exactly 1 ml of acetone was also transferred to each of 5 test-tubes, which were prepared for the standards. Five millilitres of the aqueous phase was added to the test tubes containing Pol400U(1:2). In addition, aliquots of 5 ml of various dilutions (diluted with 2M KSCN) of the aqueous phase that was being used for the extraction were transferred to the standard test tubes, the most concentrated standard having the same cobalt concentration as the initial concentration of the sample aqueous phase. To ensure equal treatment of the sample and standards all the test tubes were shaken together, and then centrifuged for 30 minutes. After extraction the Pol400U(1:2) precipitated from solution as a gum, which had assumed the deep blue colour of the tetrahedral $[Co(NCS)_4]^{2-}$. The standards and the supernatant liquid of the sample were then diluted 5 times with a diluent comprising acetone and a 2M KSCN solution in a ratio that had been predetermined to give an on-scale absorbance value of less than one. Measurement of the absorbance values at 620 nm using quartz cells with a 1 mm path length, allowed for the calibration of the cobalt extracted, by difference. A typical calibration curve is shown in Figure 7.9.

The amount of acetone in the solution will affect the intensity of the blue colour at 620 nm. Since it is likely that the acetone in the sample test tube will distribute between the "precipitated" polymer and the aqueous phase, the assumption that the amount of acetone in the standards and the sample will still be equal after extraction would lead to inaccuracies in the absolute values of the cobalt that was extracted. However, since a five times dilution with an acetone-containing diluent

was carried out, the error should not be large (a proportion of the final acetone concentration should be contributed by the diluent). In addition, the error should be present in all the samples, and the observed trends should be valid. To prevent evaporation of the acetone during absorbance measurements, the cells were stoppered.

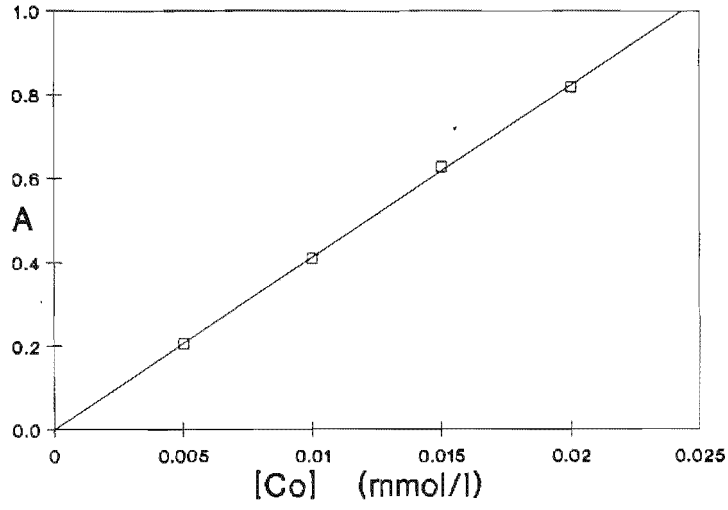

FIGURE 7.9 A typical calibration curve for the determination of cobalt in the supernatant liquid after extraction by Pol400U(1:2).

The absence of polymer in the aqueous phase was verified by evaporating the supernatant of the sample to dryness, and redissolving with water. No polymer (which is insoluble in water) was evident.

2.3(ii) Procedure for Section 1.1(ii)

Chloroform solutions of Diϕ400U with concentrations of 0.10, 0.07, 0.05, 0.03 and 0.01 $g.ml^{-1}$ were prepared from a stock solution (0.1 $g.ml^{-1}$) of Diϕ400U in chloroform. Accurately measured volumes of 1 ml of each of the Diϕ400U solutions were syringed (gas tight Hamilton syringe) into each of 5 test tubes. In addition, 1 ml of chloroform was similarly added to each of 5 test tubes, which were prepared

for the standards. Five millilitres of aqueous phase (0.08M $CoCl_2.6H_2O$ and 2M KSCN) were pipetted (Gilson adjustable pipette) into each of the sample test tubes. Into the standard test tubes, 5 ml of aqueous solution was pipetted with cobalt concentrations ranging from 0 to 0.08M cobalt and a constant KSCN concentration of 2 M. The samples and standards were shaken for 1 hour, after which they were allowed to stand for 2.5 hours. The aqueous phases of the samples and the standards were then diluted 12.5 times with ethanol, after which the absorbance at 620 nm was measured in stoppered quartz cells (1 mm path length).

For calculation of the Diϕ400U:cobalt ratio, a molar mass for Diϕ400U of 638 was used. This value was calculated by subtracting the molar mass of 2 protons from the molar mass of PEG400, and then adding the mass of two C_6H_5-NHCO- groups. This calculation is illustrated in Figure 7.10.

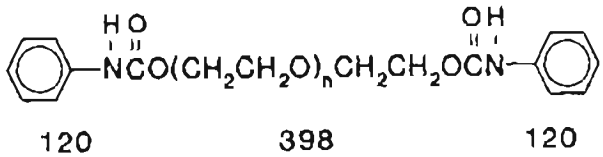

Therefore, the molar mass of Diϕ400U = 2(120) + 398 = 638.

FIGURE 7.10 The calculation of the molar mass of Diϕ400U (n = 7 - 8).

2.3(iii) Procedure for Sections 1.1 (iii) and (iv)

The urethane compounds were dissolved in chloroform to give solutions of 0.2 M for the diurethane podands and approximately 0.2 M of the repeating unit of Pol150U(1:2), Pol194U(1:2), Pol400U(1:2) and Pol400U(1:1). The large mass of Pol6000U(1:1) needed for 0.2 M of its repeating unit was not soluble in the required amount of chloroform. Hence, a concentration of approximately 0.02 M repeating

unit was used. The molar mass of the diurethane podands and the repeating units of the polyurethanes are shown below. Diagrammatic representation of these compounds may be found in Chapter 3 (Figure 3.2 and 3.3).

Diurethane podand	molar mass
Diϕ150U	388
Diϕ194U	433
Diϕ400U	638

Soluble, linear polyurethanes	molar mass of repeating unit
Pol150U(1:2)	324
Pol194U(1:2)	368
Pol400U(1:2) and -(1:1)	575
Pol6000U(1:1)	6175

The extraction and determination of cobalt was achieved as described for Section 1.1(ii). For this study, the samples and standards were diluted by transferring 0.7 ml (Hamilton syringe) of each of the samples and standards to a 5 ml volumetric flask, adding 1.3 ml water and diluting to volume with ethanol.

The amount of cobalt extracted by Diϕ194U was too small to quantify by calculating the difference in the cobalt concentration of the aqueous phase. Hence, the cobalt extracted was estimated by comparison of the absorbance at 620 nm in the chloroform solution of Diϕ194U to the absorbance in Diϕ400U (for which the extraction had already been quantified). No cobalt was found to be extracted by Diϕ150U.

2.3(iv) Procedure for Sections 1.2(i) to (v)

Double distilled water was boiled for 30 minutes and cooled under nitrogen to expel any dissolved oxygen, after which it was saturated with chloroform. Chloroform was distilled under nitrogen, and saturated with water. The above solvents were stored under nitrogen, and used for the preparation of all aqueous and chloroform solutions.

All aqueous and organic solutions were freshly prepared for each investigation. The $SnCl_2.2H_2O$ was dissolved in the required amount of concentrated hydrochloric acid (to give the correct concentration after the final dilution). After the initially formed cloudiness (due to hydrolysis products) had disappeared, the calculated amount of rhodium (accurately weighed to 4 decimal places) and, when needed, the correct mass of alkali metal salts were added, before dilution to volume with water. Care was taken to exclude oxygen during the dilution and equilibration process of the aqueous phases. The extractions were performed in a temperature controlled room at 20 ± 1 °C. Two millilitres of the chloroform solutions of the urethane compounds were shaken with 5 ml of the aqueous phase under nitrogen, in test tubes sealed with inert silicone rubber stoppers. To ensure identical treatment of the samples and standards, 5 ml of the standard solutions were shaken with 2 ml of chloroform in test tubes for the same length of time (30 minutes). The volumes of organic and aqueous phases were accurately measured with gas-tight Hamilton syringes and Gilson pipettes, respectively.

After extraction, 1 ml of the aqueous phase was transferred to a 10 ml volumetric flask. One millilitre of a 20 000 $\mu g.ml^{-1}$ $La(NO_3)_3.6H_2O$ solution was added, after which the sample was diluted to volume with 1M HCl. The standards differed from

the samples only in the concentrations of rhodium and tin, the most concentrated standard having the same concentration of rhodium and tin as the samples before extraction. Care was taken to match the matrix of the samples and standards, while the concentrations of chloroform saturated aqueous phase, hydrochloric acid concentration, alkali metal salt concentration and the concentration of the releasing agent La^{3+} of the standards were identical to those of the samples.

2.3(v) Procedure for Section 1.3(ii)

Equal volumes (1.5 ml) of the aqueous phase (described in Chapter 4, Section 1.3) and the chloroform phase {containing Pol1500U(1:2)} were shaken together and centrifuged. The complete disappearance of colour from the aqueous phase suggested quantitative extraction by Pol1500U(1:2). The aqueous phase was discarded and the organic phase was washed 3 times with 1M HCl. Acetone was added to a final volume of 2 ml to solubilize any precipitated Pol1500U(1:2) and the ^{7}Li nmr spectrum was recorded relative to an external $LiNO_3$ standard. The details are given in Chapter 4, Section 1.3.

2.3(vi) Procedure for Section 2.

The procedure is described in Chapter 4, Section 2.1. The aqueous phases were prepared, and the amount of rhodium and tin that had been extracted were determined as described in Sections 2.3(iv), 1.1 (i) and 1.1 (ii) of this Chapter.

2.4 Procedures Employed within Chapter 5

2.4(i) ^{119}Sn nmr

The aqueous phases from which extractions were made were prepared as follows. The required amount of $SnCl_2.2H_2O$ was dissolved in a calculated amount of nitrogen-saturated concentrated hydrochloric acid. After the solution had cleared, 0.100 g $RhCl_3.3H_2O$ and the required amount of KCl (if needed) were added before dilution to 5 ml with nitrogen saturated water. The solution was then equilibrated at 35 °C for a minimum of two hours. The MIBK extracts were made by shaking 1 ml of nitrogen saturated MIBK with 1 ml of the aqueous phase. A small amount of acetone-d_6 was added to the separated MIBK phase in the nmr tube for locking purposes. Portions of 0.8 g of Diϕ400U and Aliquat 336 were dissolved in 1 ml of acetone-d_6 and $CDCl_3$ respectively. After shaking each of these extractants with 1 ml of the aqueous phase, the solutions were centrifuged to separate any emulsion that formed during the shaking process. The organic extractants were separated and their ^{119}Sn nmr spectra recorded.

2.4(ii) UV-Visible Spectrophotometric Study of the Protonation of $[Rh(SnCl_3)_5]^{4-}$

It is known that chloroform reacts slowly with oxygen when exposed to air and light, giving mainly $COCl_2$, Cl_2 and HCl [9]. Since we wished to study an acid base reaction which involved the protonation of $[Rh(SnCl_3)_5]^{4-}$ in solutions of Aliquat 336 in chloroform, it was important to free the chloroform of hydrochloric acid. Hence, chloroform was refluxed under nitrogen in the dark over $CaCl_2$ to which a few pellets of KOH had been added. After distilling the chloroform was stored under a nitrogen atmosphere in the dark to prevent the photochemical formation of

phosgene and HCl. Aliquat 336 solutions (3.8170 g in 25 ml chloroform) were also stored in the dark prior to use.

The rhodium-tin solution was prepared containing 4.746×10^{-4} M rhodium, Sn:Rh = 3013:1 and 1.14 M hydrochloric acid, and allowed to equilibrate at 35 °C for 20 hours. The usual precautions were taken to prevent oxidation of Sn(II) to Sn(IV).

Five millilitres of Aliquat 336 solution were shaken with 4 ml of the rhodium solution, and centrifuged. The UV-visible study was performed on an accurately measured volume (Hamilton syringe) of the Aliquat 336 extract in stoppered 10 mm quartz cells (under nitrogen) relative to the Aliquat 336 solution free from rhodium-tin complexes. Microlitre quantities of CF_3COOH and DMF were added to the sample extract using a microlitre syringe. Since the volumes were accurately known, the absorbance values could be corrected for dilution.

2.4(iii) An Infrared Study of the Protonation of $[Rh(SnCl_3)_5]^{4-}$

The Aliquat 336 extracts were prepared as described above, using aqueous phases with higher concentrations of rhodium. The two aqueous phases used, of which one was partially deuterated (90%), contained the following:

Fully protonated solution: 0.0753 M rhodium, Sn:Rh = 20:1, [HCl] = 0.5 M, [KCl] = 1.3 M

Deuterated solution: 0.0757 M rhodium, Sn:Rh = 20:1, [DCl] = 0.5 M and [KCl] = 1.3 M (this solution was made to volume using D_2O)

The infrared spectra of the chloroform phases were recorded on a Perkin Elmer 983 Speetrophotometer using fixed pathlength KBr solution cells.

The spectra were recorded relative to an Aliquat 336 solution (of equal concentration, but free of rhodium-tin complexes) as a reference. Additions of CF_3COOH and DMF were made simultaneously to the sample and reference cells, using a microlitre Hamilton syringe.

The expected stretching frequency of the Rh-D bond was calculated as follows. The vibrational frequency can be represented by the equation [19],

$$\nu = 1/2\pi c\,(f/\mu)^{1/2}$$

while the vibrational frequency of the corresponding isotopically labelled system can be given by:

$$\nu^i = 1/2\pi c\,(f/\mu^i)^{1/2}$$

where ν = vibrational frequency,

f = harmonic force constant,

μ = reduced mass of the molecule,

c = velocity of light,

and the superscript i refers to the labelled system.

If one then assumes that the force constants are unaltered by isotopic substitution, which to a good approximation is the case [20], the expected isotopic shifts may be calculated from:

$$(\nu^i/\nu) = (\mu/\mu^i)^{1/2}$$

Hence,

$$\mu \text{ for Rh-H} = \frac{102.905 \times 1.008}{102.905 + 1.008} = 0.998222$$

$$\mu^i \text{ for Rh-D} = \frac{102.905 \times 2.008}{102.905 + 2.008} = 1.969568$$

Therefore, $\nu^i = \nu(\mu/\mu^i)^{1/2}$

$$= 1924 \times \frac{0.998222}{1.969568} = 1370 \text{ cm}^{-1}$$

3. Errors

The reproducibility of the extraction experiments using polyurethane foam and the model urethane compounds was found to be approximately 4%. This value was useful for establishing the significance of an observed difference in the amount of rhodium extracted under varying conditions. Hence, the validity of a trend could be evaluated. However a detailed error analysis of the reported %**E** and $\mathbf{D'_m}$ values was not performed since the deductions made are based upon trends, and not upon absolute values. Because the values being compared were results that had been obtained by the same procedures and apparatus, the errors are likely to be constant, and the differences observed remain valid.

REFERENCES

1 J.M.WYRLEY-BIRCH,
M.Sc. Thesis, University of Cape Town, (1984)

2 A.A.VASILYEVA, I.G.YUDELEVICH, L.M.GINDIN,T.V.LANBINA, R.S.SHULMAN,I.L.KOTLAREVSKY AND V.N.ANDRIEVSKY,
Talanta, **22** (1975) 745

3 E.PITTS AND F.E.BEAMISH,
Anal. Chim. Acta, **52** (1970) 405

4 C.E.MULFORD,
At. Abs. Newsl., **5** (1966) 88

5 D.A.SKOOG AND D.M.WEST,
"Principles of Instrumental Analysis", 2nd ed., Holt-Saunders Japan, (1980) p. 325

6 A.N.ZAIDEL', V.N.PROKOF'EV, S.M.RAISKII, V.A.SLAVNYI AND E.YA.SCHREIDER,
"Tables of Spectral Lines", Plenum Data Corporation, New York, (1970)

7 A.I.VOGEL,
"A Textbook of Quantitative Inorganic Analysis",
3rd ed., Longmans, New York, (1961)

8 S.J.AL-BAZI AND A.CHOW,
Talanta, **29** (1982) 507

9 D.D.PERRIN, W.L.F.ARMAREGO AND D.R.PERRIN,
"Purification of Laboratory Chemicals", 2nd ed., Pergamon Press, Oxford, (1985)

10 ASTM DESIGNATION : D1638-74
Annual Book of ASTM Standards, **29** (1980) 220

11 D.J.DAVID AND H.B.STALEY,
"The Analytical Chemistry of the Polyurethanes", High Polymers, Vol XVI, Part III, Wiley Interscience, New York, (1969) p.318

12 J.SCHOCH,
(Dow Chemical Company, Johannesburg), *Private Communications*

13 WATERS LIQUID CHROMATOGRAPH MANUAL

14 S.M.AHARONI,
J.Appl. Pol. Sc., **21** (1977) 1323

15 K.K.CHEE,
Pol.Commun., **27** (1986) 135

16 F.L.MCCRACKIN,
Polymer, **28** (1987) 1847

17 E.A.COLINS, J.BAREŠ, F.W.BILLMEYER,
"Experiments in Polymer Science", John-Wiley and Sons, (1973)

18 T.G.FOX AND P.J.FLORY,
J. Amer. Chem. Soc., **73** (1951) 1915

19 S.PINCHAS AND I.LAULICHT,
"Infrared Spectra of Labelled Compounds", Academic Press, London, (1971)

20 E.B.WILSON, J.C.DECIUS AND P.C.CROSS,
"Molecular Vibrations", McGraw-Hill, New York, (1955)

APPENDICES

Appendix 1 : Gel permeation chromatography

The gel permeation chromatography microprocessor cuts the chromatogram into slices and characterizes each slice by a retention time and an area. These values are given in Tables 1 and 2.

Table 1 R_t and areas of the slices of Pol150U(1:2), Pol194U(1:2), Pol400U(1:2) and Pol400U(1:1).

Pol150U(1:2)		Pol194U(1:2)		Pol400U(1:2)		Pol400U(1:1)	
R_t	area	R_t	area	R_t	area	R_t	area
17.57	1501710	16.06	264247	17.10	935750	14.04	2009220
17.79	8642850	16.33	5289100	17.33	4924050	14.37	12605500
18.01	18842600	16.60	14588600	17.56	9959750	14.70	22086500
18.23	30382300	16.87	25426600	17.79	15066900	15.03	28364600
18.45	42465700	17.14	35248800	18.02	19772900	15.36	36831100
18.67	51977100	17.41	41980700	18.25	23410600	15.69	44851500
18.89	55673600	17.68	44738800	18.48	24771400	16.02	48576500
19.11	53898900	17.95	44027700	18.71	24197100	16.35	48773700
19.33	58664000	18.22	39575800	18.94	25825800	16.68	46275900
19.55	29894100	18.49	33948200	19.17	21740800	17.01	42002100
19.77	19476400	18.76	28384400	19.40	12848500	17.34	36577800
19.99	21955900	19.03	20279800	19.63	7508250	17.67	30219200
20.21	9616210	19.30	10816400	19.86	7745630	18.00	23726400
20.43	917867	19.57	15175200	20.09	9690880	18.33	17904200
		19.84	6945210	20.32	8350910	18.66	11854800
		20.11	600460	20.55	3380480	18.99	8653710
				20.78	50056	19.32	3085370
						19.65	54151

Table 2 R_t and areas of the slices of Pol1500U(1:2), Pol1500U(1:1) and Pol6000U(1:1).

Pol1500U(1:2)		Pol1500U(1:1)		Pol6000U(1:1)	
R_t	area	R_t	area	R_t	area
16.20	1644380	14.17	270094	14.69	132830
16.44	6750520	14.47	6216850	14.95	420314
16.68	12930700	14.77	16038800	15.21	2276820
16.92	20989600	15.07	25559800	15.47	5288090
17.16	31733800	15.37	34993500	15.73	11996800
17.40	29800000	15.67	41451500	15.99	36741600
17.64	24358000	15.97	42750900	16.25	38715400
17.88	34282200	16.27	40060300	16.51	22934200
18.12	52217100	16.57	35433800	16.77	11771800
18.36	53132200	16.87	28427100	17.03	5946580
18.60	36166400	17.17	24102500	17.29	3291610
18.84	18322900	17.47	16877800	17.55	2132940
19.08	6977580	17.77	10684200	17.81	1794700
19.32	1678250	18.07	10065300	18.07	1583800
19.56	28699	18.37	9399160		
		18.67	6105770		
		18.97	2706440		
		19.27	485026		

Universal calibration was achieved by linear regression of a plot of $\log[\eta]M$ versus retention time (R_t) for the polystyrene standards (PS Stds). The intrinsic viscosity, $[\eta]$, of the PS Stds were calculated from $[\eta]_\theta = K_\theta \bar{M}^{1/2}$. Values of K_θ for PS were obtained from the literature [Chapter 3, Section 2.3(i)(*f*)]. For each K_θ value, a separate calibration curve was established. The K_θ values were 75 x 10^{-5} dl/g (calibration 1), 83 x 10^{-5} dl/g (calibration 2), and 96.8 x 10^{-5} dl/g (calibration 3). For calibration 3, $[\eta]$ was calculated from $[\eta] = K_\theta \bar{M}^{1/2} F(M/M_1)$ for $M > M_1$ (for $M < M_1$, $F(M/M_1) = 1$). M_1 = 11000 for PS. Therefore $F(M/M_1)$ was calculated according to equation 19 in Chapter 3 for standards with M = 19750 and 50000. The relevant data for calibration are given in Table 3.

Table 3. Data for the calibration curves for PS standards of low molecular weight. K_θ = 75 x 10^{-5} dl/g (calibration 1), K_θ = 83 x 10^{-5} dl/g (calibration 2), K_θ = 96.8 x 10^{-5} dl/g (calibration 3).

		Calibration 1		Calibration 2		Calibration 3		
M	**R_t**	$[\eta]$	log$[\eta]$M	$[\eta]$	log$[\eta]$M	$[\eta]$	log$[\eta]$M	**F(M/M_1)**
1350	18.52	0.0276	1.571	0.0305	1.615	0.0356	1.681	
1830	18.21	0.0321	1.769	0.0355	1.813	0.0414	1.880	
3300	17.70	0.0431	2.153	0.0477	2.197	0.0556	2.264	
9500	16.28	0.0731	2.842	0.0809	2.886	0.0943	2.953	
19750	15.49	0.1054	3.318	0.1166	3.362	0.1391	3.439	1.0228
50000	14.22	0.1677	3.924	0.1856	3.968	0.2578	4.110	1.1911

From the universal calibration curve, the retention time of each slice is translated to a value for log$[\eta]$M. Division by the $[\eta]$, which had been measured previously, (see Appendix 2), yielded the molecular weight of each "slice" of the polyurethane. M_n and M_w are calculated as described in Chapter 7, Section 2.2(iii). ($D = M_w/M_n$).

From a logM versus R_t calibration curve, the molecular weight of each slice can be obtained directly from the retention times. The data for the logM versus R_t calibration curve, which was constructed from the retention data of polystyrene standards and polyethylene glycols (PEG) are shown in Table 4.

Table 4 Retention data of PS standards and PEG for construction of a logM versus R_t calibration curve.

PS stds.		PEG	
R_t	logM	**R_t**	logM
18.52	3.130	21.55	2.177
18.21	3.263	21.32	2.288
17.70	3.519	20.29	2.602
16.28	3.978	18.46	3.176
15.49	4.296		
14.22	4.699		

Appendix 2: Efflux Times Measured for Pol150U(1:2), Pol194U(1:2) and Pol400U(1:2) in the Intrinsic Viscosity Determinations

Efflux Times

Pol150U(1:2)			Pol194U(1:2)			Pol400U(1:2)		
t_o = 97.61 seconds ±0.08%			t_o = 97.76 seconds ±0.14%			t_o = 97.64 seconds ±0.17%		
C(g.dl^{-1})	t(s)	COV	C(g.dl^{-1})	t(s)	COV	C(g.dl^{-1})	t(s)	COV
3.790	117.35	0.19	2.408	113.84	0.13	3.497	113.35	0.24
3.212	113.70	0.37		114.07	0.41	2.914	111.02	0.69
2.787	110.99	0.50		114.40	0.71	2.186	107.43	0.46
2.462	109.14	0.46	1.926	110.90	0.50	1.457	104.81	0.49
2.107	107.32	0.23		110.45	0.13	1.093	102.77	0.13
1.756	105.39	0.25	1.498	108.48	0.82	0.729	100.97	0.06
				108.06	0.30			
			1.037	105.58	0.46			
			0.613	102.36	0.46			
				102.61	0.61			

t_o = the efflux time of the solvent (THF), c = concentration, s = seconds, COV = coefficient of variation (%) of the efflux times.

Appendix 3: ^{1}H Nmr Estimation of the Molecular Weight of Linear Polyurethanes

Pol150U(1:2)

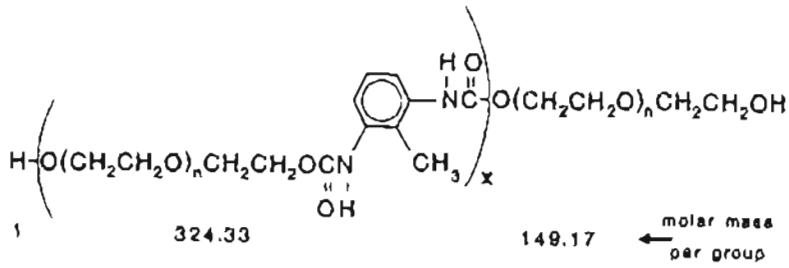

x	M	EOP/MP
0	150.2	-
1	474.5	8.00
2	798.8	6.00
3	1123.2	5.33
4	1447.5	5.00
5	1771.8	4.80
6	2096.2	4.67
7	2420.5	4.57
8	2744.8	4.50
9	3069.2	4.44

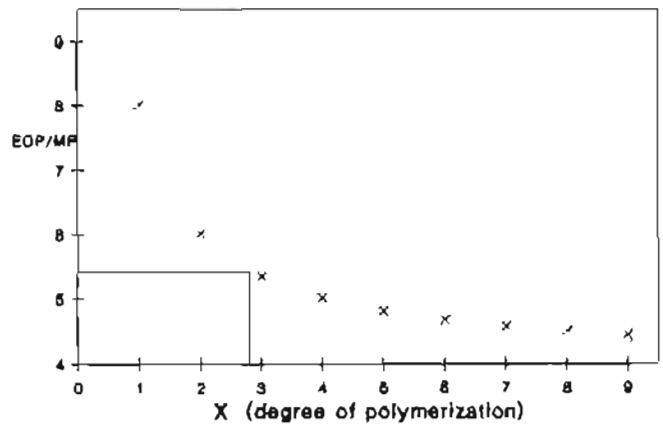

EOP = ethylene oxide protons

Mp = methyl protons

From the integrated ^{1}H nmr: EOP/MP = 5.412

therefore, from the graph: $\bar{x}$ = 2.8 and $\bar{M}_n$ = 2.8 (324.33) + 150.17 = 1058

Pol194U(1:2)

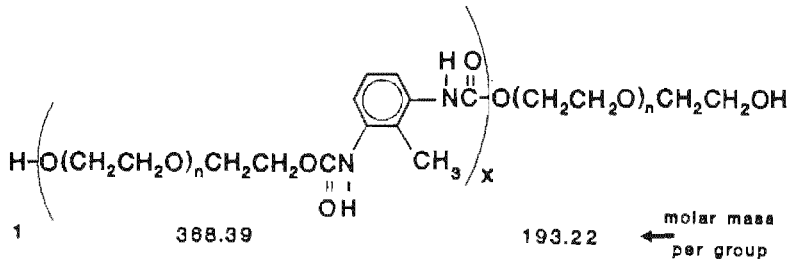

x	M	EOP/MP
0	194.2	-
1	562.6	10.67
2	931.0	8.00
3	1299.4	7.11
4	1667.8	6.67
5	2036.2	6.40
6	2404.5	6.22
7	2772.9	6.10
8	3141.3	6.00
9	3509.7	5.93

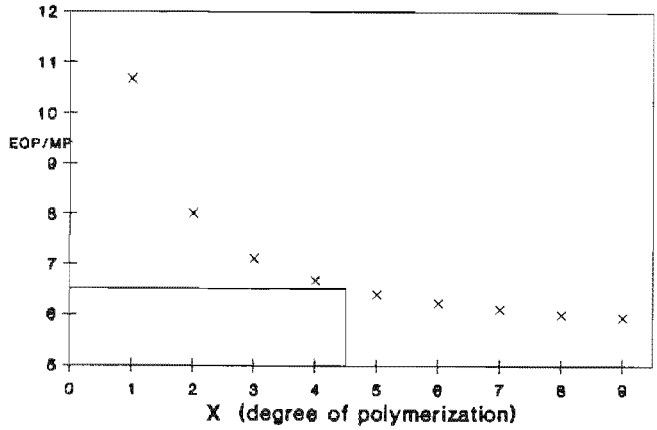

EOP = ethylene oxide protons

Mp = methyl protons

From the integrated ^{1}H nmr spectrum: EOP/MP = 6.518

therefore, from the graph: $\bar{x}$ = 4.5 and $\bar{M}_n$ = 4.5 (368.39) + 194.22 = 1852

Pol400U(1:2)

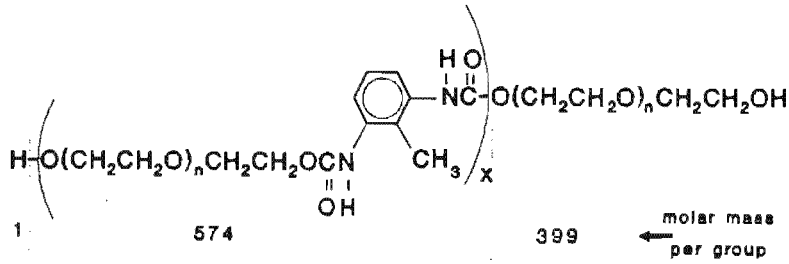

Calculation of the number of protons per oligo(ethylene oxide) group is complicated by the fact that the glycol has an average molar mass and an average number of ethylene oxide groups (n = 7-8). The number of protons (EOP) per oligo(ethylene oxide) chain was therefore calculated as follows:

PEG400 = $HO(CH_2CH_2O)_{7\text{-}8}CH_2CH_2OH$

for n=7: molar mass = 370.439 and EOP = 32

for n=8: molar mass = 414.492 and EOP = 36

We can formulate two equations, that is:

$$x(370.439) + y(414.492) = 400 \qquad (1)$$

$$x + y = 1 \text{ or } y = 1 - x \qquad (2)$$

substitute *(2)* into *(1)*: $(1-y)370.439 + 414.492y = 400$

therefore $y = 0.671$ and $x = 0.329$.

Therefore, the average number of EOP = 0.329(32) +0.671(36) = 34.684 per oligo(ethylene oxide) section with n = 7-8.

x	M	EOP/MP
0	400	-
1	974	23.12
2	1548	17.34
3	2122	15.42
4	2696	14.45
5	3270	13.87
6	3844	13.49
7	4418	13.21
8	4992	13.01
9	5566	12.85

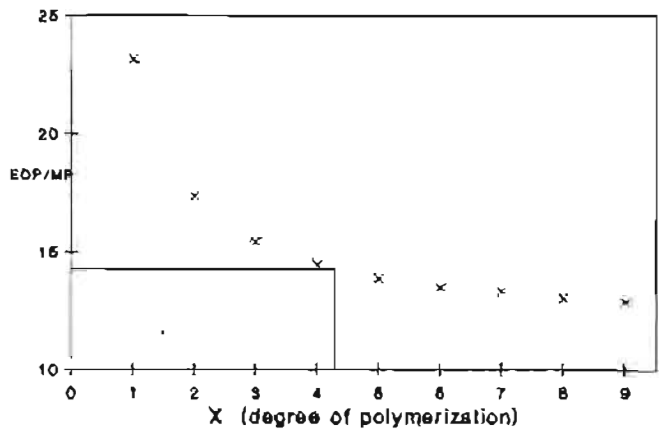

EOP = ethylene oxide protons

Mp = methyl protons

From the integrated ^1H nmr spectrum: EOP/MP = 14.27

therefore, from the graph: $\bar{x} = 4.3$ and $\bar{M}_n = 4.3(574) + 400 = 2868$

Pol400U(1:1)

A schematic representation of the structures is given in the text.

	series a		series b		series c	
	$TH(DU\text{-}PEO)_xTA$		$TA\text{-}PEO(DU\text{-}PEO)_xTA$		$TH(DU\text{-}PEO)_xDU\text{-}TH$	
x	M	EOP/MP	M	EOP/MP	M	EOP/MP
0	548	11.56	696	5.78	974	23.12
1	1122	11.56	1270	7.71	1549	17.34
2	1699	11.56	1848	8.67	2125	15.42
3	2310	11.56	2422	9.25	2700	14.45
4	2849	11.56	2997	9.63	3275	13.87
5	3424	11.56	3572	9.91	3850	13.49
6	3999	11.56	4147	10.12	4425	13.21
7	4574	11.56	4722	10.28	5000	13.01
8	5150	11.56	5298	10.41	5576	12.85
9	5725	11.56	5873	10.51	6151	12.72
10	6300	11.56	6448	10.60	6727	12.61
25			15076	11.31		
50			29455	11.34		
100					58492	11.68
2000					1.15×10^6	11.57

From the integrated ^1H nmr spectrum recorded at 30 °C: EOP/MP = 11.21

For series b: $EOP/MP = [\{x(34.684) + 34.684\} / 3x + 6] = 11.21$
therefore $x = 30.91$

For series c: $EOP/MP = [\{x(34.684) + 69.368\} / 3x + 3] = 11.21$
therefore x = a negative value

From the integrated ^1H nmr spectrum recorded at 50 °C: EOP/MP = 11.32

For series b: $EOP/MP = [\{x(34.684) + 34.684\} / 3x + 6] = 11.32$
therefore $x = 45.91$
For series c: a negative value

Appendix 4: Estimation of the Van der Waals Radius of H_3O^+

Estimation of the van der Waals radius of H_3O^+ was based upon a published crystal structure [1].

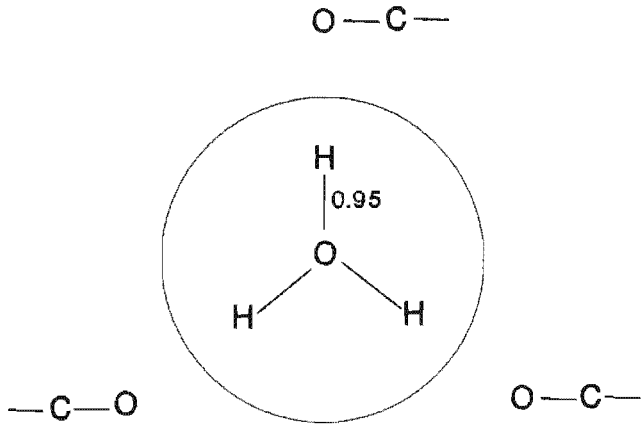

The average H-O bond length of H_3O^+ was 0.95 Å, while the average hydrogen-bond length between H_3O^+ and the chelating ligand was 1.8 Å. The hydrogen bond will in part be contributed towards by the hydrogen and in part by the oxygen atom. The Van der Waals radius of hydrogen is 1.2 Å, while that of oxygen is 1.4 Å [2]. The contribution of the hydrogen atom towards the hydrogen-bond (x) was estimated using the Van der Waals radii of the hydrogen and oxygen atoms. Hence, x = 1.2/2.6 x 1.8 = 0.83 Å. The O-H bond length plus x should be a reasonable estimate of the Van der Waals radius of H_3O^+. Therefore the radius is approximately 0.95 + 0.83 = 1.78 ≈ 1.8 Å or 180 pm.

---

[1] E.KROGH ANDERSON AND I.G.KROGH ANDERSON, *Acta Cryst.*, B31 (1975) 379

[2] F.A.COTTON AND G.WILKINSON, "*Advanced Inorganic Chemistry*", 2nd ed., Interscience, (1967)